EXTRA-LIGHT LOG TRAILER DESIGN

by

Andrzej T. Wylezinski

Dissertation submitted to the Faculty of the

Virginia Polytechnic Institute and State University

in partial fulfillment of the requirements for the degree of

DOCTOR OF PHILOSOPHY

in

Forestry, Industrial Forestry Operations

APPROVED:

William B. Stuart, Chairman

C. G. Haugh

Charles E. Knight, Jr

Richard G. Oderwald

Alfred L. Wicks

August, 1993

Blacksburg, Virginia

Extra-Light Log Trailer Design

by

Andrzej T. Wylezinski

Committee Chairman: William B. Stuart
Forestry

(ABSTRACT)

A mechanical design of an ultra-light log trailer was performed. The design process necessitated the experimental measurement of dynamic loads exerted on a log trailer and a comprehensive stress analysis of the structure.

Two light-weight, prototype, log trailers were selected to be studied, after an exhaustive survey of the existing designs. Finite element models (FEM) were developed for each of the trailers using three-dimensional tapered unsymmetrical beam elements. Static stress analysis was performed to identify critical spots in the structures and to estimate stresses encountered at these locations. These spots were selected as strain gage placements for the experimental dynamic stress analysis.

A special data acquisition system based on the STD bus computer was designed, assembled, programmed, and tested for the experimental force and strain measurements.

Experimental stress analysis of each of the selected trailers was performed. Dynamic loads and the resultant strains at critical locations were measured, both while simulating extreme situations, and during typical work cycles. The recorded service stress-time histories were then used to identify peak values of the maximum dynamic loading and the structure response. Stress distributions throughout the structures were obtained using the FEM models. The recorded service load spectra were then utilized to assess a fatigue life of each of the tested designs.

Abstract

A survey of log trailers for fatigue cracks was conducted when the dynamic stress analyses indicated that a log trailer is most likely to fail due to repeated loading. The causes for fatigue cracking of log trailers were then investigated through elastic shell element FEM modeling.

Finally, an efficient and economically feasible ultra-light design was developed based on the formulated recommendations.

The most important features of the proposed design are:

1. Reduced tare weight of 7,770 pounds.
2. Sound structural integrity.
3. Material of high strength and toughness used throughout.
4. Improved fatigue resistance (e.g., welds were replaced by elastic friction joints).
5. Movable bunks.
6. Replaceable bolsters and standards.
7. Constant tensioning device for load binders.

Acknowledgments

I would like to express my appreciation to the members of my Advisory Committee, Dr. William B. Stuart, Dr. C. Gene Haugh, Dr. Charles E. Knight, Jr., Dr. Richard G. Oderwald, and Dr. Alfred L. Wicks, for their assistance and guidance concerning this project. Their suggestions were invaluable in completing this research endeavor. Also, I would like to thank Dr. Audrey Zink for her constructive and thorough comments and for acting in the capacity of examiner during the Final Examination.

Support for this project was received from Industrial Forestry Operations Research Cooperative at Virginia Tech. Cooperative members, International Paper and Procter and Gamble Cellulose supported this research directly. I would like to thank especially Harry Archer and Buck Ford for their support and assistance in this research. Also Everett Stephenson of Union Camp Corp. deserves special thanks for his help in gathering information on light-weight trailer design and timber transportation systems in the US.

Invaluable cooperation was received from two logging firms: Regan Fox, III, Logging, Inc. and Owen's Logging, Inc., who made their trucks available for the experimental stress analysis of the selected log trailers. Their contribution included also an unlimited access to the workshops and the assistance of their mechanics during the field studies.

I am indebted to Steve Shaffer of Virginia Tech's Forestry Department, for his help in building the computer data logger, for his participation in both field experiments, help in installing the acquisition system on vehicles, and moral support when electronics seemed to be getting out of control in harsh field environment.

Sincere thanks go to my fellow graduate students and staff in Cheatham Hall for their assistance, support, and friendship. Many thanks to Joanna Banach for correcting the first draft, and Laurie Grace for reading the second draft and helpful editorial comments.

I would like to express my special appreciation to Dr. William Stuart for all his help during my time at Virginia Tech. His help included settling in Blacksburg, securing the project resources, his invaluable assistance and guidance throughout the study. Thank you for your great help and friendship.

Finally I would like to acknowledge the contribution of my family. To my wife Jola and my son Lukasz, who endured a lot of late nights and long field absences, thank you for your love, support, and patience.

TABLE OF CONTENTS

LIST OF TABLES

LIST OF FIGURES

CHAPTER 1. INTRODUCTION

Road transportation of roundwood is one of the most important components of forest industry operations. Almost all of the wood raw material in the Southeast is carried by trucks for at least part of the journey to the mill. Timber transportation constitutes over 50% of the total harvesting cost.

Hauling roundwood is different from transportation of most other commodities. Timber is an extremely heterogeneous product. The weight, shape, volume, density, and location of gravity center of the load are affected by a number of highly variable factors such as stem size, species, density, moisture content, and loading scheme. Payload determination is difficult because wood is loaded onto trucks at remote woods landings, usually without the aid of weighing devices. Load redistribution after initial loading is difficult and impractical. Log trucks often cannot carry any other loads, and few goods require transport from a yard or a mill to the forest; thus return trips are always empty. This greatly affects the productivity of the operation.

Log trucks and trailers work in a unique environment. They must be capable of withstanding the abuse of loading and unloading operations and the high energy impact loadings when driven over low-quality forest roads. Because there is no opportunity for loaded back hauls, the trucks must be resistant to fatigue due to repeated, fully reversed stresses when driven empty. Yet, they must be efficient and safe on public highways.

Trucking is the most regulated part of a timber harvesting operation. To the general public, log trucks are the most visible element of a logging enterprise. Their appearance, along with the driver's performance,

often shapes public opinion regarding the whole industry. Log truck accidents are in part responsible for high vehicle liability insurance premiums. Improving trucking safety and controlling the costs is, therefore, of great interest for the forest product industry.

Recent Trends in Timber Trucking

Trucking has undergone many changes in recent years. Today's truck tractors are more efficient than those of a decade ago. New, lightweight materials are incorporated in the design of almost all tractor components. Fuel-efficient engines and improved aerodynamics contribute to much better fuel mileage. More powerful engines, better brake systems, and improved road infrastructure allow higher travel speeds, and increased truck productivity.

Similar technological advancement is visible in manufacturing of trailers other than log trailers. Large corporate manufacturers dominate the van and flatbed trailer market. The industry has been striving to introduce new technology in trailer construction. A number of improvements have been achieved, for example the extra-light box-stressed-skin construction of aluminum van trailers similar to an aircraft fuselage design.

Dramatic advancements have taken place in designing flatbed trailers as well. Some manufacturers are now incorporating both steel and aluminum alloys in the same load-carrying structural components (Stadden, 1990). All flatbed trailers sag under load, but now, instead of building the beams straight and then heating and bending them upward, manufacturers use automated equipment to cut the webs with an upward bow. The precision necessary for this process requires automated plasma-arc cutters: 1 inch positive camber on a 45-feet long trailer creates the required curve with a radius of a quarter of a mile. Bud Reitnouer of Reitnouer Inc., Reading, Pennsylvania, proposed a revolutionary design of a flatbed

trailer (Anonymous, 1993a). Usually, the main beams and the floor are the independent components, with the floor boards overlapping flanges of the main beams. The new design incorporates six heat-treated aluminum extrusions which snap together making a 40-inch-wide continuous top flange of the main beam. The two main beams are also made as aluminum extrusions and are, at one point, 26 inches deep. Their top parts with the wide flanges and the bottom sections of conventional design are bolted together at the neutral axis, where the bending stresses vanish. Both 96-inch-wide and 102-inch-wide trailers have the platforms made of the two 40-inch-flanges, three wooden nailers, and outside rails. Solid one-piece cross members are equipped with wide flanges integral to the main beam webs allowing stresses to distribute over a much larger area. The other interesting feature of the trailers is that they use three-piece floating outriggers. The outrigger braces are not rigidly attached. Instead, the aluminum tubing outriggers slip over a mounting bracket attached to the web. The outriggers are pressed tightly against the mounting bracket when a concentrated load is placed above them. If the load is placed on the opposite side of the trailer, the outriggers slide on the mounting bracket evenly distributing stresses through the structure, instead of concentrating them in the welds. Production of these trailers is increasing very rapidly both at the original plant in Reading and at the assembling facility of Action Equipment Co. in Moundridge, Kansas.

Equipment trailers, dubbed lowboys or lowbeds, are taking advantage of high tech materials and manufacturing processes. Many of these trailers are now constructed with 100 ksi minimum yield strength, heat-treated, quenched and tempered alloy steel main beams which have a tapered design applied to both the web and the flanges (Anonymous, 1993b). The beams have large oval cutouts located in webs at the neutral axis for weight reduction. The 16-tire Murray Trailer has an expandable rear bogie to achieve the maximum payload under California permit regulations. Air cylinders expand the rear axles outboard from their normal 102-inch width to 120 inches.

Unfortunately, log trailer design and manufacture lag behind. The log trailer market is only a tiny niche of the whole truck trailer market in the US--log trailers constitute less than 1% of the total number of trailers sold every year. This market is dominated by a large number of small manufacturers. Large trailer manufacturers are reluctant to enter the market because they cannot compete with the low overheads of small welding shops and their ability to meet the customization requests of the customer. Increases in liability costs for the small manufacturers may open this market niche for the large players in the future. Currently heavy, all welded log trailers, made of easily available, low-, and medium-strength standard structural stock, prevail in the Southeast. Many of the manufacturers and loggers have started various trailer weight reduction programs, but all these activities are based on experience and common sense. Most lack the expertise, technical support, and infrastructure for comprehensive product redesign and testing.

Timber hauling has become increasingly expensive in the last several years. Vehicle ownership costs and operating expenses have been on the rise. These increases cannot be easily offset by gains in productivity. In general, a truck productivity depends on the average truck speed, payload, haul distance, and loading, unloading, and turn-around time. Maximum gross vehicle weight (GVW), vehicle overall dimensions, and maximum speed are restricted by law, and the loading, unloading and turn-around times are beyond the driver's control.

Other factors add complexity to the situation. The Federal Bridge Formula requires a precise weight distribution on truck and trailer axles (US DOT, 1982). The characteristics of timber hauled by log trucks have been gradually changing. The forest products raw material base in the South is shifting from natural to plantation stands. This results in harvesting smaller, shorter trees, and the load often reaches the legal height limit before GVW is approached.

Log - truck Transport Safety

Log transport safety is at least as important as economical performance, and it is becoming one of the tougher issues. A close examination of the equipment and methods used in log trucking shows that, in many instances, obsolete and sometimes even unsafe equipment is being used (Wilson, 1990). Cantilevered treetops overhanging the rear of the trailer, flexing freely and covering trailer tail lights create a serious hazard to other drivers. Log trucks cross and drive on public roads. Any failure in the rig can directly affect people not involved in the logging industry. News reports seldom describe the contents of a closed van if the truck pulling it is involved in an accident. Logs are visible and easy to describe and consequently commonly mentioned. A single accident changes the image of the industry in the minds of the general public. Log truck safety includes many issues: reliable truck and trailer design and manufacture, safe and convenient load securing devices, and safe operating practices are just a few. Log truck safety should be a top priority of every operator. If it is not, the forest products industry will continue to face regulatory threats and the loss of trucking privileges.

Increasing Average Payload

Given the operating environment of log trucks, there are only a few strategies available to control the costs. A rational strategy, from the operator's standpoint, would be to minimize per mile operating costs and maximize average payload. Operating costs depend on the equipment selection, the quality of maintenance practices, road conditions, and driving style. These areas have been explored by the forest products and truck manufacturing industries and a number of improvements have been introduced. It is

unlikely that significant gains in trucking profitability can be made by reducing owning and operating costs in the near future. Consequently, optimizing load sizes within the legal constraints imposed by local, state, and federal authorities is the only way available for cost control.

The payload of a log truck is usually limited for one of three reasons (Beardsell, 1986). First, the vehicle may be loaded to the point where its weight reaches the legislated GVW or axle weight limits. In this case, payload can be increased by decreasing the weight of the truck and trailer or configuring it so that axle weight limits are not exceeded before the GVW limit is reached. Secondly, payload may be limited due to uncertainty about how much wood has been loaded onto the truck. High fines for occasional overloading often make it uneconomical to aim for higher payloads. Mounting on board scales is a solution to this problem. The third limit on payload is when the load reaches legislated limits on height, width, or length before the GVW limit is reached. All these are common in harvesting plantation stands. The options are either to design a trailer with increased available loading space, or to adopt different loading strategies.

It follows that a new log trailer, characterized by: (1) a low tare weight coupled with safe performance, (2) axle configuration and spacing ensuring weight distribution in compliance with the existing restrictions, and finally, (3) increased loading space, would be a solution to achieve higher payload.

Reducing Trailer Tare Weight

Reducing a trailer tare weight by about 20% can increase an average payload of a log trailer by one half of a cord, provided the trailer is able to accommodate the larger volume. Such an increase in a trailer

payload translates to a system cost savings of $0.53 per cord for one of Westvaco's primary contractors in a typical plantation (Carruth, 1991). If the logger moves 40,000 cords of a plantation pine a year, he can save $21,200 a year. For a company buying 1.5 million tons of this material annually, the contractors' savings would amount to about $318,000 a year.

Scalehouse surveys carried out in the Southeast showed great variability in vehicle tare weight, indicating the potential of increasing a payload by careful trailer design. However, reductions in tare weight do not necessarily translate pound for pound in increased payload (Beardsell, 1986).

Tare weight reductions are achieved through careful truck and trailer selection, elimination of unnecessary equipment, and introduction of lightweight materials. All these are useful only if the vehicle is consistently able to attain the maximum legal GVW. An increased payload must not compromise safety of the operation.

A more comprehensive approach to the problem involves a complete engineering design process. The design of a lightweight trailer should be preceded by experimental measurements of the dynamic loadings exerted on the structure, and thorough stress analysis of existing designs.

Finally, it has been concluded that:

1) there is a need for a new extra-light log trailer design;

2) experimental measurement of dynamic loadings acting on a trailer should be the starting point for such a design task;

3) the design should be based on thorough stress analyses to assure safe operation;

4) the design must be resistant to fatigue;

5) the design must be economically feasible;

6) axle configuration and spacing should ensure weight distribution in compliance with existing restrictions;

7) the trailer should have an increased loading space.

Study Objectives

In 1991, the Industrial Forestry Operations Research Cooperative (IFO Coop) in Virginia Tech's Department of Forestry originated a research project focusing on lightweight log trailer design. The study was supported by International Paper, Procter and Gamble Cellulose, and other major forest products industry companies. **The overall objective was to increase an average payload of a log trailer by decreasing a tare weight, and at the same time, to ensure its safe performance.**

Four **specific objectives** were set forth for this research:

1) To use real time measurement techniques to record dynamic loadings and the resultant strains at critical points in log trailers under various work conditions;

2) To build Finite Element Models (FEM) and perform static and modal analyses of selected log trailer designs;

3) To transform field strain data into stress distributions and model dynamic performance of the structures;

4) To formulate recommendations for an extra-light log trailer design capable of economical and safe timber transportation;

In the course of the project, a need for the fast implementation of the findings was identified by the sponsoring forest products industry. Therefore, the study has been expanded to include the actual design of an extra-light log trailer which would incorporate most, if not all, of the formulated recommendations, and have a tare weight reduced by at least 25%. The design is considered to be the ultimate outcome of the study.

CHAPTER 2. LITERATURE REVIEW

This study is a continuation of research previously carried out at the Department of Forestry at Virginia Tech. In the last several years, the IFO Coop has supported a number of projects which addressed various aspects of trucking performance, efficiency, and safety (Stuart, 1992). Most recently, McCormack (1991) investigated impacts of the equipment choice, the work assignment, the road surface, the route, and the driver on the log truck performance. He used a specially designed and built computer data logging equipment for on-line automatic measurement of the vehicle speed and fuel consumption. Beardsell (1986) took a detailed look at how truck-trailer configurations and loads could be modified to increase the payload moved. Gains from improved loading practices, the use of on-board scales, and scalehouse data feedback were researched by Overboe (1988). Keesee (1990) investigated ways to reduce the amount of mud transferred to public roads by better woods road design and the installation of mud scrapers.

This literature review has been primarily based on, but not limited to, the previous IFO research, and concentrates on the subjects most crucial for the problem of extra-light log trailer design. It has been organized into the following sections:

1. Constraints on log trucking.
2. Trailer loading techniques.
3. Weight distribution models.
4. Truck-trailer configurations.
5. Frame trailer specifications.
5. Tare weight reduction.

6. Log trucking safety.

Constraints on Log Trucking

Legal Constraints

Federal and state trucking regulations affecting timber transportation in the Southeast were documented by the American Pulpwood Association (APA, 1981). However, due to the Surface Transportation Assistance Act of 1982, much of this information is outdated (Izlar, 1983). Beardsell (1986) completed a survey and analyzed current log trucking regulations in 15 southern states. Significant differences between state regulations were found, which makes it difficult to generalize recommendations for the region. Such information is crucial, especially for equipment manufacturers and loggers whose trucks cross state lines. Beardsell (1986) developed the following list of conditions which a transportation system would have to satisfy in order to meet legal requirements in every southern state[1] :

Maximum Height	13.5 feet
Maximum Width	8.0 feet
Maximum Semitrailer Length	48 feet
Maximum Combination Length	60 feet
Maximum Length Including Load	70 feet
Maximum Load Overhang	20 feet
Maximum Steering Axle Gross	12,000 pounds

[1] West Virginia and Kentucky have some additional requirements

Maximum Single Axle Gross	20,000 pounds
Maximum Tandem Axle Gross	34,000 pounds
Maximum Gross Vehicle Weight	80,000 pounds

The vehicle's maximum weight and the weight of any group axles must also conform to the Federal Bridge Formula. The maximum gross weight (W) allowed on any group of axles is given as (U.S. DOT, 1982):

$$W = 500\ [\ LN/(N\text{-}1) + 12N + 36\ ];$$

where:

L - spacing in feet between the extreme axles in the group;

N - number of axles in the group.

Total number of axles has been limited to 7. An exception is provided that two consecutive sets of tandem axles may carry a combined gross weight of up to 68,000 pounds if they span 36 feet instead of 39 feet required by the Formula. For convenience, the formula has been tabulated with the permissible loads given to the nearest 500 pounds (Table 1). The terms *inner bridge* and *outer bridge* were created to describe the application of the formula to subsets of the vehicles axles. *Outer bridge* refers to the distance between the centers of the vehicle's first and last axles, while *inner bridge* refers to any subgroup of axles (Figure 1).

A major legal constraint on timber trucking that has a great impact on hauling efficiency is that it is limited only to the daylight hours (Izlar, 1980). This may cause the cost for long hauls to become prohibitive (Wilson, 1980).

Table 1. Permissible Vehicle Loads based on the Federal Bridge Gross Weight Formula (from U.S. Department of Transportation, 1982)

Distance in feet between the extremes of any group of 2 or more consecutive axes	Maximum load in pounds carried on any group of 2 or more consecutive axes							
	2 axles	3 axles	4 axles	5 axles	6 axles	7 axles	8 axles	9 axles
4	34,000							
5	34,000							
6	34,000							
7	34,000							
8	34,000	34,000						
9	39,000	42,500						
10	40,000	43,500						
11		44,000						
12		45,000	50,000					
13		45,500	50,500					
14		46,500	51,500					
15		47,000	52,000					
16		48,000	52,500	58,000				
17		48,500	53,500	58,500				
18		49,500	54,000	59,000				
19		50,000	54,500	60,000				
20		51,000	55,500	60,500	66,000			
21		51,500	56,000	61,000	66,500			
22		52,500	56,500	61,500	67,000			
23		53,000	57,500	62,500	68,000			
24		54,000	58,000	63,000	68,500	74,000		
25		54,500	58,500	63,500	69,000	74,500		
26		55,500	59,500	64,000	69,500	75,000		
27		56,000	60,000	65,000	70,000	75,500		
28		57,000	60,500	65,500	71,000	76,500	82,000	
29		57,500	61,500	66,000	71,500	77,000	82,500	
30		58,500	62,000	66,500	72,000	77,500	83,000	
31		59,000	62,500	67,500	72,500	78,000	83,500	
32		60,000	63,500	68,000	73,000	78,500	84,500	90,000
33			64,000	68,500	74,000	79,000	85,000	90,500
34			64,500	69,000	74,500	80,000	85,500	91,000
35			65,500	70,000	75,000	80,500	86,000	91,500
36			66,000	70,500	75,500	81,000	86,500	92,000
37	Exception (see page 10)		66,500	71,000	76,000	81,500	87,000	93,000
38			67,500	72,000	77,000	82,000	87,500	93,500
39			68,000	72,500	77,500	82,500	88,500	94,000
40			68,500	73,000	78,000	83,500	89,000	94,500
41			69,500	73,500	78,500	84,000	89,500	95,000
42			70,000	74,000	79,000	84,500	90,000	95,500
43			70,500	75,000	80,000	85,000	90,500	96,000
44			71,500	75,500	80,500	85,500	91,000	96,500
45			72,000	76,000	81,000	86,000	91,500	97,500
46			72,500	76,500	81,500	87,000	92,500	98,000
47			73,500	77,500	82,000	87,500	93,000	98,500
48			74,000	78,000	83,000	88,000	93,500	99,000
49			74,500	78,500	83,500	88,500	94,000	99,500
50			75,500	79,000	84,000	89,000	94,500	100,000
51			76,000	80,000	84,500	89,500	95,000	100,500
52			76,500	80,500	85,000	90,500	95,500	101,000
53			77,500	81,000	86,000	91,000	96,500	102,000
54			78,000	81,500	86,500	91,500	97,000	102,500
55			78,500	82,500	87,000	92,000	97,500	103,000
56			79,500	83,000	87,500	92,500	98,000	103,500
57	Interstate Gross Weight Limit		80,000	83,500	88,000	93,000	98,500	104,000
58				84,000	89,000	94,000	99,000	104,500
59				85,000	89,500	94,500	99,500	105,000
60				85,500	90,000	95,000	100,500	105,500

Tandem Axle (by definition)

The permissible loads are computed to the nearest 500 pounds. The modification consists in limiting the maximum load on any single axle to 20,000 pounds.

The following loaded vehicles must not operate over H15-44 bridges: 3-S2 (5 axles) with wheelbase less than 38 feet; 2-S1-2 (5 axle) with wheelbase less than 45 feet; 3-3 (6 axle) with wheelbase less than 45 feet; and 7-, 8-, and 9-axle vehicles regardless of wheelbase.

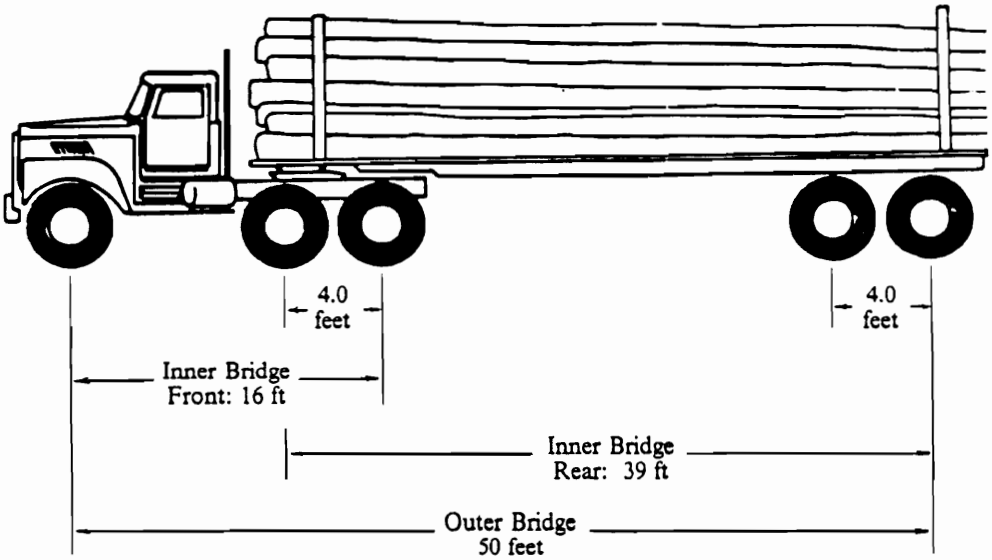

BRIDGE FORMULA RESTRICTIONS

Axle Group	# of Axles	Distance	Bridge Limit
Steering Axle	1	0.00	20,000
Tractor Bogie	2	4.00	34,000
Trailer Bogie	2	4.00	34,000
Inner Bridge - Front	3	16.00	48,000
Inner Bridge - Rear	4	39.00	68,000
Outer Bridge	5	51.00	80,000

Figure 1. Example of the Federal Bridge Gross Weight Formula Applied to a 5-Axle Tractor Trailer (from Beardsell, 1986).

Physical Constraints

The maximum legal payload of a truck is constrained by both the legal GVW and a vehicle tare weight. A loading space on the front bunk is limited by the overall legal height and width, location height of the kingpin, main beam depth at the trailer front end, and dimensions of standards and bolsters. Similarly, a loading space on the second bunk is constrained by the legal height and width, the clearance under the trailer, the main beam depth, and the required clearance between logs and the frame. Simply reducing dimensions of the load carrying structural members of the trailer, and thus the tare weight, could adversely affect its structural integrity. A comprehensive stress analysis of the trailer has to be performed to determine the loading exerted on the structure and the resultant stresses. This approach, and the use of high strength materials are proven techniques of successful weight saving in other industries.

Wood characteristics also directly affect the payload. First, the center of gravity of tree-length material may fall such that the tractor or trailer tandem axle weight limits are reached before the GVW is attained (Watson and Matney, 1981). Secondly, small trees have low specific gravity, low stacking densities, and short lengths, which may result in the legal height being reached before the GVW limit (Izlar, 1983). Therefore, center of gravity location and the weight of trees that can be packed in a given volume are of the primary interest in trailer design.

Many researchers have developed prediction equations for tree center of gravity location (Steinhilb and Erickson, 1970 and 1972; Ford, 1976; Watson and Matney, 1984). Watson and Matney's model accounted for the fact that a log had a section removed from the butt end of a tree or that the stems on the truck were trimmed to various top diameters.

Beardsell (1986) derived a formula for the center of gravity distance from the tree butt of any log cut from a stem of southern pine, expressed as a percentage of the total stem length (center of gravity percent CGP). He utilized the volume ratio equation developed by Cao and Burkhart (1980), which assumed that the green density is constant along the length of the stem.

Beardsell predicted CGP for untopped planted and natural stems to be 29% and 31% of the log length from the butt, respectively. As more of the top of the tree is removed, the CGP for the remaining log approaches 50%. Removing a 12-foot log from a 60-foot-long tree stem from a natural stand increases CGP from 30.6% to 36.4%.

The center of gravity of a load of tree-length stems depends not only on locations of centers of gravity of the individual stems, but also on how the stems are loaded onto the trailer. Beardsell (1986) investigated the location of center of gravity of a tree-length load for the three following loading schemes:

1. Butts aligned in one vertical plane.
2. Centers of gravity aligned in one vertical plane.
3. Stems randomly staggered.

He concluded that it is not possible to predict the load center of gravity location accurately by any practical procedure, and suggested the following rules of thumb which may be useful in trailer design and prediction of axle weights:

1. The load center of gravity should lie between 30% and 40% of the total load length from the butt end of the load for loads of tree-length stems with butts in the same direction.

2. The percentage will be smaller for butt aligned stems of variable lengths.

3. The percentage will be greater for larger top diameters, randomly staggered stems, and trees from natural stands.

The weight of stems loaded inside a given bunk area is greatly influenced by the tree stacking density. Lavoie (1980) defined the coefficient of effective occupancy (CO) as a ratio of the total area occupied by the tree butts to the overall available loading area. He found that for stems of the same butt diameter, CO is a linear function of the diameter. However, the relationship was not thoroughly explained and had the property of allowing CO value to exceed 1. Lavoie used the estimate along with stem volume equations, and assumed specific gravity to predict maximum payloads for a range of tree and bunk sizes.

Beardsell (1986) built five mathematical models describing the relationship between the CO and the butt diameter for loads of plantation grown loblolly pine. He experimentally estimated parameters of these expressions and compared their accuracy. A hyperbolic relationship was found to be the best by all selection criteria. A green-weight-per-stem estimate by Burkhart et al. (1972) was incorporated to estimate the weight of stems per square foot of bunk area. Finally, a relationship between green weight per unit area of the bunk, the butt diameter, and total tree height was derived (Figure 2). It can be utilized to assess the static weight acting on the trailer bolsters and standards of the given geometry.

This relationship can be also used to predict the break point between the GVW and bunk area limits on payload. For example, if the truck tare weight is 28,000 pounds, the 80,000 pounds legal GVW limit will give a maximum legal payload of 52,000 pounds. If the trailer has a front bunk area of 65 square feet and logs are loaded butts first, then a stacking density of 800 pounds per square foot of end area would be needed for the legal payload to be fully utilized.

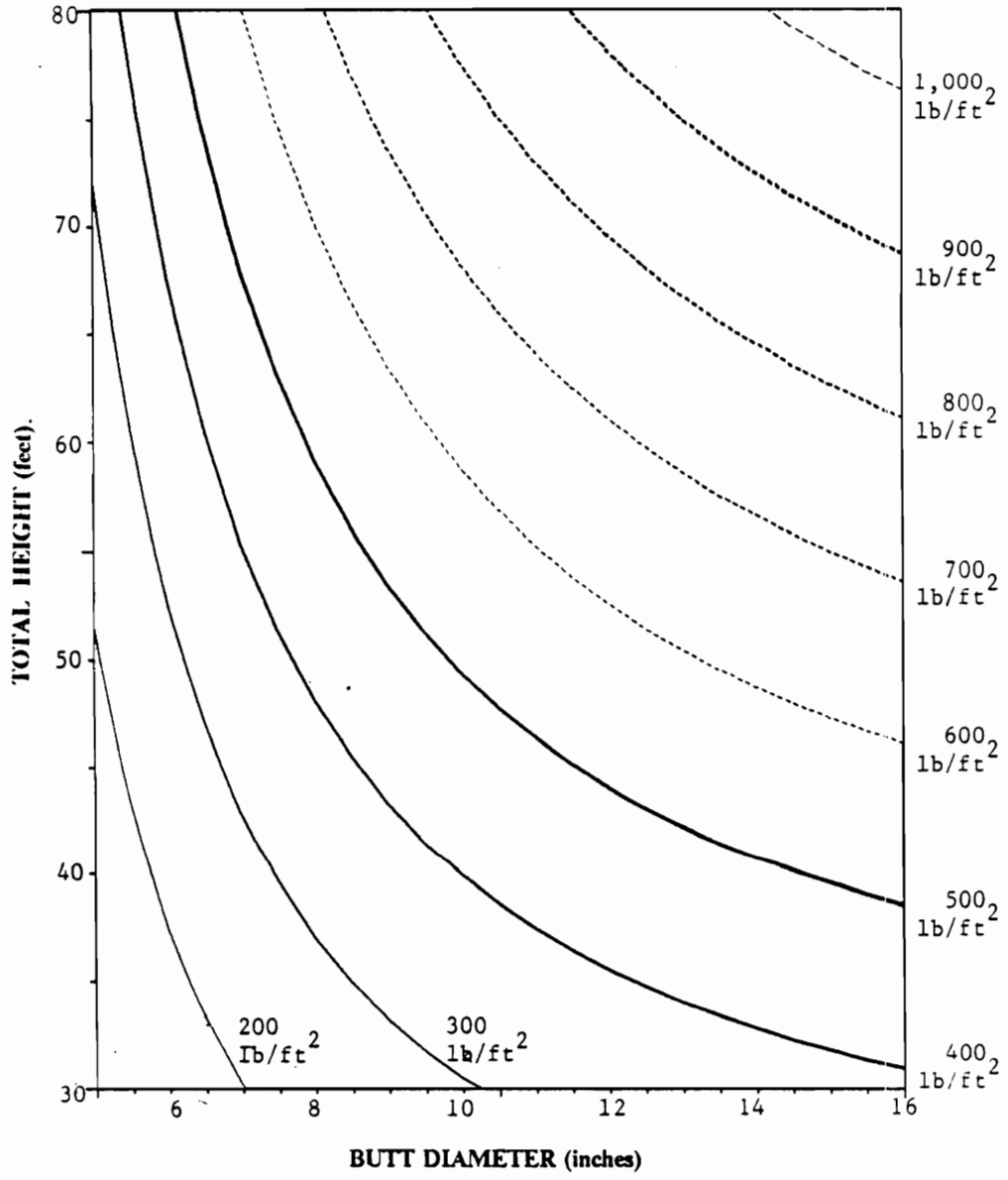

Figure 2. Response of Green Weight/Sq.Ft. of Bunk Area to Butt Diameter and Total Tree Height (after Beardsell, 1986).

For any combination of total tree height and butt diameter lying above the 800 pounds per square foot contour in Figure 2, the GVW limit will be reached before the height limit, and vice-versa.

The analysis of the model resulted in other interesting observations:

1. As tree size decreases, with other parameters remaining constant, the maximum payload decreases rapidly.

2. Load of logs contained in a given bunk is highly sensitive to butt flare and the payload can be greatly increased by staggering the stems.

3. Placing butts ahead of the bolster significantly increases the payload on a given bunk.

System Constraints

System constraints on timber trucking include the form of the product produced by the harvesting system, the loading equipment in the woods, the road network the truck must travel, and the woodyard and processing systems at the mill.

Older southern pulpmills could accept only 5-foot 3- inch shortwood that would fit on a rail car (Ilzar, 1983). In recent years, many of these woodyards have been converted to handle random-length and tree-length material as well.

Hydraulic knuckleboom loaders are the most common loaders capable of handling longwood used for in-woods operation in the Southeast. Some loggers who have small loaders use a loading technique which

requires that the loader drag stems around the front or rear standard. Because of that, standards must have sufficient stiffness to withstand these large lateral forces coupled with bending moments. The second most common loader used at the landing is the front-end-loader. Although, it uses a different loading technique, it is even more abusive to the structural members of the trailer than a knuckleboom loader.

The circular-boom loader, the mobile log stacker, and the portal crane are the most common mill unloading machines. Each type of these three machines usually has different requirements for log clearance above the trailer frame. Typically, at least 12 inches of open space is needed to permit the passing of forks or grapple tongs under the load. Quite often, these huge machines wreck trailers due to bad weather conditions and poor visibility, or simply due to carelessness of the operator. Both better trailer design and greater awareness of loader operators can decrease the number of such incidents.

Trailer Loading Techniques

When small trees are hauled, the maximum payload is usually limited by the legal height rather than by gross vehicle weight of 80,000 pounds. Wood suppliers in Louisiana who specialize in first thinning operations use a method of loading two tiers of tree-length material on a four-bolster trailer, with the back tier oriented so that butts face the rear (Nolen, 1992). Twelve- to fifteen-year-old plantation loblolly pine trees harvested in first thinning average 6 inches DBH and 28 feet in length. Single tier loads on a conventional pole trailers usually contain 275 to 300 stems per truckload, and produce maximum payload below the legal GVW limit.

A double-tier loading technique is used to enable loggers to attain full legal payload and improve hauling productivity. However, this technique slows down the unloading operation by a factor of two, and some of the unloading systems cannot handle it. A 40-foot long four-bolster trailer is used. Thirty to forty percent of the total load of tree-length stems are first loaded on the rear bunk, with approximately 12 feet of overhang and the butts facing the rear. A trailer-width log is placed across the tops of the back tier, just behind the second bolster to avoid tops being entangled with the second tier of wood. The front bunk is then loaded, butts forward, with the remaining 60% to 70% of the total load. This double-tier method of loading maximizes the payload. It allows attaining the GVW of 80,000 pounds by filling the existing loading space and also moves the center of gravity of the load to the rear, balancing the load between the front and rear axles. This loading technique is considered to be safer, as the overhang is limited to 12 feet and consists of stiffer sections of trees.

In 1987, Forest Research Institute of Canada (FERIC) conducted a study to compare the total cost of timber trucking from the stump to the mill for two alternative loading strategies: butts-first and mixed-butts loading techniques (Clark and Giles, 1988). The project was conducted in British Columbia and consisted of three phases. During the first one, observations of hauling productivity were carried out for three truck configurations: a 2-axle pole trailer, a 3-axle doglogger, and a 3-axle tractor-jeep trailer pulled by a 3-axle tractor in each case. Each trial was repeated for two log lengths: 15 and 19 meters (49 and 62 feet). Four types of loading equipment were tested: Wagner L120 log stacker, Caterpillar 215 and Prentice 600 knuckle-boom loaders, and Caterpillar 980B front-end-loader. The predominant species was lodgepole pine. The second phase monitored woodyard activities at a mill to evaluate the influence of log-butt orientation on woodyard equipment productivity and log breakage. The last component of the study was designed to detect changes in the Lumber Recovery Factor (LRF) due to alternate log orientation at a sawmill. Loading operation on landing was closely monitored. The operation was stopped whenever the

overall height limit, gross vehicle, or gross axle weight limits were reached (each truck was equipped with on-board scales).

The results obtained in the study showed no difference in productivity between butts-first and mixed-butts loading strategies for 15-meter-long logs. However, a Hitachi UH122 loader had to reposition the grapple due to insufficient boom-reach when loading 19-meter-long logs. This resulted in longer (about 5 minutes) loading times. Nevertheless, this did not have any significant influence on either truck trip times or daily loading productivity.

The mixed-butt loading scheme increased the maximum payload by 2% for the pole trailer loaded with shorter logs, and by 14% for the doglogger loaded with longer stems. With all butts first, only the pole trailer could achieve maximum legal payload with 15-meter-long logs, and none of the tested trucks attained the full legal GVW with the 19-meter-long stems. However, all the three trailer configurations tested were able to attain the full legal load when butts were mixed, regardless of log length.

Reducing the allowable maximum rear bunk overhang from 6 to 5 meters further reduced an average payload for butts-first hauling by 1.9% for a doglogger trailer, and by 5.7% for a tractor-jeep configuration.

Butt orientation had no significant influence on the productivity of woodyard equipment. Log breakage increased only for the knuckle-boom loaders. Logs handled by tops would break with the frequency of from 2% to 13% for the loaders tested. However, highdecking bundled truck loads with the Wagner L120 stacker reduced log breakage by 10% over the sorting and highdecking with knuckle-boom loaders.

Finally, the total landing-to-mill economic evaluation of the two loading strategies proved that annual net savings of about 804,000 Canadian dollars ($1.79 per cubic meter) would be achieved due to the mixed-butts scheme.

Beardsell (1986) experimented with five different alternative loading strategies. A trial was conducted in which the same stems were loaded on a double-bunk trailer using the following schemes: conventional, top one-quarter layer stepped back to a second standard, butts staggered, combined random length and longwood, double bunk random length, and butt to top loading strategies.

The technique of dropping the top one-quarter to one-third of the load back to the second pair of standards has been used by Union Camp Company in Georgia for stems from final harvest of about 50 feet in length. Beardsell reported a payload increase by 13% to 15% with this loading scheme. Besides the increase in bunk occupancy, this strategy improves axle weight distribution by transferring more weight to the trailer tandems--the center of gravity of the load was found to move 2 to 3 feet to the rear. The technique had no effect on a in-woods loader productivity. It was observed that the unloading operation would be unaffected if the load could be handled as a single unit. Possible problems could occur if the woodyard required butt alignment to facilitate reclaim from inventory, or because of a slasher design.

Staggering butts on a trailer has been used by Weyerhaeuser Company in North Carolina with tree-length pine thinning material of an average length of 35 feet. This loading strategy offers about 18% greater payload when compared with the conventional butts-first scheme. Essentially, this strategy has the same advantages as the set back method. Loading and unloading productivities were practically unaffected, but again if the woodyard requires precise butt alignment, this technique may be impractical.

Loggers delivering wood to Catawba Timber Company in South Carolina often load the rear trailer bunk one-third to one-half of the height of the standards with random length longwood and then place tree-length stems on the trailer in the conventional manner. This loading strategy increases the payload by about 25%. However, reductions in productivity of both loading and unloading operations were observed.

The technique of loading two bunks with random-length logs could increase the maximum payload by as much as 30%. However, currently it is seldom implemented, because it sacrifices the efficiency of tree-length handling.

Beardsell indicated that butt to top loading in two tiers offers the greatest load space utilization (up to 35%), but at the same time may present the biggest barriers to implementation. The weight transferred to the trailer tandems is the greatest of all the tested alternatives, and can be controlled by varying the percentages of stems loaded in each direction. Serious loader productivity reductions can be avoided by skidding trees onto the landing from two directions. Also, butt to top loading is easier if the tractor is not attached to the trailer during the loading operation allowing stems to be drag loaded from both directions. Common objections to this loading strategy include jackstrawing during unloading and reclaim operations, less efficient use of circular storage systems, and hang-ups in the slasher deck and conveyer system. All of these difficulties can be eliminated by switching butts in the same direction during unloading. This procedure is easily facilitated by separating the oppositely formed tiers with two logs laid crosswise on the first pile. Then a front-end-loader can easily pick off each tier separately. The same procedure can be used with an overhead portal crane without the truck repositioning if the separating cross logs are large enough. However, in both cases operation times would be doubled for single-grip unloaders.

After this exhaustive review of log trailer loading techniques, a conclusion emerges that from the standpoint of trailer design, the very last loading strategy (i.e. butt-to-top loading in two tiers) and the conventional double bunk method (when hauling shortwood) should be assumed for a static stress analysis. The two methods are equivalent in terms of the weight distribution on the trailer and correspond to the worst loading scenario on the trailer when the bending moments along the trailer frame are the greatest.

Load Distribution Models

The weight distribution over the axles of a log vehicle is vital because axle weight limits can restrict payload before the maximum legal GVW is reached. Axle weights constitute a part of the overall loading acting on a trailer's frame, and therefore, knowing them is necessary for a stress analysis of the structure, and for its safe design.

In most cases, a log vehicle has at least three axles, and it is necessary to make an assumption how a reaction force from the road is conveyed through the tandem to the frame. It is justified to assume that the force acts at a midpoint between the axles only when the axles are equalized in a tandem. Then the problem becomes statically determinate, and the axle weights can be computed from the equilibrium condition.

Baumgrass (1975) developed a load distribution model for tandem axle trucks commonly used in West Virginia. After making an assumption about the reaction force acting through a tandem, the model considers a simple beam, supported at one end by the steering axle, and at the other by the tandem drive axles. The model was used to calculate the required wheel base and cab length for a desired axle weights.

The load distribution for a tractor-trailer configuration is more complex. Essentially, the vehicle can be modeled as two simply supported beams. The tractor beam is supported by the steering axle at one end and by the drive tandem at the other. In addition to the reaction forces from the road, the beam is loaded with the tractor's weight and the load from the semitrailer at the kingpin. The trailer beam is supported at the kingpin by the tractor on one end and by the trailer's axle tandem on the other. In addition, it is loaded by both the payload and the trailer's tare weight.

Beardsell (1986) developed a weight distribution model for the tractor-semitrailer which facilitated the simultaneous consideration of all legal constraints on vehicle design. Beginning by calculating the weight distribution in a conventional way, he expressed the axle weights in the form of mathematical functions, where the distance between the load center of gravity and the kingpin was the independent variable. He imposed then the legal weight limits on the steering axle, the tractor's and trailer's tandem axle weights, and on the gross vehicle weight in the form of inequalities. Finally, he plotted these relationships in one graph (Figure 3). The figure clearly shows that an interval exists for the values of the load center of gravity location for which the maximum payload of 80,000 pounds can be reached. This flat area on the maximum payload curve, named the *sweet spot*, has the following properties:

1. The size and location of the *sweet spot* depend on vehicle geometry, tare weight distribution, and axle weight restrictions.

2. The wider the *sweet spot*, the easier it is for the loader operator to place the actual load center of gravity within its boundaries.

3. It is more likely that the rig exceeds one of the tandem axles' legal weight limit than the gross vehicle weight limit.

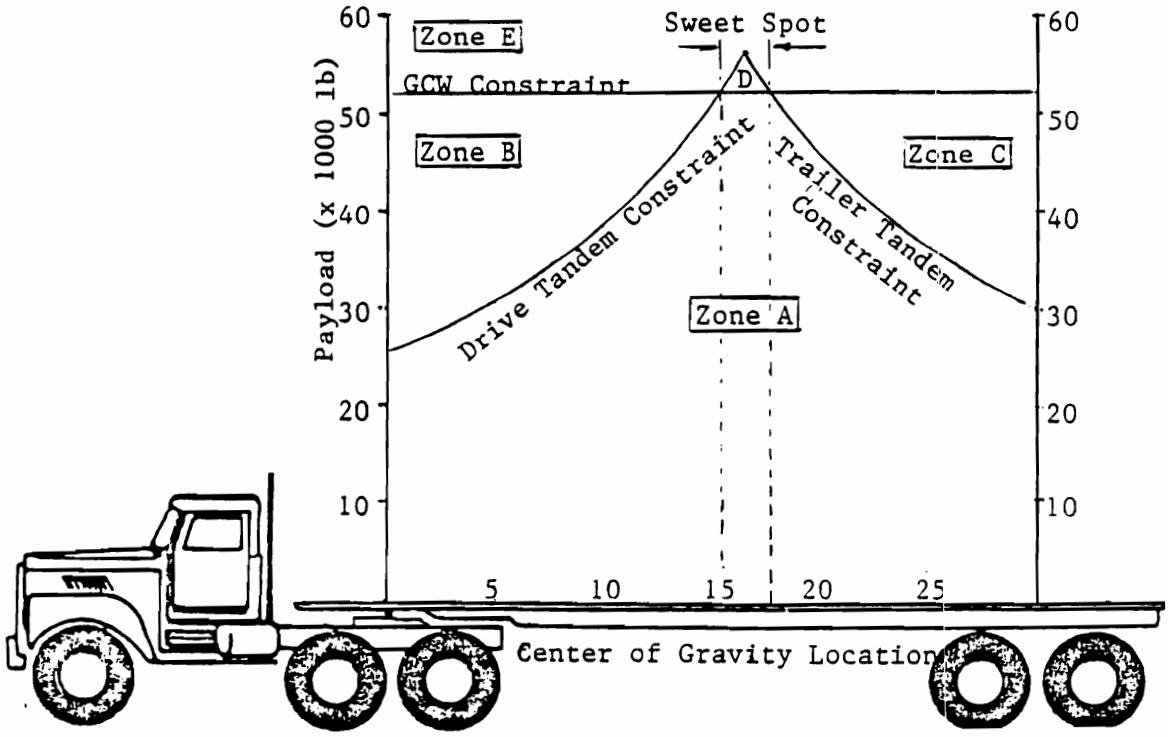

Figure 3. Weight Constraints for Hypothetical Log Truck of 30-foot Trailer Wheel Base (after Beardsell, 1986).

The general version of the model also included all the Federal Bridge Formula restrictions and had the form of a computer spreadsheet template. The model was used to experiment with various adjustments to the vehicle geometry and to see their effects on the legal payload curve. For instance, we can quickly find a solution to the common problem of reaching the tandem axle weight limit before attaining the GVW limit. One way to solve the problem is to transfer weight to the tractor steering axle by setting the tractor fifth wheel ahead of the tractor tandem center. An 18-inch offset increases the legal payload by about 3,000 pounds for a typical tractor-trailer configuration.

Experimenting with different vehicle configurations, Beardsell arrives at the interesting conclusion that adding a third axle to a tandem semitrailer could be the best alternative. Assuming that the extra axle adds 1,500 pounds to the 28,000 pounds of an average tandem trailer tare weight, the maximum legal payload of 50,500 pounds and a sweet spot width of almost 3 feet are achieved. Mounting single wide tires on all three trailer axles could then further increase the maximum legal payload.

Truck - Trailer Configurations

There is a great variety of possible log-truck configurations. Each is characterized by the number and spacing of axles, the number and location of articulation points, the arrangement of bunks which hold the load, and the form of wood it is carrying.

A three-axle tractor and two-axle semitrailer is a standard configuration for longwood and tree-length roundwood road transportation in the South (Bearsdsell, 1986). Tractors may vary in a wheel base and a

cab style, but almost invariably have a single steering axle with single wheels, and tandem drive axles with dual wheels.

Configurations used in the South

Frame and pole trailers are the most common types of log trailers in the South. Both types of trailers attach to the tractor by means of a kingpin and fifth wheel coupling and are supported at the rear by tandem axles. Frame trailers are designed to support log loads at intermediate points between the kingpin and axles. Various bunk arrangements are possible, depending on the wood form being hauled. Their great advantage is their versatility: they can be used to transport shortwood, logwood, or tree-length material. Several main frame forms are available: straight frame, gooseneck, cutout-frame, center-drop, and tapered with web cutouts. The gooseneck trailer has a 15- to 16-inch drop in the main beam. The second bolster is usually set flush with the web of the main beam. The combination of these two features permits a 20% increase in loading space. Pole trailers have only two bolsters and two sets of standards. The first bolster is usually located just over the fifthwheel, approximately just over the midpoint of the tractor tandem. A heavy pole connects it with the trailer bogie. The second bolster is mounted right above the trailer tandem midpoint. The whole simplicity of the pole trailer design lies in the fact that the load weight is conveyed directly to the road. The pole serves only as a coupling and does not bear any weight of the logs. Consequently, this type of a trailer is 3,000 to 3,500 pounds lighter than a frame trailer. However, the scalehouse data clearly demonstrated that pole trailers do not utilize their reduced tare weights (Beardsell, 1986). Their average cross-sectional loading area is 61 square feet, while the average area for a gooseneck trailer is about 75 square feet (Ford, 1993). Pole trailers are characterized by significantly higher off-tracking, especially when traveling empty. Because of the more consistent payloads and versatility, frame trailers are more common across the Southeast. Recently, folding pole trailers are becoming quite popular due to the reduced brake and tire wear, quicker turn-around times,

lower fuel consumption when they drive empty, and greater maneuverability of the tractor in the woods. Introducing a folding frame trailer, which would combine the versatility and strength of a frame design with the very useful feature of self loading for the return trip, could be a significant advancement in log trucking in the Southeast.

West Coast Configurations

Three types of log trucks: the "stinger steer" trailer, the self loader tractor-semitrailer, and the short logger are common in the western United States (Dykstra and Garland, 1978). The most common configuration is the three-axle tractor and the tandem-axle "stinger steer" trailer. The trailer differs from southern pole trailers in the location of points of articulation. Its first bunk is mounted over the tractor tandem on a swivel base and the second is similarly mounted over the trailer bogie. The tractor frame terminates in a framework--the "stinger"--which attaches to the trailer by means of a special compensating head which slides in and out. Both the specific location of the point of articulation and the compensating head force the "stinger steer" trailer to follow the tractor in almost the same tracks. Thus, the trailer off-tracking is reduced to a minimum and the vehicle is able to negotiate very tight curves safely. The manufacturer argues that the cost of building narrower roads for the "stinger steer" trailer is significantly lower than the cost of road construction necessary for semitrailers (Peerless, 1986). After the load is removed from the truck, the trailer is loaded on the tractor for return trip. This has many advantages: trailer tires are subject to only about two thirds of the wear that a "towed" trailer would receive, turn-around times are quicker, the shorter vehicle has better maneuverability in the woods, additional weight on the driving axles of the empty tractor increases its traction. "Stinger steer" trailers are built light--their construction is primarily based on the formed and welded T-1 high-tensile steel. Usually, they are equipped with rubber mounted two-spring or walking beam suspension. On-board electronic or hydraulic scales for protection against overload fines are the standard option. The design of most of the trailer wear points (the center bearing,

and the flat friction blocks in the swivel base of the bunk, the friction bearing of the compensating head) incorporates UHMW plastic--an excellent abrasion resistant, low friction coefficient, and high energy absorption material (Stephenson, 1993). Only the fifth wheel area and axles are conventionally lubricated.

The self loader truck is essentially a "stinger steer" trailer configuration, except that the tractor frame is extended to allow a hydraulic knuckle-boom loader to be mounted behind the cab. This solution sacrifices a portion of the trailer's payload, but the trucker is independent of the loading/unloading equipment at the mill.

The third log truck configuration used on the West Coast is the short logger. This combination consists of a three-axle truck and a two-axle full trailer. Both a truck and a trailer have two bunks, so that each can carry a load of 20-foot-long logs. A simple full trailer is ideal from the standpoint of weight distribution. The load center of gravity usually falls exactly at the midpoint between the axles; thus, the maximum legal weight on each axle can be utilized. However, shortwood systems have been phased out in the region during last several years.

Foreign Configurations

The three most common log truck configurations in Canada were studied by Smith (1981). The three-axle tractor and a tandem-axle pole trailer had an average GVW of 95,400 pounds. A six-axle configuration, of an average GVW of 112,777 pounds, consisted of a three-axle tractor and a three-axle frame trailer. The third configuration tested was a three-axle tractor pulling a train of two semitrailers. This configuration averaged at GVW of 126,053 pounds. There was a tremendous difference in payloads for the above three truck configurations, but no significant difference was found between their unit transportation costs.

The New Zealand Logging Industry Research Association (LIRA) carried out several log truck transportation cost studies over the last 15 years. Gordon (1980), Stulen (1985), and Taylor (1989) compared truck hauling costs for 17 different 5-, 6-, and 7-axle configurations, for the Class I, and Class II roads, and for off-highway transportation. The road class category was defined by the road load-carrying capacity. Class I roads permit larger axle weights, and thus, greater vehicle payloads. The pertinent costs and payload data for each configuration were compiled from various scientific and industry surveys. A model based on average values of the important parameters was derived for calculating operating and fixed costs of the selected configurations. The major assumptions of the model were that the truck travels 50,000 miles per year, uses 3- or 4- axle tractor with 290 HP engine, average loaded haul distance it covers is approximately 25 miles one-way, three-quarters of the distance is over highways, and the 2- and 3-axle trailers are piggybacked on tractors when they are empty.

Truck operating and fixed costs have been found to constitute from 80% to 90% of the total cost of a rig. Therefore, the cost of the whole vehicle can be compared only for the same types of tractors.

The analysis showed that an average cost per ton of the combination is by far more sensitive to the number and spacing of axles, thus the associated maximum legal payload, than to the fixed and operating costs of the particular trailer. Table 2 summarizes the transportation costs per ton for different tractor-trailer combinations capable of longwood hauling, broken down for the two road categories. Over the years, 6-axle combinations; 3-axle tractor and 3-axle trailers, have proven to be the most economical over the both road categories. The differences were highest for Class II roads, and amounted to 24%. The most common combination, 3-axle truck with 8-feet spread tandem-axles pole trailer, was found to be more expensive by 5% and 16% than the most economical configurations over Class I and Class II, respectively. The three cheapest truck trailer combinations for longwood road transportation, regardless of road category, are shown in Table 3.

Table 2. Trucking Cost Comparison for Different Truck Trailer Configurations in Australia: Longwood trucks.

CLASS I LIMITS	CARTAGE COST ($/TONNE)	% DIFF.	CLASS II LIMITS	CARTAGE COST ($/TONNE)	% DIFF.
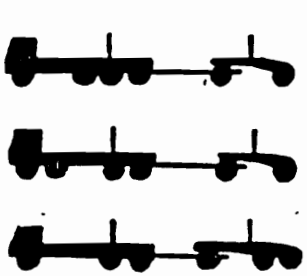	6.80 - 6.85	Cheapest	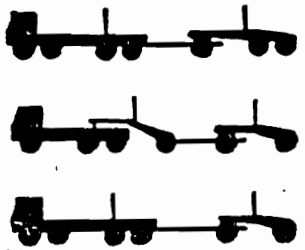	7.10 - 7.25	Cheapest
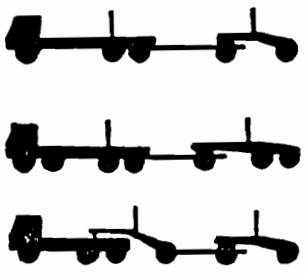	7.05 - 7.15	4%	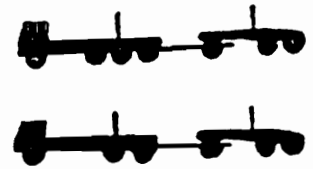	7.35	2%
				7.45	4%
					
				8.15 - 8.45	16%
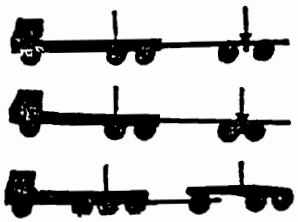	7.25 - 7.35	5%			
			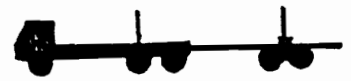	8.90	24%

Table 3. Trucking Cost Comparison for Different Truck Trailer Configurations in Australia: The three cheapest combinations for longwood haul over Class I and Class II road categories, combined.

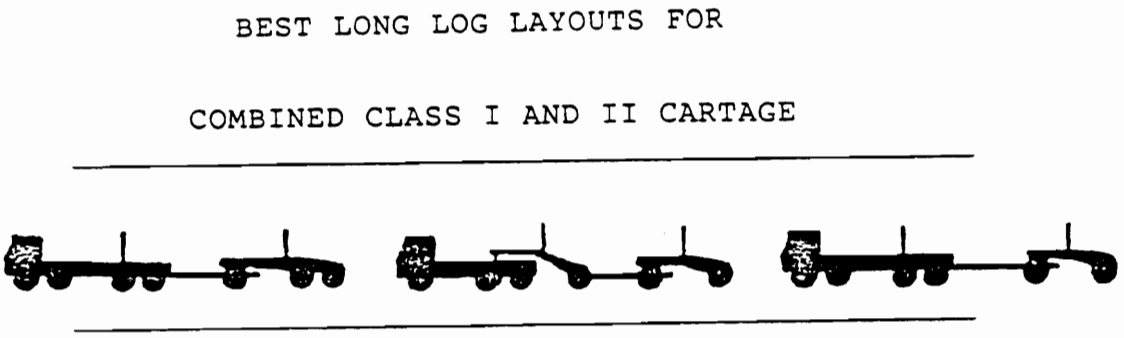

Observations made over the last decade indicate that in choosing a trailer economics have not necessarily been the most important criterion. Many other factors affect the equipment choice. Criteria such as regional conditions influencing load types (shortwood vs. longwood) and rig versatility have determined the selection of other units, such as Bailey Bridge trailers, which are not the most economical. The other vehicle combinations gaining popularity in recent years in New Zealand are: the twin-steer 4-axle trucks (especially popular for shortwood transportation), 3-axle drive trucks (the extra axle is lifted when traveling empty), and the folding Bailey Bridge trailer.

The rapidly increasing popularity of the folding Bailey Bridge trailers stemmed from the introduction of the new weight and dimension regulations in February 1989, which aligned the New Zealand laws more closely with the Australian transport legislation (Taylor, 1989). The New Zealand version of the folding Bailey Bridge is the folding frame trailer built by Evans Engineering Co. in Tokoroa. Its chassis is manufactured out of high tensile steel alloy folded plate, with another plate welded along the bottom edge.

The beam has web sections cut out for reduced tare weight. Other weight-saving refinements include super single tires and aluminum rims, high tensile steel standards and bolsters, and single-leaf springs. All these resulted in the tare weight of only 11,576 pounds. The most important feature of the trailer is its ability to mount and dismount onto the tractor unit unaided. The process is controlled by two hydraulic cylinders located at the pivot point of the trailer. The operation consists of: breaking the frame with the aid of the cylinders, backing up the tractor while applying the trailer brakes, releasing the trailer brakes and reactivating the cylinders to load the trailer onto the tractor (Figures 4 to 10). The process takes only about one minute. The trailer is placed on the tractor without impact. Comparison of the economic performance of the trailer with those of the other configurations has shown that this design is characterized with quicker turn-around times due to higher average speed of the empty trailer, and by the increased in-woods maneuverability (Taylor, 1989).

Figure 4. Self Loading Sequence for Evans Folding Frame Trailer: Folding the third bolster and standards.

Figure 5. Self Loading Sequence for Evans Folding Frame Trailer: Folding the front and then the second bolsters and standards.

Figure 6. Self Loading Sequence for Evans Folding Frame Trailer: Breaking the frame--operation consists of breaking the frame with the aid of two hydraulic cylinders, backing up the tractor while the trailer brakes are engaged.

Figure 7. Self Loading Sequence for Evans Folding Frame Trailer: Folding frame.

Figure 8. Self Loading Sequence for Evans Folding Frame Trailer: Loading trailer on the tractor.

Figure 9. Self Loading Sequence for Evans Folding Frame Trailer: The final phase of loading--hydraulic cylinders are engaged once again to put the trailer finally in place.

Figure 10. Self Loading Sequence for Evans Folding Frame Trailer: Trailer loaded on tractor and ready for a return trip.

An Australian manufacturer, Elphinstone Engineering in Tribunana, Tasmania, built the first of the folding Bailey Bridge log trailers, dubbed a "Fold-A-Skel" , in 1986 (Elphinstone, 1992). The Fold-A-Skel uses fabricated, tapered I-beams made of high tensile steel and a unique tri-beam steel/rubber suspension (Figure 11). The tri-beam suspension was originally designed for a 3-axle log-jinker trailers (folding pole trailers). It has exceptional abilities to distribute loading evenly over the three trailer axles, which provides greatly increased stability while the trailer is cornering or passing over obstacles (Figure 12). The other very important feature of the trailer is that it is capable of self loading onto the tractor with no help of hydraulics or pneumatics. According to the manufacturer, a skilled truck operator requires as little as 30 seconds for the operation. Trailer brakes are used to fold the frame. A bank of dirt is required for the final placing of the trailer on the tractor. The sequence is shown in Figures 13 to 17. Two Fold-A-Skel trailers are combined in the design of the B-Double trailer (Figure 18). This trailer train utilizes a 7-axle layout, and thus has an increased payload.

Recent Michelin Tire Company research revealed that the trailer tandem contributes 42% to the total rolling resistance of the 5-axle tractor-semitrailer (Stephenson, 1993). This again indicates the need of loading a log trailer onto the tractor for empty return trip.

A German manufacturer, Doll Fahrzeugbau GmbH, offers a set of self-steering two-axle trailers which have some exceptional features. The Mercedes 3-axle tractor with the self-steering Doll tandem trailer is a common configuration in Germany, and has very successfully entered markets in Africa and Asia. The basic feature of the trailer design is that the load is used as a structural member joining the trailer to the tractor; the load itself bears vertical and sideways loadings and conveys them onto the trailer frame, and originates a mechanical signal to hydraulic system of the trailer for the self-steering action. The logs are bound tightly with a steel cable by means of an on-board winch to make performing these functions possible.

Figure 11. Elphinstone "Fold-A-Skel" Trailer, Tribunana, Australia.

Figure 12. Elphinstone Tri-Beam Suspension.

Figure 13. Self Loading Sequence for "Fold-A-Skel" Trailer: Backing up on a ramp to engage the beam breakers.

Figure 14. Self Loading Sequence for "Fold-A-Skel" Trailer: Moving from the ramp after initial breaking the beams.

Figure 15. Self Loading Sequence for "Fold-A-Skel" Trailer: When trailer folds, bolsters close automatically by means of a special mechanism.

Figure 16. Self Loading Sequence for "Fold-A-Skel" Trailer: Now a driver releases trailer breaks while still reversing the truck.

Figure 17. Self Loading Sequence for "Fold-A-Skel" Trailer: Trailer loaded on the tractor.

Figure 18. "B-Double" Trailer: Combination of the two "Fold-A-Skel" trailers.

Two of the Doll trailers, the "Kompact-Selbstlenker" and "Ratio- Selbstlenker " have only the front axle steerable, while the "Holzkombinationszug" design has both of the axles steerable.

When the vehicle drives around a curve, it articulates at two points: over the tractor tandem and at the trailer bogie. The logs on the rig change their position with regard to the tractor and also to the trailer. Thus, the bolster is forced by the load to swivel with the rotary table of the trailer. This angular motion of the bunk on the trailer is the mechanical signal which begins the self steering action. A single hydraulic cylinder or a set of four cylinders cross-connected receive the hydraulically amplified signal and perform the steering function. The feature enables the vehicle to successfully negotiate right angle corners on narrow, mountainous, woods roads.

Some of the other obvious benefits of the design include: (1) increased payload due to a lower tare weight of the trailer (due to lack of main beams), (2) increased safety of the vehicle because of the exceptional maneuverability, (3) reduced tire wear (due to the self-steering), (4) lighter construction as some of the sideways forces acting on the self-steering trailer are reduced, and (5) shorter turn-around times as the trailer is carried on the truck while unloaded. An additional feature of the trailers is that they have rubber pads incorporated in the construction of the bunk bases to cushion shocks exerted on the trailer chassis and to isolate bolster-standards assemblies from the main beams.

Doll is installing Exte standards and bolsters on some of its trailers. Exte Fabriks AB, located in Farila, Sweden, is one of the leading manufacturers of wood transportation systems in Scandinavia. This enterprise specializes in extra-light aluminum and steel alloy bolsters and standards for log vehicles. The complete series of bolster/standards sets ranges from 3.6-ton capacity and 200-pound tare weight to 16-ton capacity and 1,000-pound tare weight. Exte standards are usually designed as separate components from bolsters. Special mechanisms are employed to quickly connect and disconnect them from the bolster, and

in some configurations, for self unloading of the trailer. In most designs, standards are equipped with chains to bind their tops together when loaded. The objective is to limit the loading exerted on the bottom section of standards, which allows for reduction of their cross-sectional area, and thus of their tare weight.

The manufacturer has developed a whole set of clamping devices to mount the complete bunks on the top flanges of the trailer's main beams. They are characterized by simplicity and reliability of operation (Figures 19 to 22). Some incorporate elastic elements for cushioning the vibrations transferred between the members. The manufacturer also builds moveable banks for self-loading trucks.

Another Swedish manufacturer, the Laxo Mekan AB in Laxa, builds standards of exceptionally low weight (Table 4). The lightest set of a bolster and two standards weighs only 250 pounds, which for a standard double-bunk trailer translates into weight saving of about half of a ton. Laxo bolsters and standards are made of extruded aluminum and steel alloys. Therefore, the sections are without welds, and the material is of uniform structure giving the members enormous strength and toughness against fatigue compared with the welded designs. Standards have an octagonal cross-sectional shape. They are attached to a bolster with four long, fatigue-resistant, pre-stressed, special bolts. If needed they can be removed from the bunk quickly by loosening the bolts.

The new Laxo Cradle System 80 is equipped with an automatic tensioner (Figure 23). The objective is to constantly tension the cable around the load to prevent it from moving on the trailer. The tensioning mechanism is built completely inside a bolster, which protects it from water and debris. When the vehicle is driven empty, the cable is stored under the bolster or in a special box. The tensioner is powered by a pneumatic cylinder hooked up to the truck air system.

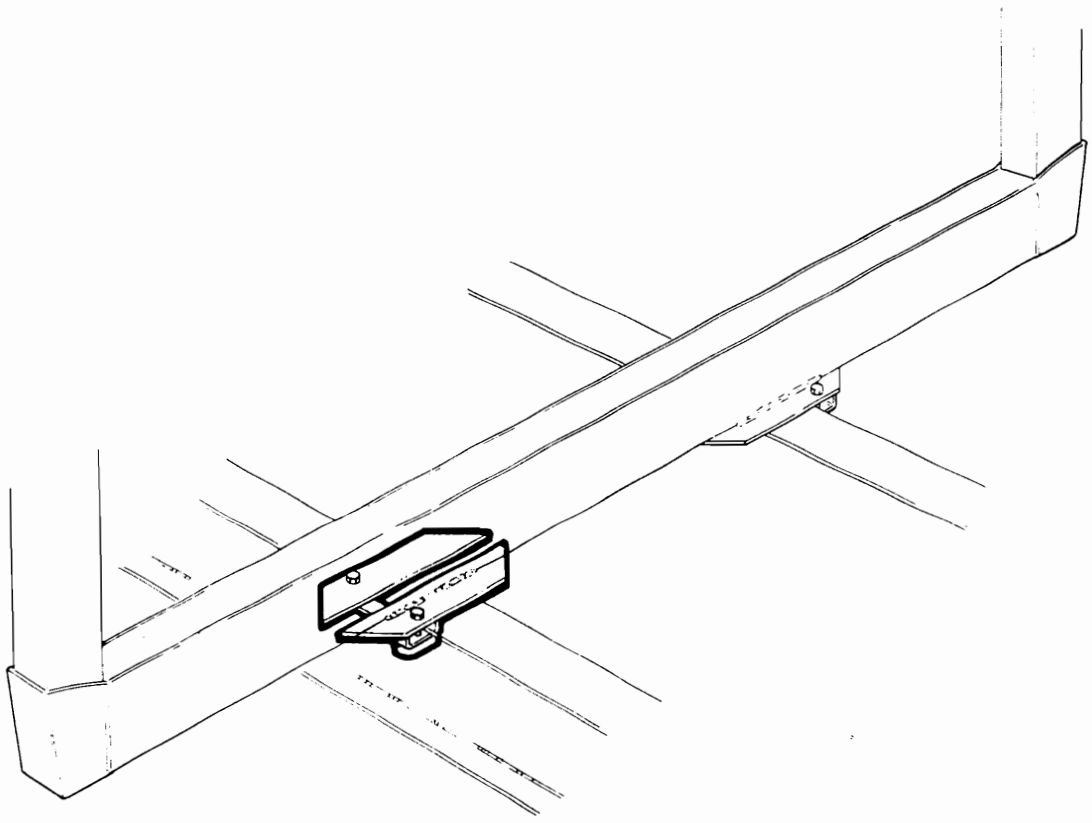

Figure 19. Clamping Fixtures to Mount Complete Bunks on Top of Main Beams Developed by EXTE Fabrics AB, Farila, Sweden: Bolted design (EXTE, no date).

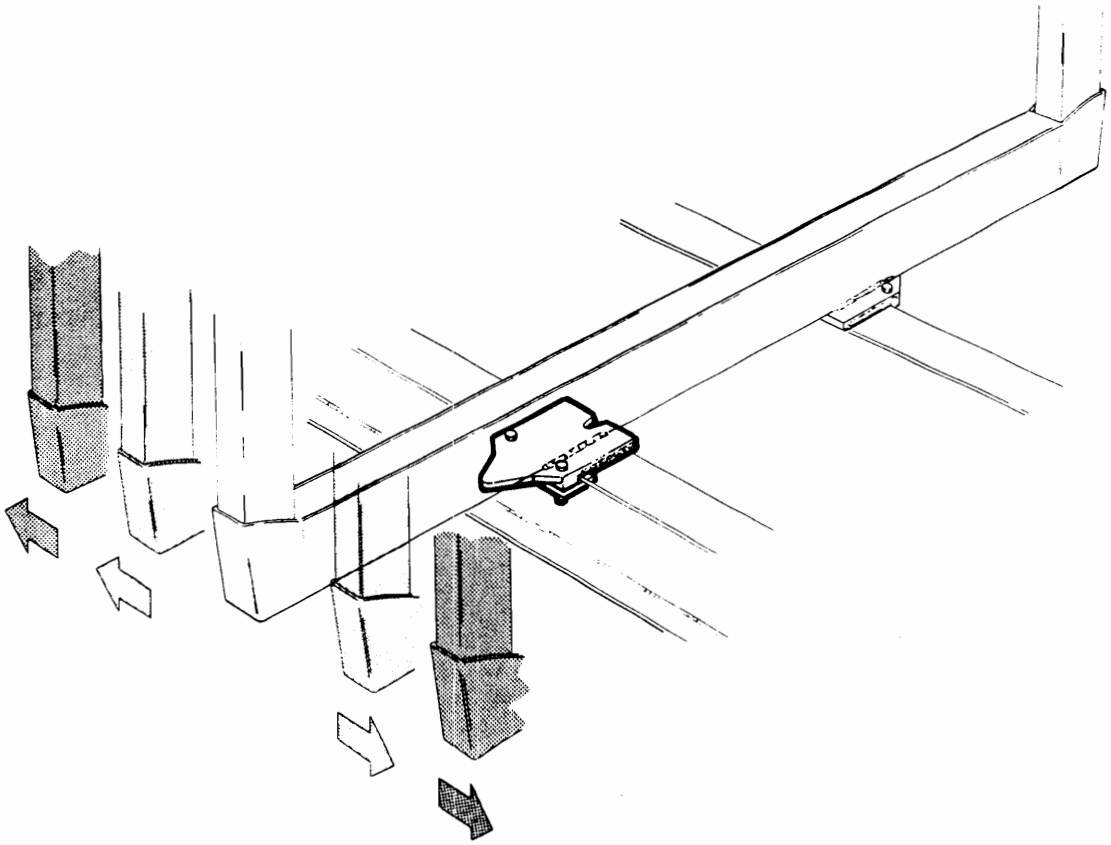

Figure 20. Clamping Fixtures to Mount Complete Bunks on Top of Main Beams Developed by EXTE Fabrics AB, Farila, Sweden: Moveable connection; design incorporates a low-friction pad for easy sliding of the bunk along the main beam (EXTE, no date).

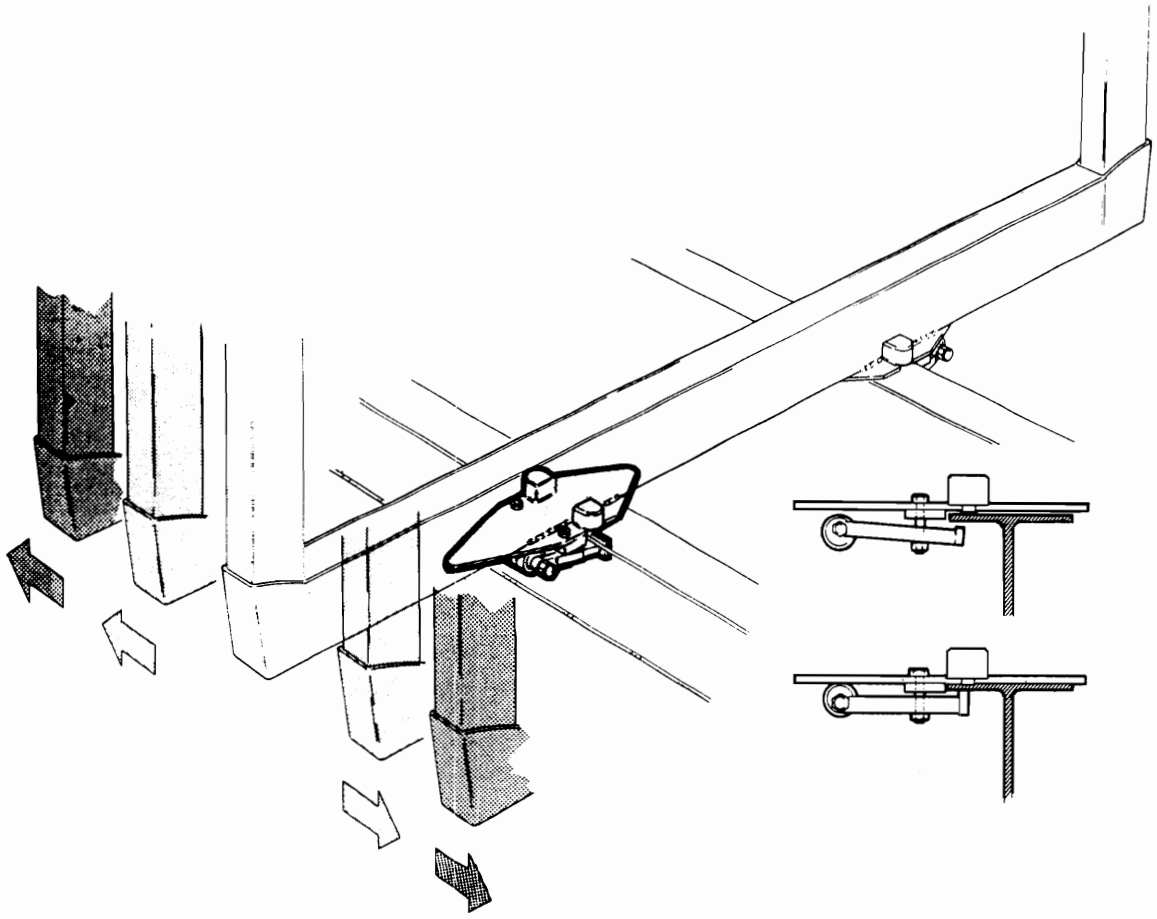

Figure 21. Clamping Fixtures to Mount Complete Bunks on Top of Main Beams Developed by EXTE Fabrics AB, Farila, Sweden: Quick connect/disconnect device; version 1 (EXTE, no date).

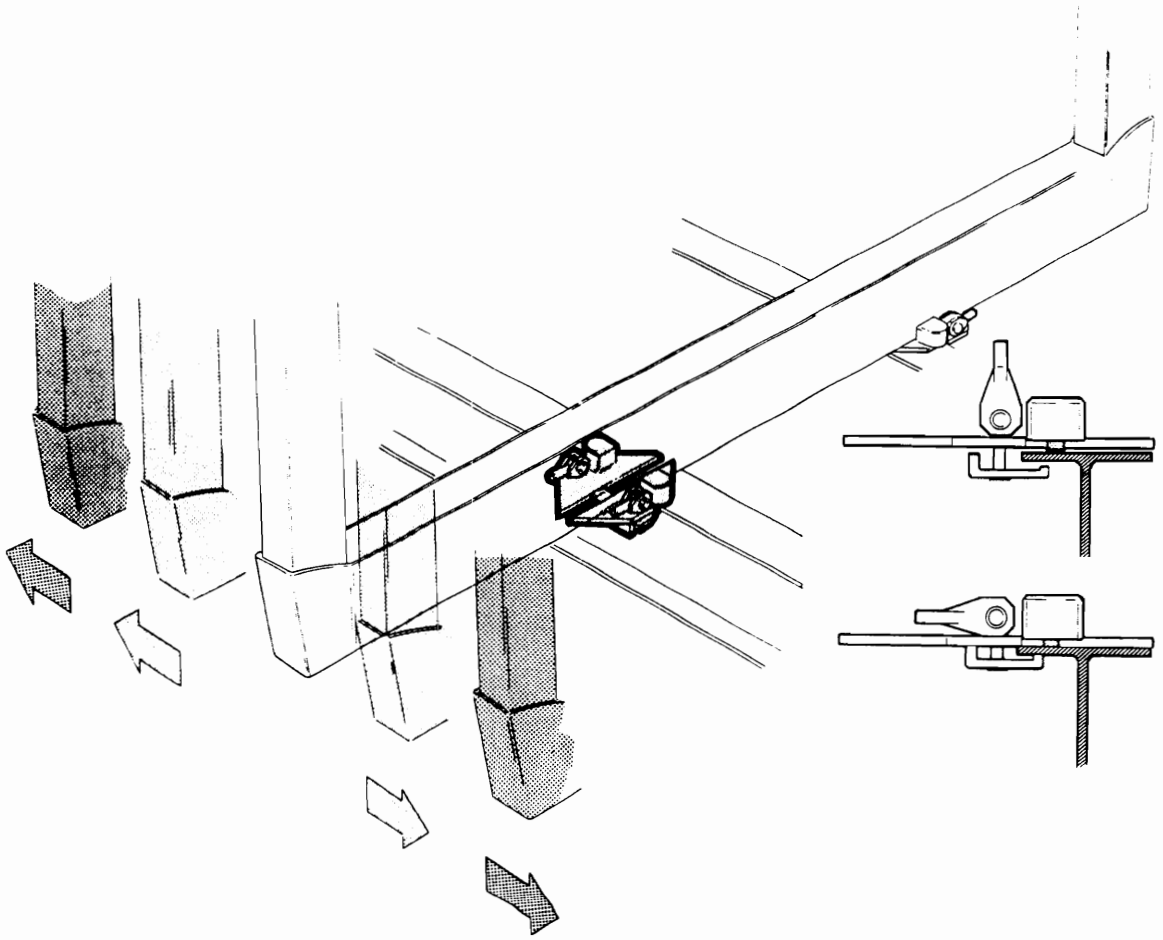

Figure 22. Clamping Fixtures to Mount Complete Bunks on Top of Main Beams Developed by EXTE Fabrics AB, Farila, Sweden: Quick connect/disconnect device; version 2 (EXTE, no date).

Table 4. Weights (kG) and Dimensions (mm) for LAXO Standards and Bolsters (LAXO, no date).

Weights (kg) and dimensions (mm)

Bolster System 80	Bolster	Stanchion	Outside width 2500 Inside load width	2600	Load height	Weight of 2600 units*	Remarks
All aluminium	80 Aluminium	Aluminium	2210	2310	2600	120	**
All aluminium	80 Aluminium	Aluminium	2210	2310	2800	130	**
All aluminium	80 Aluminium	Aluminium	2210	2310	2800	112	
All aluminium	80 Aluminium	Aluminium	2210	2310	3000	120	
Alumin./steel	80 Aluminium	21/80 Steel	2275	2375	2800	132	
Alumin./steel	80 Aluminium	21/80 Steel	2275	2375	3100	141	
All steel	80 Steel	21/80 Steel	2275	2375	2800	169	
All steel	80 Steel	21/80 Steel	2275	2375	3100	178	
Automatic tensioner	80 L incl. chain					36	

*Aluminium bolster 2500 wide: weight reduction 2 kg
Steel bolster 2500 wide: weight reduction 3 kg
**Complete stanchion
The Laxo System 80 bolster provides many options, so you can select the one that suits you best.

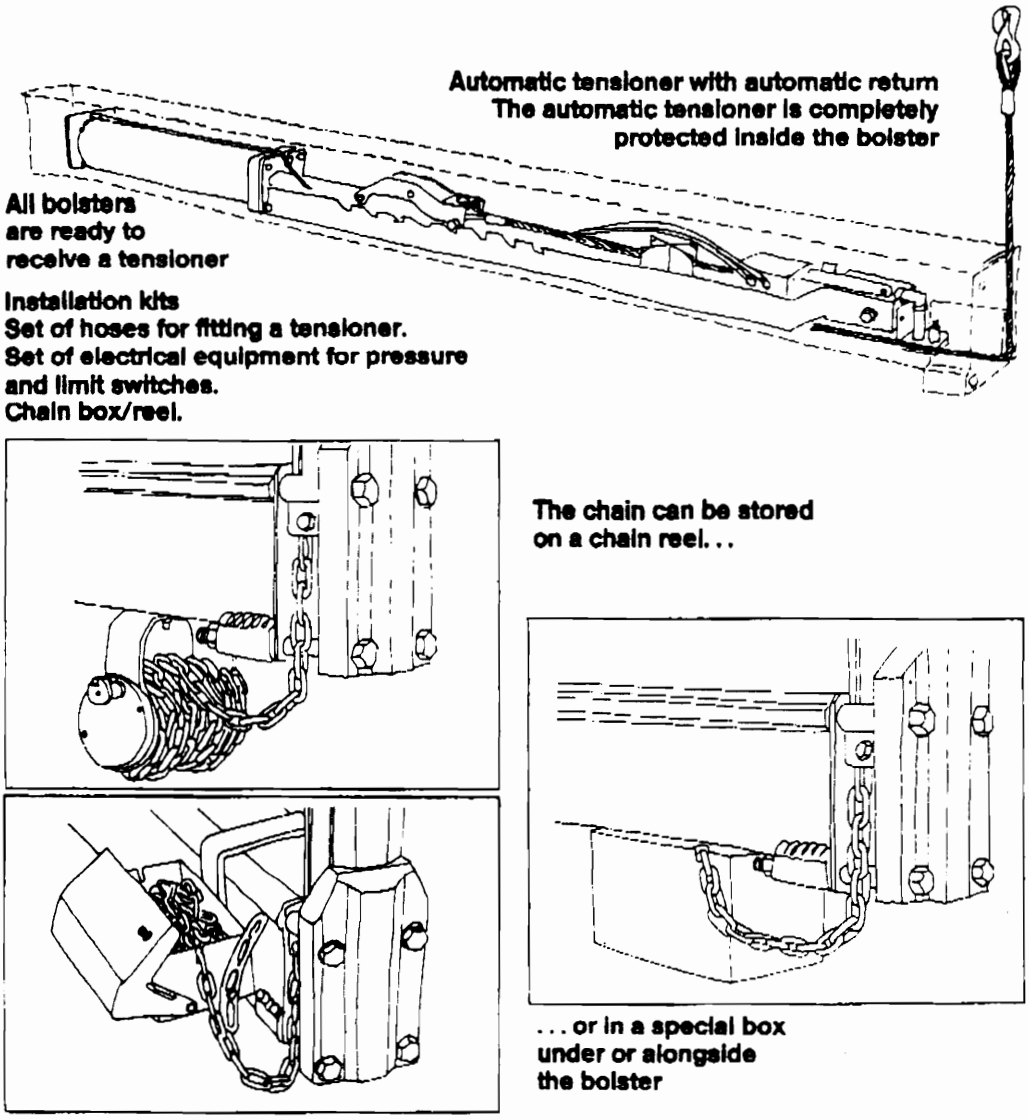

Figure 23. Laxo Cradle System 80 with Automatic Cable Tensioner (LAXO, no date).

Futuristic Log Truck Configuration

A radically new conceptual design of a log vehicle was proposed by Wilson (1980). It would consist of a 3-axle tractor and 3-axle trailer of the capacity of 15 cords. The main feature of the concept lies in that the tree butts would be loaded to the rear and the tops would be extending over the tractor cab. The design has some advantages; the load would not be cantilevered over the rear of the trailer, and tail lights of the trailer would be easily visible, allowing night operation. However, the concept requires that the maximum vehicle gross weight limit be increased to at least 103,000 pounds, which seems very unlikely in the near future.

Frame Trailer Specifications

Table 5 shows the most important technical specifications of a contemporary frame log trailer. Tare weights usually range from 11,000 to 13,000 pounds. A tractor pulling a log trailer typically weighs between 16,000 and 18,000 pounds thus; given the legal limit on the GVW, the maximum legal payload is typically somewhere between 25 to 26 tons. However, there are a few lighter trailers which may achieve higher maximum payload. The extra-light prototype tree-length trailer built by the Clark Trailer Service, Inc. in Andalusia, Alabama, weighs only 8,800 pounds (Figures 24 through 27). Its theoretical, maximum payload is about 27.5 tons, provided the trailer can accommodate that volume of logs. To increase the loading space, the trailer has an overall width of 102 inches and the two front bolsters recessed in webs of the main beams. The typical overall dimensions for a frame trailer, however, would be: length - 40 feet, height - 13.5 feet, and width - 8 feet. Clark's trailer uses a lighter 5th-wheel plate having the thickness of 5/16 of an inch; typically a 3/8 inch thick plate is utilized. The trailer's kingpin is set at the height of 48 inches and at 20 inches from the front of the trailer.

Table 5. Typical Modern Log Frame Trailer Specifications.

ITEM	SPECIFICATIONS
Max. Legal Payload	25 - 26 ton
Total Length	36' 0"- 45' 0"
Total Height	13' 6"
Total Width	8' 0" (8' 6")
5th Wheel Plate Height	47"- 52"
Kingpin Plate	3/8 " thick, 36" long, welded to the trailer
Kingpin Setting	17.5"- 24"
Tare Weight	10,000 - 13,000 lbs
Main Frame	W 18" WF I-Beam @ 35 lbs/ft with bow-string truss 4" x 1/2" underneath; ASTM A36 (36 ksi yield) or A572 (50 ksi yield)
Drop in Main Frame	0" (straight frame) - 20" (gooseneck frame)
Log Clearance	20" (min. 10")
Cross Members	from C Channel 10" deep @ 15.3 lbs/ft (ASTM A36) on 6 feet centers to JR. I-Beam M 6" deep @ 4.4 lbs/ft (ASTM A36) on 3 1/6 ft centers
Standards	from 6"or 5"O.D. Sched. 40 to 80 Pipe @ about 19 lbs/ft to 5"x 5"x 5/16" Square Tubing @ 15.62 lbs/ft (36 ksi to 70 ksi yield); up to 96" max. overall height
Bolsters	from 8"x 6"x 3/8" Rectangular Tubing @ 32.58 lbs/ft to 9"x 5"x 1/4" Rectangular Tubing @ 22.42 lbs/ft (ASTM A500 Gr. B or HSLA-70)
Landing Gear	Heavy duty steel box, hand crank cable folded or telescopic and gear operated

Table 5 Continuation. Typical Modern Log Frame Trailer Specifications.

Suspension	3 Point 4 Spring Mechanical Suspension, 3 up to 8 leaf springs; Hutch H-7700 fabricated suspensions are far the most common
Axles	5" Tube 1/2" or 5/8" wall thickness - 22,500 lbs capacity; DANA K21 or D22 Series with Stemco Oil Seals
Wheels	20" 6 Steel Spoke
Rims	20"x 7.5 ", 2-Piece
Tires	10:00-20, 12 Nylon or Steel Ply - Range F
Brakes	Federal Standard 16 1/2" x 7" x 3/4" Air
Winches	from 2 to 4, cable or synthetic strap 25' long with hooks

Figure 24. Double-Drop Trailer built by Clark Trailer Service, Inc., Andalusia, Alabama.

Figure 25. Double-Drop Trailer: Trailer's neck.

Figure 26. Double-Drop Trailer: Rear section.

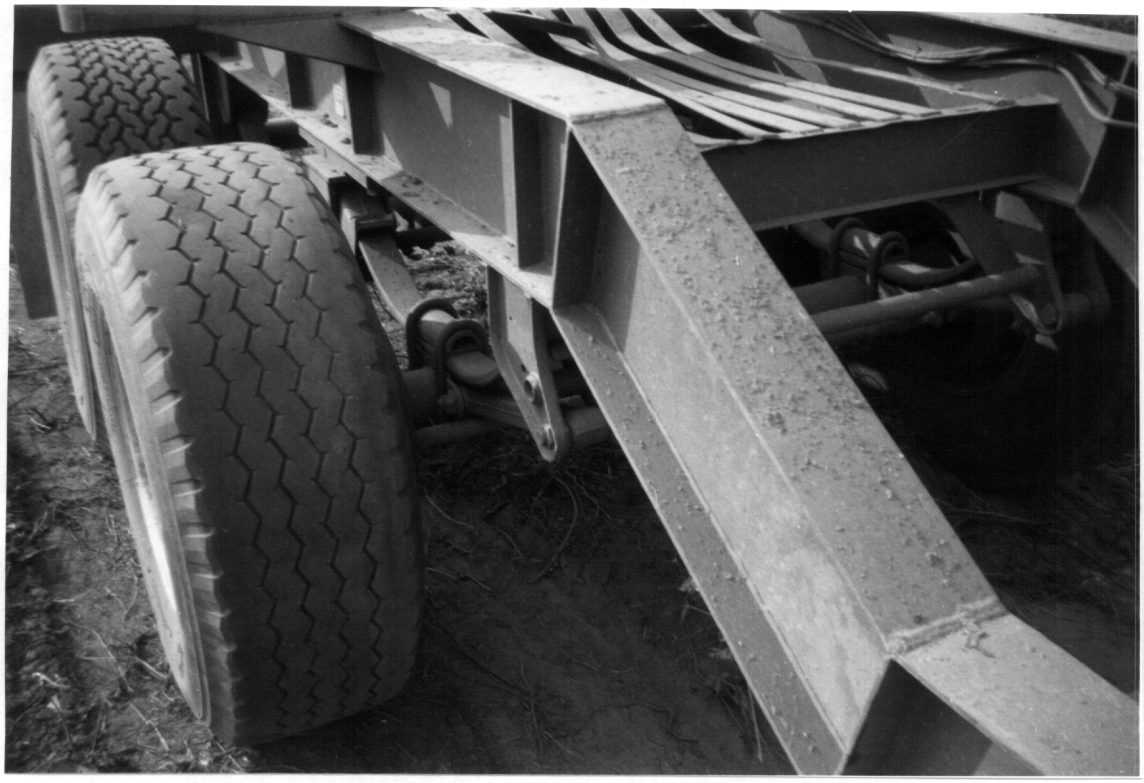

Figure 27. Double-Drop Trailer: Super-wide-singles and one-leaf spring suspension.

Usually, the kingpin is set at 17.5 inches from the front and at the height of 48 to 50 inches. The increased distance of the kingpin location from the trailer's front combined with moving of the first bolster to the very front, limits bending moments acting on the main beam front section, allowing a reduction of beam depth in the neck area.

The main feature of the Clark's trailer--the low tare weight--was achieved by using specially fabricated main beams. These beams have a depth of 9 inches in the kingpin area, which increases in the neck to the maximum of only 12 inches in the center section. Low depth and light tare weight have been made possible by the use of high tensile materials. A quarter inch thick plate made of 50 ksi yield strength steel was used for the webs, and the 3/8"x 6" bar of 80 ksi yield strength low-alloy steel, was used for the flanges. It is interesting that Emil Doll uses slightly stronger material for webs than for the flanges in building fabricated main beams on their trailers. Theoretically, the very corner of the web-flange junction is the most stressed point in an I-beam section. This is the location of highest residual stresses from welding. If an automated welding process (possibly with pre- and post-heating) is employed, the effect of residual stress should be significantly reduced and the required large radius of the fillet in the weldment obtained. An increased cross-sectional area is introduced at the critical location distributing high stresses over a larger area. There are two basic advantages of fabricating I-beams rather than using standard wide-flange sections. The manufacturer has a better control over the geometry of the beam, and thus, over the section modulus, and can further control the resisting bending moment (RBM) of the beam by selecting a stronger steel. Clark's beams weigh only 26 pounds per feet. Their RBM is 2,435 thousands inch-pounds. Until recently, the wide flange I-beam 18-inch deep made of ASTM A36 steel was almost exclusively the standard material for building main beams. This beam weighs 35 pounds per foot, but its RBM is only 2,074 thousand inch-pounds. For this reason, 18-inch deep wide flange section is commonly reinforced by a strap trussing when used for main beams on log trailers.

A trailer frame can be designed as a straight frame (a simple I-beam with or without reinforcement underneath), where the minimum log clearance of about 10 inches is obtained by placing bolsters on pedestals. This design limits the loading space on the trailer. In recent years, gooseneck, center double drop and center frame cutout frames became very popular. Examples are the Pitts thinning trailer, Union Camp's Company "possum belly" trailer, Peerless plantation trailer, and Clark's trailer discussed earlier. These designs provide the required log clearance of about 17 inches, crucial for fast and safe unloading with one-grip portal cranes. Placing the second bolster behind the drop and flushing it into main beam's web increases loading space up to 75 square feet (Ford, 1993).

The number and spacing of cross members, their dimensions and cross-section properties, are decisive for strength and stiffness of a log trailer frame. The survey of the trailer designs indicates that there is no widely accepted standard for designing these members. On some trailers, C-channels 10-inch deep (@ 15.3 lbs/ft) on 6-foot centers are used; others use junior I-beams 6 inch-deep (@ 4.4 lbs/ft) on light units. The material for cross members is usually ASTM A36 steel. In most cases, the frame is fabricated by welding. Fatigue cracks usually appear in the cross member-beam joints where residual stresses were induced by welding. Log trailer manufacturers have kept increasing the number and size of the cross members to avoid premature cracking of the frame. It has been found out, in the course of this research, that replacing welds with friction joints and bolting up the trailer's frame would allow to use fewer and smaller cross members without the danger of accelerated cracking. Stresses would be distributed over larger areas. Reducing the number and size of cross members should permit diminishing the trailer tare weight to some extent.

Carbon steel pipes of 5-inch or 6-inch nominal diameter are commonly used for standards. These sections are available in the standard strength category (i.e., Schedule 40) as well as in the extra-strength category (i.e., Schedule 80). The 5-inch and 6-inch Schedule 40 pipes weigh 14.62 lbs/ft and 18.97 lbs/ft,

respectively. The Schedule 80 counterparts weigh 20.78 and 28.57 lbs/ft. The minimum mechanical properties of the steel are: the yield strength: 35 ksi, and the ultimate tensile strength: 60 ksi. Standards heights are uniform on double-bunk trailers at 8 feet. Trailers with a drop frame or designated for only longwood have standards varying in height from 6 to 8 feet.

Almost exclusively, 8" x 6", 3/8" wall thickness rectangular tubing (@ 36.58 lbs/ft) or 9" x 5", 3/8" wall thickness tubing (@ 32.58) are used for bolsters. This stock is available in ASTM A500 Grade B steel, which has 46 ksi yield strength and 58 ksi ultimate strength. Standards are joined to bolsters rigidly by welding. Usually, gussets of 5/16" plate are used to reinforce the connection. Four complete sets of bolsters and standards typically weigh as much as 2,500 pounds, which constitutes up to 25% of the total trailer's tare weight. Bunks offer good potential for weight reduction.

Bunks are usually welded to the top flanges of main beams. These weldments are again common places for fatigue cracks initiation. Manufacturers try to alleviate the problem by gusseting the joints. However, residual stresses are induced from overheating and high temperature gradients. The joints do not necessarily become stronger; instead, commonly, only an increased trailer tare weight is obtained.

The suspension system is the single group of components that probably has the greatest impact on load capacity, ride characteristics, and safety of a log trailer. It attaches axles to the trailer frame, keeps them in alignment with the chassis, keep the wheels in a contact with the road, and provides uniform ride characteristics by filtering and dampening vibrations and reducing the forces entering the frame. There are three basic types of suspensions used on frame log trailers: the 3-point 4 leaf-spring suspension, the single-point suspension, and the air-bag suspensions. Walking beam suspensions are popular on the stinger steer trailers on the West Coast.

The most popular 3-point, 4-leaf-spring suspension on log trailers is the Hutch-7700 series. These suspensions provide a full equalization between the axles for greater stability. The number of springs varies from one for the lightweight version to the standard number of 7 or 8. Usually, the capacity is in the range of 44,000 to 60,000 pounds.

The Hutch-900 and the recently released new version Hutch-9700 are the most popular single-point suspensions used on log trailers. These suspensions are usually rated higher, at 50,000 to 60,000 pounds tandem capacity.

Truck-trailer combinations equipped with air-bag suspensions are rapidly gaining popularity in over-the-road transportation. These vehicles are characterized by superior ride characteristics, better driver comfort, lower tire wear, improved braking efficiency, and reduced vibration-related maintenance (Stephenson, 1988). These suspensions are built primarily for highway use, and none are ideally suited for logging operations. Shock absorbers, brake chambers, air bags, and transverse torque rods on many units are low, and/or exposed to damage in rough terrain. Some lack adequate articulation for good traction on uneven terrain, and thus require a controlled traction differential. However, the equipment manufacturers continue to experiment with new designs to develop an air suspension suitable for on/off-road heavy duty application.

For several years, Union Camp Company in Georgia has been operating a number of rigs using the "possum belly" frame trailers mounted exclusively on air-bag suspensions. The trailer was designed by Everett Stephenson of Union Camp in Savannah, Georgia. The trailer is equipped with the C-400-27 over mount Cascade Air Ride suspension weighing 870 pounds. The total tare weight of the trailer is about 12,000 pounds. Among the other interesting features of the trailer are air scales hooked up to the vehicle air system, and the ability to raise and lower the fifth wheel on the tractor as much as 6.5 inches to

facilitate coupling to set-out trailers. The front bolster is set back 30 inches to accommodate flared butts. It has been estimated that this design feature enables the trailer to carry 3,000 pounds more payload of swell-butted wood.

Tare Weight Reduction

The log vehicle's legal payload cannot exceed the difference between the maximum sanctioned GVW and its tare weight. Obviously, the only way to increase payload is to reduce tare weight. Beardsell found that each pound of unnecessary weight in a truck-trailer costs $5 over the life of the rig (after Stuart, 1992). Reducing the tare weight of a combination by 2,000 pounds will return a profit, if the cost is less than $11,400, and provided the rig's life is not reduced by more than 50,000 miles or annual operating costs are not increased by more than $2,700.

In practice, it is often easier to ignore than to remove additional weight on the rig (Stuart, 1992). There are few log haulers who really need a sleeper-cab. Oversized fuel tanks are doubly expensive: they are unnecessary weight and a source of problems associated with moisture condensation. Many impressive looking and expensive headache racks do not offer any better cab protection than the conventional well designed and lighter versions. Many loggers, over the years, have encouraged trailer manufacturers who build their trailers stronger so that they can withstand the abuse from loaders and mill wood yard equipment. Some trailers have extra cross members in the center so that the frame will not be distorted if the mill's overhead grapple pinches the frame or the front-end-loader rams into it. Added heavy rear standards, to provide for drag loading tree-lengths with a small loader, may only seem to save a few dollars on the loader in a short run. In reality, that additional weight has to be carried around everywhere

and increases the operating costs over the whole life of the trailer. Hasty repairs, such as welding an additional piece of plate to cover a place where the loader damaged the trailer, also costs in the long run.

Table 6 shows the tare weight breakdown of a typical double-bunk log trailer. The largest contribution to weight comes from the running gear. Not surprisingly, this is the area where the most significant weight reductions have been achieved. The modifications to the running gear of a trailer include the use of: super-wide single tires instead of the typical duals, radials instead of ply tires, and aluminum instead of steel rims.

The use of super-wide single tires in logging operations has several advantages (Anonymous, 1992). Operators can reduce the tare weight of their haul vehicles achieving larger legal payloads. During wet weather, state and local governments ban hauling wood due to the excessive amount of mud on paved roads. Most of this mud comes from between dual tires and is thrown out when the vehicle accelerates. The use of super-wide singles eliminates this problem; the amount of mud carried on the roads is significantly reduced. Super-wide singles also offer less rolling resistance. Tire manufacturers claim 5% fuel savings. Singles also simplify operation: they do not require the difficult matching of duals, are easier to maintain, and create a system of reduced number of parts.

The drawback of using singles is that they increase ground pressure, which may result in the vehicle getting stuck in difficult terrain. Singles are also quicker to lose traction on ice or snow. It has been observed that when a driver operating a vehicle with a trailer equipped with duals has a flat tire, he will often continue to drive to get to a repair shop. If he does so, he often totally ruins the flat tire and puts himself and other road users in risk in case of a blow-out of the other tire. All that is impossible with super-wide singles. In a long run, the driver is always better off calling for a road service.

Table 6. Tare Weight Breakdown for Typical Double-Bunk Log Trailer (after Beardsell, 1986).

ITEM	MATERIAL	QUANTITY	WEIGHT
RUNNING GEAR	Includes: Springs, Axles, Wheels Rims, Brake Drums & Tires	-	4,000 LB
MAIN FRAME	18" WF @ 35 LB/FT	80 FT	2,800 LB
CROSSMEMBERS	12" WF @ 14 LB/FT	35 FT	490 LB
STANDARDS	5" SCHEDULE 80 PIPE @ 21 LB/FT	64 FT	1,330 LB
BOLSTERS	8" x 6" x 3/8" RECTANGULAR TUBE @ 33 LB/FT	32 FT	1,060 LB
LANDING GEAR		ONE	350 LB
FIFTH WHEEL PLATE	40" x 40" x 3/8" PLATE	ONE	170 LB
BUMPER		ONE	150 LB
MISCELLANEOUS			250 LB
TOTAL			10,600 LB

Mike Macedo of the International Paper Company in Freedom, New Hampshire, reported that super-wide singles increased life from about 60,000 miles per conventional tire to 85,000 miles per super single (Anonymous, 1992). Retread costs are reduced: $180 per dual set of 11R24.5 versus $135 for a super single.

It is possible to use singles with the standard axles and rims, but this reduces sideways stability of the trailer and should be avoided. Offset rims must be used. In turn, using standard axles and the offset rims results in greater side-loading of the wheel bearings (Stephenson, 1991). Therefore, it is strongly recommended that super-wide single tires be used with the longer axles.

Deck Trevitt, an independent logger from the middle Georgia region, achieved over 200 pounds of tare weight reduction by placing super singles and offset rims on his trailer axles (Trevitt, 1991). A reduction up to 450 pounds can be achieved by using more expensive aluminum rims. Tests by the International Paper company in New Hampshire resulted in 1,000 pound tare weight reduction due to using super singles (425/65R22.5), instead of the conventional duals (11R24.4), on tri-axle shortwood trailers (anonymous, 1992). The total cost of converting to super singles amounted to $5,950 (rims, hubs/brake drums and tires).

Trevitt achieved 1,200 pounds weight reduction by using lighter, 14-inch custom fabricated I-beams, lightweight landing gear, three bolsters instead of four, along with the super-wide tires with aluminum rims. Additional weight reduction can be obtained with 3-point, single-leaf, 4-spring suspension. Trevitt estimated that a truck-trailer combination total weight reduction of about 3,000 pounds cost him $2,000.

Log Trucking Safety

Log trucking safety is a complex issue involving many problems. Reliable truck and trailer design and manufacture, safe and convenient log securing binders, safe loading, hauling and unloading practices are just a few.

Highway accidents involving log vehicles are a special concern to the forestry community, since they cause injuries and deaths, expose businesses to liability, and are very visible to the public. A single accident can dramatically change the image of the industry in the minds of the society. The Transportation Committee of the Georgia Forestry Association has been obtaining data on log truck accidents for the last three years (Green and Jackson, 1992).

The analysis comparing logging trucks and tractor-trailer units with other types of heavy trucks from the standpoint of the accident data brought interesting results. Logging trucks were found to be about 3 times as likely to have mechanical failures in accidents as were other heavy trucks. Mechanical failure was the most often cited contributing factor in accidents of log vehicles, while it was the ninth most often cited factor with other types of heavy trucks. Log trucks had a significantly higher rate of brake failure, improper lights, steering failures and slick tires than did other heavy trucks. Logging trucks (13.6 years) were older than log tractor-trailers (10.6 years), which were, in turn, older than other heavy trucks (9.3 years). Drivers of logging trucks and log tractor-trailers were under influence of alcohol or drugs in 1.97% and 1.19% of accidents, respectively, compared to 0.52% of drivers of other heavy trucks involved in accidents. The results have been used by the Transportation Committee to identify the most acute training needs and problem areas.

Shaffer and Stuart (1987) give a long list of tips how to keep log trucking a safe operation. Contractors should hire only safe, well trained, and properly licensed drivers. Trucks should be kept highway safe. Safety equipment such as flares, reflectors, mud flaps, mud scrapers, lights, and tail light extensions for the ends of tree-lengths should be always present on the truck. New tires rather than recaps should be used, especially on the front wheels. This reduces serious accidents caused by blowouts. Installing speed limiting governors on tractors might be a way to lower maximum speeds.

Load size is an important safety element of a log vehicle. A too heavy, too high, or too long load on a trailer is frequently a source of hazard. Weight control measures, such as installing electronic scales, are very helpful in avoiding fines and rig failures.

Brake failure is the most common mechanical cause of crashes. Refitting brake drums with automatic adjusters or ordering anti-lock brake systems on new trucks are very helpful in increasing reliability. Performing regular safety inspections cannot be overemphasized.

The second most common cause of the accidents is the driver unbinding the load manually at the mill's woodyard. On the average, one driver per year is killed by a falling log. Weyerhauser Company in Amory, Mississippi, designed and built a log truck unbinding rack (Alt, 1990). Essentially, it provides drivers with a safe location to remove the load-securing ties just before the actual unloading operation. The rack's safety arms are designed to prevent any loose logs from falling off the top of the load onto the driver below. Tests with the unbinding rack showed reliable and fast operation. In addition, unbinding at the rack speeds up the actual unloading operation. The yard's crane operator does not have to wait for unbinding after the truck is positioned in the unloading area. The truck driver is safe, standing away from the vehicle.

Reliable and convenient load securing devices are very important for the safe log truck operation. Their primary objective is to prevent the logs from moving on the trailer. Steel cables, chains, or synthetic straps are usually used as the load binders. There are a number of methods of placing the ties over the load (Lavoie, 1981). They include: using a grapple of a loader to lift the securing chains and let them fall on the opposite side of the trailer, using the boom of a hydraulic nuckleboom loader, the driver throwing the straps or light cables over the load, and finally the driver climbing the load to throw the ties from the middle of the pile so that they fall on the other side or his climbing the load on the opposite side to grasp the end of the tie. Operations involving climbing the load are the most common and at the same time the most dangerous of all methods. Using a loader is much safer but not convenient and not always feasible. In most cases, the binders are pre-tensioned by using various tightening devices, of which winches are the most common.

During the development of a tree-length/long-log railcar, Union Camp Corporation recognized the need for a load securing device which would accumulate and lock in any slack in the tie (Stephenson, 1991). A constant-tension winch was developed using a synthetic web strap of 16,000 pounds rating. The winch weighs about 55 pounds and develops the tensile force of about 200 pounds in the strap. The winch is tightened with a pointed bar in a conventional way. Then a power spring in the opposite end of the winch housing is preset and held under tension by a second ratchet. If the load settles and strap tension declines, the power spring advances the drum, while the primary ratchet locks in accumulated slack. After the railcar is unloaded, straps are wound into the enclosed winches and hooked to a staple welded to the inner surface of the doors. The power spring is reset, so that spring tension holds the door and prevents theft of straps.

It is recommended that the ties on log truck be tensioned regularly during the whole trip to the mill to ensure their proper operation as the load tends to settle due to vibrations.

Unlike Stephenson, who selected synthetic web straps for his constant-tension winches, Lavoie's choice was the 8 millimeter aircraft steel cable. The cable had 7 strands, each containing 19 wires. It has an important capability of not forming kinks when wound onto a small-diameter drum. It also costs 85% less than heavier chains of the same breaking strength. The experimental trials showed that the cable can be successfully thrown over the load if its cross-sectional area is less than 16 square meters. Lavoie designed a winch which was equipped with: a stainless tubular housing, toothed wheel mounted to the housing and a pawl on the drum, and a bronze bearing (Figure 28).

While, most of the major private industry and government research organizations in forest products sector have separate divisions studying log trucking profitability and safety, and literature on the problem is piling up, only one publication has been found dealing with an experimental measurement of dynamic loading acting on a log trailer.

"Safety in Log Transport" by Baas and Stulen (1985) brings results of load securing device testing under various operating conditions. The study was carried out by Logging Industry Research Association and a number of other organizations in New Zealand. A conventional Kenworth W924R logging truck towing a 2-axle jinker pole trailer was selected for the tests. Cables, chains, and synthetic straps used as alternative load securing devices were equipped with tension links. Strain gages were then installed on the links as well as on standards and bolsters of the trailer. A series of tests were carried out using radiata pine and eucalyptus logs. Dynamic stresses were recorded during loading, unloading, traveling over various road surfaces, low and high speed cornering, and wraparound cable failure simulation tests. The effectiveness of a number of chain and cable configurations was checked in stopping load movement under conditions of hard braking.

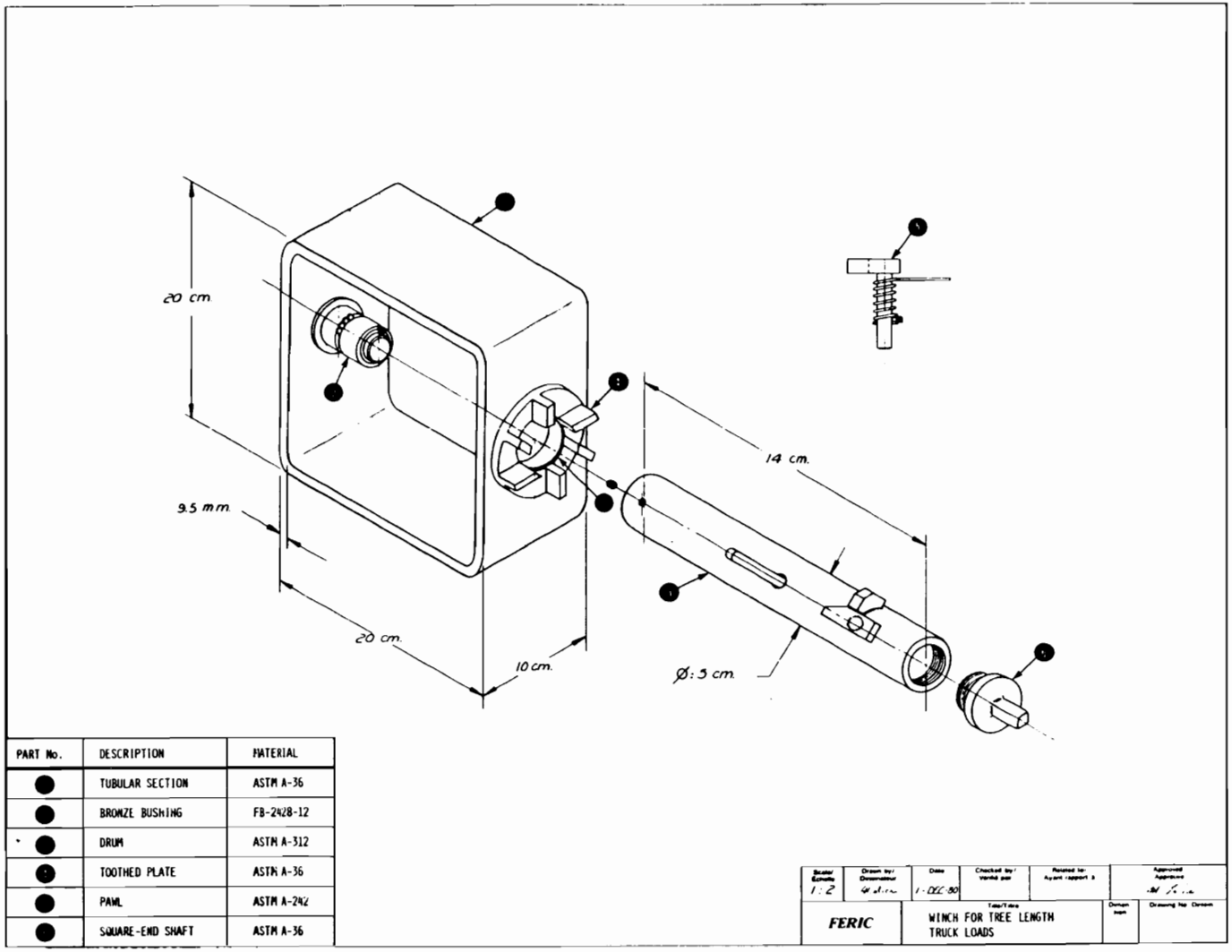

Figure 28. Load Securing Binder Tensioner Suggested by Lavoie (after Lavoie, 1981).

The following maximum dynamic loadings acting on a log truck were recorded. The maximum vertical acceleration of 2.2 g was detected while the trailer was passing over a bump, forward acceleration of 0.78 g when it was hard braking, and 0.45 g as the maximum sideways acceleration for low speed hard cornering.

The greatest stresses in standards and bolsters during the whole experiment were recorded during unloading operation and amounted to 31.29 ksi and 35.67 ksi, respectively. Tests showed that a log grapple loader produced higher stresses than a CAT 966 front-end-loader and a Wagner fork stacker. The second most stressing situation for the trailer was a tight cornering at low speed (27.84 ksi and 31.62 ksi in standard and bolster, respectively). The maximum tension of 9.15 tons in load ties was recorded for maneuvers on a wood yard (again during tight turns at low speeds).

Design criteria for standards, bolsters, and load securing ties were set. It is required that standards and bolsters be capable of withstanding a horizontal force of 6.6 tons applied at the top of the standard. Ties should have a safe working load of at least 2.2 tons. Among the other conclusions, it was stated that synthetic straps could not be used to restrain the load due to a low friction coefficient between the strap and logs.

CHAPTER 3. METHODS AND PROCEDURES

Introduction

The ultimate objective of this study was to design an extra-light log trailer. In general, a mechanical design consists of several distinct phases: a recognition of a need, definition of the problem, gathering of information, synthesis, evaluation, and communication of the design (Dieter, 1983). The basic characteristic of this process is its iterative nature - a designer returns to the earlier steps many times before the design is completed (Shigley, 1977). The research approach of this project reflects the general structure of a mechanical design.

Recognition of Need

For years, the need for an extra-light log trailer has been recognized by all parties involved in timber harvesting process. Productivity and cost sensitive loggers have been introducing various truck and trailer weight reduction programs. Trailer manufacturers specialized in customizing their designs to better fulfill the specific user needs. Forest products industry and government research organizations initiated several research studies in this domain. The need for safer log trailers has been articulated in the concern about the log trucking safety by the transportation authorities and general public.

Definition of Problem

There is a distinct difference between the statement of the need and the identification of the problem. The problem is much more specific and is usually defined by stating precise specifications and outlining the scope of the design.

The following are the most common criteria used in mechanical design arranged in the order of importance (Peters and Hopkins, 1986):

- function;
- safety;
- reliability;
- cost;
- manufacturability;
- marketability.

The inclusion of safety and reliability at or near the top of the list is a function of recent developments in government regulation, expanded product liability actions, and implementation of government and manufacturer associations standards, all occurring in the last two decades (Peters and Hopkins, 1986).

Three major criteria, of equal importance, were set forth for the extra-light log trailer design: to decrease tare weight by at least 25% (i.e., 2,500 to 3,000 pounds) as compared with the weight of current designs, to increase loading space, and to insure safe performance.

Scope of the Study

As has been discussed earlier, the suspension system has a great impact on dynamic loadings acting on a trailer and the resultant stresses; therefore, this study was limited to the trailers equipped with the most common suspension system, i.e. the 3-point, 4-leaf spring suspension. The extra-light trailer design uses a conventional tandem axle layout (2 axles spaced 49 inches apart) and the Hutch H-7700 suspension system.

To be fully versatile, the trailer had to be capable of hauling short-wood, long-wood, and tree-lengths. Also, all possible loading schemes must be permitted.

It was planned that the trailer would have moveable bunks and replaceable standards and bolsters.

Synthesis

Information was gathered on various aspects of log transportation by trucks as a part of the synthesis phase of the design process. This included a survey of the existing designs, trailer loading techniques, weight distribution models, and the existing constraints on log trucking.

Experimental measurements of dynamic loads acting on a log trailer were required because literature contained very little information, and trailer manufacturers either did not have this information or considered it proprietary. Next, the resultant stresses in structures of various designs had to be determined. **The first two fundamental approaches of this research were the real-time measurement of the dynamic loadings exerted on the structure and a comprehensive stress analysis of the existing light-weight designs.**

A survey of trailers for fatigue cracks and fatigue analysis of selected designs was conducted, when the analysis of selected designs indicated that a log trailer is most likely to fail in fatigue due to repeated loading.

Two experimental lightweight frame log trailers were selected to be tested: the gooseneck thinning trailer (Figure 29) manufactured by Pitts Trailers of Pittsview, Alabama, and the full-tree trailer (Figure 30) built by Tuten's Welding, Inc., of Perry, Florida. A conventional double-bunk frame trailer was included in the study as a control design (Figure 31).

The results of the experimental trials, engineering parameters, models and insights were utilized to formulate specifications for the ultra-light log trailer design.

Finally, the actual design was developed. Light-weight and high-strength materials, and a special design emphasizing fatigue resistance were utilized to achieve the required light construction and strength.

Evaluation

Due to time and financial constraints, the proposed design has been evaluated on a limited scale. A finite element model using unsymmetrical elastic beam elements was built and static stress analysis performed. The objective was to determine the design factor (the theoretical safety factor) of the proposed structure under various loading scenarios.

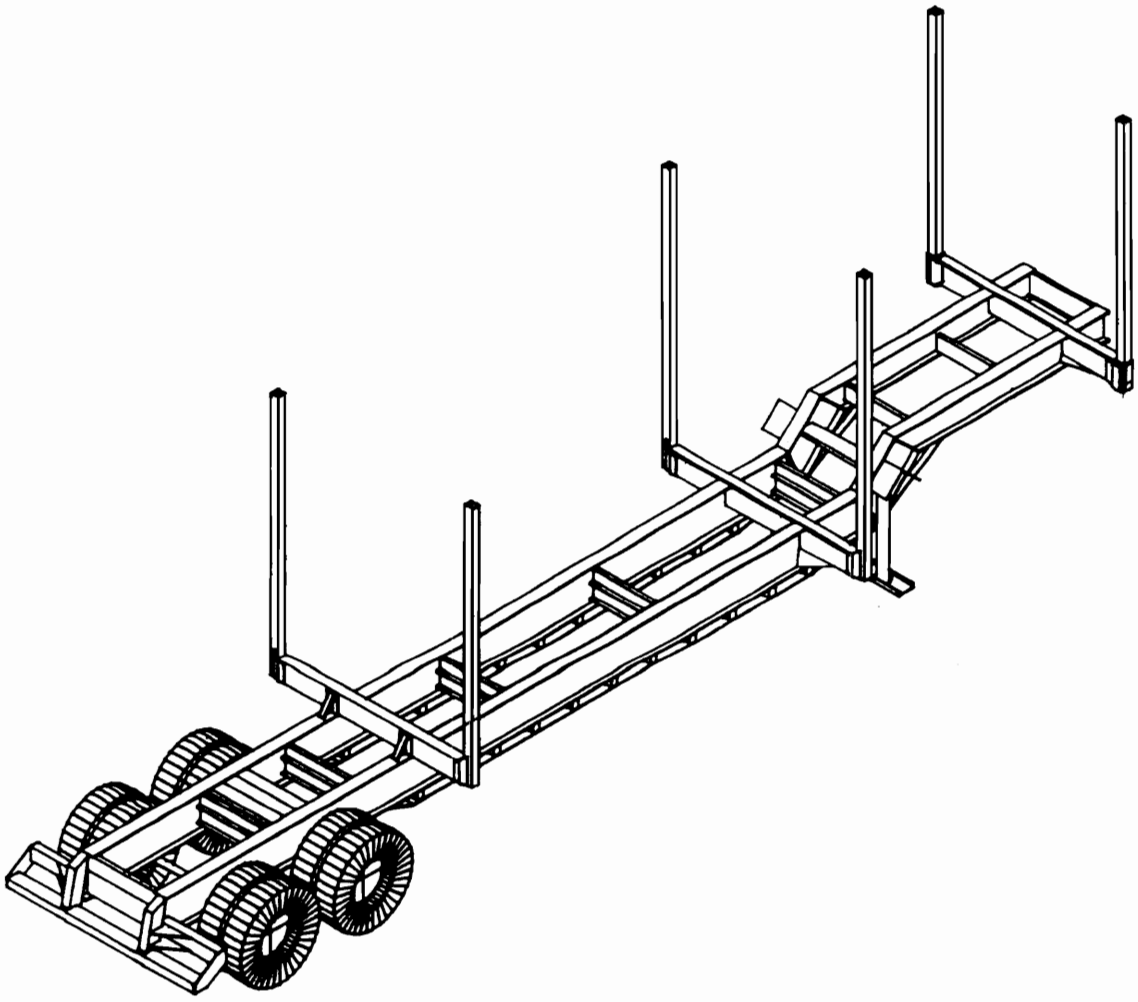

Figure 29. The Gooseneck Thinning Trailer Built by Pitts Trailers, Inc., Pittsview, Alabama.

Figure 30. The Extra-Light Full-Tree Trailer Built by Tuten's Welding, Inc., Perry, Florida.

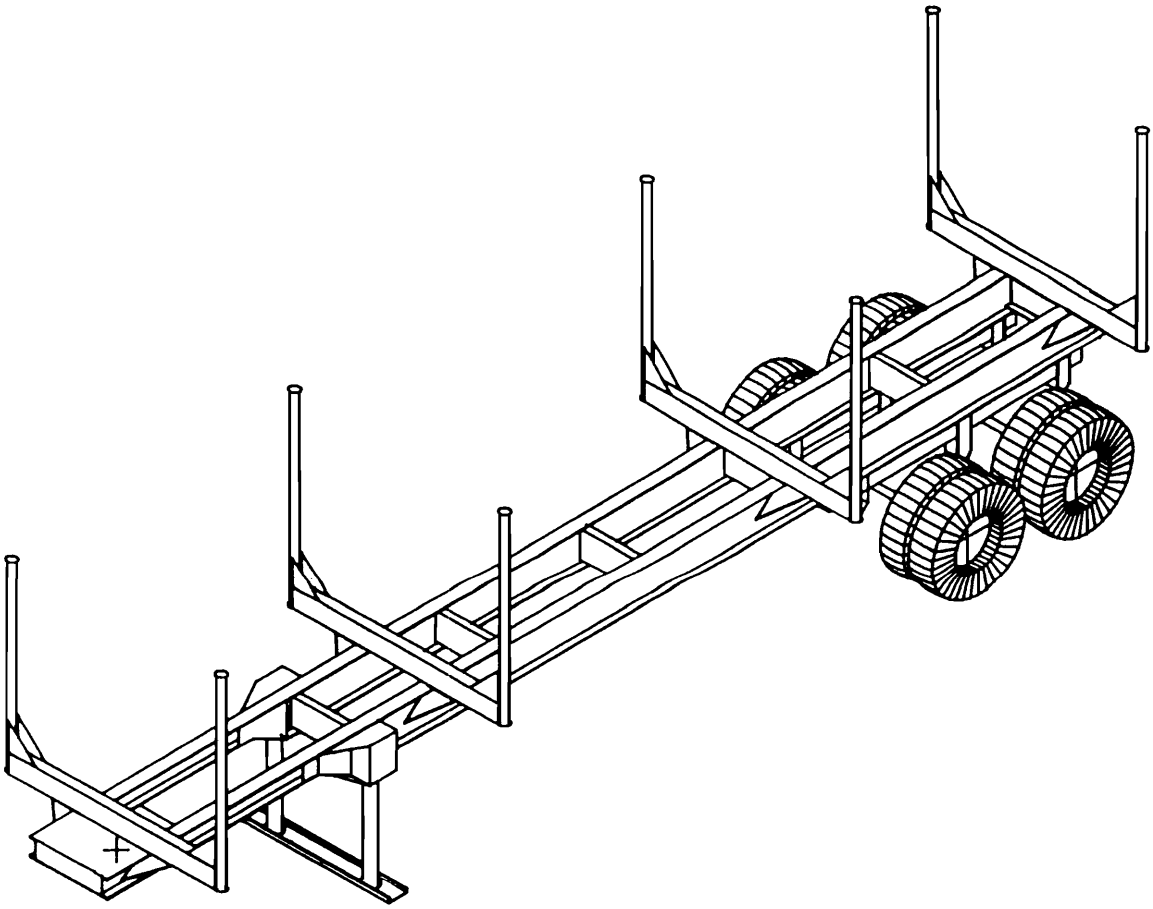

Figure 31. A Standard Double-Bunk Trailer.

Communication of the Design

The extra-light design was documented and evaluated through detailed engineering drawings, coupled with technical data from the manufacturers of frame members and other components, and the static stress analysis results. The design concepts and specifications were presented to log trailer manufacturers for further evaluation and development of final product design. At the time of writing this dissertation, three major manufacturers are preparing preliminary designs of the extra-light log trailer for manufacturing.

It is planned that the design process will be completed by a comprehensive product testing.

Major Research Activities

The following major research activities were undertaken to meet the project objectives:

1. Redesign of the existing harsh environment data logger for the experimental stress analysis of the selected trailers. This phase also included programming and testing the data logger and associated transducers.

2. Development of data retrieval, storage, and processing programs.

3. Preliminary stress analysis of selected trailers to determine strain gage locations and estimate stress magnitudes at these locations.

4. Planning and execution of the field experiments.

5. Development of three-dimensional elastic beam element finite element models of the trailers to transform the field strain data into stress distributions.

6. Building finite element models of other extra-light log trailers.

7. Surveying trailers for fatigue cracks.

8. Development of elastic shell element finite element models of simple frames to perform their static analysis and verify hypotheses about fatigue cracking of the trailers.

9. Fatigue analysis of the selected designs.

10. Designing an extra-light log trailer for safe and economical timber transportation.

Finite Element Method

The objective of this design effort was a light-weight load carrying structure. Safety and reliability were also of the highest importance. Therefore, stress analysis was employed heavily throughout most of the phases of the design process to assure all concerns were met.

The structure of a log trailer is a three-dimensional frame structure with many cross-section changes and multiple supports, subject to complex load distributions. Such a structure can be analyzed by the application of the elastic beam theory, but the solution would be very tedious to develop by hand, especially if the problem is multiply statically indeterminate. However, such a problem is readily solved using of the finite element method (FEM).

FEM is a numerical procedure for analyzing structures and continuums. The method originated as a method of stress analysis. Today it is applied in many fields of science and engineering; however, the widest use is still in stress analysis. FEM is an exceptionally powerful procedure. Problems that previously were utterly intractable are now solved routinely (Cook et al., 1989).

The basis of FEM for the analysis of structures may be summarized in several steps (Knight, 1990). The domain of the solid structure is divided into small parts called "elements". Neighboring elements are interconnected at a finite number of points called "nodes". The assembly of elements constitutes a model of the structure. Behavior of a single element is described by a general solution for the governing equation. The specific solution for each element is a function of the unknown solution values at the nodes. Application of the general solution form to the whole structure yields a finite set of algebraic equations to be solved for the unknown nodal values. The structure loads and displacement boundary conditions must also be translated to nodal entities because the problem solution unknowns are nodal values.

The first two sources of error inherent in the method are that the element solution is usually not an exact solution, and the precision of the algebraic equation solution is a function of the computer accuracy. Both can be minimized with good modeling practices. The other errors of the method include: modeling errors (if there are major discrepancies between a physical system and its mathematical model), manipulation

errors (associated with a particular equation solver employed by the FEM software), and numerical errors (stemming form bad modeling practices, e.g. a stiff element connected to a soft region).

Structural elements are formulated using the same general assumptions about their behavior as those used in the respective structural theories. Therefore, a finite element solution using structural elements cannot be any more accurate than a solution by the appropriate customary methods. However, it is much easier and faster to obtain a finite element solution on a computer. Computer FEM programs are very useful in producing graphics displays, which makes it much easier to understand and evaluate the model and the results obtained. FEM is an indispensable tool when it comes to modeling a structure response to different load distributions, simulating the use of different materials, or various design alternatives.

The finite element method has also its disadvantages. It is a numerical method; thus it provides no closed-form solutions. A computer, a reliable program, and intelligent use are essential (Cook et al., 1989). Experience and good engineering judgment are needed to define a good model. Numerous input data are required, and voluminous output must be sorted and understood. A computer program in no way supplants the user's responsibility to do approximate engineering calculations (Knight, 1990).

In many cases defining boundary conditions for a given problem represents a real challenge for the analyst. The following problems are difficult to analyze with finite element modeling:

- assembly stresses;
- residual stresses;
- problems of unknown load distribution;
- elastic-plastic behavior of the material.

The objective of the preliminary stress analysis of the selected trailer designs was to identify the critical stress locations in the structures and to estimate the stresses encountered at these locations. These spots were then used as the strain gage locations for the experimental stress analyses.

Conceptual models were developed as a first step in the analysis after determining that a finite element formulation was needed. Precise information on the geometry of the structure was gathered; detailed engineering drawings were acquired for that purpose. Typical load configurations as well as possible overload conditions were determined for each trailer loading strategy. Alternative models were developed to determine loadings on standards because of the lack of pertinent information.

Three-dimensional elastic beam elements are best suited for correct modeling of a log trailer because of the trailer geometry, loading patterns, and its structural behavior. Only half of the trailer (obtained by cutting it along its longitudinal axis of symmetry) needed to be represented in the model due to the symmetry of the structure and symmetry of loading. Exploiting symmetry reduces usually the effort required to create a model, limits the number of computations, and increases numerical accuracy.

Preliminary 2-D Analysis

A three-dimensional analysis always requires that a two-dimensional simplified solution be prepared as an initial step to gather insight into the nature of the problem and provide some experience for developing a good three-dimensional model (Knight, 1990).

Completion of the conceptual FEM model provided the information needed to choose the proper computer program. The Finite Element Personal Computer Program (FEPC), developed by Dr Charles E. Knight of the Department of Mechanical Engineering at Virginia Tech, was selected for the preliminary 2-D

analysis of the first trailer to be studied. The choice of the computer code was dictated by its availability and compactness which allowed for quick and efficient analysis.

FEPC includes an interactive pre-processor for mesh generation and a post-processor for graphic display of the results. It runs on an IBM PC or compatible with 640 K Byte memory. With this memory size, 600 nodes and 600 elements are dimensional limits. The program is also limited by the a nodal bandwidth size limit. A node bandwidth of 15 or less is required to complete a solution of 600 node model. Larger bandwidths may be accommodated by using fewer nodes in a model (Knight, 1989).

The 2-D formulation required that the trailer structure be broken down to simple components: main beams, bolsters and standards. Cross members and the running gear of the trailer were not considered in the preliminary static analysis. Each of the components was modeled separately. Model definition included input and generation of all node point coordinates, selection of the elastic beam element from the program's element library, input and generation of node connectivity, definition of all elements, and input of material and cross-section properties. Nodes were created at every location where a change of cross-section property, or a force, or a moment, had been applied. Elements were reduced in size in regions of anticipated high stress gradients. Displacement boundary conditions and loads were specified. This resulted in input data file for the analysis processor (Knight, 1990).

A static stress analysis for a 10% and 19% overload was performed for the Pitts gooseneck trailer. First, a solution for all node displacement components was obtained. These were then used, along with the element formulation matrix, to find the element strain components. Stresses in each element were calculated using material properties.

The post-processor reads the results files and allows a user to create graphic displays of the structural deformation and stress components. A plot of a deformed shape of the structure was analyzed for agreement with the applied boundary conditions and the anticipated deformation. This provided a check that the model was done correctly. Node displacements are single-valued, but stresses are calculated within each element so node stresses are multi-valued if more than one element is attached to a given node. Node stresses are usually obtained by averaging the values from all elements attached to the node.

Preliminary FEM static analysis of the gooseneck trailer was performed using FEPC program. The results obtained were then validated by the conventional stress analysis methods. Two approaches were employed: double integration of the elastic curve differential equation method and the superposition principle in solving the statically indeterminate problems.

3-D Analysis

Three-dimensional models of the selected trailers were developed to verify the results obtained by the preliminary analysis and confirm the strain gage locations. The university version of the ANSYS program, by Swanson Analysis Systems, Inc., was obtained for this purpose. It is a popular, commercial, general purpose finite element program. Its capabilities include 3-D static, modal, transient dynamic, and harmonic response analysis; solid modeling and design optimization; as well as thermal and other field analyses. The full version of ANSYS (version 4.4A with a 200 DOF wave front limit) for a 80386 DX processor personal computer was utilized.

The 3-D formulation represented the entire structure (i.e. a symmetric half) in one model. Displacements, stresses, and reactions at points of support were solved for the general three-dimensional loading. The 3-D

elastic symmetrical beam elements STIF4 were employed, in the first models, and the 3-D tapered unsymmetrical beam elements STIF44 in the refined formulations.

The STIF4 and STIF44 are uniaxial elements with tension, compression, torsion, and bending capabilities. The elements have six degrees of freedom at each node. The STIF44 allows a different unsymmetrical geometry at each end, and permits the end nodal points to be offset from the centroidal axis of the beam. Effects of shear deformation are included in both of the elements. The geometry, nodal point locations, loading, and coordinate systems for these elements are shown in Figure 32 and Figure 33 for the STIF4 and STIF44, respectively.

Each element in the model was defined by two end nodes and the orientation node (or an angle of orientation for STIF4), and the element real constants. The latter described an element in terms of the pertinent cross-sectional properties. The STIF44 has an option for cross-section shear center offset effects to be included in stress computations.

Output data for these elements included, along with the nodal displacements, the axial, bending, combined axial and bending, torsional and average shear stresses.

The gooseneck trailer used a single insert on the second bolster for hauling thinning material, and two inserts for hauling tree-lengths. In the refined models, friction interaction between the insert and bolster was modeled utilizing the 3-D interface element STIF52 (Figure 34). The element represents two surfaces which may maintain or break physical contact and may slide relative to each other. It is capable of supporting only compression in the direction normal to the surfaces and Coulomb friction force in the tangential direction. Each element has three translational degrees of freedom. The elements may be preloaded in the normal direction, or they may be given a gap specification.

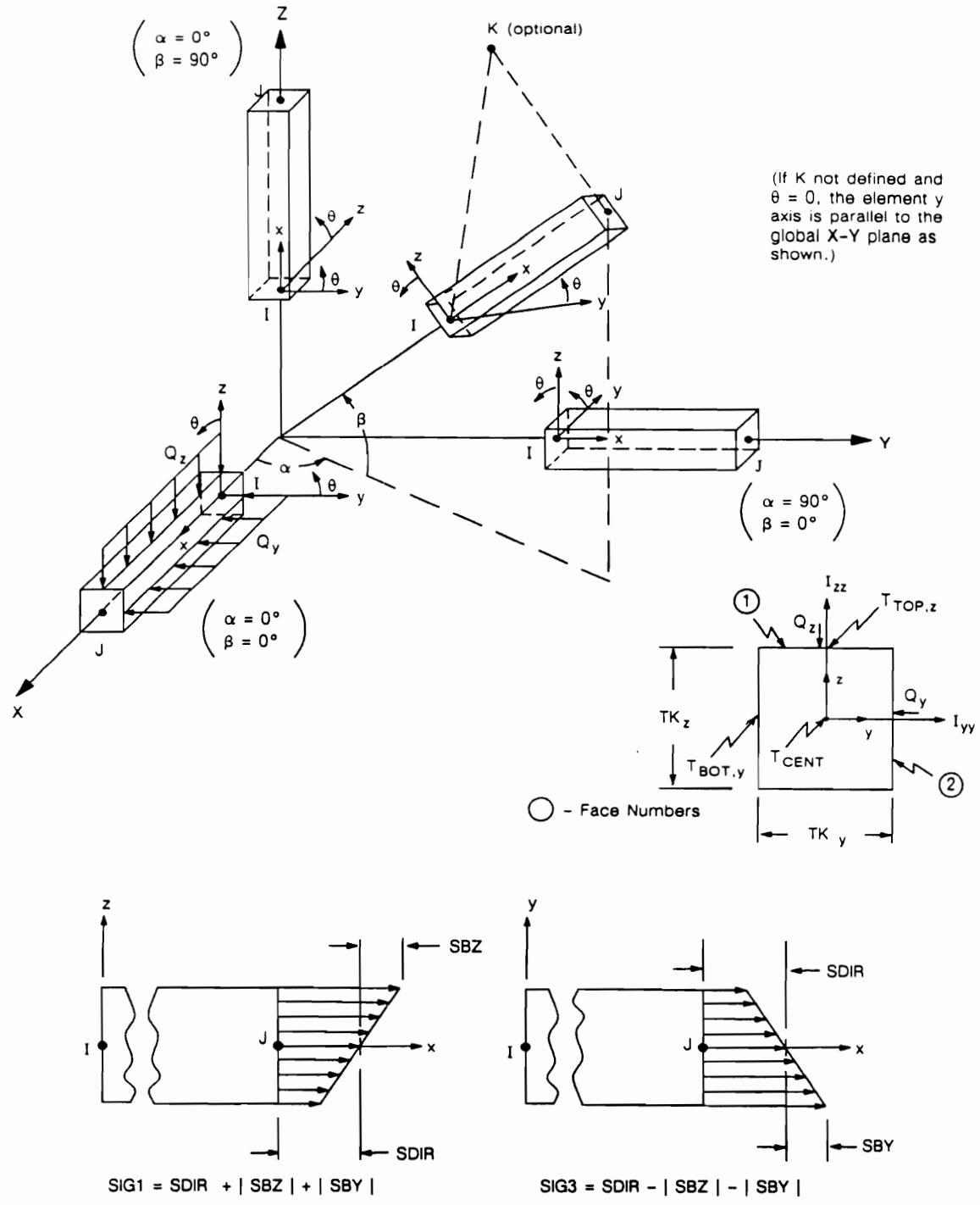

Figure 32. The Geometry, Nodal Point Locations, Loadings, and Stress Components for the 3-D Elastic Beam Element STIF4 (Swanson Analysis Systems, 1989). (Reprinted with special permission from Swanson Analysis Systems, Inc.).

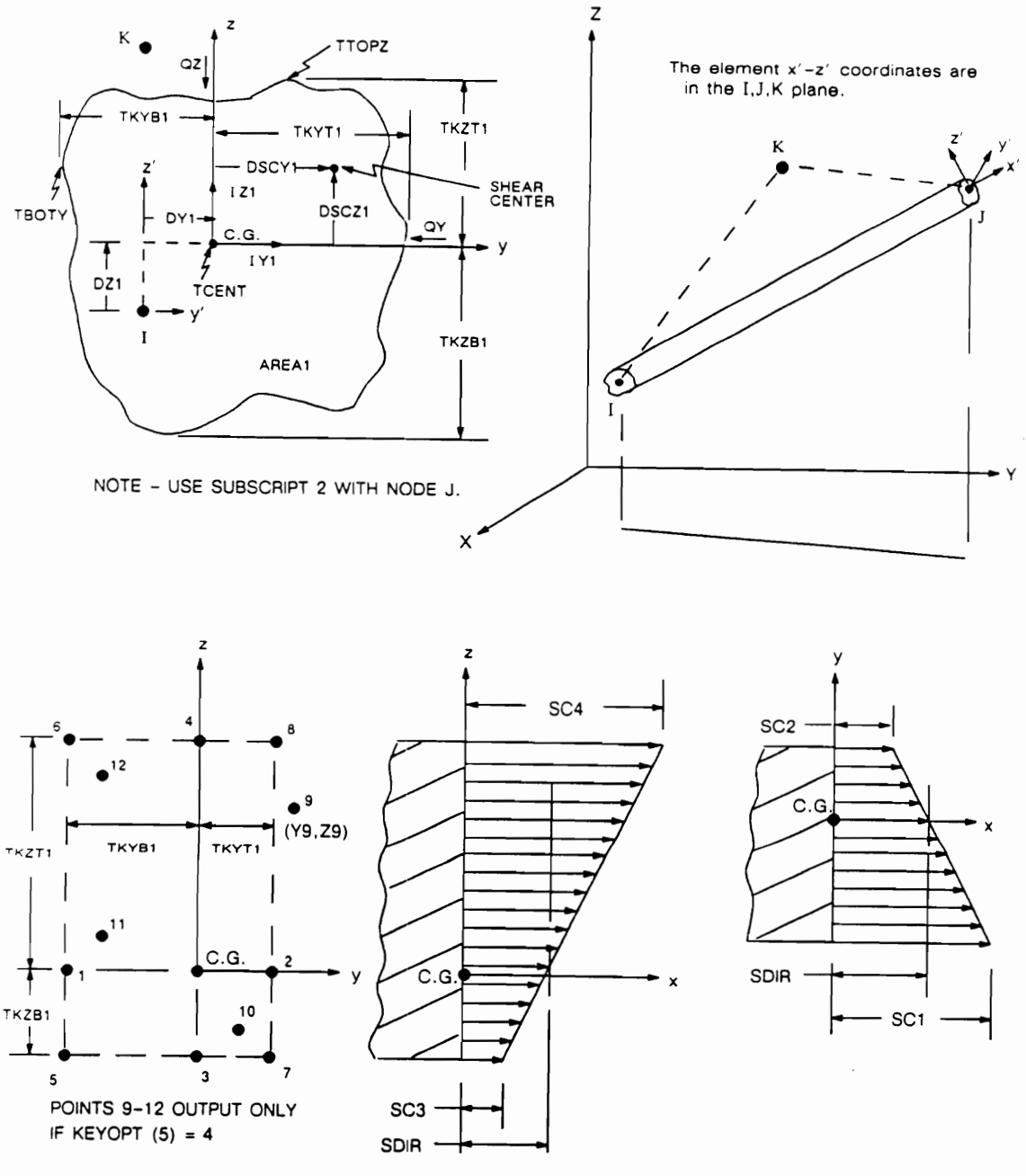

Figure 33. The Geometry, Nodal Point Locations, Loadings, and Stress Components for the 3-D Tapered Unsymmetrical Elastic Beam Element STIF44 (Swanson Analysis Systems, 1989). (Reprinted with special permission from Swanson Analysis Systems, Inc.).

The element operates bilinearly and requires an iterative solution until convergence is obtained. The convergence criterion for the analysis was set equal to +/- 10% tolerance in equilibrium. In the analysis of the gooseneck trailer, 60 iterations were usually required for the solution to converge.

The kingpin connection between the trailer and tractor, and the trailer running gear were represented as rigid simple supports in the early models. This is a conservative approach, and it leads to slight overestimation of stresses in the frame. In modified 3-D models, spring-damper elements STIF14 (Figure 35) were employed to model the effect of the flexing of the trailer running gear, as well as the tractor suspension system.

The damping capability of STIF14 was not accessible for the analyses performed (i.e. static and modal). The total flexing of the running gear of the trailer was modeled by three spring-damper elements supporting the trailer's frame at the hangers and equalizer locations. Assumptions about spring constants of these elements were made based on observations about how much the rear of a trailer lowers under the full load capacity of the suspension. A similar assumption about a spring constant of the element simulating the kingpin/fifthwheel coupling was made.

The refined models for the selected light-weight trailers were used to perform static and modal analyses.

The objective of these analyses was to determine stress distributions in trailers under different loading scenarios. Data obtained from the experimental static measurements were used to validate the models. Finally, the stress distributions under static conditions were utilized to interpolate dynamic stress values at the locations different from measurement points.

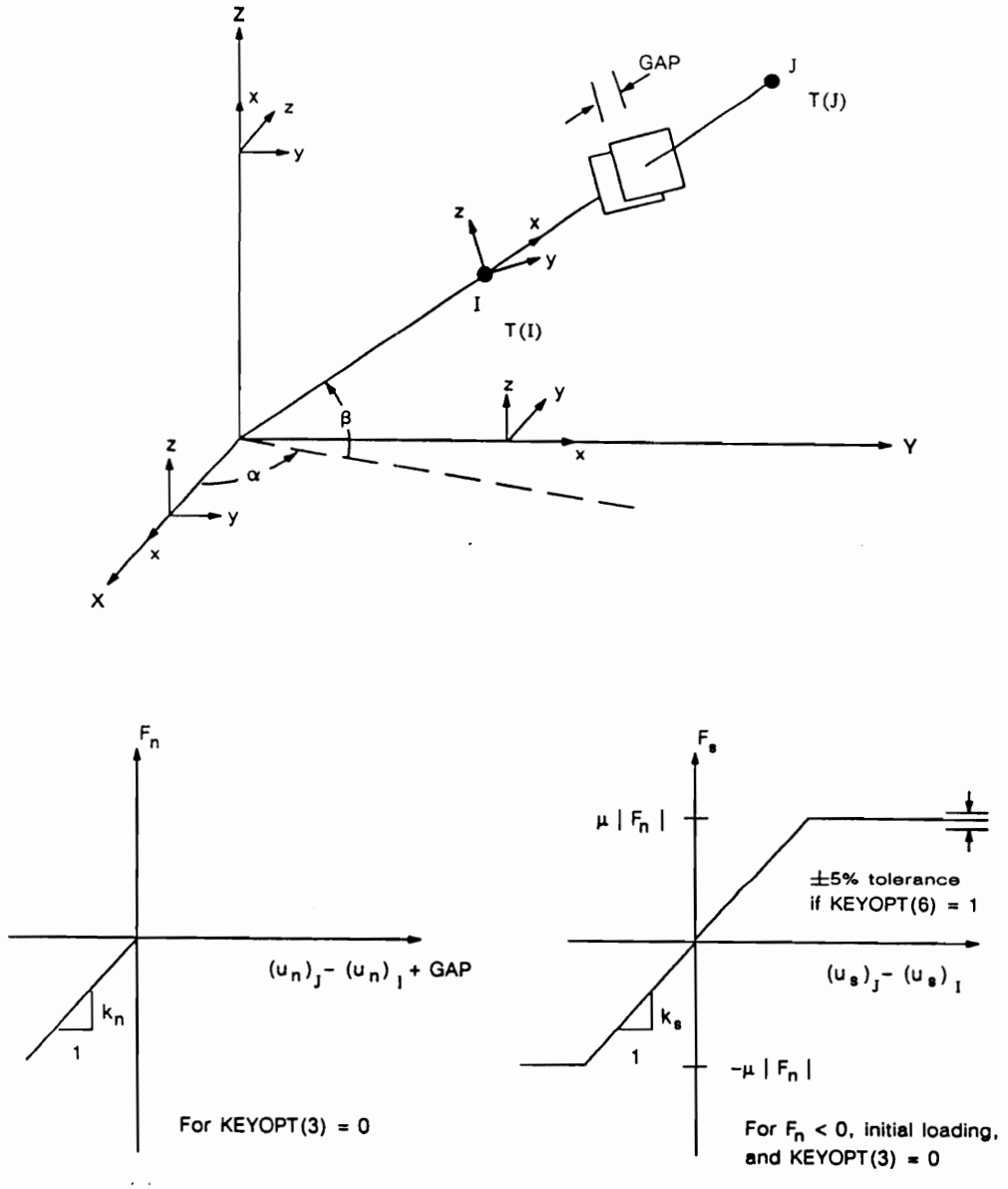

Figure 34. The Geometry, Nodal Point Locations, and Element Coordinate System for the 3-D Interface Element STIF52 (Swanson Analysis Systems, 1989). (Reprinted with special permission from Swanson Analysis Systems, Inc.).

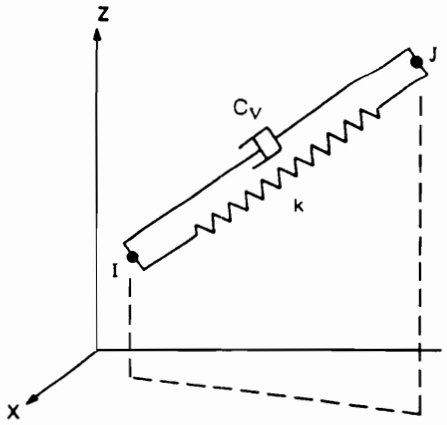

Note - Two-dimensional elements must lie in the X-Y plane

Figure 4.14.1 Spring-Damper

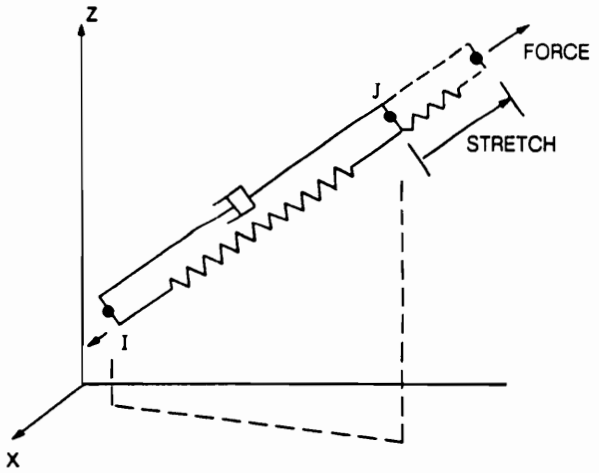

Figure 35. The Geometry, Nodal Point Locations, and Element Coordinate System for the 3-D Longitudinal Spring-Damper Element STIF14 (Swanson Analysis Systems, 1989). (Reprinted with special permission from Swanson Analysis Systems, Inc.).

The objective of the modal analysis was to determine the first lowest natural frequencies associated with the observed most common vibration modes of the trailers. These frequencies were then compared with the ones measured during the experimental dynamic stress analyses of the designs.

Shell Element Model

Static analysis using 3-D beam elements provided information about the distribution of nominal stresses in the trailers. These nominal stresses are a function of the overall geometry of the trailer (structure classified as a frame) and of the nature of the loading exerted on the structure (pressures along bolsters and standards, assumed concentrated forces on main beams, bending moments). Stresses in regions of stress concentrations are usually several times higher than the nominal ones. Concentrated stresses are usually developed at locations of abrupt cross-section changes, interconnection of members, load application, places of structural support, and other stress risers. These stresses are beyond the scope of the 3-D elastic beam formulation.

Experimental stress analysis of the selected lightweight trailers indicated that the maximum nominal stresses are below the material yield strength, and that the failure due to excessive yielding seems unlikely under "normal conditions" (excluding situations of obvious trailer misuse). However, careful examination of a number of log trailers revealed the existing fatigue cracks in many of the structures.

In the course of the study, an attempt was made to identify the reasons for this phenomenon. In order to verify the hypotheses put forward, finite element models of simple frames simulating a front section of a log trailer were developed. Building a shell element model for the entire structure of a log trailer was impossible due to the 200 degrees of freedom wave front size limitation imposed on the university version. Building a model by substructuring was still feasible, but would be very time-consuming.

The 4-node elastic quadrilateral shell elements STIF63 were employed in building the models. The STIF63 elements have both the bending and membrane capabilities (in-plane and normal loads are permitted). The geometry, node point locations, loading and coordinate system for this element are shown in Figure 37. Elements in the model were defined by four nodal points, plate thickness, and material properties. The element loadings were specified as surface pressures on any face of the element, and nodal forces. Data output for each element contained information on the nodal displacements, stresses in middle, top and bottom surface, as well as the element bending moments (MX and MY) and the twisting torque (MXY) (Figure 36).

Locations of stress concentration were specified in the model to estimate the maximum stresses at stress risers. The keypoints about which area mesh would be skewed were defined prior to mesh generation. Elements were generated circumferentially about, and radially away from, the stress concentration point during the mesh operation.

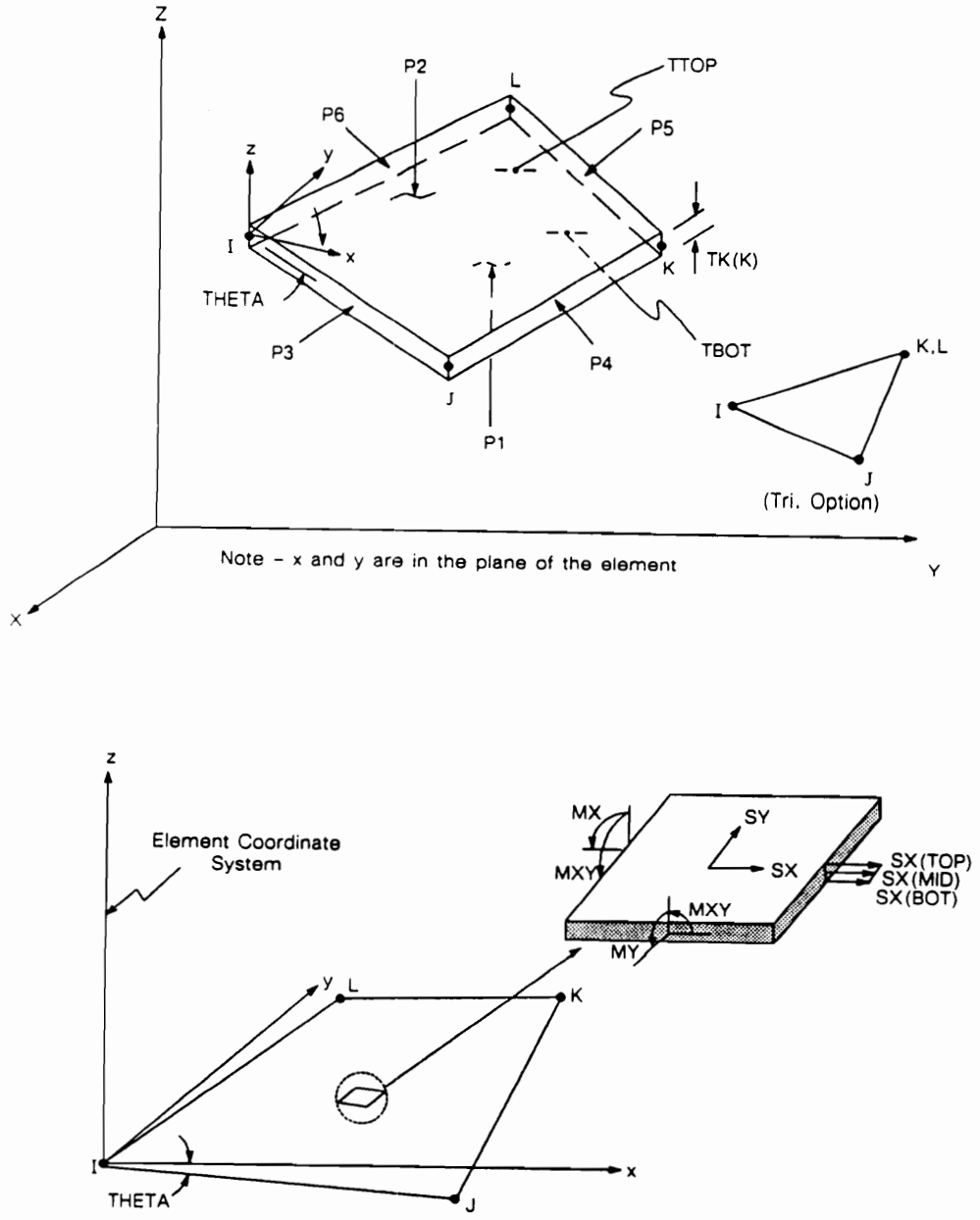

Figure 36. The Geometry, Nodal Point Locations, Loadings, and Stress Components for the Elastic Quadrilateral Shell Element STIF63 (Swanson Analysis Systems, 1989). (Reprinted with special permission from Swanson Analysis Systems, Inc.).

Experimental Stress Analysis

Experimental stress analysis is used to determine and improve the mechanical strength of structures and machines by experimental means. In doing so, it does not remain a mere counterpart of theoretical methods of stress analysis. It encompasses those, utilizing all the conclusions reached by theoretical considerations, and goes beyond them in maintaining direct contact with the true physical characteristic of the real world problems (Hetenyi, 1950). Often, the experimental approach is the only means of investigating mechanical strength problems. Theoretical considerations are based on simplified assumptions which represent a certain detachment from reality. For instance, modeling boundary conditions creates serious difficulties when using the popular finite element method. Pinned, roller, or fixed supports are often used to restrain the structure from movement. However, such ideal joints do not exist in reality, and in most cases the stiffness of joints is unknown. Often, only experimentation can determine whether such idealization was justified. No such doubt enters experimental approach, especially when it is done under actual service conditions. All the factors due to the material properties, methods of manufacture, and the condition of operation are fully represented (however not measured). It is possible to determine the stress distribution in the structure or machine part in actual operation without prior knowledge of the nature of the loading acting on the member.

Several principal methods of experimental stress analysis and literally hundreds of individual strain indicating devices are accessible to today's stress analyst (Table 7). The electrical resistance strain gage technique and photo-elastic coating method (called "PhotoStress" method) are the most common and effective techniques of experimental stress analysis applied to practical engineering problems.

Table 7. Experimental Strain Measurement Methods (after Rinn, 1992)

	METHOD	APPLICATION	ADVANTAGES	DISADVANTAGES (COMMENTS)
Widest Range of Applications and Measurement Information	Electrical resistance foil strain gage	Static and dynamic testing for both service and residual stresses.	Relatively inexpensive and easy to apply. Remote data collection. Used over wide temperature range.	Averages strain under grid. "Point measurement" only.
	PhotoStress (photoelastic coating)	Similar to foil strain gages.	Full-field analysis of both static and dynamic strains on most any material.	Must have visual access. Limited temperature range. More work than strain gages.
Limited to Specialized Measurement Applications	Semiconductor strain gage (piezoresistive)	Mostly dynamic testing and measurement of low strains.	High gage factor (high output).	Sensitive to temperature. Expensive. Gage factor inconsistency. Fragile.
	High-temperature strain gage (resistive or capacitive)	Static and dynamic testing up to 1000°C.	High temperature testing.	Expensive and more difficult to use than foil gages. Less accurate.
	3-D photoelasticity (stress freezing)	The only practical experimental test method for complete 3-D stress analysis.	Full-field analysis of both surface and interior stresses.	Complex. Time-consuming.
	Moiré	Strain and deformation analysis mostly of flat surfaces.	No reinforcement. High-temperature applications.	Mostly lab testing. Sensitive to motion.
	Holography	2-D strain and deformation analysis.	Non-contacting.	Lab testing only. Expensive. Complex. Sensitive to motion.
	Thermal emission (Spate)	Strain analysis under dynamic conditions.	Full-field analysis. No reinforcement. Non-contacting.	Test part must be vibrated. Very expensive. Measures $\sigma_x + \sigma_y$.
	X-Ray	Measures surface strains. Mostly used for residual stress analysis.	Non-contacting.	Expensive. Mostly limited to lab testing.
Generates Only Partial Information	Brittle lacquer	Determination of strain distribution. Proof testing.	Very inexpensive. No instrumentation.	Limited information and accuracy. Mostly qualitative. Very sensitive to temperature and humidity.
	2-D photoelasticity	2-D model analysis. Mostly static testing. Preliminary design study.	Full-field analysis. Accurate, simple, and fast.	Plane stress only. Can't simulate nonhomogeneous materials. (Simulates geometry only).

Strain gages are extremely sensitive; they detect strain with 1 μ-strain accuracy. The principal limitation of the strain gage technique is that it provides a point measurement and that the value indicated is actually an average of strain over the gage grid length. Strain gages are much cheaper and very convenient for remote automatic strain measurements when compared to the "PhotoStress" method. Measurements can be performed at many points on the surface of the structure simultaneously. Gages work over a wide temperature range and are capable of being used in hostile environments.

The approximate maximum strain sensitivity of the "PhotoStress" method is 10 times lower (10 μ-strain). The photo-elastic coating is a full field stress analysis technique. It is used in both static and dynamic testing. The "gage length" is virtually zero in this case. Installation is not affected by humidity or time. The "PhotoStress" method easily reveals directions of principal stresses and indicates strain gradients. However, "PhotoStress" technique is limited to only 100 ^{o}F, and is much more expensive than the strain gage installations.

The strain gage technique was selected for experimental stress analysis of the selected trailers after considering the purpose of the investigation, its field character, the need for continuous automatic recording of the service load spectra, and the time and financial resources available. It was believed that the experimental approach, combined with the full stress field analytical method of finite elements, would insure a comprehensive stress analysis of the structures. Contrary to the opinions of some theorists and of some experimentalists, the two aspects of the discipline are not separable, and overemphasis on either one is likely to decrease the cost-effectiveness of the stress analysis effort (Perry, 1982).

Electrical Resistance Strain Gage Technique

The principle of the electrical resistance strain gage was discovered by Lord Kelvin when he observed that the resistance of a wire alters when it is subject to strain. No use was made of this principle until the 1930's when it was rapidly developed into one of the most useful tools in experimental stress analysis. The idea of bonding the resistance element directly to the test piece was conceived at California Institute of Technology. In this first application, made by Simons, 40 feet of constantan wire was laid longitudinally on four faces of a bar in zigzag fashion and coated with glyplar as a binder. The unit was used as a dynamometer for impact testing. At about the same time, Ruge at Massachusetts Institute of Technology originated an idea of bonding the wire to a paper and then cementing the strain gage to the structural member being tested (Dohrenwend and Mehaffey, 1950).

There are two constructions of the strain gages. An older construction consists of a continuous length of resistance wire of about 0.001-inch diameter, wound tightly and cemented to a backing. The newer version of the gage uses the conductor in the form of a metallic foil "ribbon", 0.0004 to 0.001 inches thick, mounted on a thin epoxyethylene backing (Hendry, 1964). The strain gage is firmly bonded to the specimen. The length and cross-sectional area of the conductor change, as the surface of the member under the active gage grid extends or contracts in the direction of the winds, as a result of loading, resulting in the corresponding increase or decrease in electrical resistance. The change in resistance is, within a wide range, proportional to the strain in the specimen:

$$\varepsilon = (1/F) * (\Delta R/R);$$

where the constant F is termed the gage factor, and ΔR and R are the change in the resistance and the original resistance of the conductor, respectively.

It can be shown that based on the pure geometrical changes of the conductor, the gage factor would be (1 + 2*μ), where μ is Poisson's ratio. However, for most materials, the specific resistance of the conductor changes with strain, and the gage factor is about 2.0.

Although a gage is intended to measure a strain in the direction of its length only, the short lengths of the conductor perpendicular to the axis of the gage introduce some degree of sensitivity to transverse strain. Fortunately, this effect is small enough (about 0.2% of longitudinal sensitivity in foil gages) to be neglected in engineering applications when single-segment gages are used. If three-segment rosettes are employed, the experimental data must be corrected for transverse sensitivity. Standard formulas for 45 ° rectangular rosettes were used in the process of field data correction.

Today's commercially available gages are of metal foil structure and cover a very wide range of applications. They are made of a variety of materials, of different dimensions, grid arrangements, and electric resistances. Measurements Group, Inc. located in Raleigh, North Carolina, is a leading worldwide strain gage and strain measurement instrumentation manufacturer. The characteristics of their most common strain gages are shown in Tables 8 and 9 (Figure 37).

Measurements Group's universal general-purpose CEA series gages were selected for this study. The gages utilize constantan alloy (A-alloy) for the strain sensitive grid which is completely encapsulated in polyamide. This provides the ruggedness and excellent grid protection required in field application. The 0.001 inch thick polyamide film in the encapsulation is very flexible and does not reinforce the grid. A long-term gage stability is achieved, because the grid cannot be contaminated during installation by fingerprints or other agents. Also, the CEA series features large, rugged, copper-coated terminal tabs, greatly simplifying soldering operation.

Table 8. Strain Gage Sensing Alloys for a General Stress Analysis Application (Measurements Group, 1992). (Reprinted with special permission from Measurements Group, Inc.).

ALLOY TYPE	APPROXIMATE GAGE FACTOR①	STC AVAILABILITY	FATIGUE PERFORMANCE	MAXIMUM ϵ RANGE
A (CONSTANTAN)	2.0	YES (00-50)	GOOD	6%
P (ANNEALED (CONSTANTAN)	2.0	NO (08)	POOR	20%
K (MODIFIED KARMA)	2.1	YES (00-15)	VERY GOOD	2%
D (ISOELASTIC)	3.2	NO (DY)	EXCELLENT	2%②

① GAGE FACTORS LISTED ARE ROOM TEMPERATURE (75°F/*24°C)* VALUES

② NONLINEAR AT STRAIN LEVELS OVER ±0.5%

Table 9. Strain Gage Matrices (Backings) for a General Stress Analysis Application (Measurements Group, 1992).(Reprinted with special permission from Measurements Group, Inc.).

TYPE	CONSTRUCTION	OVERALL THICKNESS (INCHES)	COMMENTS
CE	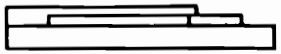 Cast Polyimide	0.0022	General Stress Analysis Large Copper-Coated Tabs
E	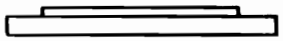 Cast Polyimide	0.001	General Stress Analysis Numerous Options Available
W	 Glass-Epoxy-Phenolic	0.0028	Stress Analysis & Transducers Fatigue Resistant Leads Widest Temperature Range
S	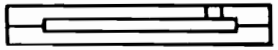 Glass-Epoxy-Phenolic	0.002	Stress Analysis & Transducers Wide Temperature Range Solder Dots
S2	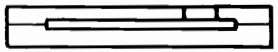 Laminated Polyimide	0.0025	Used For Testing Composites High Resistance Grids Large Solder Pads

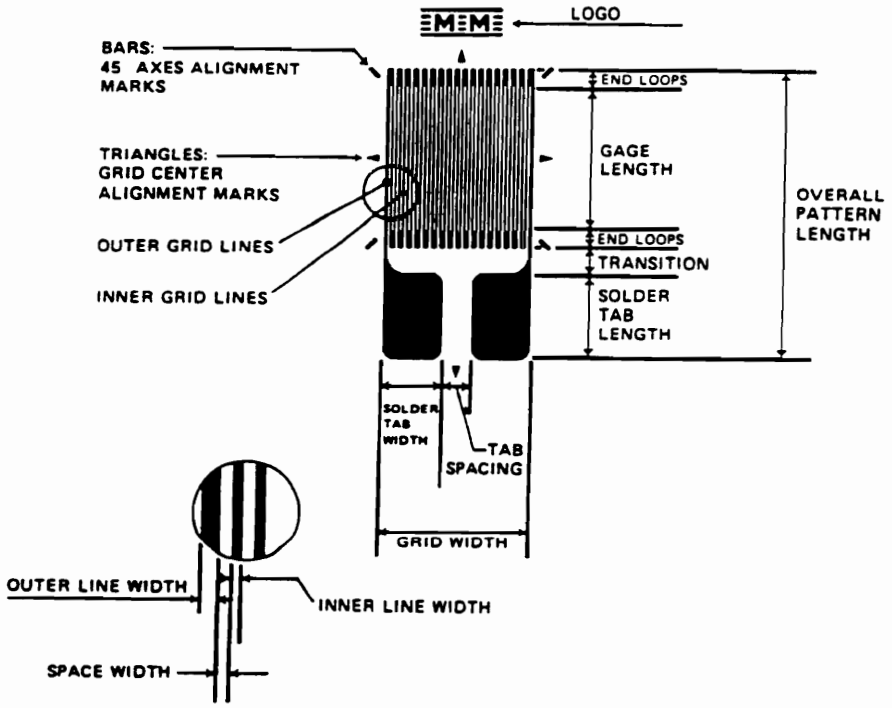

Figure 37. Measurement Group's General-Purpose Single-Segment CEA Strain Gage (Measurements Group, 1992). (Reprinted with special permission from Measurements Group, Inc.).

These gages are subject to a special thermal process to obtain a self-temperature-compensation feature when used on steel, aluminum, and other most common materials. This means that the gages produce minimum thermal output (i.e. temperature-induced apparent strain) over the temperature range from about -50 to +400 °F. This effect has been achieved by ideally matching the thermal expansion coefficients of both materials: strain gage grid alloy and the specimen material. Since the gages were used in the temperature range from 10 to 90 °F, temperature-self-compensation did apply and their calibration for thermal output was not necessary.

Two gage patterns were used: single-segment gages and rectangular rosettes. Single-grid gages were employed at the locations were the state of stress at a point was identified as the uniaxial by the preliminary analysis. Gages of electrical resistance of 350 Ohms were selected for the study to reduce the heat generation in a gage, the long leadwire effect, and to improve the signal-to-noise ratio. Preliminary tests with the control double-bunk trailer in Southeast Virginia indicated that the narrow general purpose gages CEA-06-250UN-350 of a quarter-inch active grid length represented the best compromise in view of the strain averaging under grid, space for gage installation, gage price and ease of installation. These gages are capable of measuring strains in the range of +/- 3% (30,000 μ-strain) which was adequate for this application.

Single-plane CEA-06-250UR-350, 45 ° rectangular rosettes were used at the locations where the directions of principal stresses on the surface of the structure varied with the nature of loading exerted on the trailer. Again, a quarter-inch long active grid length was found appropriate.

The usual method of measuring the change of resistance in a strain gage is by means of a Wheatstone bridge circuit (Figure 38). The output from the Wheatstone bridge can be expressed as:

$$e_o / E_i = \{ R_1 / (R_1 + R_2) \} - \{ R_4 / (R_3 + R_4) \};$$

where e_o, E_i, R_1, R_2, R_3, R_4 are the bridge output, bridge excitation, and the resistances in the bridge arms, respectively. When the bridge output is zero it is in balance. Then:

$$R_1 / (R_1 + R_2) = R_4 / (R_3 + R_4);$$

which can be rewritten as:

$$R_1 / R_4 = R_2 / R_3$$

A change of resistance of one of the resistors unbalances the bridge so that an output signal is produced. If the R_1 resistor is an active strain gage that has undergone a change of resistance, ΔR_1, when the test specimen to which it is bonded has been subjected to stress, and assuming that all resistances were of the same initial value R, the bridge output can be expressed as:

$$e_o / E_i = (\Delta R / R) / \{ 4 + 2 (\Delta R / R) \};$$

The bridge output can be then expressed in terms of measured strain, because the relative resistance change of a strain gage ($\Delta R/R$) is equal to the product of the gage factor (F) and the produced strain:

$$e_O = F * \varepsilon * E_i / (4 + 2F * \varepsilon).$$

The term $2F*\varepsilon$ in the denominator gives rise to some nonlinearity for the strain measurement using this bridge configuration. However, the magnitude of this error is approximately only 0.1% per each 1000 μ-

train (Lineback, 1987). It can be shown that a configuration obtained by placing four active gages in the arms of the bridge (i.e. full bridge circuit) attached to a beam in bending produces a linear output which is four times the value of the quarter bridge output.

Usually, only one arm of the bridge is an active strain gage. The other arms required to complete the circuit must either be inactive strain gages or high precision resistors.

The initial balance of a strain gage bridge is affected by a differential heating of the bridge arms. A "dummy gage" opposite the measuring gage in the bridge is frequently used. This second gage eliminates any unbalance of the bridge arising either from changes in ambient temperature or from self heating. To properly perform its functions, the dummy gage must be identical to the active gage, unstrained, mounted on the same material as the specimen, and located close to the actual test piece. In practice, self-temperature-compensated gages are used. It is cheaper and more convenient to do so.

Long leadwires were used in the installations due to the large physical sizes of the structures. The three-leadwire method of the active gage connection with the quarter bridge arrangement was employed to provide for automatic compensation of leadwire temperature effects, to minimize the initial unbalance due to the leadwires, and to reduce their desensitizing effect on bridge output (Figure 39).

Eight Wheatstone bridges were built using Measurement Group's 350 Ohm precision resistors for each of the 8-channel A/D boards, and enclosed in a separate box. Two units; one for each of the A/D boards were used during experiments.

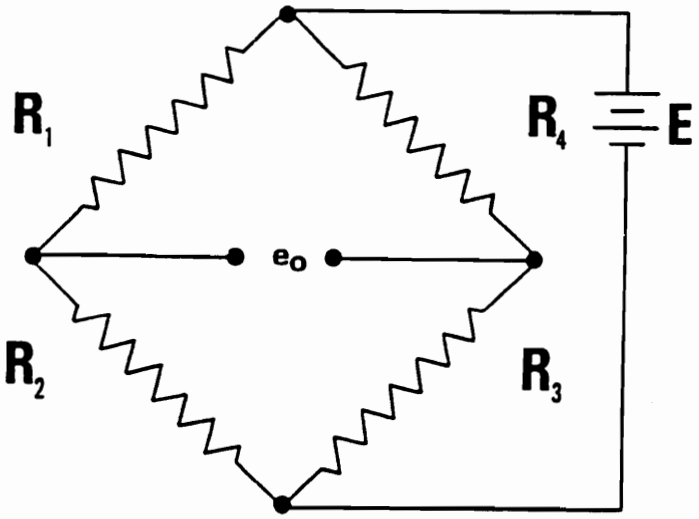

Figure 38. Wheatstone Bridge Used as Primary Circuit for Strain Measurement (Measurements Group, 1992). (Reprinted with special permission from Measurements Group, Inc.).

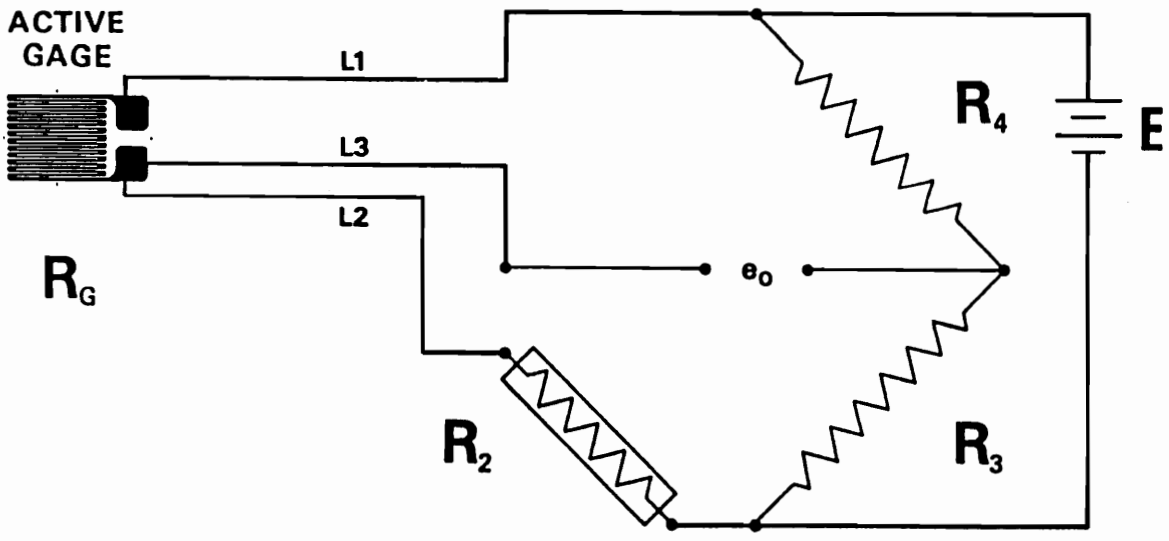

Figure 39. Three-Leadwire Method of Active Gage Quarter Bridge Connection (Measurements Group, 1992). (Reprinted with special permission from Measurements Group, Inc.).

Data Acquisition System

There are several types of computer data logging systems currently being used in research. Off-the-shelf systems are available for most major laboratory monitoring functions. However, they are not suitable for forest harvesting application due to their size, power requirements, and harsh environment of forest operations. Single-board devices, which are readily available, are robust, low-power, small, and capable of measuring, and storing significant volumes of data. However, data retrieval and flexibility in application remain a difficulty (McCormack, 1990).

A more common solution is to use an intermediate sized multi-board micro computer system. This has the advantage of larger capacity for data collection and storage, and ready peripherals for data exchange (i.e. floppy disk or tape drive).

The STD bus was designed 20 years ago as a universal arrangement of signals that any microprocessor at that time could use. Thus, the STD bus started out being processor-independent, which most of the other existing bus systems were not. This means that it should be possible to design new STD bus CPU cards as new microprocessor chips become available, and these new cards should work in old systems, simply because all of the signals and pin assignments on the edge connector were previously defined for a general-purpose CPU chip. After two decades, some of the newer processor cards are CPU specific. It is still relatively easy to put together a whole system based on the STD bus. Customers can purchase 80% to 90% of the required cards, depending on their application, from various manufacturers. The remaining 20% to 10% of the cards have to be designed and built by the end user (Titus et al., 1982).

The STD bus cards for industrial process control and real-time measurements are widely available. This permits ready configuration of specialized measurement boards from different manufacturers to meet user needs. McCormack successfully used the STD bus computer for speed and fuel consumption measurement on log trucks, proving the utility of such a system for the forest harvesting application. The data logger was redesigned for the use in this project.

The data acquisition system involved the following major groups of components (Figure 40):

1. external transducers, which produced signals to be measured and which included:

- strain gages measuring strains at critical locations on a trailer;
- accelerometers measuring accelerations in the three directions in space;
- vehicle speed transducer;
- brake monitor;
- event switch box.

2. the data logger which was monitoring the signals coming in from the transducers, measuring, pre-processing, and subsequently storing the readings, and which consisted of (Figure 41):

- STD Bus computer;
- system monitor and control console.

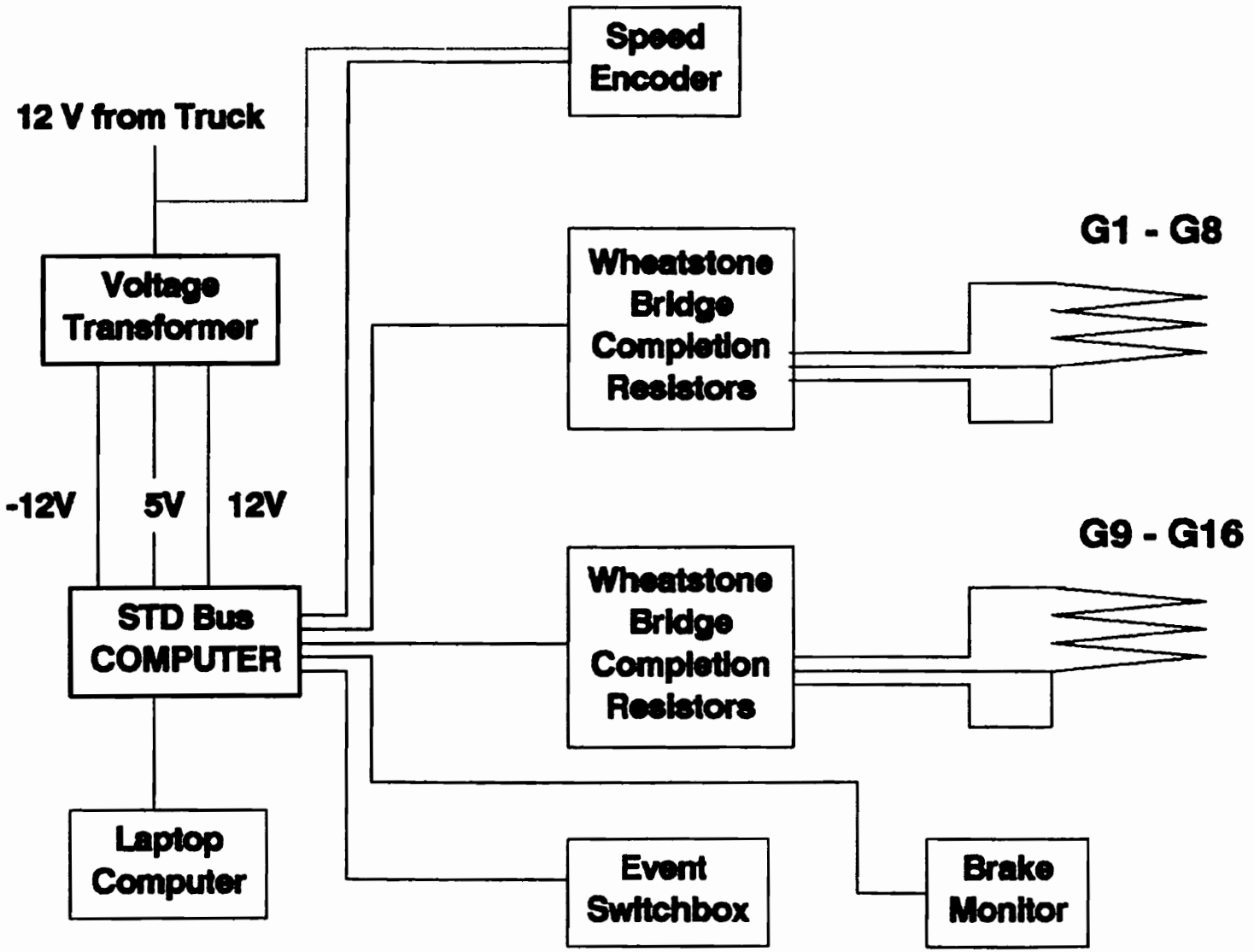

Figure 40. Data Acquisition System Interconnection Schematic.

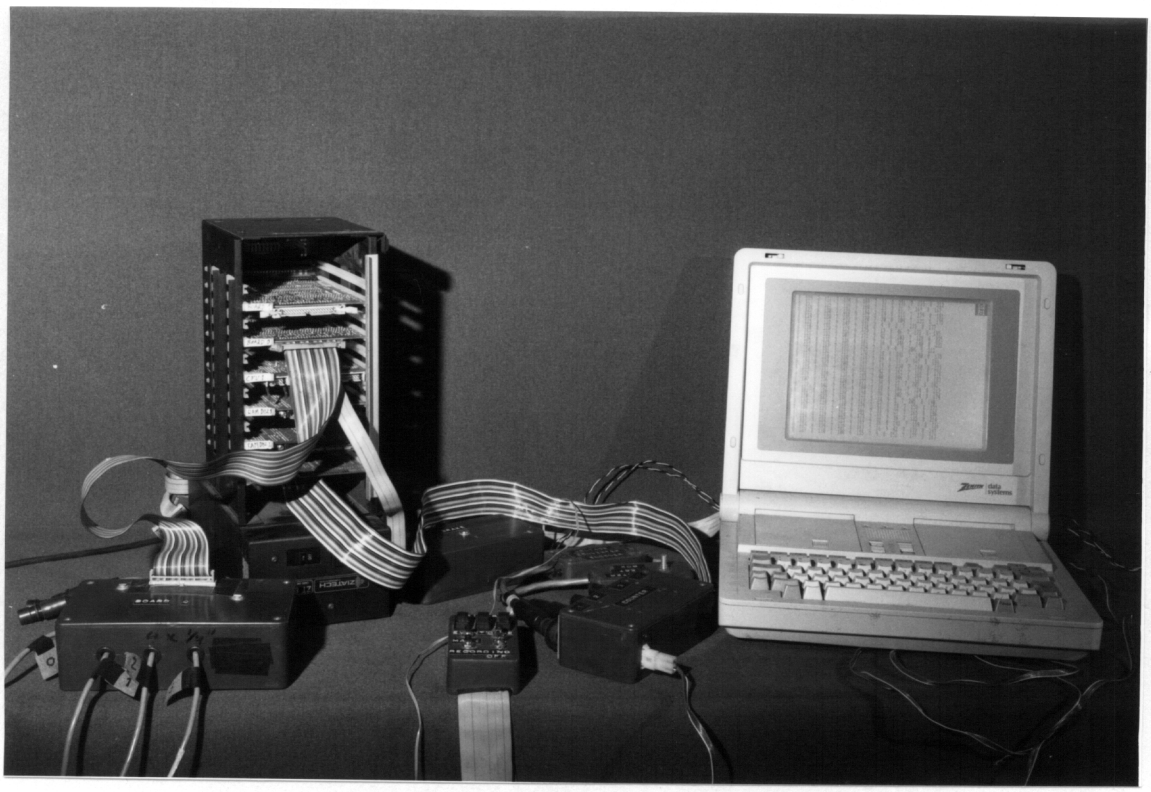

Figure 41. Data Logger Computer System.

Computer Data Logger

The computer data logger built for this project comprised:

Ziatech ZT8809 Microprocessor Board (384 K Byte memory)

Ziatech ZT8825 Extended Memory Boards

Ziatech ZT8853 3 1/2" Floppy Disk Drive

Ziatech ZT8852 IDE 80 Meg Byte Hard Disk

7409 Sensoray Signal Conditioning Analog Input Boards

Matrix 7911/ADC-12 12-Bit Analog-to-Digital Converter Card

MSI C730 21 Channel Counter and Digital I/O Board

MATRIX 8 slot card cage and backplane

Melcher AM3000 DC-DC Power Supply

The CPU card used the NEC V20 microprocessor operating at 8 MHz speed. The system emulated an IBM PC - XT and worked under a ROM-based DOS version 3.3. Component boards were all designed for a high vibration and wide temperature range environment. A Zenith Laptop Computer was used as a system control console and monitor. A special software, the Virtual System Console (VSC), written by Ziatech, would subdue the laptop's microprocessor to the host CPU of the STD bus computer and make it possible for the two units to work together.

The two 7409 Sensoray Boards used during all three field experiments were specially designed to interface strain gages and strain gage transducers. Each was configured to accept 8 voltage differential signals. Each channel was provided with a gage excitation and would compensate for initial bridge unbalance. The

on-board microprocessor continuously scanned trough the eight channels. Pulsed excitation was provided in order to minimize self heating effects. As each channel was scanned, the sensor signal was amplified, filtered, digitized, linearized, and converted into engineering units. Then the data was immediately accessible to the host CPU. The boards utilized a 14-bit A/D converter. Cycle time of internal software was 17 milliseconds per channel. The frequency of sampling was about 5 times a second. The final resolution of strain measurement was +/- 9.44 μ-strain. The two boards could interface 13 strain gages and 3 accelerometers at a time during the test.

For faster strain/stress measurements, especially when a trailer was driven empty, the Matrix 7911ADC-12 general analog-to-digital converter card was used. It was configured to accept 8 voltage differential signals at a time. The input signal ranged from +/- 10 mV to +/- 10 V, depending on the user-specified amplifier gain. The board required special on-board wiring utilizing a 2 V DC battery to provide strain gage excitation. Thanks to the fast 12-bit successive approximation A/D converter, the sampling frequency of all the eight sensors reached over 35 Hz. Strain measurement had 37.76 μ-strain resolution with this board.

The MSI C730 21-Channel Counter and Digital I/O Board was used for counting signals from the speed sensor and monitoring the event switch box.

The two ZT8825 Extended Memory Boards were configured as a single 2 Meg RAM Disk. This memory capacity would suffice for approximately one hour of continuous recording with the 7409 Sensoray board and 18 minutes for the Matrix 7911 board, given its high frequency of data sampling. Once all the memory was filled up, the truck was stopped for the data transfer to the ZT8852 IDE 80 Meg Hard Disk. The advantage of using the hard disk was that it could accept data files of the size up to the RAM disk

capacity (i.e. up to 2 Meg). It had to be installed in the cage for the data transfer and then removed each time, because this component was not vibration resistant. The files were later divided into smaller sizes. The overall system dimensions after mounting on a foam vibration insulation base were 14" x 12" x 8". This met the size requirement for mounting on the floor in front of the passenger seat. Boxes with Wheatstone bridges for the strain gage circuits were placed under the seat.

Voltage Transformer

A Melcher AM3000 DC-DC inverter power supply was used to generate the voltage levels +/- 12 V and +/- 5 V required by the computer and some of the transducers. Voltage input was supplied from the truck 12-volt electric system. A common ground with the truck system was maintained because of the requirements of several of the transducers.

Strain Gages

As it has been earlier discussed, Measurements Group's general-purpose temperature-self-compensated CEA-06-250UN-350 single-element gages, and 45 ° rectangular, single-plane CEA-06-250UR-350 rosettes were used. The quarter bridge and three-wire circuits were employed.

Accelerometers

Three strain gage type accelerometers monitored the vertical, sideways, and longitudinal dynamic loading exerted to the trailer in terms of "g"--the gravity acceleration. They were all mounted rigidly at the midpoint of the cross member closest to the anticipated load center of gravity location. Accelerometers measuring vertical, sideways, and longitudinal acceleration had a range of +/- 5 g, +/- g, and +/- 0.5 g,

respectively. The dynamic load measurement resolution depended on the transducer range and the A/D converter card. It ranged from +/- 1.9 10e-3 g to +/- 0.02 g for the 14-bit Sensoray A/D card and the fast Matrix 12 bit A/D card, respectively.

Vehicle Speed Sensor

A 360-count-per-revolution optical encoder was used as the speed transducer. The encoder was attached to a wheel hub oil seal bolt circle of the driver side front wheel. The front wheel on the driver side was used because it was not subject to the power-induced wheel slip, it was less sensitive to weight transfer rolling radius changes between loaded and unloaded condition, and usually experienced better road surface conditions than the off-side wheel. The bearing mounted encoder housing was restrained from turning by a PVC pipe extension slip mounted in a ring attached to the truck fender. This allowed the vertical displacements and horizontal rotation with steering of the encoder. The transducer output was a 5 V pulse train, about 36 counts per foot of distance. The distance (and the speed) measurement relied on constant tire rolling radius.

Brake Monitor

Brake application was monitored from the brake lamp circuit. This arrangement provided automatic indication of brake usage, but no information on brake intensity. The intensity of the braking force was measured by the longitudinal accelerometer.

User Switch Box

The user switch box was designed as a seven-switch panel. The computer monitored it every 5th data sampling cycle (i.e. approximately once a second). Five latching switches and two push-to-contact switches were used. The first three switches were used to denote, in binary code, the road category in the computer file. Five road categories were distinguished: the unformed and formed forest sand roads, gravel forest roads, one-lane paved roads, and state highways. Two other switches were used to code, in the same fashion, the three pre-defined events: a bump on the road, curve/corner, and road intersection. One *push-to-contact* button inserted a sequence number in the data set. The event was also entered in a trip log, with a short description associated with the sequence number. The last switch (a push to contact type) was used to switch off and on data recording. This last utility was especially important to control the data amounts and limit recording to the actual experiment.

System Calibration and Testing

First, the two Sensoray 7409 and the fast Matrix 7911 boards, were calibrated for precision and stability using a precision voltage generator. The MSI C730 counter and digital I/O board were also tested at that time.

The A/D cards were calibrated for strain measurement using a specially prepared calibration beam. An aluminum bar with a single-segment gage installed as shown in Figure 42 and strained in bending was utilized for this purpose. The Measurement Group's portable strain indicator model P-3500, certified at the factory, was employed for precise stress measurement under a "standardized" loading condition. Calibration of the strain gage instrumentation included comparing the data logger computer recording with the strain indicated by the P-3500 indicator.

A conventional double-bunk trailer, selected to be included in the study as a control trailer, was instrumented with strain gages for the initial implementation of the data acquisition system. The data logging computer was installed in the cab of the tractor. The testing took place around Pembroke, Virginia. The dynamic loading and the resultant stresses in the trailer were monitored during loading, unloading, and traveling loaded while the trailer was hauling pine saw logs.

The Tektronix 2232 Digital Storage Oscilloscope with recording capability was employed for sampling the dynamic strains induced at different measurement points. It was determined that the frequency of the measurement equal to 5 Hz, of which the Sensoray 7909 card is capable, would be sufficient for the stress analysis of a log trailer. This data sampling was a compromise between excessive data collection and acceptable accuracy. Monitoring incoming data on the laptop computer was set at a one per second rate.

Procedures for Field Experiments

Dynamic loadings acting on a trailer, the resultant stresses at various critical locations, and the situations in which these occurred were measured and automatically recorded during the field experiments for the two basic conditions:

- when simulating extreme situations, and
- during typical work cycles.

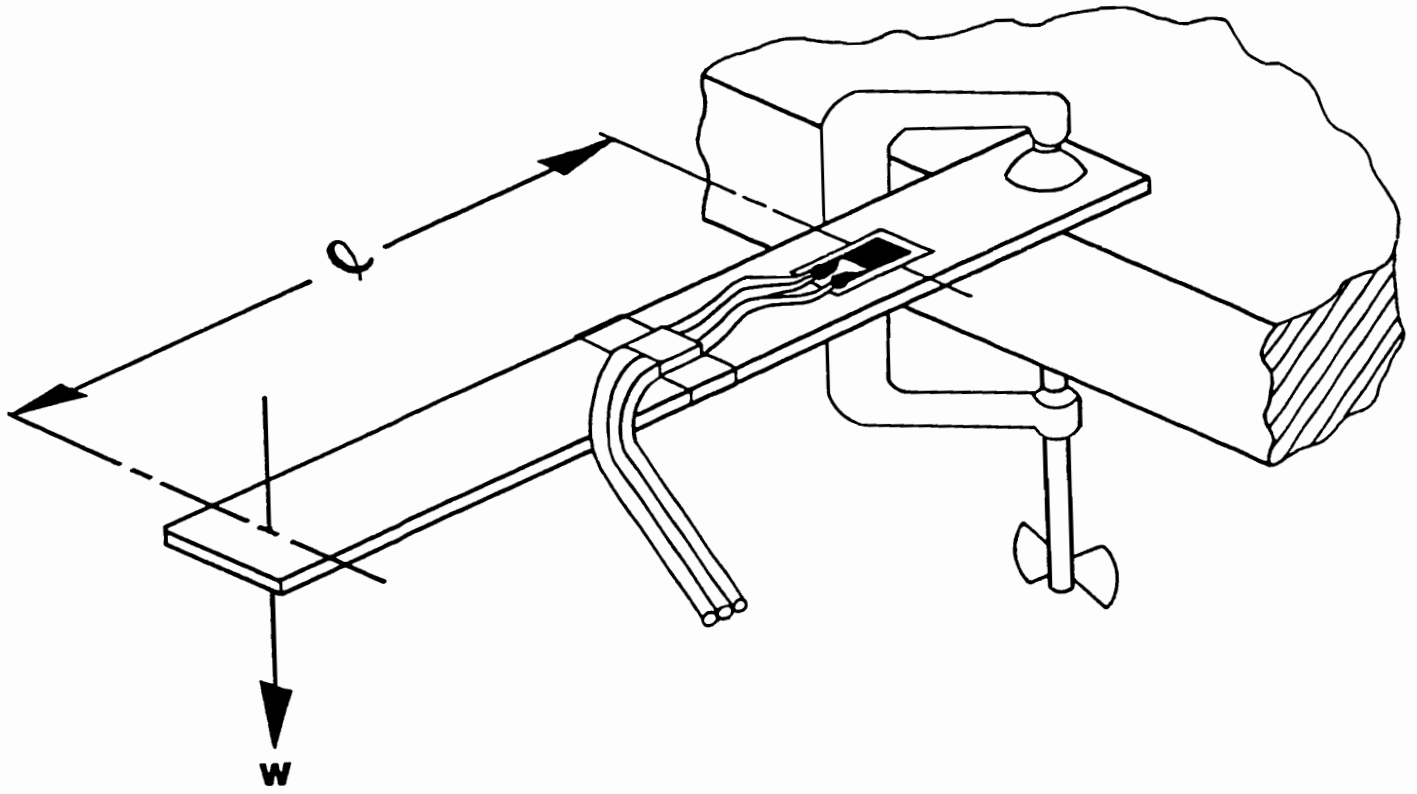

Figure 42. Simple Cantilevered Beam with Installed Single-Element Strain Gage Used for System Calibration.

In the first part of the experimental stress analysis, a trailer was overloaded by up to 30% and driven along a closed loop over rough, unpaved surface. The driver was asked to drive with an increasing speed up to the maximum at which he still felt safe.

Next, the trailer was tested during hard cornering, braking, and forward acceleration. The procedure was repeated for a well sealed surface: asphalt or concrete. Then the trailer was subjected to repeated loading and unloading operations with different equipment. Trials included tests with knuckle-boom loader, front-end-loader, forklift loader, and one-grip portal crane. Whenever possible, the operator was asked to be rough (but not abusive) during the operation to simulate extreme loading conditions. Trailers loaded with maximum legal payload were driven along randomly selected sections of public roads. State highways, two-lane and one-lane community roads, as well as sand unformed, formed and gravel forest roads were covered. Trials were repeated for two loading patterns: logs resting on all the three bolsters versus resting on the second and the third bolster (thinning material), and two load types; they were also repeated for pine versus hardwoods. Experiments were also performed while the trailer was driven empty over different road surfaces.

During the second part of the study, the dynamic loads and the resultant stresses were monitored during typical service cycles. The first part of the trials would usually take two days, whereas the second component of the experiment lasted three days for the gooseneck, and a week for the full-tree trailer.

Data sets of over 20 Meg size were created each time. Before analysis could begin, the data files were reduced to standard computer storage files for easy handling by analysis software. Commercial spreadsheet algorithms were used to graphically edit the data as time series. The data was than searched for the maximum values and the situations in which they occurred. Typical service load spectra were identified for members of trailer for fatigue analysis.

Fatigue Analysis

There are, in general, many different modes of structure failure. It can occur under static load by:

1. Ductile fracture in tension, compression or shear.
2. Buckling.
3. Creep.
4. Brittle fracture.

Under dynamic, repeated loads failure occurs by fatigue.

Fatigue failures of structures and machines in service far outnumber all the other causes of failures. The estimated cost of fatigue fracture and its prevention is 80% of the total cost associated with failures and failure prevention of all structures and machines (Dowling, 1993).

The mechanism of fatigue failure in metals may be described in the following steps (Marsh and Frost, 1968). The process begins with the initiation of a surface microcrack. Many experiments demonstrated that crack initiation is confined to the surface grains of the material. After microcrack initiation, it subsequently extends and penetrates into the body of the metal. The direction of microcrack development is initially that of the slip planes between grains of the metal. It remains so, until a microcrack is of such a size that the amount it opens and closes becomes sufficient to affect a large enough volume of material along its edge for it to grow as in continuum. The growth process is now associated with the magnitude of the tensile strain range in the volume just ahead of the crack tip. The growth direction becomes normal to the direction of the nominal maximum cycling tensile stress, being now independent of any crystalline slip

directions. The crack (now termed macrocrack) grows at a rate much faster than that of the initial microcrack, and it spreads rapidly through the metal. The component fails when there is not enough effective cross-section area left to support the nominal load. The brittle appearance of a fatigue fracture results from the fact that during the microcrack growth stage, the cyclic plastic strain occurring at any instant is confined to a small volume of material just ahead of the crack tip. Fatigue fracture occurs unexpectedly at nominal stress levels much lower than those causing the material to yield under static conditions.

Fatigue failures which occur in practice result primarily from fatigue cracks originating at some sort of discontinuity. Many of these occur because all real engineering materials contain flaws of one sort or another. The flaws may be inherent in the material (e.g. inclusions), caused by fabrication (e.g. welding defects), or inherent in the geometry of the component. The latter is a consequence of lack of attention to detailed fatigue design. This is the greatest single factor responsible for failures. Therefore, the merit of any design of a structure subject to dynamic loadings depends to a great extent on the skill of the designer in avoiding unnecessary stress concentrations.

At present, there are three major approaches to analyzing and designing against fatigue failures. The traditional approach is to base analysis on the nominal (as computed with ordinary equations) stresses in the region of the component being analyzed. The method is called *stress-based approach*. The nominal stress amplitude that can be resisted under cyclic loading is determined by considering the mean stress, and by making adjustments for the effects of stress raisers, type of loading, size of component and surface quality. The method employs relationships between the nominal stress amplitude and life, called S-N curves. Another approach is the *strain-based approach*. It considers the variations in the local stress and strain at critical location, such as a stress raiser. It is similar to the nominal-stress approach in that it uses a form of S-N curve, but differs in that strain is the variable related to life, and also in that plastic

deformation effects are specifically considered. Finally, there is the *fracture mechanics approach*. It analyzes cracks and their growth rates. Only the form of fracture mechanics based on linear-elastic stress analysis has been sufficiently developed that it can be considered a design tool. The primary variable employed is the special parameter called the stress intensity factor, K. Rates of change of crack length with number of cycles are used to obtain the life of the component until the crack obtains a predefined unacceptable size.

The *nominal-stress* approach was used to assess a fatigue life of the two trailers tested. The method assumes a uniform cycling stress extracted from the stress-time history for the component, and neglects sequence effects. More appropriate approach would be to consider the cumulative effect of some percentage of the greatest overall stress ranges experienced by the member during service. In most cases the 10% of all overall strain/stress ranges that are the greatest will cause more than 90% of the fatigue damage (Fuchs and Stephens, 1980). The recorded stress-time histories would be analyzed for identifying major overall ranges by the rainflow cycle counting method, for instance. This would have been a time consuming task given the large data sets created for each trailer tested, and was not planned to be performed in this study.

CHAPTER 4. PRELIMINARY STRESS ANALYSIS

The objective of the preliminary stress analysis of the selected trailers was to identify the stress critical spots in the structures and to estimate stresses encountered at these locations. These locations were then used as strain gage placements for the experimental measurements.

The Gooseneck Trailer

The prototype gooseneck log trailer built by Pitts Trailers was the first structure studied. The trailer was intended to maximize payloads from longwood thinnings. Butt loading area was increased by introducing a 16.5-inch drop in the frame. The trailer tested had three sets of bolsters and standards, and weighed 10,900 pounds. It was capable of a consistent 25 ton payload of tree-lengths from thinnings.

Precise measurements of the trailer geometry were made. Individual axle and total gross weight for two loads of tree-length material from thinnings were obtained, and paired with the same weights for the empty tractor and trailer combination. The distance between butts and the kingpin was recorded. The two payloads were extra heavy: 54,100 (Case 1) and 58,320 pounds (Case 2) corresponding to a 10% and 19% overload, respectively. This information allowed the computation of theoretical force distributions and locations of centers of gravity for the trailer, tractor, and payloads for both configurations from the equilibrium condition of the vehicle. Loading on each structural member was then derived assuming a symmetric load distribution on the trailer. The above computations were presented in Appendix A.

2-D Model

It is always recommended that a two-dimensional analysis be performed before proceeding to the three-dimensional one. The 2-D simplification gives insights concerning the nature of the problem and provides experience for developing a good 3-D model. The Finite Element Personal Computer (FEPC) program was used for the preliminary finite element stress analysis.

Elastic beam elements were best suited for proper modeling of the trailer. Nodes were created at every location where a change of a cross-section existed or a concentrated force or moment was applied.

The 2-D formulation of the trailer required that the structure be broken down to simple components: main beams, bolsters, and standards. Each component was modeled separately.

Main Beam

The main beam of the trailer was modeled using 112 elements and 113 nodes (Figure 43). Forces exerted on the member were computed from the equilibrium condition. Displacement boundary conditions included those applied at the kingpin (where both vertical and horizontal displacements were restrained) and at the suspension point (where only a vertical displacement component was restrained). The trailer suspension was modeled as a simple roller support at the equalizer location. This conservative approach leads to a slight overestimation of the stresses.

Modeling Loads on Standards

Modeling the loadings exerted on the standards is a complex problem. Two methods were suggested for this analysis. The first method used a hydrostatic pressure concept. It assumes that logs have very small diameters with respect to the standard height and the bolster length, and that there is very little friction between them. Logs are treated as a fluid filling the space of a bunk. Horizontal forces and bending moments acting on each consecutive cross section of the standard are then determined as shown in Figure 44 (see Appendix A). This is a conservative method yielding an overestimation of the stresses. However, upper bounds of the stresses are generated.

The second method of the analysis assumed that a pile of logs confined in the cross section area of an equilateral triangle is supported exclusively by a bolster. Half of the remaining load on the given bunk is partially distributed to the standard. Logs were assumed to have large cross sectional areas in comparison with the bunk dimensions, and there is considerable friction between the logs. The portion of the load acting on a standard was treated as a rigid body. The horizontal force and bending moment acting on the standard were determined from the equilibrium condition of this portion of the load (Figure 45). This method is more realistic and stresses computed using this method provided the lower bound for the static stress magnitudes in standards and bolsters.

Bolsters

Loads acting on each bolster included: a linearly distributed force (determined as a ratio of the weight on the given bolster to the inner length), a horizontal force and bending moment exerted on each standard and conveyed to the bolster, and the structure weight.

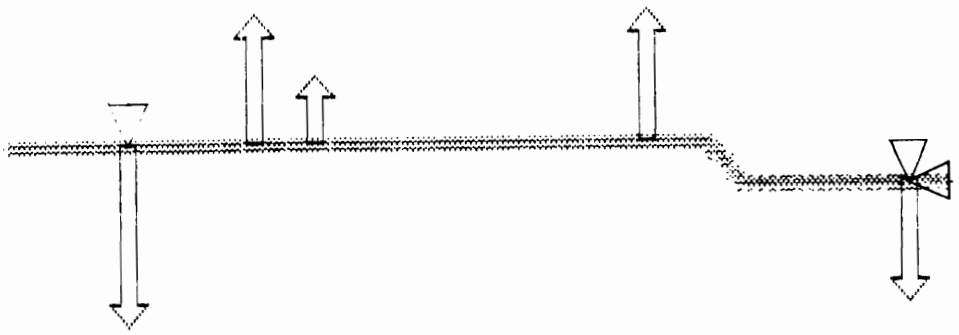

Figure 43. The 2-D FEM Model of the Gooseneck Trailer Main Beam.

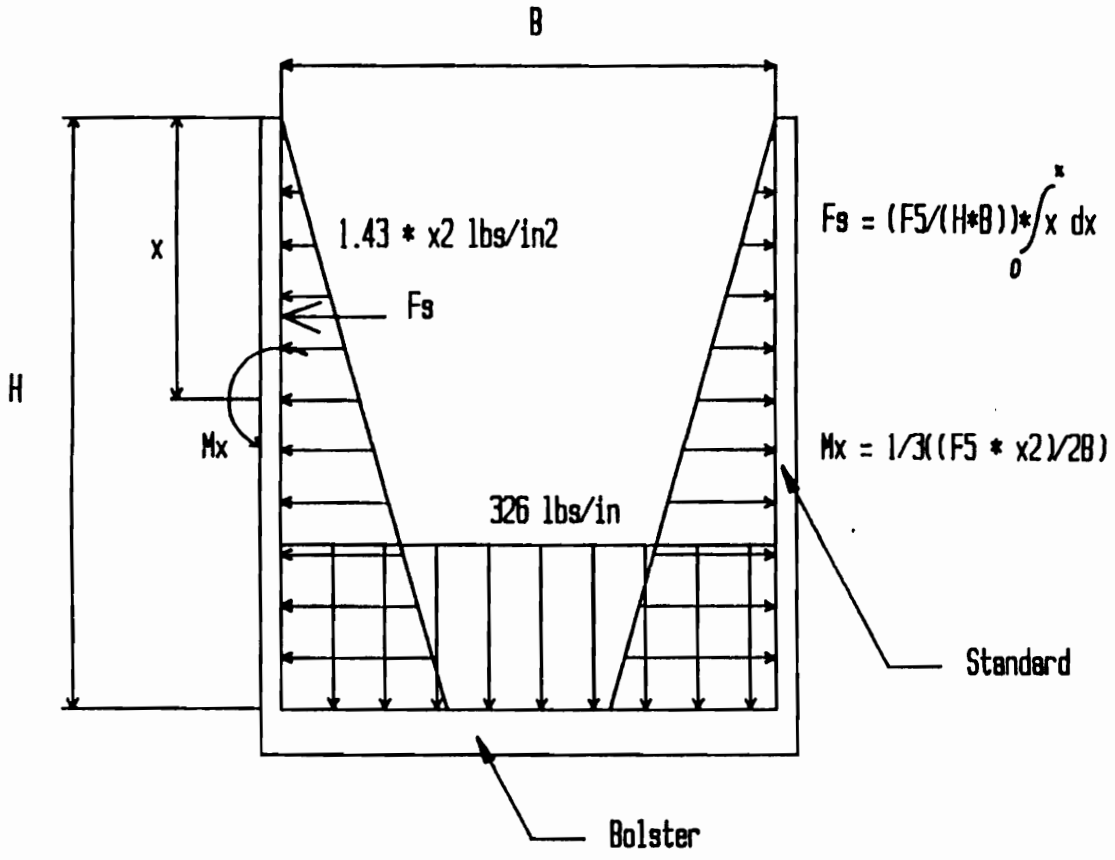

Figure 44. Method 1 of Computing Loadings on Standards: The "hydrostatic pressure" concept.

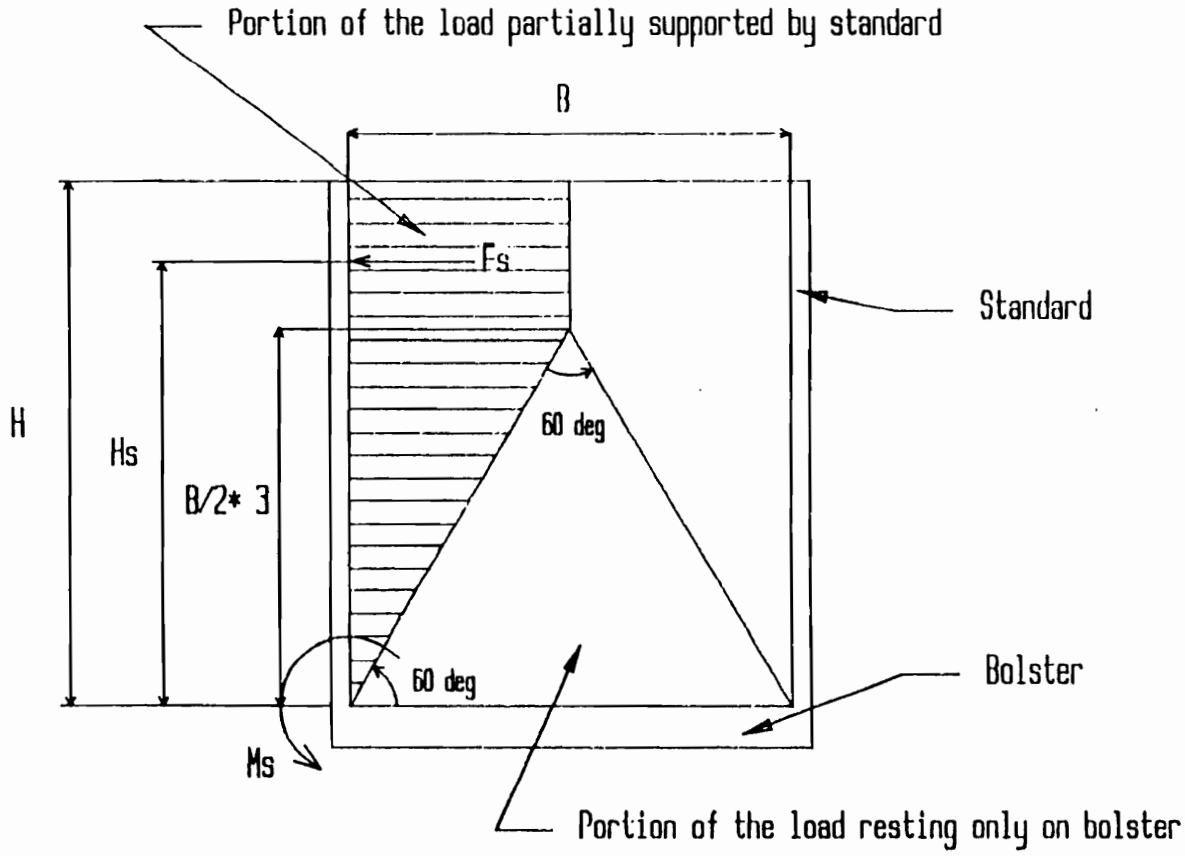

Figure 45. Method 2 of Computing Loadings on Standards; This concept assumes that a portion of the load partly rests on the standard.

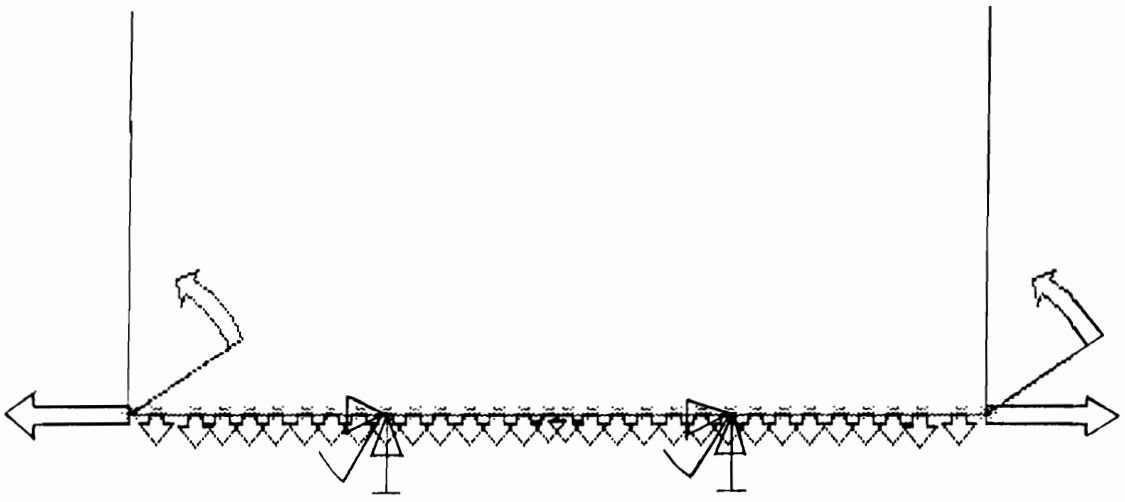

Figure 46. The 2-D FEM Model of the Gooseneck Trailer Second Bolster.

The second bolster was modeled with 31 elements and 32 nodes (Figure 46), while the third bolster was modeled with 47 elements and 48 nodes. Displacement boundary conditions were applied at the support points (where bolsters are welded to the I-beams). Vertical and horizontal displacements and rotations were restrained at these locations.

Standards

Standards on the second and third bolster were modeled using 25 elements and 26 nodes, and 21 elements and 22 nodes, respectively. Figure 47 shows the 2-D model of the second bolster. Displacement boundary conditions for each standard were imposed at joints with bolsters; vertical and horizontal displacements and rotation were restrained there.

RESULTS

A static stress analysis of the gooseneck trailer was performed for both methods of computing loads on standards and for the two payloads. The results are shown in Tables 10 and 11.

The maximum normal stresses in the main frame took place in the cross-section under the second bolster. The beams were made of the ASTM A36 steel with a minimum yield strength of 36 ksi. Therefore, the computed stresses correspond to a design factor (the theoretical safety factor) equal to 1.78 and 1.29 for the Loading Cases 1 and 2, respectively. The considerably higher stresses for the second payload are the result of both a higher load and the load center of gravity being shifted closer to the kingpin.

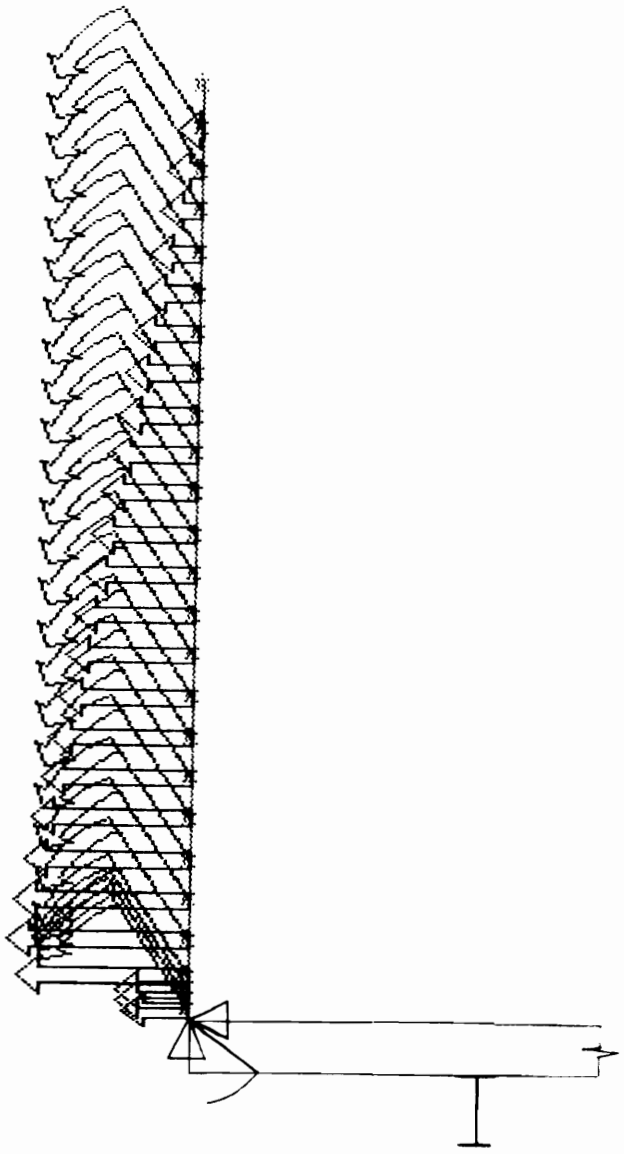

Figure 47. The 2-D FEM Model of a Standard on the Second Bolster (Method 1).

Table 10. Maximum combined bending and axial stresses and maximum strains induced in the gooseneck trailer when loaded with 54,100-pound payload (2-D analysis).

	Method of Computing Loadings	
	1	2
FRAME		
Max. combined stresses	20,220 psi	
Max. displacements	x=0.093 in. y=0.989 in.	
2nd BOLSTER		
Max. combined stresses	29,152 psi	16,970 psi
Max. displacements	x=0.001 in. y=0.034 in.	x=0.0004 in. y=0.021 in.
3rd BOLSTER		
Max. combined stresses	31,845 psi	19,208 psi
Max. displacements	x=0.0013 in. y=0.046 in.	x=0.0004 in. y=0.0287 in.
STANDARDS on 2nd Bolster		
Max. combined stresses	147,223 psi	89,230 psi
Max. displacements	x=0.000 in. y=7.092 in.	x=0.000 in. y=5.337 in.
STANDARDS on 3rd Bolster		
Max. combined stresses	132,026 psi	81,400 psi
Max. displacements	x=0.000 in. y=5.381 in.	x=0.000 in. y=4.280 in.

Table 11. Maximum combined bending and axial stresses and maximum strains induced in the gooseneck trailer when loaded with the 58,320-pound payload (2-D analysis).

	Method of Computing Loadings	
	1	2
FRAME		
Max. combined stresses	27,900 psi	
Max. displacements	x=0.114 in.	y=1.284 in.
2nd BOLSTER		
Max. combined stresses	32,971 psi	19,433 psi
Max. displacements	x=0.001 in. y=0.043 in.	x=0.0004 in. y=0.0267 in.
3rd BOLSTER		
Max. combined stresses	33,124 psi	19,970 psi
Max. displacements	x=0.0014 in. y=0.0469 in.	x=0.0004 in. y=0.0298 in.
STANDARDS on 2nd Bolster		
Max. combined stresses	164,100 psi	99,480 psi
Max. displacements	x=0.000 in. y=7.904 in.	x=0.000 in. y=5.950 in.
STANDARDS on 3rd Bolster		
Max. combined stresses	137,300 psi	84,670 psi
Max. displacements	x=0.000 in. y=5.596 in.	x=0.000 in. y=4.450 in.

This indicates the importance of moving the center of gravity to the rear of the trailer to reduce the maximum stresses. However, the latter solution could in some cases worsen the weight distribution between the tractor and trailer axles. A deformed geometry of the trailer I-beam is shown in Figure 48 a.

The analysis indicated that the most stressed spots in the bolsters are in the cantilevered sections, just at the tips of the reinforcing gussets. The computed stresses correspond to the ranges of the design factor: from DF=1.23 to DF=2.12 for the second bolster, and from DF=1.13 to DF=1.8 for the third bolster. Lower values corresponded to Method 1 of computing loadings on standards (the hydrostatic pressure concept) and the heavier payload (Loading Case 2). Figure 48 b shows a deformed geometry of the second bolster for the Method 1.

The analysis revealed that the maximum stresses in a standard are encountered in the very bottom cross-section of the member. These locations were found to be the most stressed spots in the entire structure.

The computed high stresses indicate the necessity of designing the standard-bolster joint very carefully. The large differences between the stresses computed with the use of the two methods indicate the uncertainty about the magnitudes of the stresses encountered in these cross-sections. The methods provided upper and lower bounds for the values.

Figure 49 shows a deformed geometry of a standard on the second bolster. When designing a log trailer, it should be remembered that tops of standards move outward by at least 2 to 2.5 inches under typical (legal) payloads. The overall width of an empty log trailer should accommodate this increase in width.

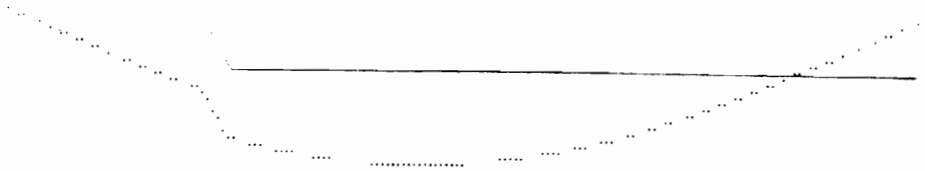

a)

b)

Figure 48. Deformed Geometry: (a) of the Main Beam, and (b) of the Second Bolster.

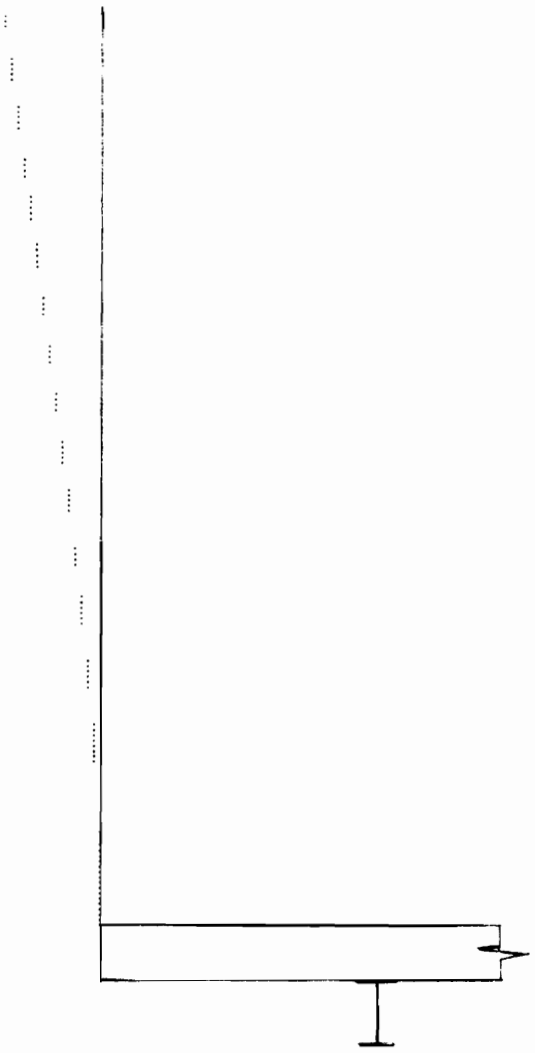

Figure 49. Deformed Geometry of the Second Standard.

Analysis Using Conventional Methods

Two conventional methods of stress analysis were employed to validate the results obtained from the FEM computer modeling. The double integration of a differential equation of an elastic beam method represents a universal approach toward statically indeterminate beam problems. In practice, such problems are solved using the method of superposition. The latter approach requires that formulas for deflections and slopes of beams, appropriate for the particular loadings and types of support present in the problem, be found in structural or mechanical engineering handbooks. However, only the most common beam configurations are represented, which may necessitate using a more general approach.

Both conventional methods were applied in static stress analysis of the structure. The traditional computations yielded results differing no more than 1% from the results obtained from the FEPC program. This confirmed the validity of the 2-D FEM analysis. Appendix B contains sample computations using the two conventional methods discussed.

3-D Formulation

The 3-D formulation takes into account the entire three-dimensional structure of the trailer. All the components are represented in one model. Displacements, strains, and stresses are solved for the general three-dimensional loading, i.e. forces, bending moments, and twisting torques acting in any arbitrary direction in space. Stresses in each section of a member represented by a single node are computed as a vector sum of axial and bending stresses due to lateral forces in vertical and horizontal planes. Shear stresses in torsion were negligible because of the symmetrical loading and geometry of the trailer. Shear

stresses due to the lateral forces were also minimal in this analysis, as the structure consists primarily of long, straight beams.

All input data: the information on the geometry of the gooseneck trailer, the payloads, locations of centers of gravity, spacings of axles, etc.; were taken from the 2-D analysis.

ANSYS STIF4 3-D elastic beam elements were employed to build the preliminary 3-D model of the trailer. The model was characterized by a higher level of detail. It consisted of 368 nodes and 368 elements, with 50 different cross-sections and sets of cross-sectional-area properties incorporated into the analysis. Only half of the trailer needed to be represented in the model due to the symmetry, obtained by cutting the trailer along its longitudinal axis. The two methods of computing loadings on standards were applied.

The following boundary conditions were imposed on the structure of the trailer:

1) displacement restraints:

a) symmetry plane boundary conditions at midpoints of each cross member:

- linear displacement restraints in the direction of the global y-axis;
- rotation displacement restraints in both x-y and z-y planes;

b) displacement restraints at points of structure support:

- at the kingpin; along all axes of the coordinate systems;
- at the suspension midpoint, where only the vertical displacement was restrained;

2) loadings:

a) horizontal forces exerted on a standard at each node and acting along the negative direction of the y-axis;

b) bending moments about nodal y-axis exerted at each node of a standard in the vertical x-z plane;

c) pressures representing linearly distributed forces acting on the second and the third bolster, and finally,

d) gravity acceleration; which allowed computation of the stresses due to the weight of the structure itself.

Figures 50 and 51 show the 3-D model and the imposed boundary conditions for the first and the second method of computing loadings on standards, respectively.

RESULTS

The 3-D static stress analysis was carried out only for the Loading Case 2: the 58,320 pound thinning tree-length payload.

The displacements of the tops of the standards on the second and third bolsters were found as the maximum for the entire structure. The deformed shape and undistorted geometry of the trailer are shown in Figure 52 (see also Table 12).

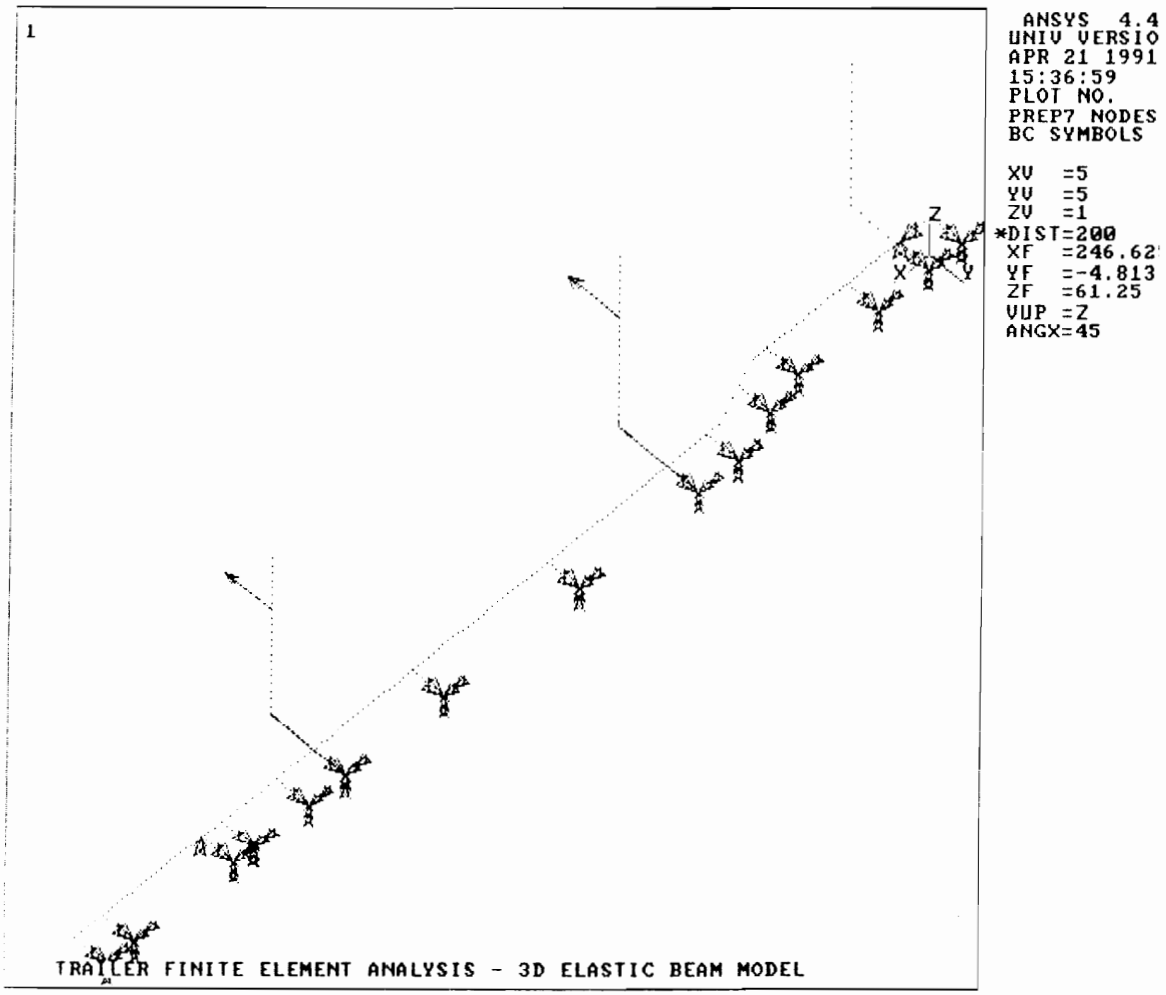

Figure 50. The 3-D Preliminary FEM Model of the Gooseneck Trailer: Method 1 of computing loadings on standards.

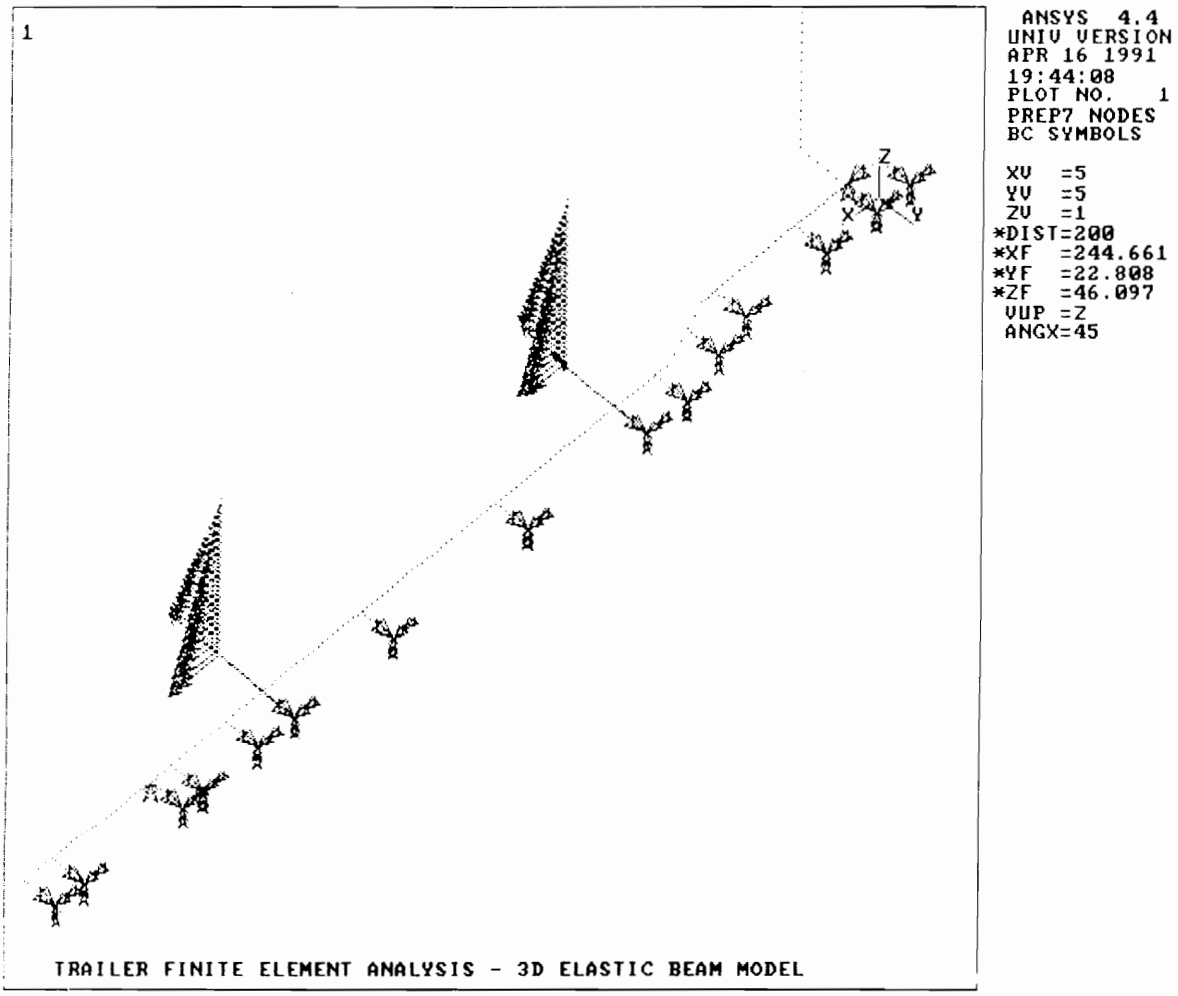

Figure 51. The 3-D Preliminary FEM Model of the Gooseneck Trailer: Method 2 of computing loadings on standards.

Table 12. Maximum combined bending and axial stresses and maximum strains induced in the gooseneck trailer when loaded with the 58,320-pound payload (3-D analysis).

	Method of Computing Loadings	
	1	2
FRAME		
Max. combined stresses [psi]	-23,295	-23,188
Max. displacements [in.]	x=-0.170 y=-0.320 z=-1.230	x=-0.170 y=-0.970 z=-1.240
2-ND BOLSTER		
Max. combined stresses [psi]	38,091	24,342
Max. displacements [in.]	x=-0.1700 y=-0.0027 z=-1.2900	x=-0.1700 y=-0.0008 z=-1.2300
3-RD BOLSTER		
Max. combined stresses [psi]	36,055	23,426
Max. displacements [in.]	x=-0.1700 y=-0.0027 z=-0.7900	x=-0.1700 y=-0.0008 z=-0.7100
STANDARDS on second Bolster		
Max. combined stresses [psi]	- 171,396	-102,992
Max. displacements [in.]	x=-0.2800 y=-8.8400 z=-1.2900	x=-0.2800 y=-6.5300 z=-1.2300
STANDARDS on 3-rd Bolster		
Max. combined stresses [psi]	-125,239	-83,014
Max. displacements [in.]	x=-1.020 y=-6.240 z=-0.790	x=-1.020 y=-4.860 z=-0.730

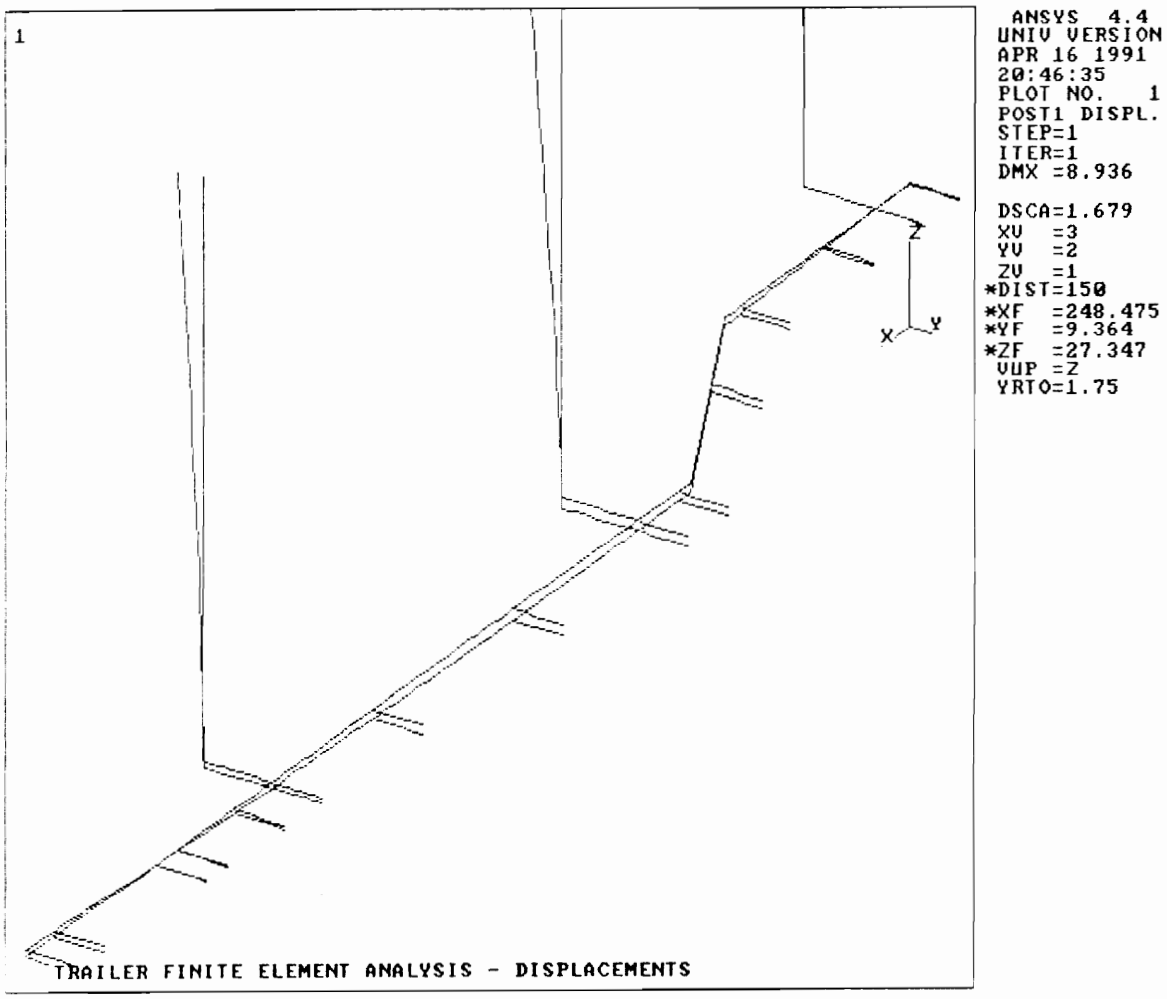

Figure 52. The Deformed Geometry of the Gooseneck Trailer: Loading Case 2 (i.e. 58,320-pound payload).

The prevailing stresses in each cross-section of the trailer are the maximum normal stresses due to bending in vertical planes (about the nodal y-axes). These stresses have been plotted along the structural members of the trailer in Figure 53. Figure 54 shows maximum normal stresses from bending in the horizontal planes (about the nodal z-axes). The analysis confirmed that both the bolsters and the main I-beams at the gooseneck are the only members of the structure stressed significantly by axial forces (Figure 55).

A vector sum of all stresses for each node was plotted along the trailer components in order to obtain a complete picture of the stress distribution (Figure 56). Figure 57 shows the distribution of the algebraic sum of maximum absolute values of stresses along the geometry of the trailer (Table 12).

The 3-D analysis confirmed that the most stressed components of the trailer are the very bottom cross-sections of standards. The tensile strength of the structural T-1 steel (also designated as ASTM A514), which was used for fabricating the standards, is estimated to be equal to 120,000 psi minimum (Reyson, 1989). The computed maximum stresses result in design factors (against tensile strength) in the range of SF=<0.70;1.17> and SF=<0.96;1.45> for the standards on the second and third bolster, respectively, depending on the method of computing loading on standards.

All other structural components of the trailer were manufactured from ASTM A36 steel, which has a tensile strength equal to 58,000 psi. The following design factors are associated with some of the components; second bolster: SF=<1.52;2.38>, third bolster: SF=<1.61;2.48>, main beam: SF=<2.49;2.50>.

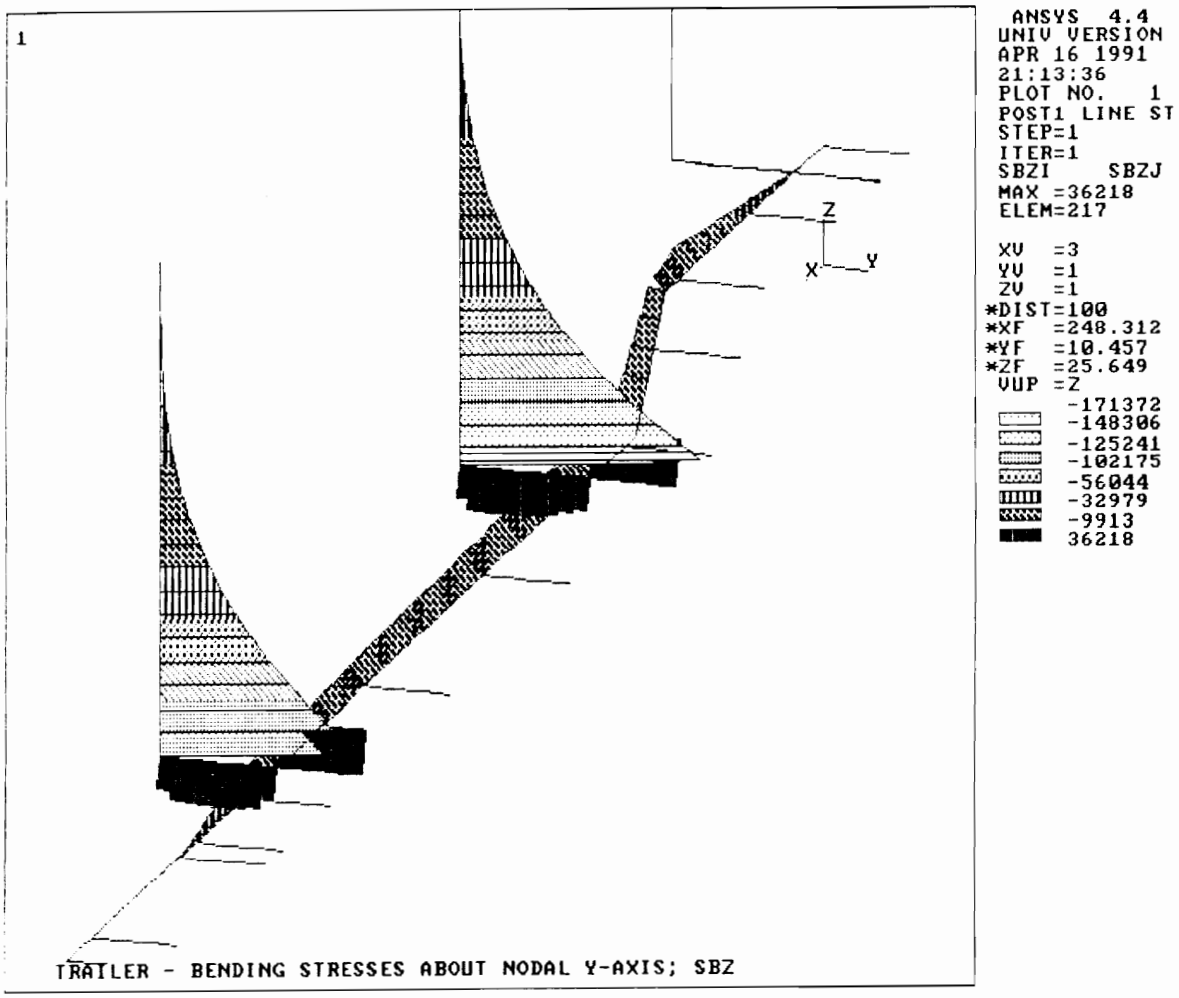

Figure 53. Results of the 3-D Elastic Beam Element Stress Analysis of the Gooseneck Trailer: Bending stresses about a nodal y-axis (bending in vertical plane).

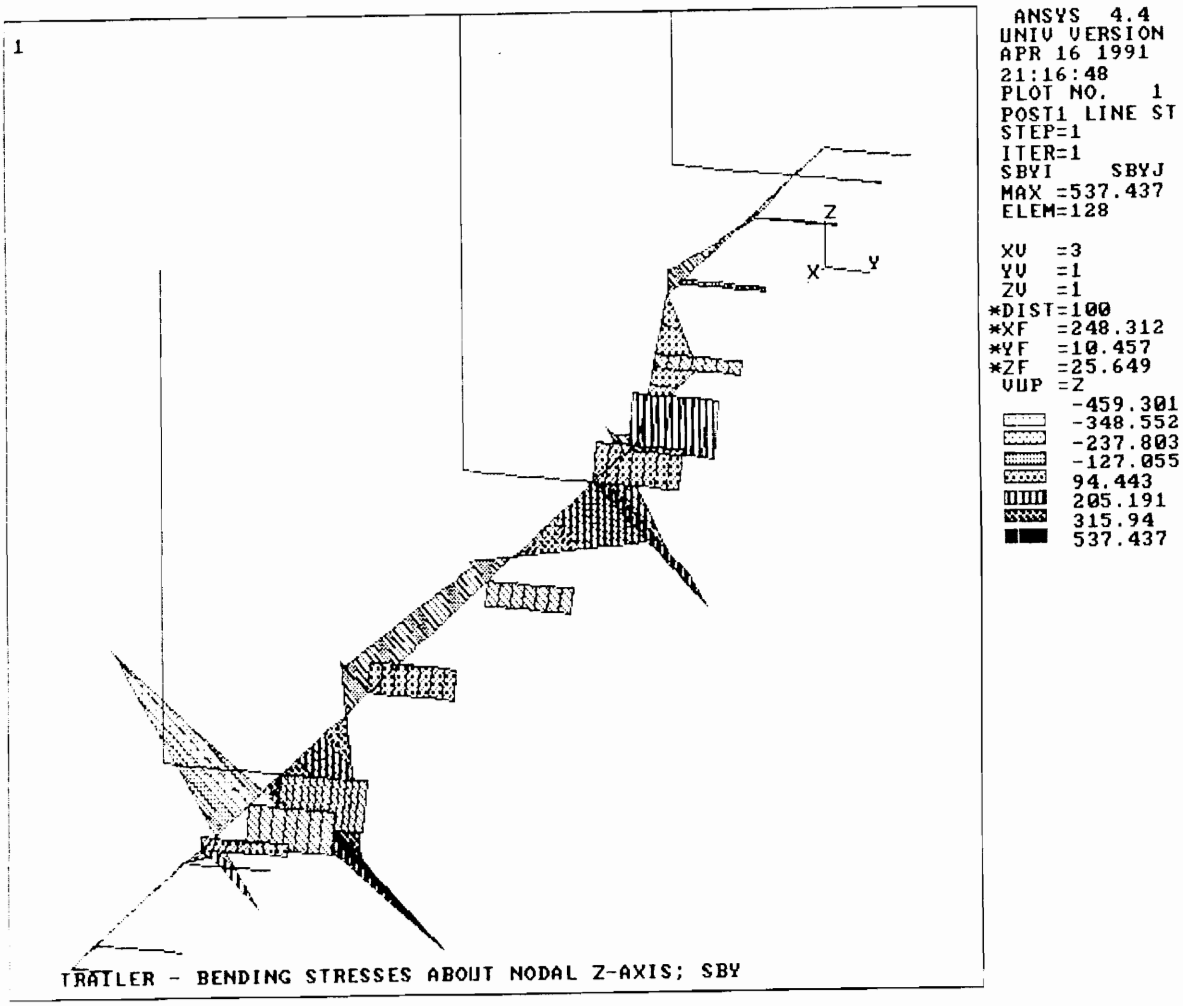

Figure 54. Results of the 3-D Elastic Beam Element Stress Analysis of the Gooseneck Trailer: Bending stresses about a nodal z-axis (bending in horizontal plane).

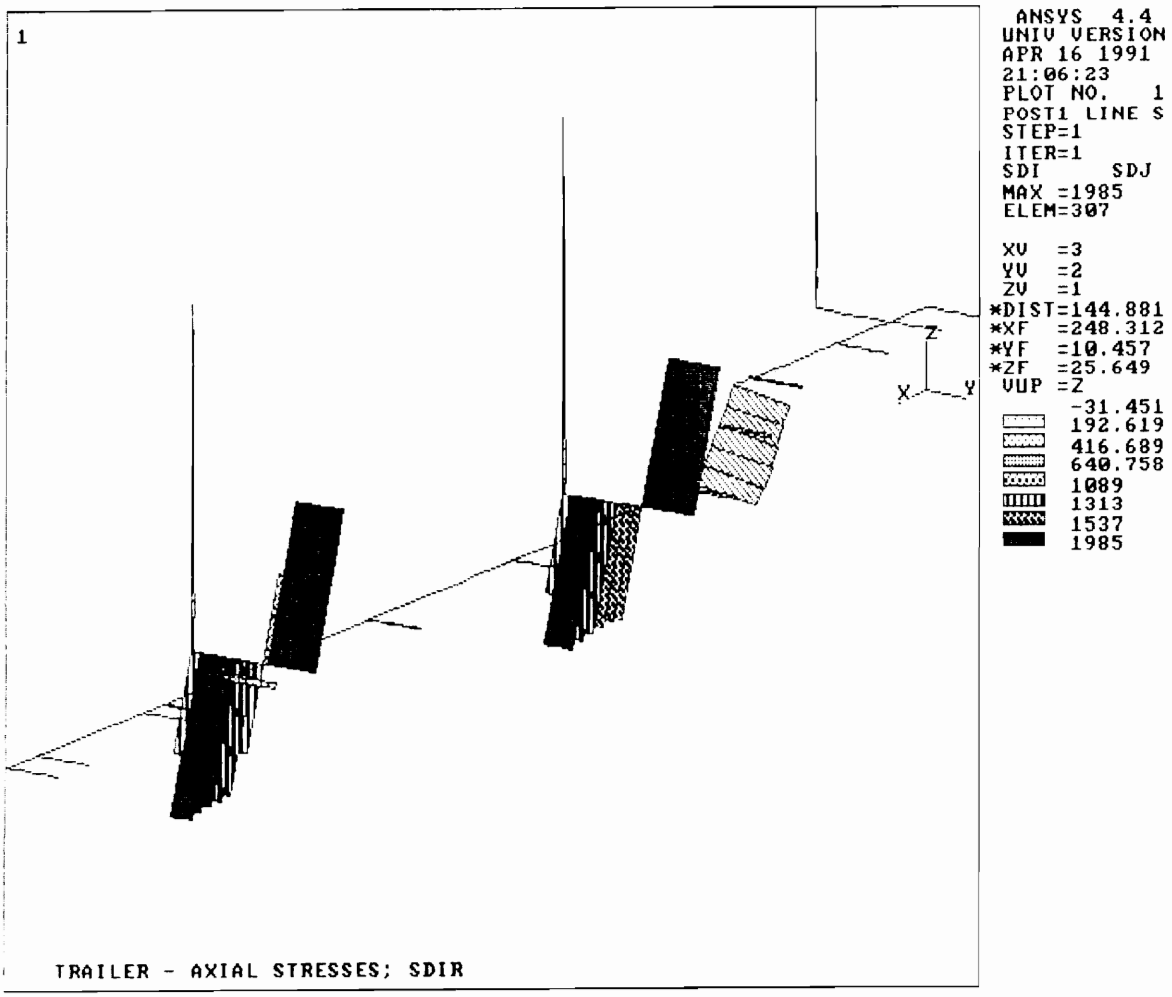

Figure 55. Results of the 3-D Elastic Beam Element Stress Analysis of the Gooseneck Trailer: Axial stresses plotted along the trailer geometry.

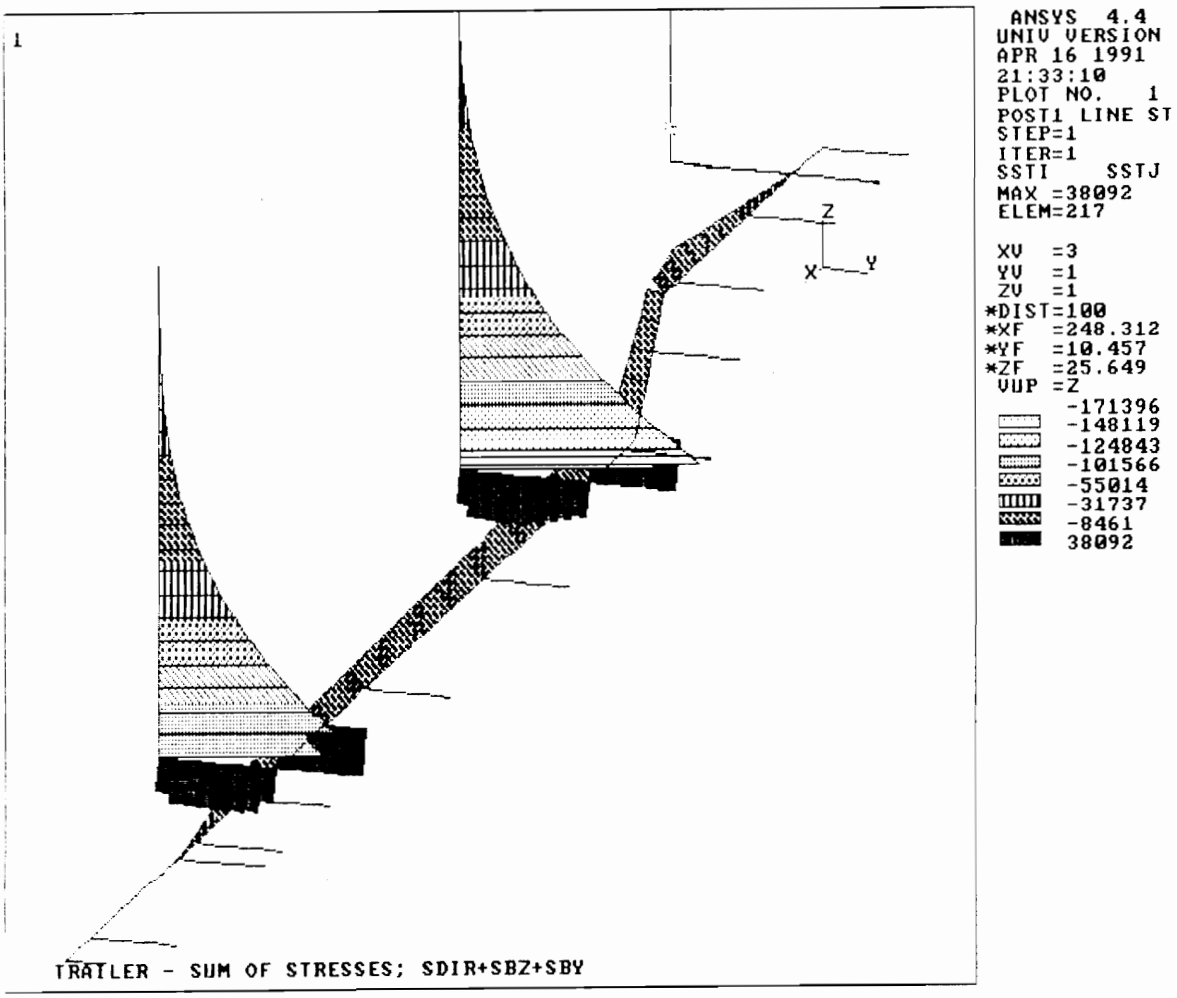

Figure 56. Results of the 3-D Elastic Beam Element Stress Analysis of the Gooseneck Trailer: Vector sum of maximum normal stresses.

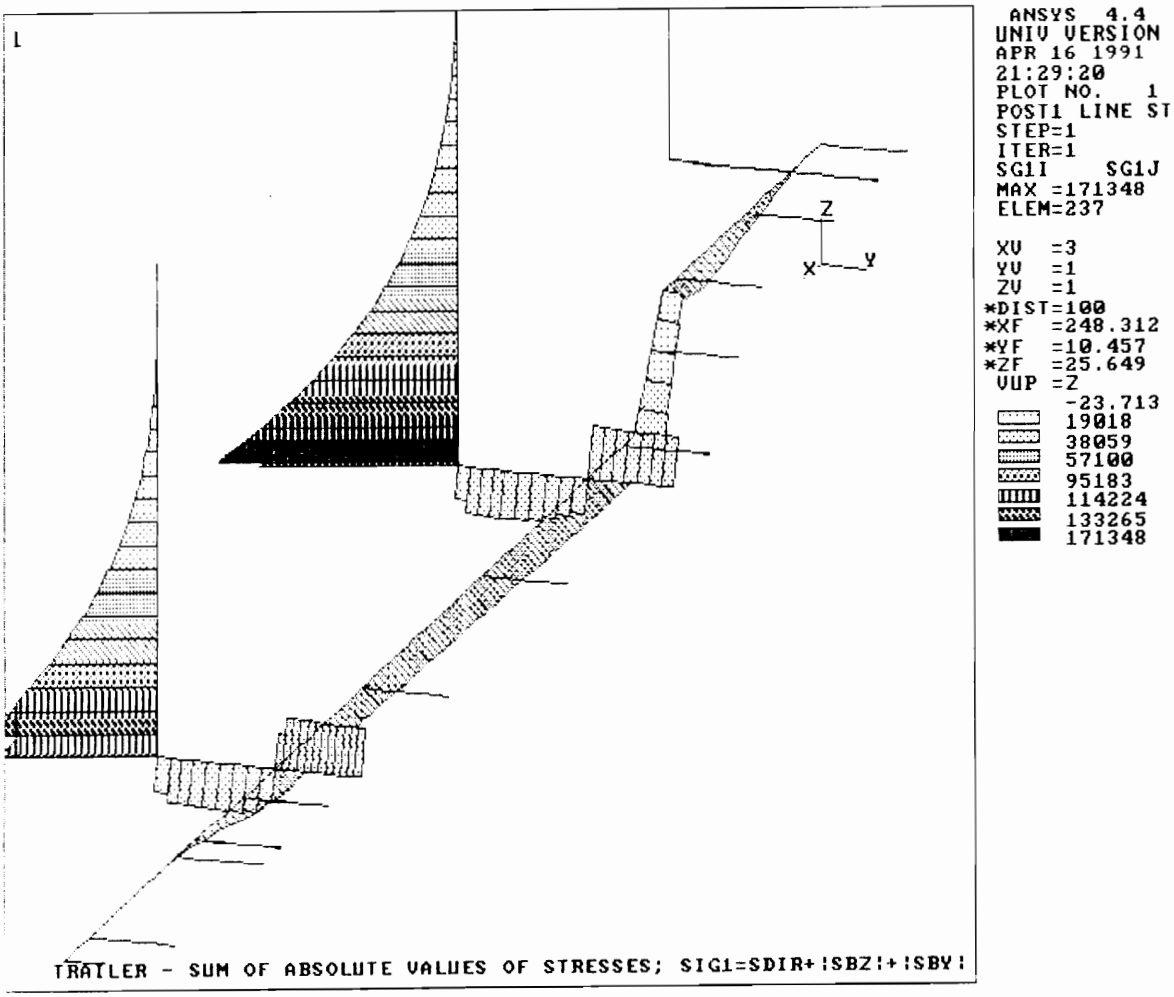

Figure 57. Results of the 3-D Elastic Beam Element Stress Analysis of the Gooseneck Trailer: Algebraic sum of absolute values of the maximum normal stresses.

CONCLUSIONS

The 3-D analysis confirmed the results obtained by the previous 2-D analysis. The same overall stress distribution pattern was computed for the trailer. Minor differences in the stress magnitudes originated primarily from the higher precision of the 3-D model (over 50 different cross-section properties were employed, whereas the FEM analysis was limited to 10 per model). Also, the simplifying assumptions of the 2-D formulation had an impact on the values of the computed stresses.

The first method of computing loadings on standards (i.e., the hydrostatic pressure concept) highly overestimated the stresses induced into the structure. The results were verified in the field by using the same boundary conditions as those imposed in the model. The trailer was loaded with approximately the same payload as was used in the analysis, and the joint displacement of standards' tops was measured. The second method of computing loadings on standards (i.e. group of logs partially supported by a standard approach) proved to be more realistic and should be used in further analysis.

The preliminary analysis of the gooseneck trailer indicated that the bottom sections of the standards on the second and third bolsters on the trailer are over stressed (the highest design factor was only DF=1.45). A modification of the standard design was recommended to the manufacturer. The modification was soon made on the existing three prototypes of the trailer, enhancing safety of the structures.

The following locations were identified as stress critical, and selected for strain gage placements for the experimental stress analysis:

1. Bottom flanges of the main beams at the cross sections under the second and the third bolsters, and at the gooseneck of the trailer;

2. Bottom sides of the cantilevered sections of the bolsters at the tips of the reinforcing gussets;

3. Outer sides of standards at the bottom cross-sections (at the level of the tips of the reinforcing gussets);

4. Locations on the main beam web at the neutral axis of a cross-section were selected to detect shear stresses in torsion due to twisting torques combined with shear stresses resulting from lateral forces. Locations on the neck, in the drop between the second and third bolsters, and behind the third bolster were selected for this purpose.

Figure 58 shows the selected locations for strain gage placement on the gooseneck trailer.

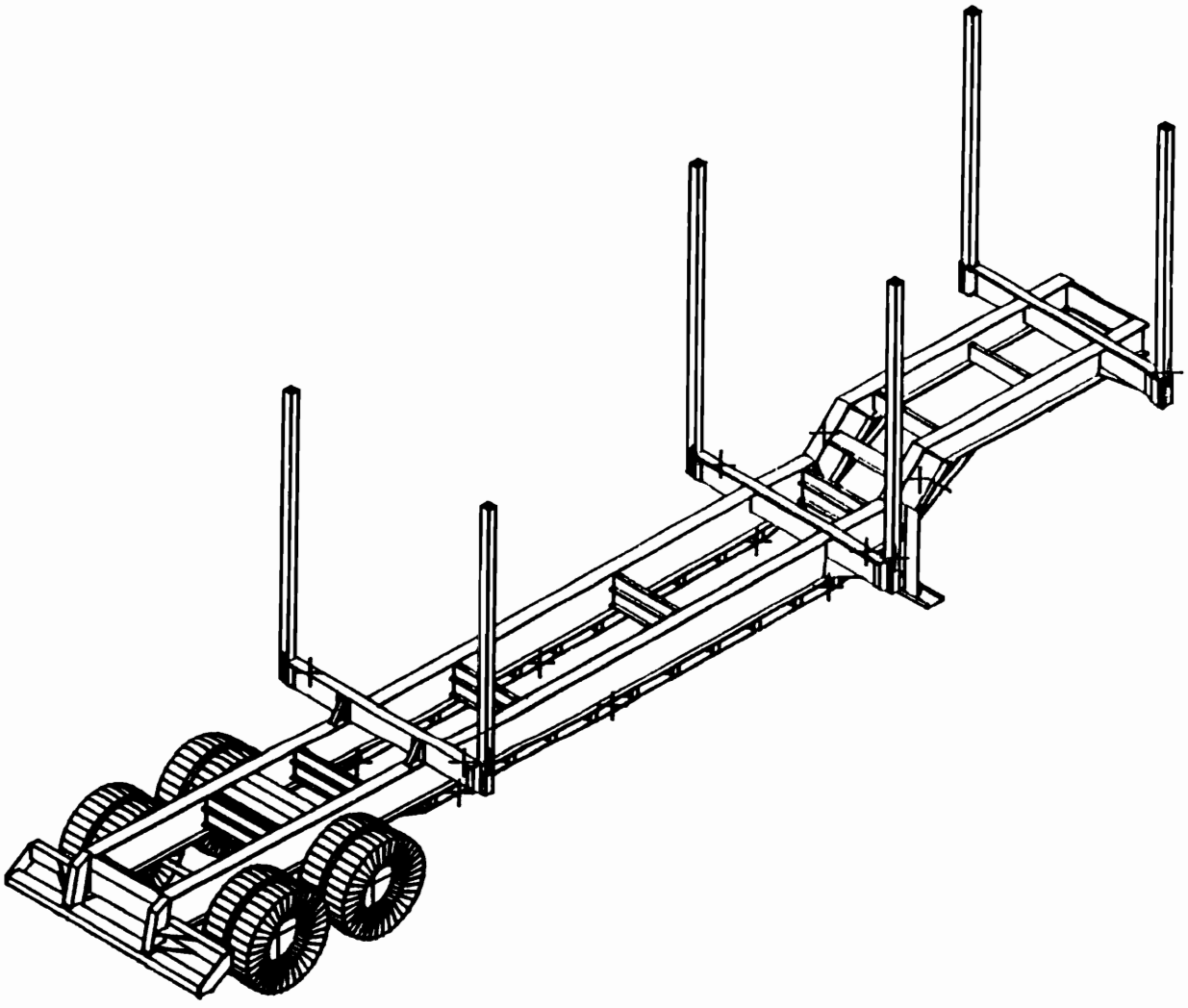

Figure 58. Locations of Strain Gage Placement for Experimental Stress Analysis of the Gooseneck Trailer.

CHAPTER 5. EXPERIMENTAL STRESS ANALYSIS

Introduction

A log trailer is subject to loads varying with time throughout its service life, similar to any other vehicle. A designer is faced with the uncertainty of the nature of the service-load histories exerted on the structure. The operational loads must usually be determined experimentally to design the structure without unnecessary expenditure of material and effort (Buxbaum, 1979).

A log trailer is an elastic mechanical system, its natural modes of vibrations are excited by time-varying operational loads. The recorded structure response is in the form of stress-time history at a point of measurement, thus at locations away from the point of load introduction. Therefore, it usually shows significant differences with regard to the characteristics of the actual load-time history because a stress-time history contains both the effects of external loadings and the elastic behavior of the structure. Therefore, the experimental trials of the selected trailers included measurements of the dynamic loads in terms of accelerations in three directions of space. In general, it is impossible to observe the external loads when investigating only the structure response. Recording stress-time histories was also key for approximating fatigue life of the existing light-weight designs. Such predictions provide an objective evaluation of various trailer design techniques.

Field measurements should cover all possible loading cases, preferably in the same time proportion as the trailer experiences in its service life. The tests, therefore, included simulating extreme situations as well as monitoring the loads and the resultant dynamic stresses during normal work cycles.

Theoretically, there are two possible failure modes of a log trailer: by plastic deformation due to an excessive impact loading exerted on the structure, and by fatigue due to repeated loadings. The data recorded during the field experiments were used to detect peak values of the dynamic loading and to isolate typical service load spectra on the trailers.

Field Trials

The gooseneck thinning trailer was selected to be tested first. Locations for strain gage placements were determined through the preliminary stress analysis. The experimental dynamic stress measurements of the trailer were carried out during weeks July 8 and July 15, 1991, in Perry County, Mississippi.

Altogether 18 strain gages, 13 single-segment and 5 three segment 45 ^{o} rosettes, were installed on the trailer. Three strain gage accelerometers measured vertical, longitudinal, and sideways accelerations which were associated with the dynamic forces exerted on the load and the trailer. The accelerometers were installed on the trailer at a midpoint of the cross member closest to the calculated vehicle center of gravity.

First, the trailer was subjected to simulated extreme situations. The trailer was overloaded by 12% to 30% and driven over a closed loop on an abandoned shortwood yard (Figure 59). The road conditions corresponded to those of a formed sand forest road. The surface was rough, with numerous shallow, transverse ridges; some of the sections were covered with bark, small limbs and other wood debris. The

surface was dry and dusty. The driver was asked to drive with increasing speed up to the maximum speed at which he still felt safe.

The trailer was tested during hard cornering, braking, forward acceleration (Figure 60), and loading and unloading with a knuckleboom loader (Figure 61). Experiments were repeated for two loading patterns: logs spanning all three bolsters versus logs resting on the second and the third bolsters only (thinning material), and for two load types: pine and hardwoods.

The trailer was then driven along a 30-mile closed loop, over randomly selected roads. Unformed and formed sand and graveled forest roads, a one-lane community road, and a two-lane state highway were included.

In the second part of the study, the dynamic loading and the resultant stresses in the log trailer were monitored during typical service. The trailer was loaned to Owen's Logging Inc. in Wiggins, Mississippi, an independent contractor, for two days. During that time it carried five loads of pulp logs and one heavy load of poles. Stresses were measured and recorded during loading with a Barko 160A on an in-woods landing (Figure 62), and during unloading with a Barko 275 knuckleboom loader at the woodyard, and with a Caterpillar front end-loader at a pole plant (Figure 63).

The second set of field trials, with the light full-tree trailer, were carried out in Taylor County, Florida, in March of 1992. The procedures for the experiments were the same as those used for the gooseneck trailer. A knuckleboom loader, forklift (Figure 64), and an overhead portal crane (Figure 65) were included as loading and unloading equipment during the study. Monitoring dynamic loadings and the resultant stresses during normal work cycles was performed when the trailer was operated by Regan Fox Logging, Inc., an independent logging contractor based in Perry, Florida, and current owner of the trailer.

Figure 59. Experimental Stress Analysis of the Gooseneck Trailer: Simulating extreme situations--hard cornering.

Figure 60. Experimental Stress Analysis of the Gooseneck Trailer: Simulating extreme situations--hard braking.

Figure 61. Experimental Stress Analysis of the Gooseneck Trailer: Simulating extreme situations--loading with a knuckle-boom loader.

Figure 62. Experimental Stress Analysis of the Gooseneck Trailer: Monitoring the dynamic loading and the resultant stresses at critical locations--loading with a Barko 160A knuckle-boom loader on in-woods landing.

Figure 63. Experimental Stress Analysis of the Gooseneck Trailer: Monitoring the dynamic loading and the resultant stresses at critical locations--unloading with a Cat front-end loader at the pole plant.

Figure 64. Experimental Stress Analysis of the Full-Tree Trailer: Monitoring the dynamic loading and the resultant stresses at critical locations--unloading with a forklift on the sawmill wood yard.

Figure 65. Experimental Stress Analysis of the Full-Tree Trailer: Monitoring the dynamic loading and the resultant stresses at critical locations--unloading with a single-grip crane on the pulp mill wood yard.

The trailer was used to haul full trees to the Procter and Gamble Cellulose pulp mill in Perry, and to deliver saw logs to a local sawmill.

Results

Maximum Dynamic Loading

The two selected lightweight trailers were tested for a total of three weeks. The primary objective was to monitor dynamic loading exerted on a log trailer. The peak values of the dynamic loads were of fundamental interest. Knowing magnitudes of these values should enable the designer to choose a required design factor for the given yield strength of the material to minimize the possibility of failure by excessive plastic deformation.

Two different loading conditions for the trailer were observed: when the trailer was driven empty, and when it was carrying a load. The two modes were characterized by completely different mass-to-stiffness ratios of the structure. When empty, the trailer weighs about 5.5 times less than when loaded, but the stiffness of the running gear is then somewhat greater (less deflected tires are stiffer).

The following maximum dynamic loadings exerted on a log trailer for the empty mode, expressed in terms of gravity acceleration "g", were detected in the course of the entire experiment:

1. Vertical = 2.75 g (in addition to gravity);
2. Sideways = 1.20 g;
3. Longitudinal = 0.66 g;
4. Resultant (vector sum) = 3.99 g (including gravity).

The maximum magnitudes of dynamic loading were encountered when the full-tree trailer was driven over Florida State Highway 19. The signal was recorded at the moment the vehicle was passing over a pot hole at a speed of about 55 mph (Figure 66). The resultant maximum loading, computed as a vector sum of the three rectangular components, was determined to be 3.99 g. This loading is rather theoretical since it is unlikely that all maximum dynamic loadings will take place exactly at the same instance. Stresses caused by dynamic loads were well below yield strength of the material. It is unlikely that the trailer could be plastically deformed under normal conditions (unless tipped over or crushed in a road accident). However, these loadings contribute to the cumulative fatigue damage of the structure.

The following maximum dynamic loadings were exerted on a log trailer in the loaded mode (expressed in terms of gravity acceleration "g"):

1. Vertical = 1.10 g (in addition to the static load);
2. Sideways = 1.12 g;
3. Longitudinal = 0.25 g;
4. Resultant (vector sum) = 2.39 g (including static load).

The maximum vertical loading of 2.10 g (which includes the static load) was measured when the trailer, loaded with a 51,920-pound full-tree payload, was driven over a formed sand road at about 35 mph (Figure 67). The trailer was passing over a bump at the moment when the signal was recorded (Figure 68). The maximum sideways and forward dynamic loadings were detected when the vehicle was braking for another bump on the road, a minute later (Figure 69). The total resultant maximum loading on the trailer, computed as a vector sum of the three rectangular components was determined equal to 2.39 g (including static load). Again, this resultant loading should be treated as theoretical since it is unlikely that all three maximum loading would occur at the same instant.

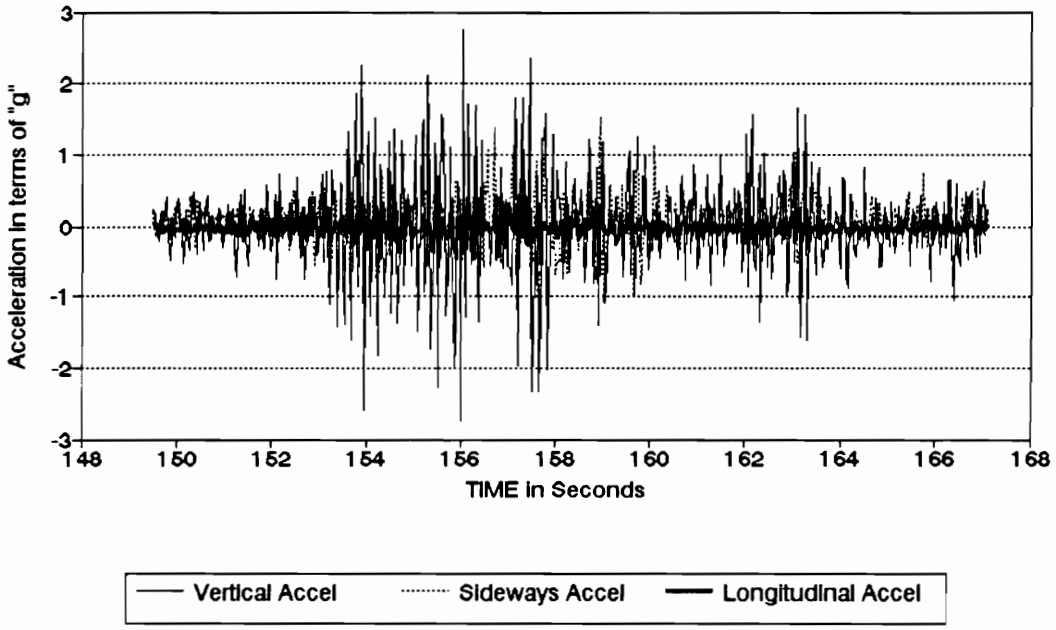

Figure 66. Maximum Vertical Dynamic Loading Acting on a Log Trailer for the Empty Mode.

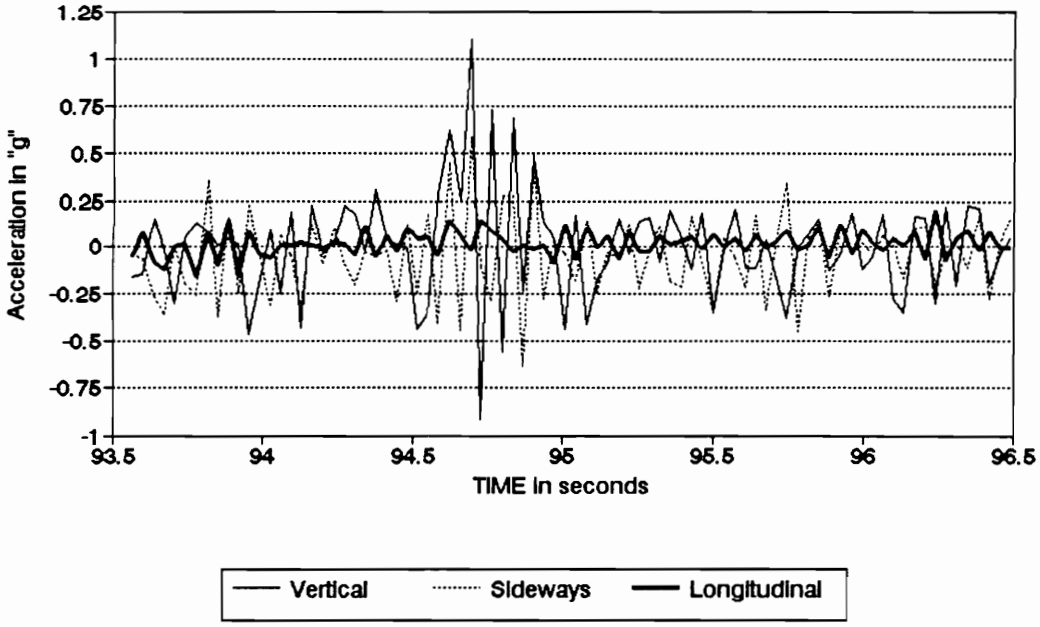

Figure 67. Maximum Vertical Dynamic Loading Acting on a Log Trailer for the Loaded Mode.

Figure 68. Situation for which the Maximum Lateral and Forward Dynamic Loading were detected.

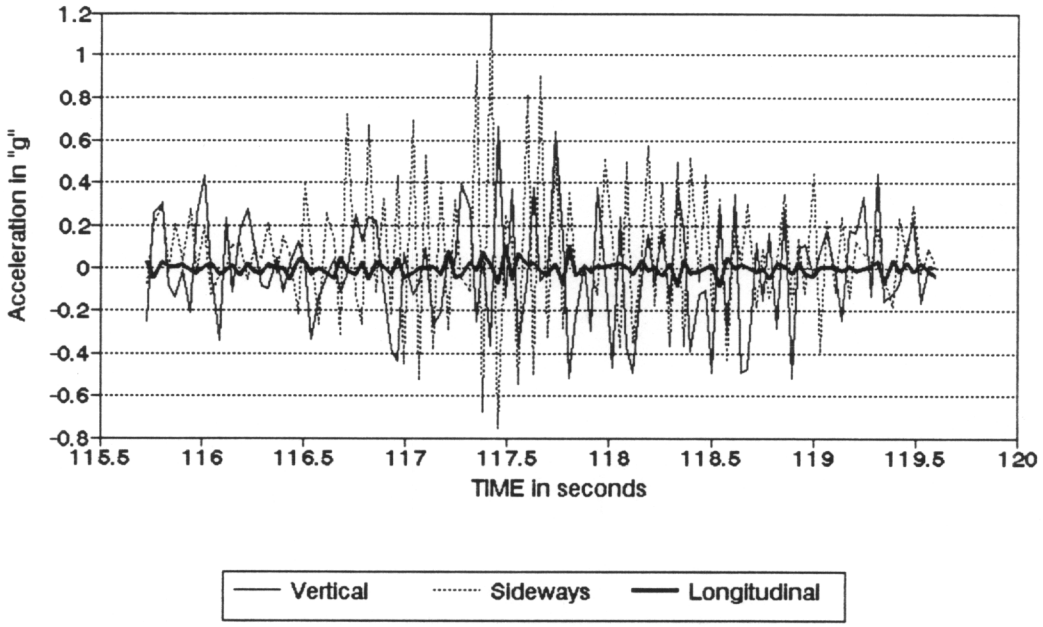

Figure 69. Maximum Lateral Dynamic Loading Acting on a Log Trailer (Loaded Mode).

A slightly lower sideways dynamic loading, 1.05 g, was recorded when the gooseneck trailer was accidentally hit hard on the front standard by a grapple during loading with the Barko 160A nuckleboom loader in the woods.

In general, it was observed that larger amplitudes of dynamic loadings occurred when trailers were driven empty over a highway at a highest legal speeds. However, for the loaded mode, greater amplitudes of the loading were observed when traveling at 30 to 40 mph over low quality roads with numerous bumps and pot holes. It was also found that the trailers were frequently subject to a large impact loads during loading and unloading operations.

These findings lead to the conclusion that a design of a log trailer should incorporate a design factor (as computed as a ratio of the minimum yield strength of the material to the maximum computed static stress) greater than 2.10, to exclude the situations when local plastic behavior develops at the most critical locations under dynamic conditions. The 2.10 value is the absolute minimum design factor and assumes a "normal operation" of the trailer (excluding the situations of obvious misuse). Because of the difficulty of predicting the conditions under which a trailer will operate, it is recommended that the design factor be taken as 2.5 or 3.0 to create a buffer to accommodate unforeseen surges in dynamic stresses.

When local plastic behavior develops, the structure is still able to carry more load up to the full plastic load. The difference between the fully plastic load (when trailer fails due to excessive deformation) and the load corresponding to initiation of yielding at highly stressed points in the critical cross-section acts as an additional safety buffer. Local initiation of plastic deformation must not be permitted, however, because it induces residual stresses in the structure. Surface tensile residual stresses contribute to accelerated fatigue damage of the structure.

Trailer Dynamic Response

A dynamic response is unique for a given structure and reveals strengths/shortcomings of the particular design. For structures consisting of the same members, and having similar construction, however, it is very beneficial to generalize their dynamic behavior for the purpose of a lightweight design. A discussion of a generalized dynamic response of the tested trailers follows.

The dynamic response of the trailers was measured in terms of stress-time histories at critical locations on the trailer. The signals varied as a function of member type and depended on the characteristic of the dynamic loading. This resulted in a wide range of the trailer responses.

Figures 70 and 71 show two different responses in the front standard of the full-tree trailer as a result of dynamic forces exerted during loading with a nuckleboom loader (Barko 160A). The dynamic stress variation shown on the first plot occurred from a group of logs being dropped on a corner of the standard-bolster junction. This caused forced vibrations in the member. The induced dynamic stress in the standard bottom cross-section is characterized by a high amplitude of about 16 ksi and high frequency as a result of the force being applied at a low height on the standard. In contrast, Figure 71 shows the dynamic response in the front standard when an impact load was first applied at approximately half of the standard height as the loader grapple pushed a group of logs down to the bolster. The high mechanical energy was absorbed by the member, which is revealed by the high stress and duration of the surge. This last plot exemplifies a situation in which a standard may fail due to excessive impact loading. It is impossible to state any exact numerical value for the design factor for a standard. It is recommended, however, that a high tensile steel (of at least 100 ksi yield strength) be used to fabricate standards to maintain both low tare weight and the high resisting bending moment (RBM) of the member.

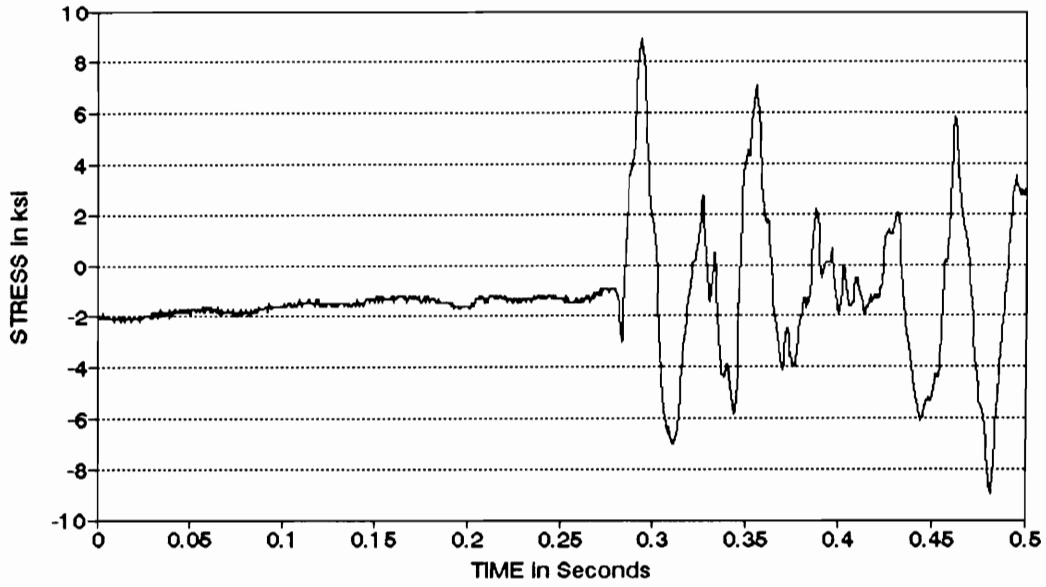

Figure 70. Dynamic Stress in the Front Standard Recorded During Loading with a Knuckleboom Loader.

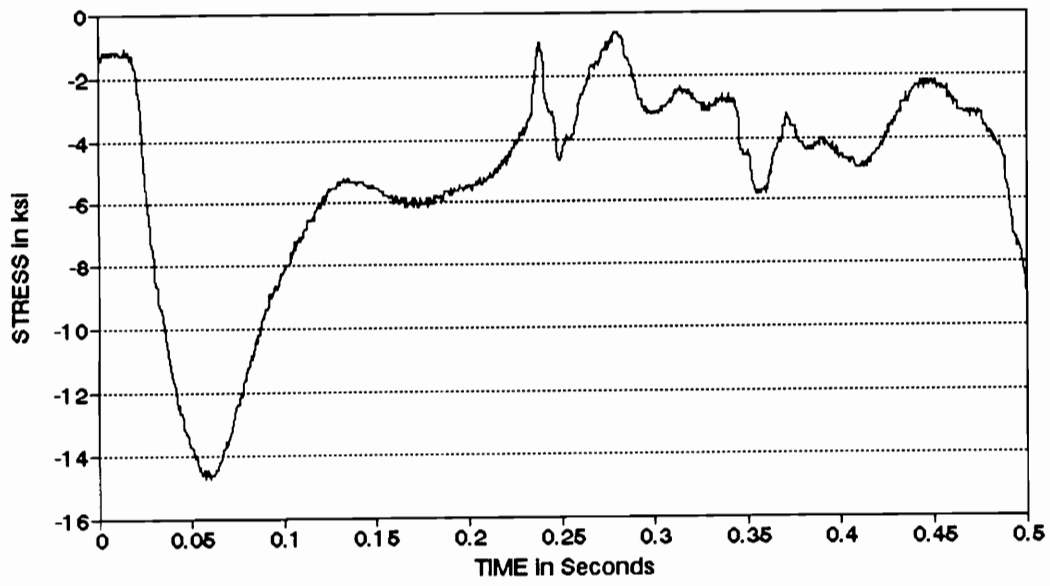

Figure 71. Dynamic Response in the Front Standard on the Impact Load During Loading with a Knuckleboom Loader.

A high tensile material has also the advantage that it deflects proportionally more (almost three times more than the standard ASTM A36 steel), and thus, allows for easier and quicker load redistribution to the other members. However, large displacements are sometimes not acceptable .

A trailer's response to a dynamic load from the road is shown in the following two plots of dynamic stress in the main beam of the gooseneck trailer. Figure 72 shows a signal of about 3 ksi amplitude and 1.8 Hz frequency--the excited vibrations of the trailer frame at the second bolster. The stress was recorded when the trailer carrying a 64,660 pound tree-length payload was driven over a forest sand road with deep ruts. The signal corresponds to a "smooth" ride--there is only a slight mean stress variation present, but the amplitude and frequency stay fairly constant. The dynamic stress induced at the same location when the trailer encountered a shallow ditch in the road is shown in Figure 73. Both the amplitude and frequency of the signal changed: the amplitude rose up to 5 ksi and the frequency increased slightly to about 2.2 Hz. This stress run exemplifies mechanical forced vibrations with strong damping because the excitation was out of phase with the trailer's natural vibrations. The effect of an excitation acting in phase with natural vibrations of the main beam is shown in the next two plots. Figure 74 represents dynamic stress when the full-tree trailer was driven loaded over a formed sand forest road at a speed of about 35 mph. The static stress was 12.5 ksi. The dynamic loading resulting from a ripple in the road and a movement of the vehicle was out of phase with natural vibrations of the loaded trailer. The resultant stresses are characterized by high frequency but rather low amplitude - about 3 ksi. However, when the trailer slowed down so that the excitation adjusted in phase with the natural vibrations of the trailer, a "mechanical resonance" response was obtained (Figure 75).

The same behavior was observed for the other members of the trailers. Figure 76 shows forced vibrations in the front bolster when the full-tree trailer was driven loaded (51,920 pound payload) over a sand road at about 20 mph. The source of the dynamic load on the vehicle was again the ripple on the road.

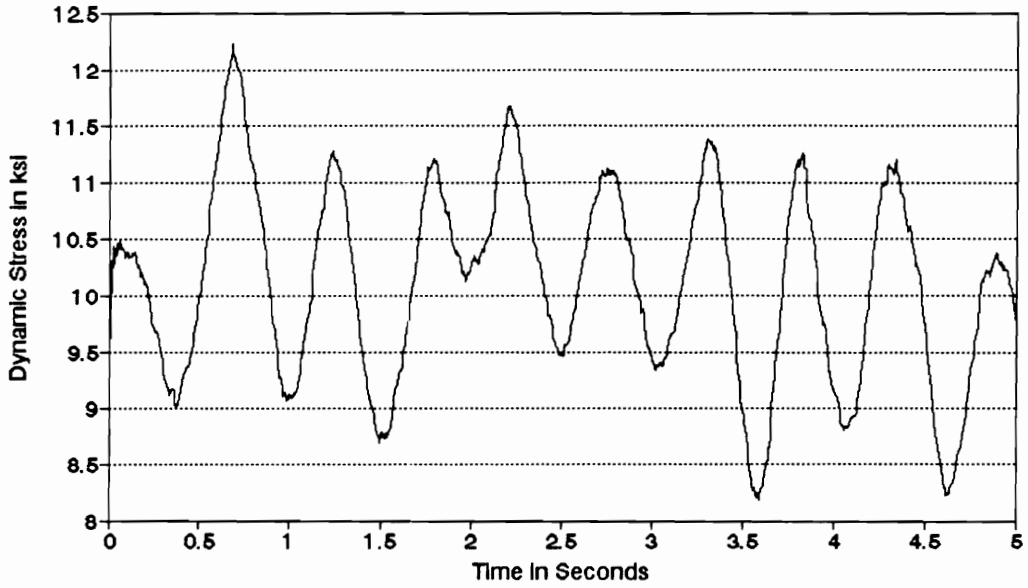

Figure 72. Dynamic Stress in the Main Beam of the Gooseneck Trailer While the Trailer Was Driven Loaded over Sand Road.

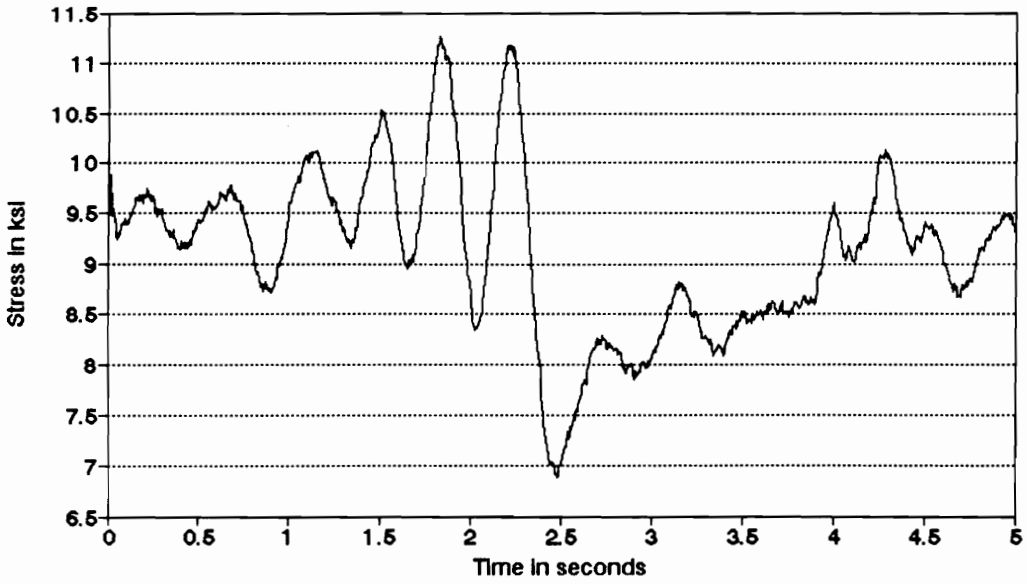

Figure 73. Dynamic Stress Recorded at the Same Point While the Trailer Was Passing over a Ditch.

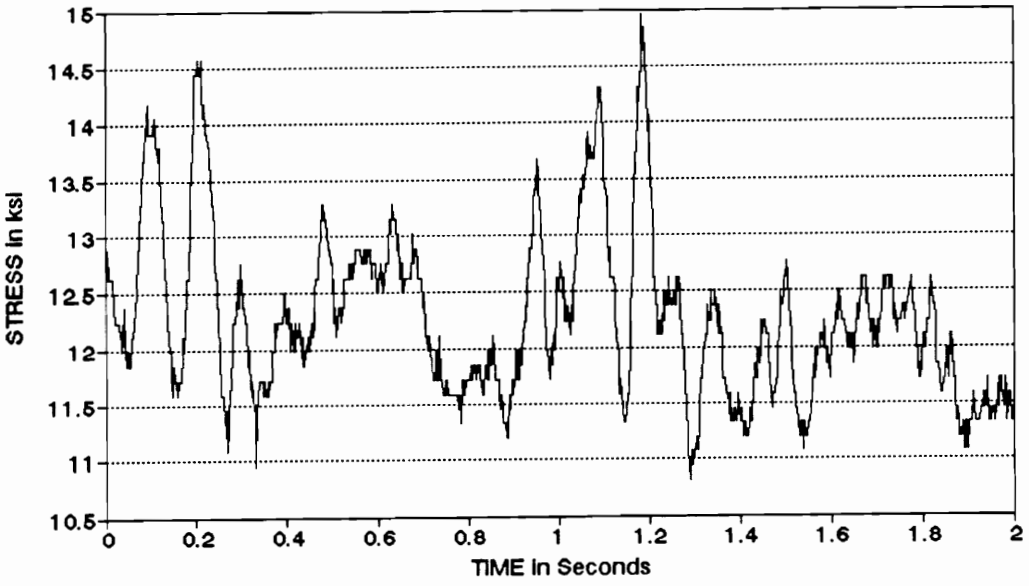

Figure 74. Dynamic Response in the Second Bolster While the Full-Tree Trailer Was Driven Fast over a Sand Road.

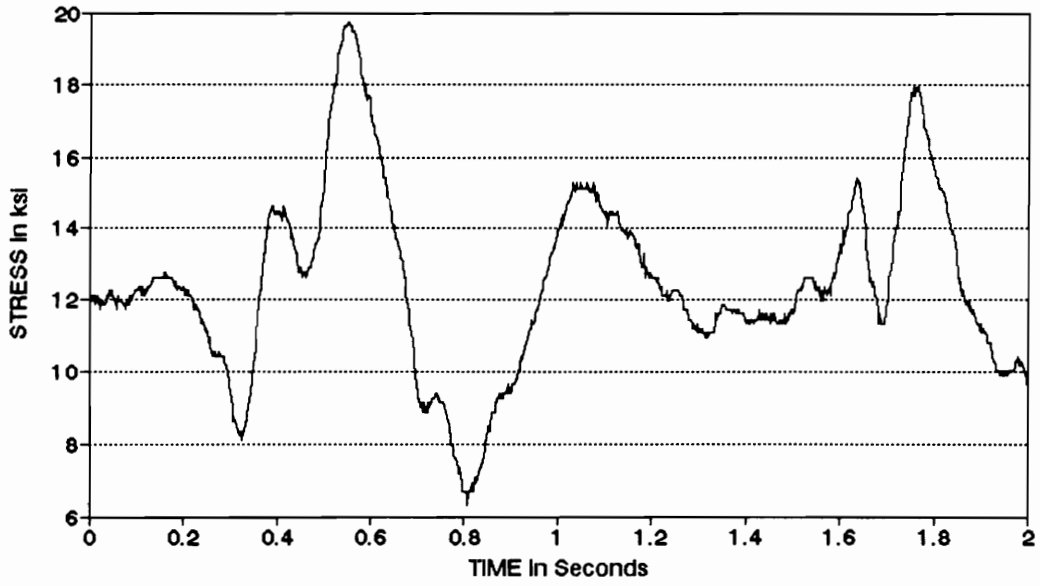

Figure 75. Resonance Response in the Same location When the Trailer Slowed Down While Passing over a Large Bump on the Road.

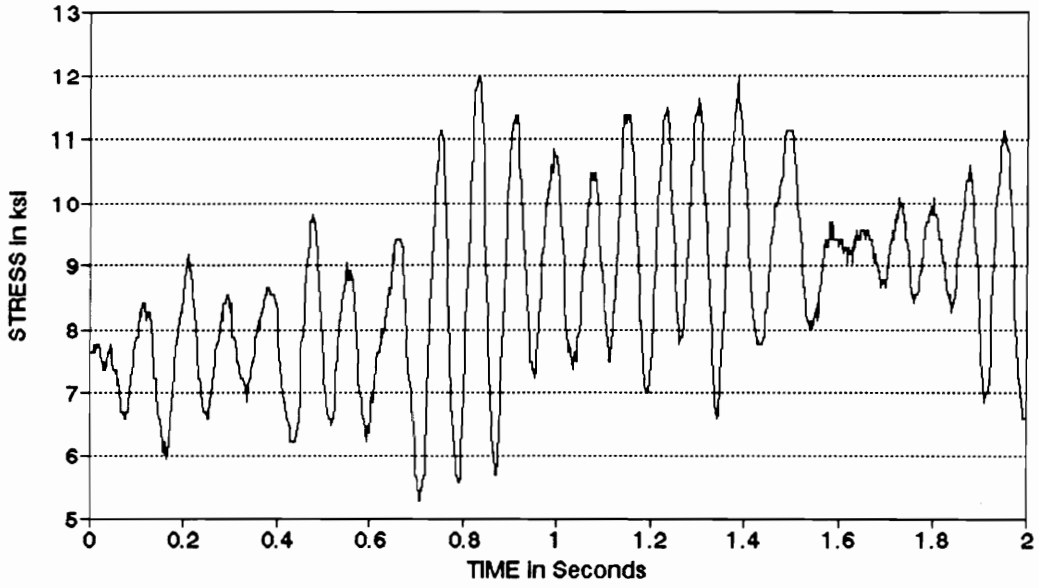

Figure 76. Stress in Front Bolster Recorded When the Full-Tree Trailer Was Driven over a Sand Road at 20 MPH.

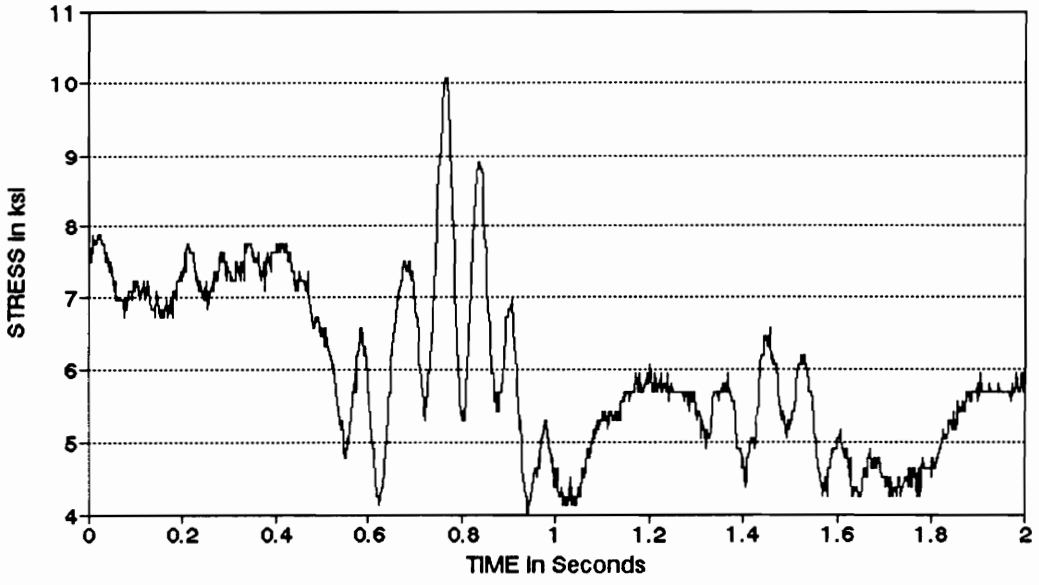

Figure 77. Stress in the Same Point Recorded While the Trailer Was Passing over Railway Tracks.

The static stress in the bolster was 9.3 ksi. Figure 77 represents a similar situation, when the trailer was crossing railway tracks on a highway. This time, however, an increase in the amplitude was accompanied by a change in "mean" stress due to the load shifting when the trailer was leaning to one side.

Examination of the dynamic stress variation in various members of a log trailer for the empty and loaded modes of operation revealed the following important observation. A typical dynamic response in a main beam under the second bolster when a trailer was driven empty is shown in Figure 78. The signal corresponds to a "smooth ride" over a highway at about 45 mph. It is characterized by a low amplitude (4 ksi) and high frequency (approximately 8 Hz). However, when the trailer was passing over a road patch or railway tracks, the signal is in a form of a high energy, forced vibrations (Figure 79), or even of a mechanical resonance (Figure 80). The amplitude approached 10 ksi, while the frequency stayed at the same high level (about 8 Hz).

Figure 81 shows a representative run of the dynamic stress in the main beam of the trailer when it was driven loaded over the same section of the highway.

The static stress, 9.5 ksi, is represented in the plot as the reference zero. The amplitude was about 12 ksi, but the frequency decreased to about 2 Hz. Thus, the amplitude of the dynamic stress for the loaded mode and the resonance response was only about 20% higher than for the empty mode in the same situation. However, for the empty mode, the trailer is subject to the fully reversed dynamic stress four times more frequently. This relationship between dynamic stresses in the main frame when the trailer was driven empty versus the situation when it was driven loaded was observed for other road surfaces. The dynamic responses for a formed forest sand road for the empty and the loaded modes are shown in Figure 82 and Figure 83, respectively. The same behavior was found for the other structural members of this trailer (Figures 84 and 85) as well as for the second trailer included in the study.

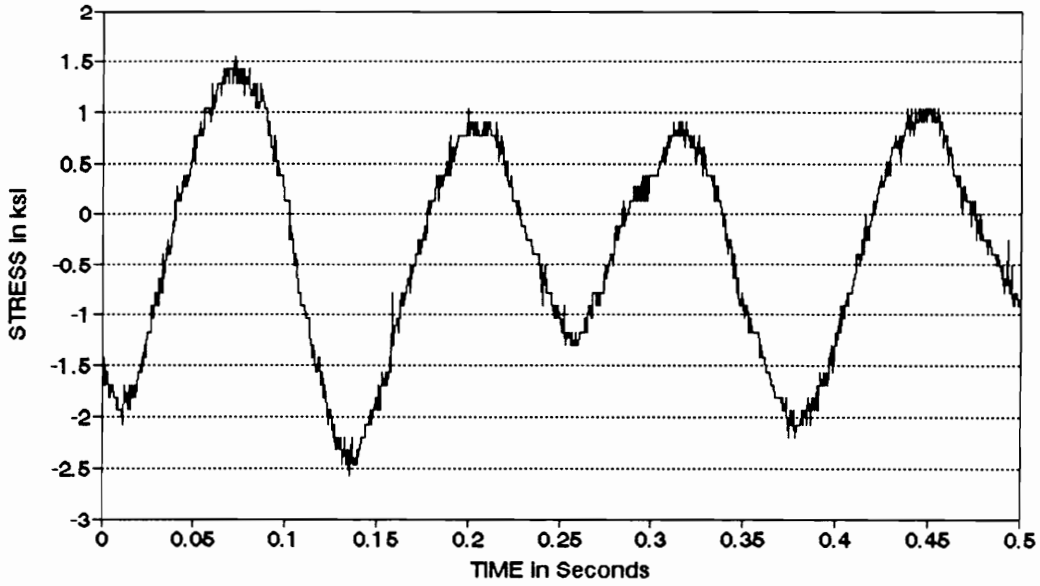

Figure 78. The "Smooth Ride" Dynamic Response in the Main Beam of the Full-Tree Trailer.

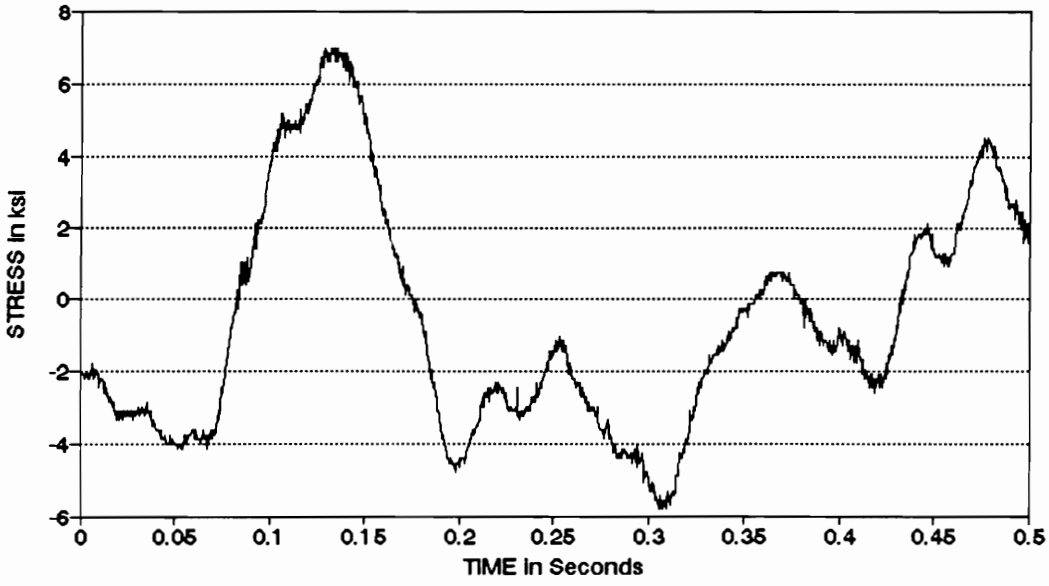

Figure 79. Dynamic Stress in the Main Beam Recorded When Passing over Railway Tracks on State Highway.

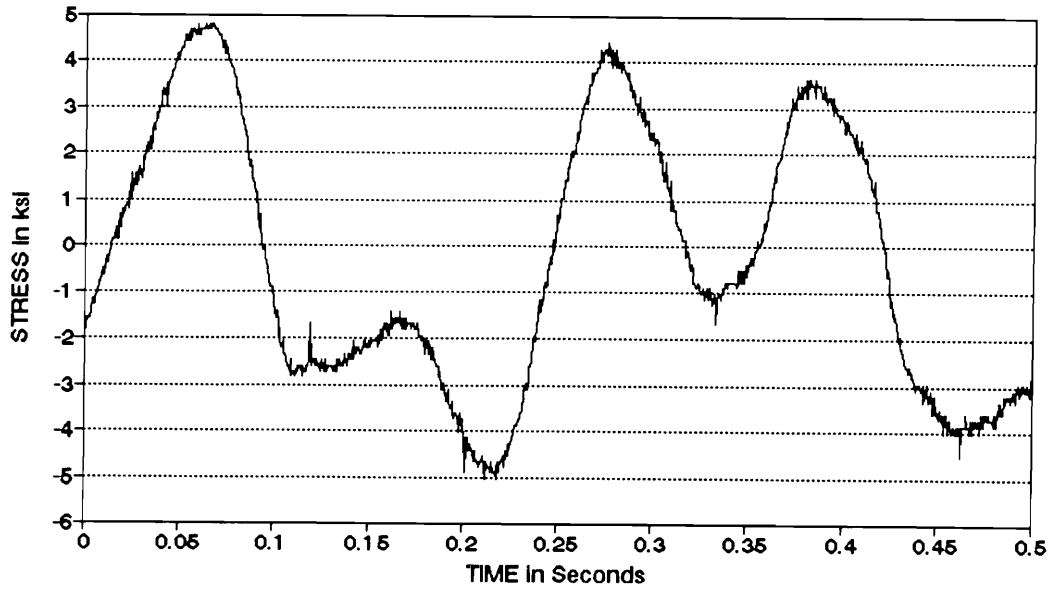

Figure 80. Mechanical Resonance Recorded for the Main Beam When the Trailer Was Driven Empty over State Highway.

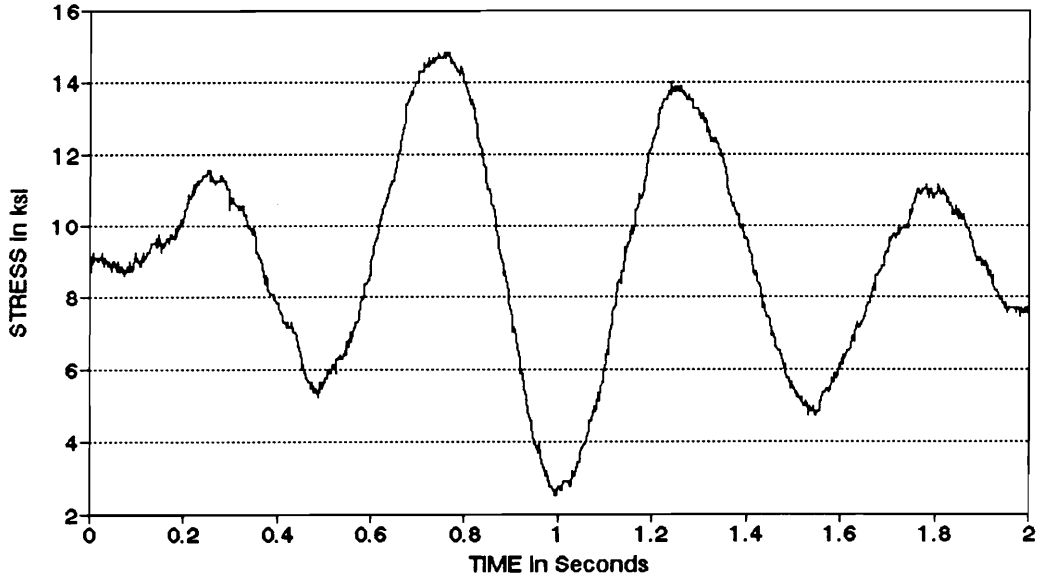

Figure 81. "Resonance" Response for the Main Beam When the Trailer was Driven Loaded over the Same Section of the Highway.

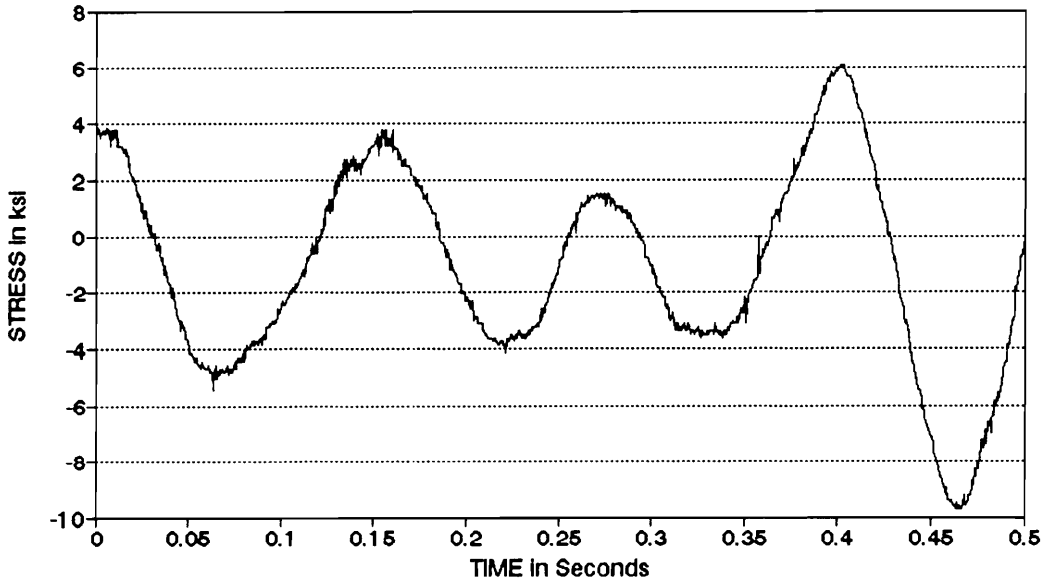

Figure 82. "Resonance" Response for the Main Beam When the Trailer Was Driven Empty over Sand Road.

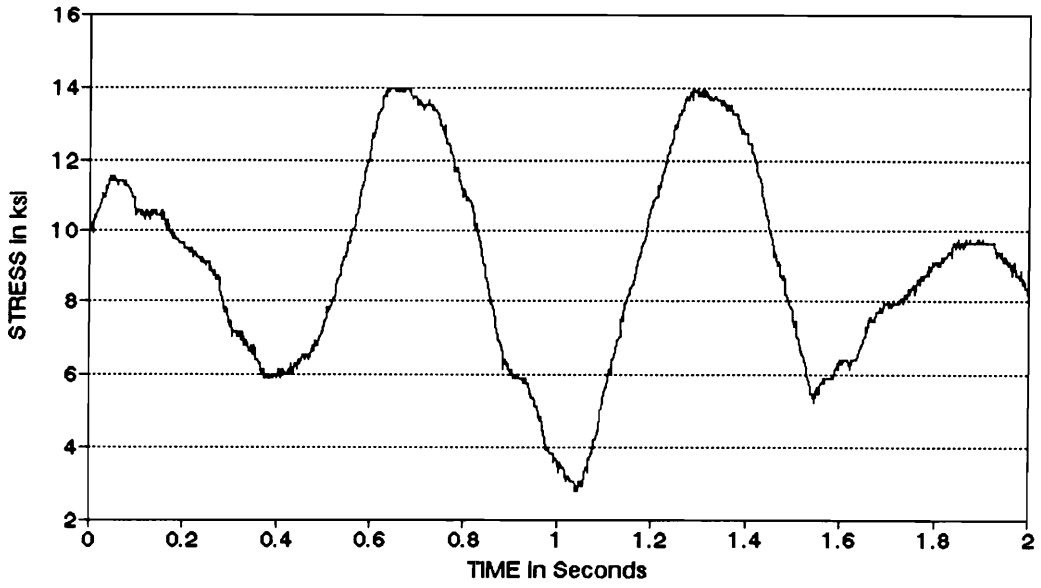

Figure 83. "Resonance" Response for the Same Member and the Same Section of the Sand Road When the Trailer Was Driven Loaded.

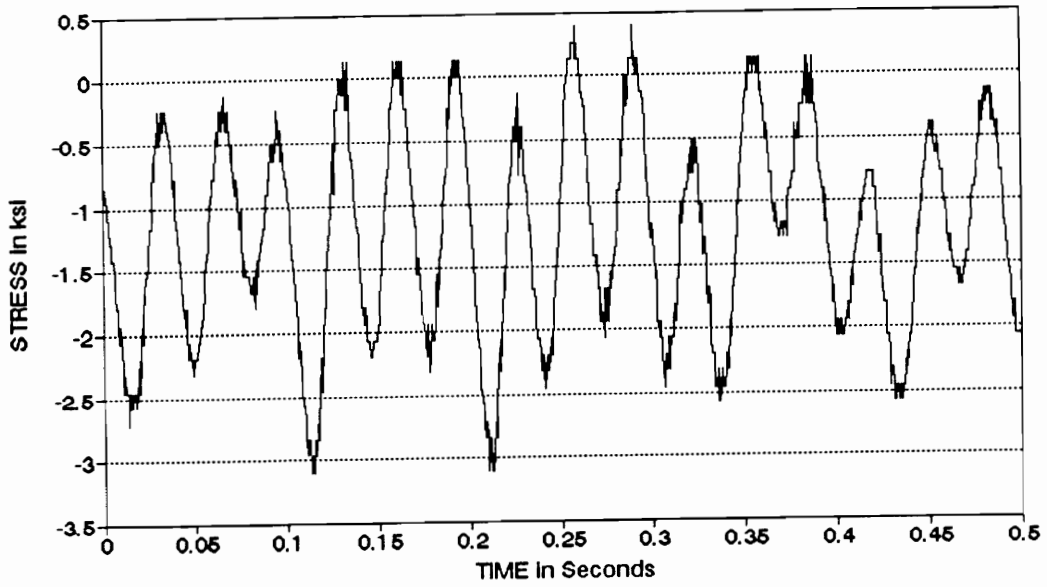

Figure 84. Dynamic Stress in Front Standard When the Trailer Was Driven Empty over State Highway.

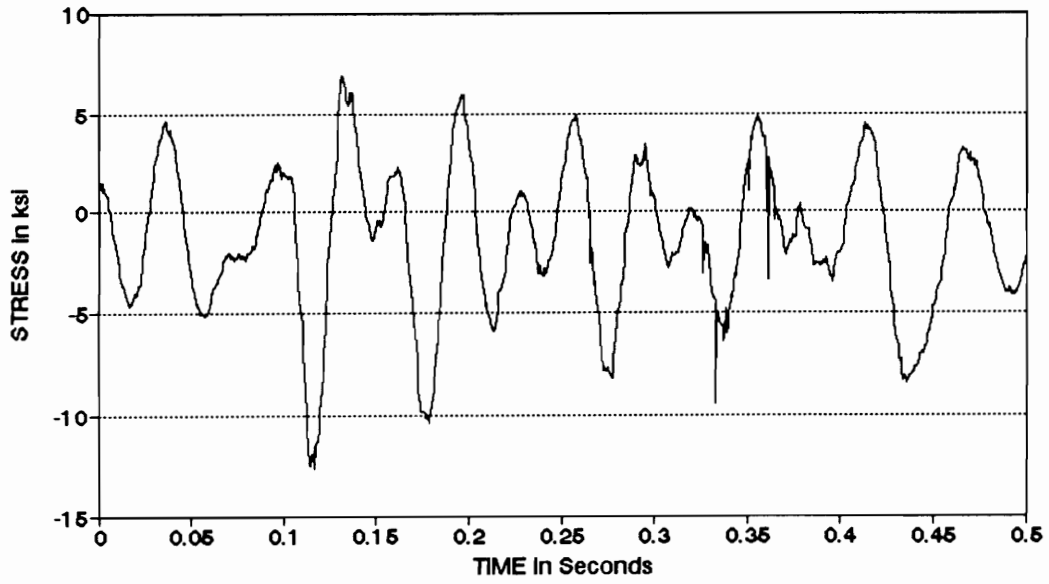

Figure 85. Dynamic Stress in the Standard When the Trailer Was Driven Empty over Sand Road.

It follows that traveling empty contributes significantly to the cumulative fatigue damage of a log trailer. The mean stress for the empty mode is zero, but the dynamic stress is fully reversed; the number of stress cycles for the same section of the road is four times higher, and the amplitude is only 20% lower.

There are a number of possible ways to alleviate the negative impact of the empty mode of operation on the fatigue strength of the trailer. A mechanical suspension system having a variable spring rate, depending on the load carried, or preferably an air suspension system with controlled air pressure could be selected so that the trailer's lowest natural frequencies for the empty mode would be removed from the 7 to 8 Hz range. The second solution would be making the trailer axles movable with respect to the frame.

Changing suspension position would automatically modify the natural frequencies. The design of the frame could be also altered so that the frequencies for the empty mode are outside the frequency range of the excitation, however this approach would not be that easy as the others.

It appears that building a trailer as a folding frame design would be the most advantageous solution for the problem. Folding and loading a trailer on the tractor for the return trip have additional advantages; reduced brake and tire wear, and decreased fuel consumption are just a few.

Maximum Stresses in the Gooseneck Trailer

The absolute maximum value of the dynamic stress in the entire structure of the gooseneck trailer was recorded 55.8 ksi for the front standards. This stress magnitude corresponded to a safety factor equal to 1.61 (against the yield point of the T-1 steel). The stress was measured while the trailer was tested for extreme situations while carrying 64,660 pounds of pine tree-length pulpwood (30.3% overload). The logs spanned all three bolsters. The trailer was driven over rough surfaces simulating a formed sand forest road

on an abandoned woodyard. At the instant when the stress was recorded, the vehicle was negotiating a very tight curve at a speed of approximately 7 mph (Figure 86). At that moment, normal stress measured in the bottom of the front bolster was equal to 14.5 ksi in compression. The whole vehicle was leaning to one side due to the quasi static loading with the centrifugal force. Similar surges in dynamic stresses were observed in all structural members on one side of the trailer during negotiating tight curves at high speeds.

Maximum stresses in the main I-beams and bolsters were recorded for a similar situation, when the truck and trailer were negotiating a tight turn, which coincided with a pot hole in the road. The trailer was loaded with 55,920 lbs of hardwood pulpwood (12.7% overload). The factor that elevated stresses for this lower payload was the loading pattern - the logs were placed between the second and the third bolsters. This load configuration was found to induce greater stresses into the structure. The trailer was driven at an average speed of 10 mph. The maximum dynamic stress recorded in the main I-beam was 27.45 ksi (Safety Factor = 1.31) under the third bolster, 24.33 ksi (Safety Factor = 1.48) at the second bolster, and 18.12 ksi (Safety Factor = 1.98) at the gooseneck, all in tension. The maximum dynamic stress recorded for a bolster occurred at the same instant and was equal to 21.24 ksi (Safety Factor = 1.69) in compression.

The second most dangerous situation for the trailer, in terms of the magnitudes of the dynamic stresses, occurred when the trailer was being unloaded by a front-end loader. When the loader hit a top of the standard with logs during the unloading operation (Figure 87), the stress in the bottom of the standard on the second bolster amounted to 47.9 ksi (Safety Factor = 2.08). The dynamic stresses induced into the structure of the trailer, during a loading operation were compared for a front-end-loader and a knuckleboom loader. The stress amplitudes occurring in the structure while unloading by a front-end-loader were found to be 15% higher than those measured during loading the same load with a Barko 160A

knuckleboom loader. The frequency of the dynamic response of the trailer during the unloading by the front-end-loader was several times higher.

Dynamic stresses at the most critical locations in the trailer were interpolated, based on the recorded values of the stresses at points of measurement, using the static stress distributions obtained from the 3-D FEM stress analysis. The maximum combined normal stresses computed for the most critical locations and the corresponding safety factors (SF) were:

1. bottom sections of standards: 60 ksi (SF = 1.83);
2. front bolster: 16 ksi (SF = 2.25);
3. middle and rear bolsters: 25 ksi (SF = 1.44);
4. the main I-beams:
    - under the middle bolster: 30 ksi (SF = 1.20);
    - under the rear bolster: 27 ksi (SF = 1.33);
    - at the gooseneck: 20 ksi (SF = 1.80).

The gooseneck trailer could be strengthened by replacing ASTM A36 steel with a high-strength low-alloy structural steel for bolsters and main beams (and not changing the geometry of the trailer). For instance, ASTM A572 grade 50 steel (designated also as INX or Ex-Ten) has a yield strength of 50 ksi minimum. Besides providing high strength, this steel offers good workability and weldability at a comparatively moderate price (Ryerson, 1989). Thus, welds with the difficult T-1 steel, which was used to manufacture the standards, should be more reliable. Also, A572 (G50) has much higher toughness and fatigue strength. Its atmospheric corrosion resistance is the same as that of plain carbon steel. A572 (G50) is now one of the most common steels used in manufacturing railroad cars, trucks, cranes, excavating equipment, and fabricating structures.

Figure 86. Maximum Dynamic Stress in the Entire Structure of the Gooseneck Trailer Was Recorded for the Front Standard and Took Place When the Trailer Was Tested During Extreme Cornering.

Figure 87. The Second Highest Stress for the Gooseneck Trailer Was Recorded for the Second Standard During Unloading with Front-End-Loader.

Using this steel would also allow a designer to decrease the tare weight by redesigning the geometry of the trailer. Other beam cross-sections can be used for building the members to increase their stiffness. For instance, a fabricated simple I-beam of a greater depth or thicker or/and wider flanges would be lighter and have still larger section modulus than the standard wide flange W18x35 section.

Maximum Stresses in the Full-Tree Trailer

The absolute maximum value of the dynamic stress in the entire structure of the full-tree trailer was recorded equal to 42.3 ksi at the third bolster. The stress was measured while the trailer was carrying a 51,920-pound pine full-tree payload (gross vehicle weight was 78,100 lbs) and was driven over a formed sand forest road. At the moment when the stress was recorded the vehicle was passing over a large bump at a speed of approximately 20 mph. This stress magnitude was very close to the yield strength of the ASTM A500 steel (46 ksi) used to build the bolster. Thus, at the time of this dynamic loading the safety factor was only 1.08 (computed against the yield point of the material). The recorded stress magnitude indicates that the trailer's third bolster could be overloaded and might need to be replaced with a stronger one.

Maximum stresses in the main I-beams and standards were recorded for the same payload when the trailer was negotiating a corner at approximately 15 mph while driving over the same section of the sand road. The maximum stresses in the main beam were 19.30 ksi (SF = 1.89) at the third bolster, and 14.01 ksi (SF = 2.57) at the second bolster. The maximum stresses in the second bolster were 21.7 ksi (SF = 2.13). The front and the second standards were subjected to the following stresses: 12.55 ksi (SF = 2.86) and 20.30 ksi (SF = 1.77), respectively.

A number of factors contributed to overall lower maximum nominal stresses and higher safety factors for the full-tree trailer than those for the gooseneck thinning design. These included differences in the type and size of payloads and loading patterns, as well as the differences in trailers designs. The gooseneck trailer was capable of accepting larger payloads due to the increased loading space, and the stresses were proportional to the loading (elastic behavior of the structure). Thinning material placed between the second and the third bolsters, was located at some distance from the points of support and induced larger bending moments in the main beams. This pattern of loading also brought about the excessive leaning of the trailer and significant surges of stresses on one side of the structure when the trailer was negotiating a corner. I-beam sections undergo large displacements when subjected to a combination of bending and twisting loads (Figure 86). Finally, the full-tree trailer uses five bolsters: two in the front, one intermediate, and two in the cage. The trailer's standards and bolsters, except for the third bolster, were loaded proportionally less than the two or three bolsters on the gooseneck trailer. The third bolster on the full-tree trailer was heavily loaded due to the close proximity to the center of gravity of the full-tree payload. Even though the overall nominal stresses measured for the full-tree trailer were lower than those for the gooseneck trailer, the former revealed many fatigue cracks. It was found that the cracks originated and propagated at stress concentration points in the trailer.

The second most dangerous situation for the full-tree trailer, in terms of the magnitude of the dynamic stresses, occurred when the trailer was loaded and unloaded, which was similar to the results obtained for the gooseneck trailer. Maximum stresses induced by the overhead portal crane were found to be lower than those caused by a knucklebone loader and a front-end-loader.

In a process of upgrading a design of the full-tree trailer, the joints between the members (e.g. bolster mounting on the main beams) should be redesigned, and the main beam cross-section should be replaced by a simpler design, both to avoid stress concentrations.

Statistical Analysis of Data

Preliminary inspection of the stress-time series indicated that, in general, the trailers revealed two distinct types of dynamic response. The first, associated with traveling over low quality forest roads, was characterized by high amplitude and low frequency. In contrast, stresses recorded while the trailer was driving along paved roads, were of high frequency and low amplitudes. A hypothesis was formulated that, log trailers have two possible failure modes: plastic deformation due to dynamic overloading (while driving over dirt roads or loading/unloading operations), and fatigue fracture due to the accumulated effect of repeated stress cycles of magnitudes below the yield strength of the material (while riding on paved roads). Verifying this hypothesis was important for the extra-light log trailer design.

A random sample of 150 data points (evenly distributed between road categories) were drawn from the original data set for the gooseneck trailer using the random number generator within the NPSP statistical package (Pirie, 1988). The analysis was designed to compare the dynamic stresses occurring in the main beam while the trailer was driving loaded over roads of different categories. The *a priori* hypothesis was that the highest stresses occurred on sand roads, followed by those on one-lane paved roads, and then by those on highways. The null hypothesis stated that the median (mean) differences between the measured dynamic stresses equaled zero for all possible pairs of the road categories tested. The alternative hypothesis was that for at least one pair of the road types, the median (mean) difference of the stresses was different from zero.

Assumptions

The procedures used in the analysis required the following assumptions about the data to validate statistical inference:

1. Dynamic stresses induced in the main beam while the trailer is driven loaded are due to no other influences than the category of the road and random variation.

2. The observations of dynamic stresses in the main beam are independent of each other.

3. The observations come from a continuous distribution.

4. The observations are symmetrically distributed.

5. The observations come from the same population.

6. Random variability in the observations of dynamic stresses comes from some Gaussian distribution.

Table 13 shows the required assumptions for each parametric and nonparametric test used in the analysis.

Table 13. Assumptions Required by the Procedures Used to Validate Statistical Inference.

Procedure	Assumption					
	1	2	3	4	5	6
Kolmogorov -Kuiper		X	X		X	
Kruskal-Wallis	X	X	X		X	
Jonckheere	X	X	X		X	
One-way ANOVA	X	X	X	X	X	X

Validation of Assumptions

The trailer was designed to maximize tree-length payloads from commercial thinnings. Such loads are placed between the second and the third bolsters. The trailer can also carry longer material from clear cuts, by loading butts at the front of the trailer. The three parameters: loading pattern, load size, and material type, have an impact on the magnitudes of the stresses induced in a log trailer. A constant payload of fresh pine tree-length pulpwood was used during the trial to control the effects of the above factors.

Temperature changes of the strain gages was the second major factor that could have a direct systematic effect on the measured stresses. The period during which the measurements were being taken was sufficiently long that the gages could elevate their temperature due to the electric current passing through them and due to changes of the ambient temperature. However, since the dynamic stresses were measured, and not the static ones, this issue is of minor importance.

The assumption of the mutual independence between the observations can be easily violated by the load movement on the trailer. Load shifts could create dependence of the consecutive measurements until the truck passed over another bump and the load moved to a new configuration. During the study, we were able to detect the impact of load settling on the measured stresses, even though two pretensioned cables tied the load to the trailer.

Dynamic stress is a continuous variable. However, due to analog-to-digital conversion in the computer data acquisition system, the stress was reported as a discrete data. This created numerous ties in the data. The biggest group of ties included 13 observations. However, as the data logging hardware was capable of

measuring stress to the nearest 0.03 psi, the potential for violation of this assumption was not significantly greater than of that the other assumptions.

There were a variety of factors which could have led to violations of assumptions 5 and 6. These factors were: changing load configuration on the trailer due to log settling, road conditions within sections of the same category, driver's behavior, and changing temperature of the strain gages. However, for all the measurements taken from the same location, the same transducer, and the same data acquisition system were used for recording the data, so the potential for violating these assumptions should be relatively small.

Results and Discussion

Visual analysis of the data was inadequate to confirm the normality of the distributions tested. The distributions appear fairly symmetrical (Figures 88 and 89). However, slight skewness is present in each case. Also, the box plot of the stresses recorded for a one-lane paved road reveals two extreme (low) and two moderate (high) outliers, which indicate that the distributions may be heavy tailed.

Both the Stephen's Modification of the Kolmogorov-Smirnov and Kuiper goodness-of-fit tests failed to reject the null hypothesis ($p>0.15$) only for the distribution of the stresses when the trailer was driving over a sand road, indicating that the distribution might have been normal (Table 14). For the data recorded when the trailer was driven on a one-lane paved road, Kolmogorov-Smirnov test fails to reject ($p>0.15$), while Kuiper gives moderate evidence against the null hypothesis ($0.05>p>0.025$) that the distribution is Gaussian-like. In case of the highway data, both tests agree ($p<0.025$ for K-S, $p<0.01$ for Kuiper), indicating that the distribution is not normal.

Both the parametric (One-Way ANOVA) and nonparametric (Kruskal-Wallis) tests for location provide very strong evidence ($p<0.0001$ and $p<0.001$ respectively) that the dynamic stresses occurring in the main beam are different at least for one pair of road categories. The visuals strongly support this conclusion. If the data were normally distributed, the one-way ANOVA would only be slightly more powerful than the Kruskal-Wallis test. However, since there is a reasonable evidence that at least two samples come from other than Gaussian-like distributions, the appropriate procedure to use is the Kruskal-Wallis test.

The nonparametric protected LSD test revealed that the dynamic stresses recorded when the trailer was driven over forest sand roads were higher than those recorded for paved roads, and that those in turn were higher than the dynamic stresses recorded on highways. Visuals strongly support these results.

Similarly, both the Fisher's protected LSD and Ducan's multiple range tests (normal theory) showed significant differences between each pair of the samples. The a priori hypothesis was that stresses occurring on highways were the lowest, and that those on one-lane paved roads were lower than on forest sand roads. Therefore, the Jonckheere test was performed for this a priori ordered alternative. It provided a very strong evidence ($p<0.00001$) that the above mentioned relationship is valid. Since the Jonckheere test is a one-sided test of ordered alternative, it provided more power ($p<0.00001$) than the Kruskal-Wallis test ($p<0.001$). A logical contrast would be to compare the dynamic stresses in the main beam of the trailer while driving over forest sand roads with the respective stresses for the other two road categories tested. The median increase in the dynamic stress for sand roads compared to that for one-lane paved roads and highways was found to be equal 1.49 ksi.

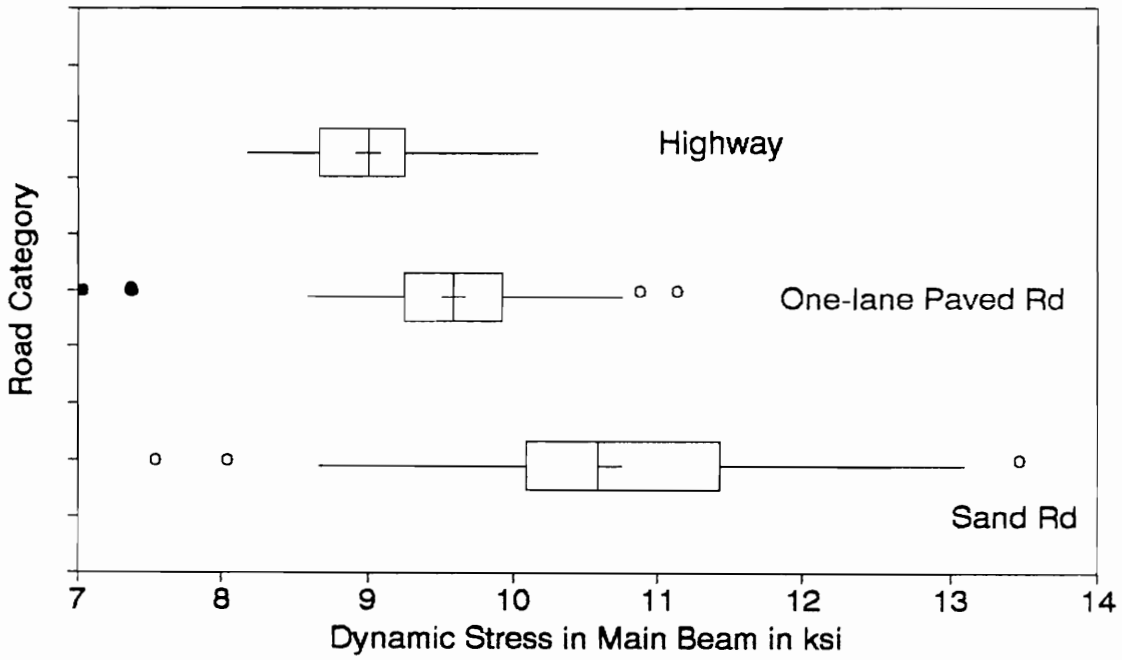

Figure 88. Box Plots for the Data of Dynamic Stresses Recorded on Three Types of Roads.

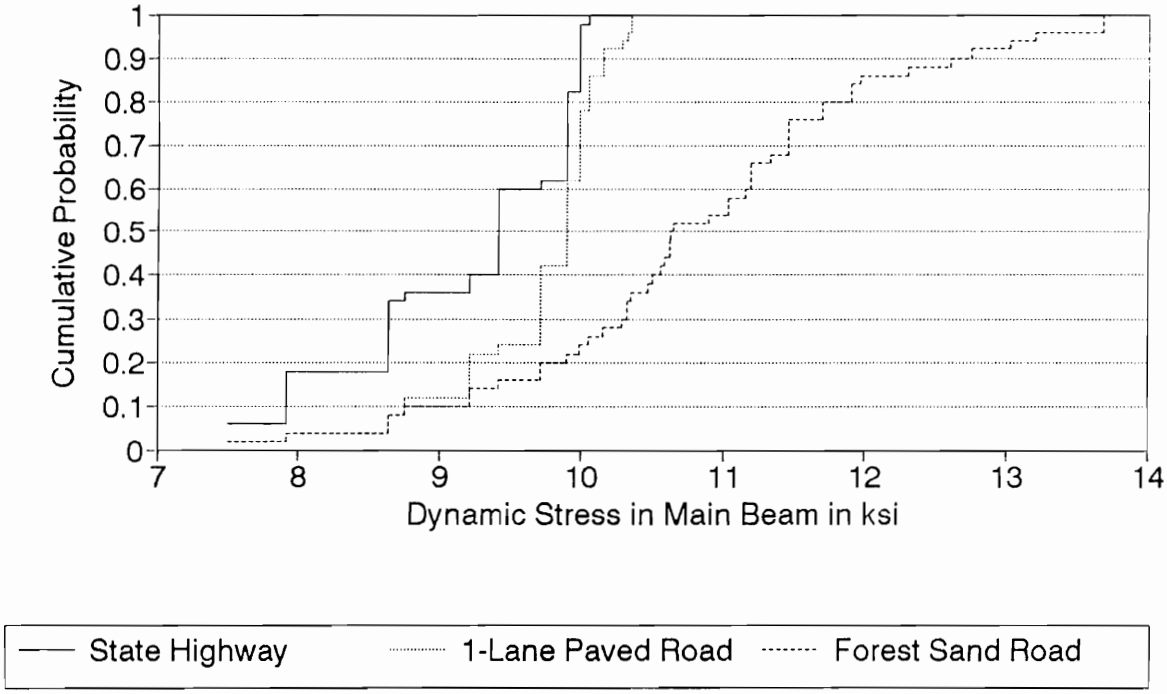

Figure 89. EDF Plots for the Data.

Table 14. P-Value Table for Various Statistical Tests Used to Verify the *a priori* Hypothesis.

Procedure		p-value
K - S	Highway	0.025>p>0.01
	1-Lane Paved Rd	p > 0.15
	Forest Sand Rd	p > 0.15
Kuiper	Highway	p < 0.01
	1-Lane Paved Rd	0.05>p>0.025
	Forest Sand Rd	p > 0.15
Kruskal-Wallis		p < 0.001
Jonckheere		p < 0.00001
One-way ANOVA		p < 0.0001

Conclusions

1. The dynamic stresses occurring when a log trailer is driven over forest sand roads are of the highest magnitudes. These stresses should be considered as the maximum working stresses, and used for dimensioning trailer structural members (after incorporating a predefined safety factor).

2. Dynamic loading acting on a log trailer when it is traveling over low quality forest roads is characterized by low frequency but high amplitudes, which in an extreme situation, can cause a failure by plastic deformation.

3. The second possible failure mode of a log trailer is associated with the fatigue fracture due to accumulated effect of a great number of repeated stress cycles, most of which are created while the trailer is driven over paved roads.

4. The extra-light log trailer should be designed to withstand high stresses when driving over dirt roads and during loading and unloading operations, and to be fatigue-resistant against the repeated loadings. Both strength and low tare weight can be achieved by using high tensile, heat treated steel. Designing and building trailer free from stress concentration places will warrant its fatigue resistance.

5. Due to the significant load movement on the trailer, when load securing cables/chains are used with initial pretensioning only, it is strongly recommended that a trailer be equipped with a constant tensioning device. Tying load to the trailer is very beneficial. It significantly limits dynamic loading on standards and bolsters, adds stiffness to the trailer's frame, and enhances safety of the hauling operation. Also, such a device can make possible a remote removal of straps from the load at a woodyard. This in turn would significantly increase the safety of unloading operation at a mill.

CHAPTER 6. FINITE ELEMENT MODELS

Introduction

Detailed finite element models were built for the two trailers (i.e. the gooseneck and the full-tree trailer) and for the extra-light longwood trailer built by Clark Trailer Service, Inc. (see Chapter 2). The objective was to evaluate merits of various existing designs. Once the models were developed and verified, they provided efficient and powerful tools for further analysis. Experiments with different loading schemes and auxiliary equipment configurations were also performed.

Gooseneck Trailer 3-D Model

Three types of elements were used to build the final models. 3-D tapered unsymmetrical beam elements were employed for modeling the trailer's structural members. STIF44 elements allowed for a convenient representation of tapered sections of beams, and permitted end nodal points to be offset from the centroidal axes of members. The effects of shear deformation were included in the analysis. Output consisted of nodal displacement data, axial stresses, normal stresses from bending, the combined normal stresses (i.e. the sum of the axial and bending stresses), torsional shear stresses, and the shear stresses due to lateral forces.

Figure 90 shows the final model of the gooseneck trailer. Three linear, spring-damper elements (STIF14) were used to model the trailer's running gear. The elements are represented by three vertical line sections supporting the rear of the trailer at the hangers and the equalizer locations. Spring constants of the elements were derived from the observation that the trailer displaces about 3 inches under the full legal tandem weight (i. e. 34,000 pounds). A similar assumption was made about the stiffness of the tractor and trailer coupling at a kingpin. The actual physical connection between the tractor and the trailer was simulated as a single spring-damper element.

The gooseneck trailer used an insert on the third bolster for hauling tree-length material from thinnings to provide the required clearance between logs and the frame, and to raise the load over the trailer's bumper and the rear lights. The interaction between the insert and bolster was modeled with the use of 3-D interface elements (STIF52). Each represented two flat surfaces which would either maintain or break contact and slide relative to each other. Each was able to support the normal compression and the frictional tangential forces. The elements were nonlinear and required iterative solutions.

Figure 91 shows the gooseneck trailer model with all boundary conditions represented. These included: the symmetry plane boundary conditions at midpoints of each bolster and cross member, displacement restraints at locations of structure supports, and finally the static load on the trailer: concentrated forces exerted on standards, and pressures on bolsters. A 55,920-pound payload of thinning material, identical to the one during the experimental stress measurements, was assumed. Load distribution and loadings on each trailer's member were derived using the computations showed in Appendix A. Lateral, horizontal forces exerted on the second and the third standards were computed using Method 2 (i.e. the concept of a group of logs partially supported by a standard).

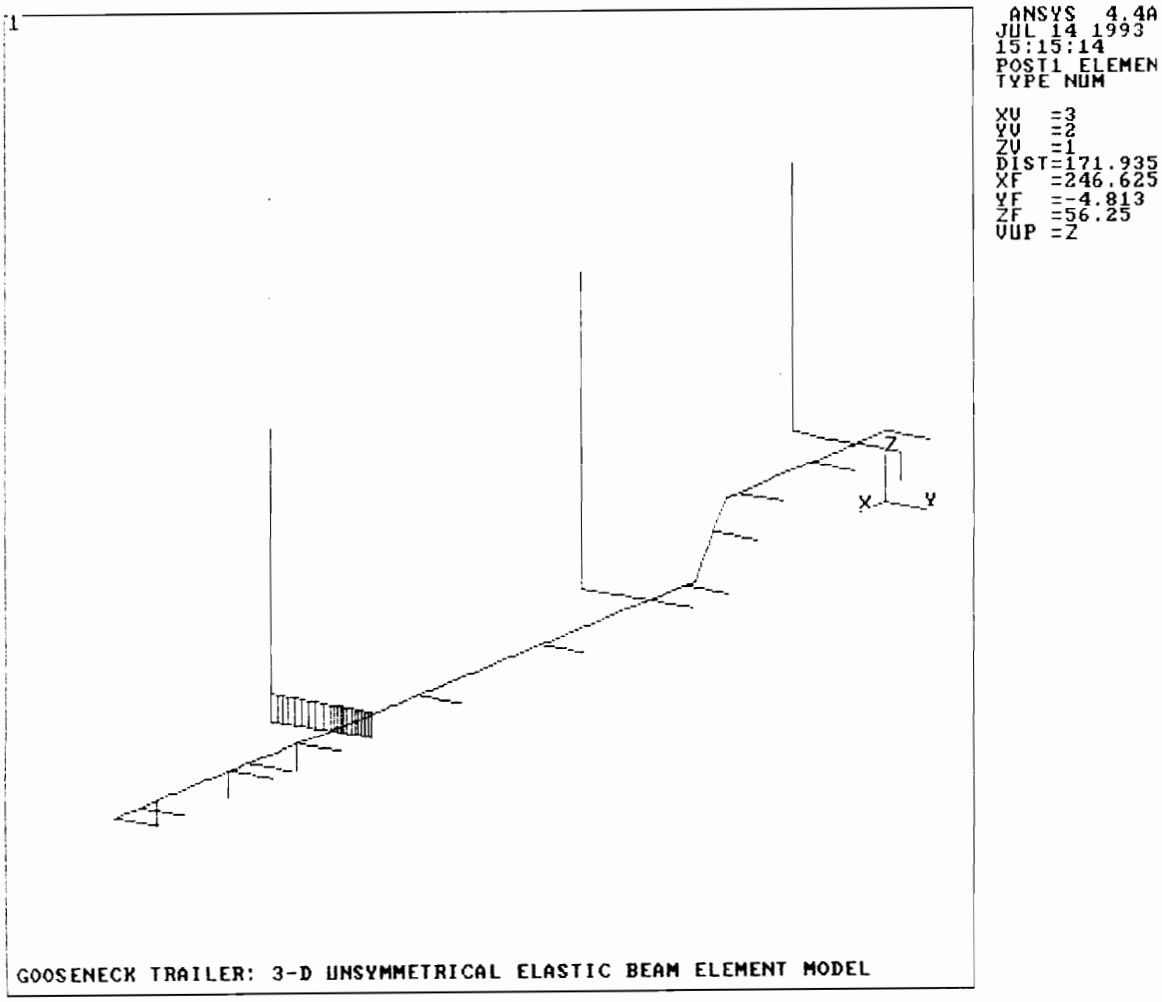

Figure 90. The 3-D Tapered Unsymmetrical Elastic Beam Model of the Gooseneck Trailer.

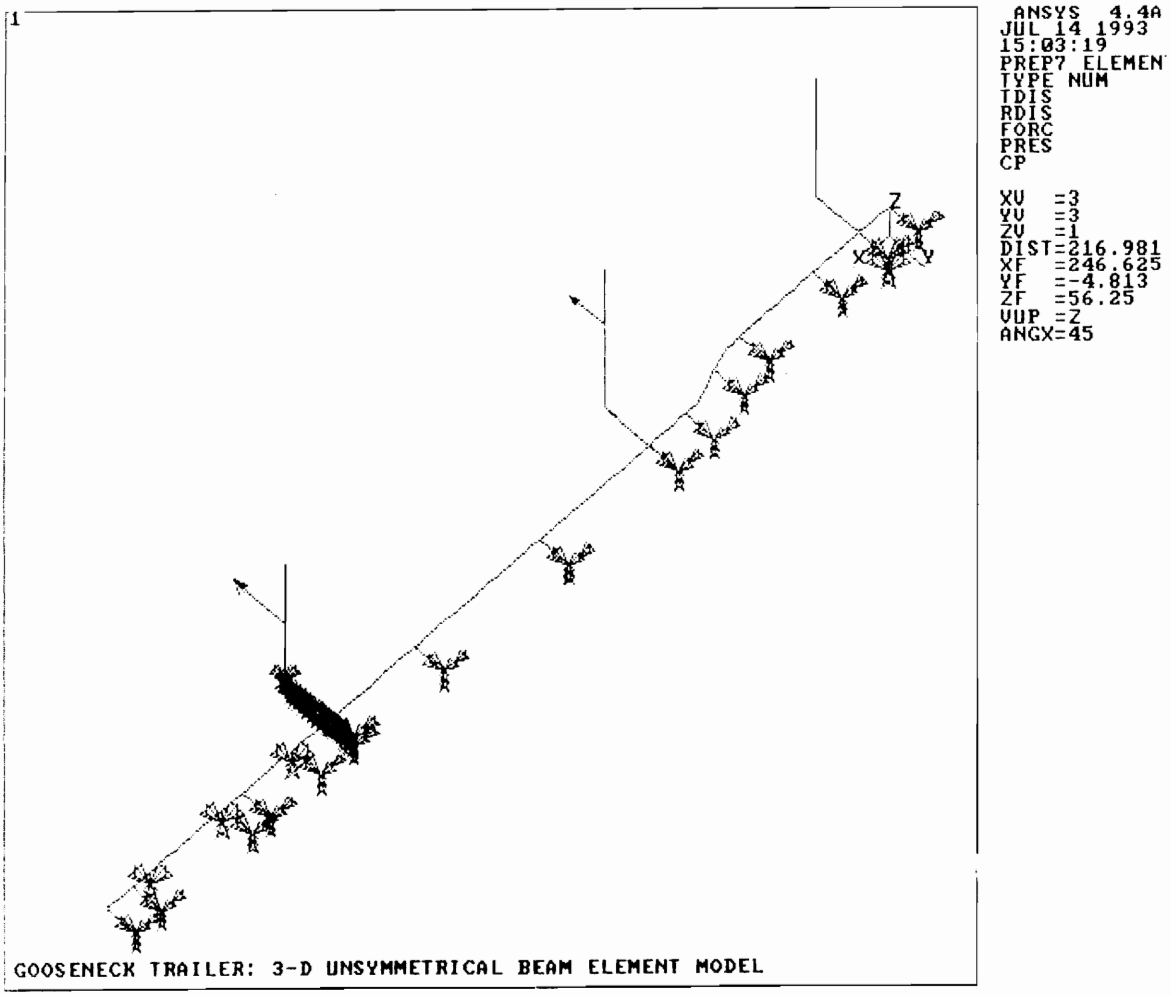

Figure 91. The Gooseneck Trailer Model with All Boundary Conditions Represented.

A static stress analysis was performed. A convergence required for the solution was obtained after 66 iterations. Figure 92 shows the distorted geometry of the trailer. The top of the second standard was predicted to displace the most, 1.682 inches sideways (i.e. y_{max} = -1.682). Its total joint displacement in space with regard to the global rectangular coordinate system was 4.087 inches.

Figure 93 shows the plot of the computed maximum combined normal stress distribution in the trailer. It was found to agree with the results obtained in the preliminary stress analysis.

Results from the earlier experimental static stress analysis of the gooseneck trailer, under the identical payload and load distribution, allowed for the model verification. The computed maximum combined normal stresses at measurement points during the experimental stress analysis were sorted out from the stress output data. These values were then compared with the experimental data. Table 15 contains both the FEM solution and the measured values.

The FEM results differed by +/- 5.2% from the static strain measurements with the exception of the 3rd bolster and the 2nd standard. Stresses on the 3rd bolster at the point of measurement were computed 8.1% lower than actually measured. It is believed that the difference stemmed primarily from the difficulty of simulating a complex friction interaction between the insert and the bolster. Only 21 three-dimensional interface elements were used to model this interaction. A greater number of elements representing the bolster, insert, and their interaction, as well as setting the friction force tolerance in equilibrium to less than 10% would certainly help to obtain a better agreement. However, the analysis would require a much larger number of iterations, and thus more computer time. Some shortcomings of FEM certainly influenced the results, but it should also be kept in mind that there is at least 2% to 3% of measurement error associated with the strain gage technique. All these factors, combined, contributed to the obtained differences in the stress values.

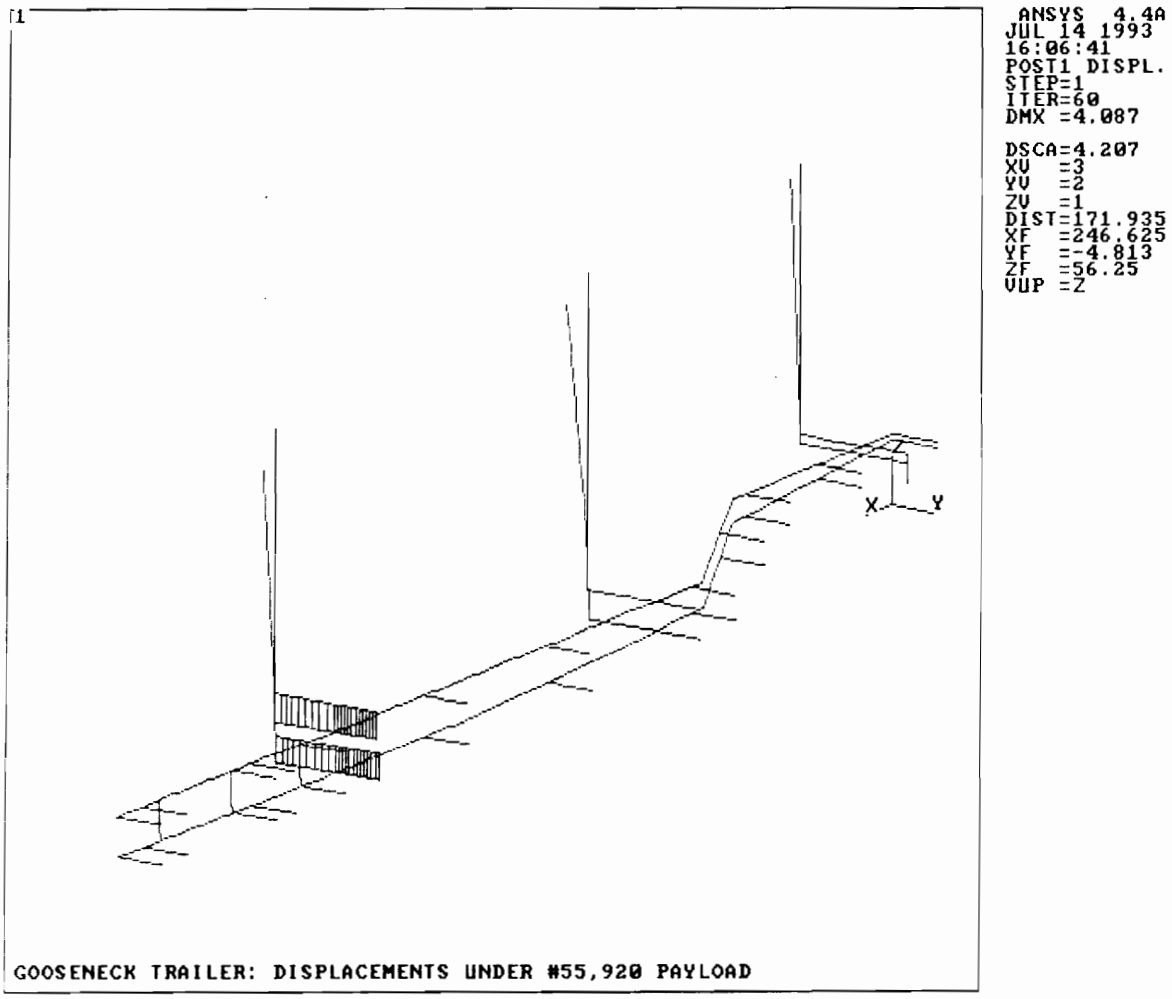

Figure 92. Computed Displacements of the Structure under 55,920-Pound Payload.

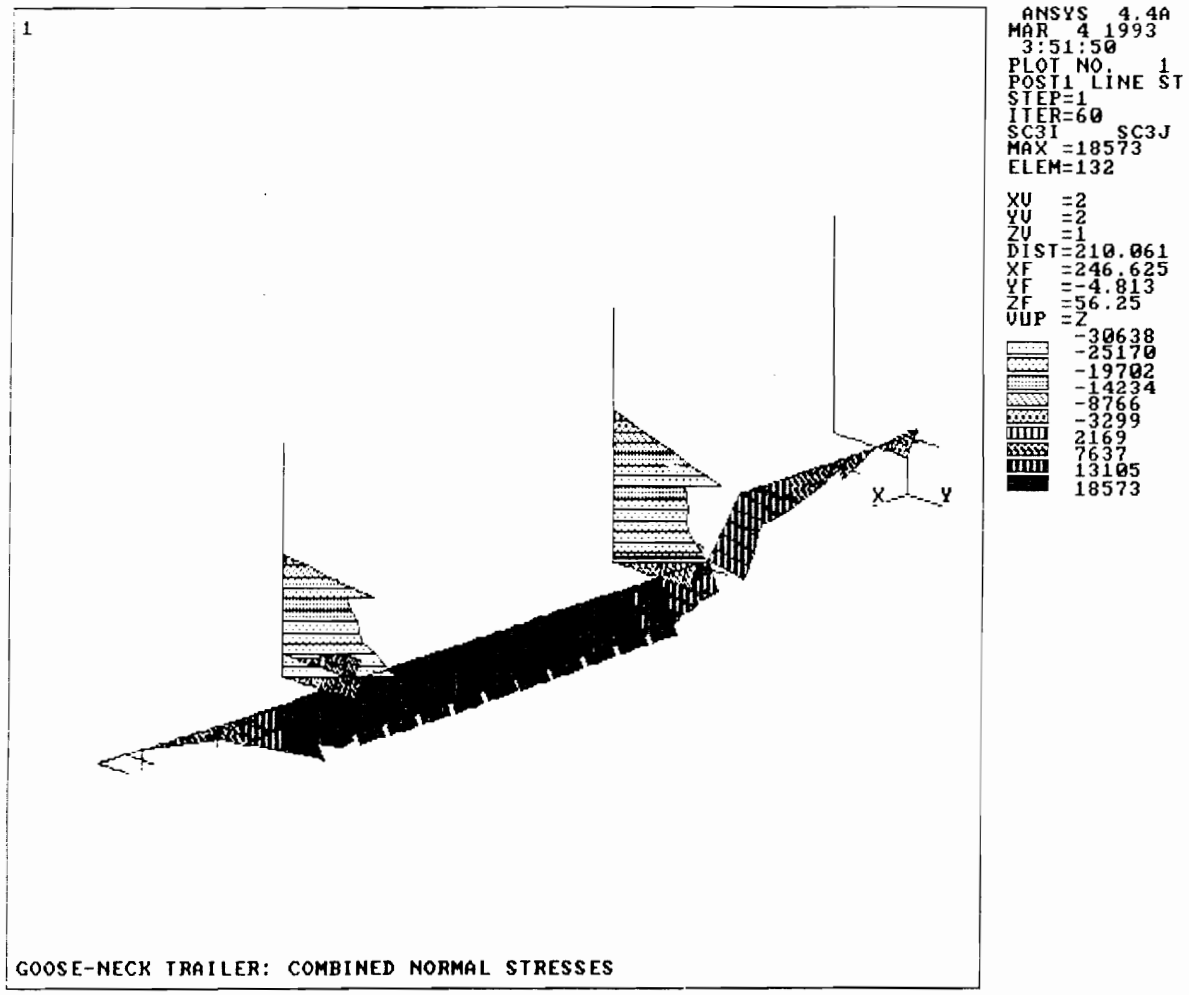

Figure 93. Combined Maximum Normal Stresses under the 55,920-Pound Payload.

Table 15. Comparison of FEM Stress Analysis Results with Experimental Data.

Stress at Characteristic Spots [psi]			
Spot	FEM Stress Analysis	Experimental Data	Percent Error
I-Beam @ Gooseneck	9,041	8,760	3.6%
I-Beam @ 2nd Bolster	14,278	14,700	-2.8%
I-Beam @ 3rd Bolster	16,125	15,840	1.8%
2nd Bolster	-10,222	-11,070	-5.2%
3rd Bolster	-5,735	-6,240	-8.1%
3rd Standard	-25,185	N/A	N/A
Insert (on 3rd Bolster)	-9,897	N/A	N/A

Maximum normal stresses in standards were computed 30.5% higher than the measured ones. This difference again illustrates the difficulty in modeling the static loadings exerted on standards. In practice, some log trailer manufacturers use a rule of thumb that a standard must withstand a horizontal force equal to one third of the weight on the given bolster applied at the height of the load cross-sectional area CG (Baas and Stulen, 1985). This method results in slightly higher computed stresses in the member than the method assumed in the study. The experimental stress analyses revealed that the ratio of the maximum dynamic stress to the maximum static stress at the bottom cross-section of a standard was between 1.8 and 1.9. These locations are also the most stress-critical spots on a trailer. Therefore, it is recommended that the computed stresses (i.e. higher than measured by about 30%) be considered in a trailer design. This obviously conservative approach is justified for safety reasons. If load binders could be continuously tensioned to remove any slack due to load settling, and to tie the logs firmly to the frame, the dynamic loadings on standards and bolsters would be reduced to the point where the lower values of stresses (i.e. the measured ones) could be considered in the design.

Number of Bolsters

It was observed that the loading scheme, and thus load distribution, on the trailer has a decisive influence on the stress levels in members of a log trailer. Figure 94 shows the stress distribution in the main beam of the gooseneck trailer for two identical payloads. Figure 94a corresponds to the situation when thinning material is placed between the second and the third bolsters, while Figure 94b shows the stress distribution when tree-lengths span all three bolsters. The location for the maximum combined normal stresses changes, and the values of the stresses change as well. Maximum normal stresses in the main beam decrease significantly (by about 25% in this case) when the logs are placed on all four bolsters.

a)

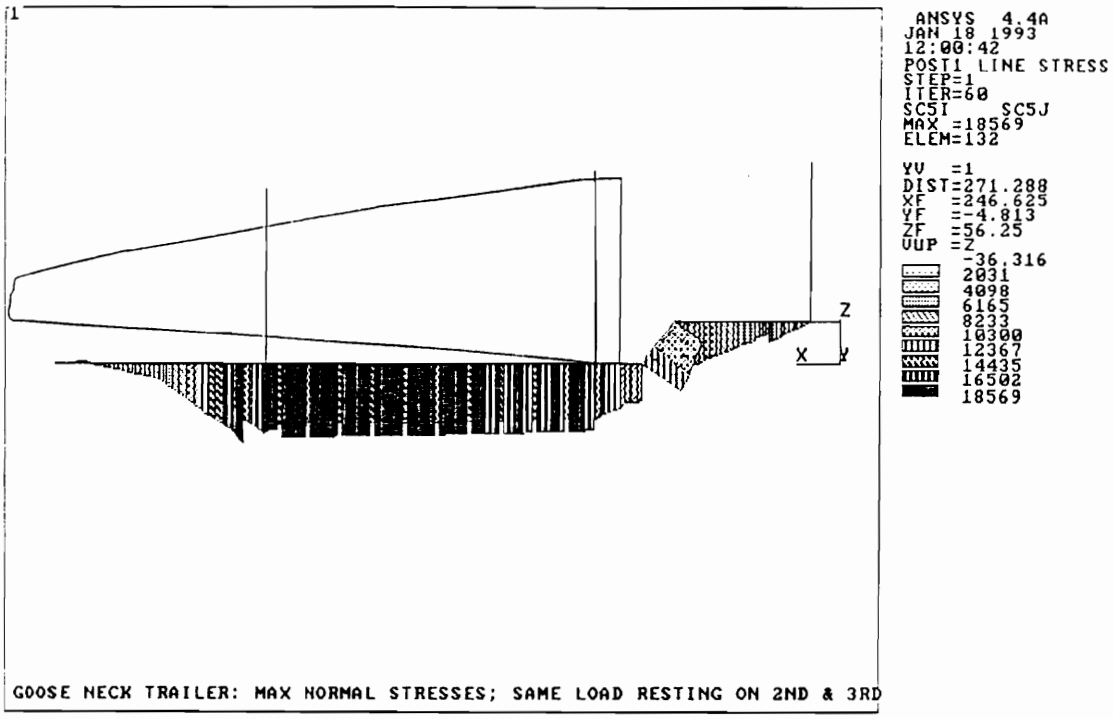

b)

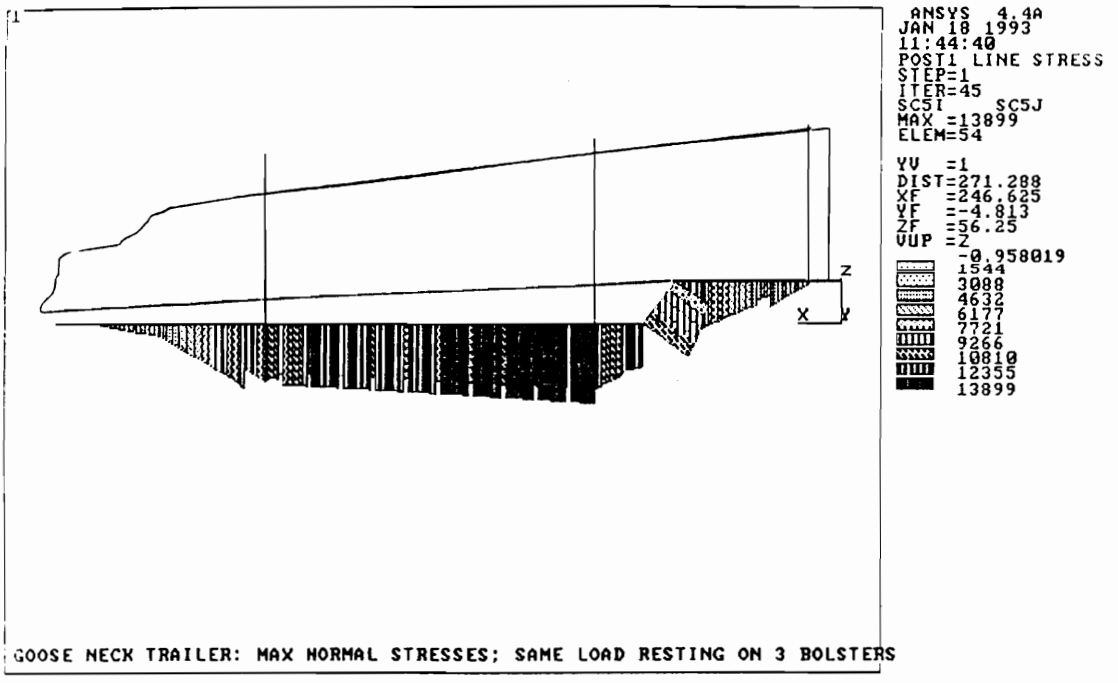

Figure 94. Stress Distribution in the Main Beam of the Gooseneck Trailer for Two Loading Schemes; (a) when the load rests on the 2nd and 3rd bolster, and (b) when it spans all bolsters.

The 16.5-inch drop in the trailer's neck was introduced to increase the loading space for short trees from thinnings. It is very advantageous to utilize this enlarged space to increase payloads. However, it is recommended that loading be performed in two stages when possible. First, a bottom layer of logs (i.e. the bottom tier) should be placed behind the gooseneck up to the level of the trailer's neck section. Then, long material (e.g. tree-lengths) should be loaded across all three bolsters, filling the available loading space on the trailer. This loading scheme should accommodate about 20% more small trees from thinnings, and at least 4% more payload when the trailer is hauling tree-lengths. The insert on the second bolster would be removed as for the thinning material, freeing 328 pounds (i.e. the insert's weight) for increased payload. The two tiers in load will have to be separated by two short logs placed across the trailer to facilitate unloading.

Insert Cradling on Standards

Inserts on bolsters are frequently used to facilitate the unloading operation, and to lift the back of the load above the trailer's bumper and taillights. These inserts, however, could significantly decrease loadings on standards and bolsters as well. Inserts in use slide on bolsters in between the standards, and do not cradle around the standards.

The 3-D FEM model developed for the gooseneck trailer was used to experiment with various auxiliary equipment configurations. In the first analysis it was assumed that the insert on the third bolster is equipped with some kind of cradling mechanism to restrain the standards.

Figure 95 shows stress distributions in the bolster for both situations: the conventional insert (Figure 95a), and when the insert cradles the standards (Figure 95b). The results reveal that by introducing this simple design element, maximum combined stresses in the bolster are reduced by a factor 2.86! At the same time, the maximum combined stresses are diminished by 18% (Figure 96b) in the standard, and by 26% in the insert itself (Figure 97b).

Cable between Standard Tops

Theoretically, it would to be advantageous to tie tops of the standards on the same bolster together with a cable or strap after loading is completed. This should significantly diminish stresses in the standards, standard-bolster weldments, and bolsters.

This hypothesis was verified in the FEM analysis. A three-dimensional spar element with a uniaxial tension-only capability (i.e. of bilinear stiffness matrix), the STIF10 element, was used to model a cable placed between the tops of the standards. The element has stiffness removed whenever it goes into compression simulating a slack in a cable. The initial state of the element was initial strain. The element is nonlinear and requires an iterative solution.

A 3-D FEM static stress analysis was performed for the two following configurations. In the first situation, a cable is placed between standard tops, after the trailer is loaded, and the cable is pretensioned with a 100-pound pull. The second configuration consisted of the same pretensioned cable accompanied by an insert on the bolster, with cradling mechanisms clamping around the standards. Figures 98, 99 and 100 show stress distributions in the bolster, standard and insert for the two scenarios, respectively.

a)

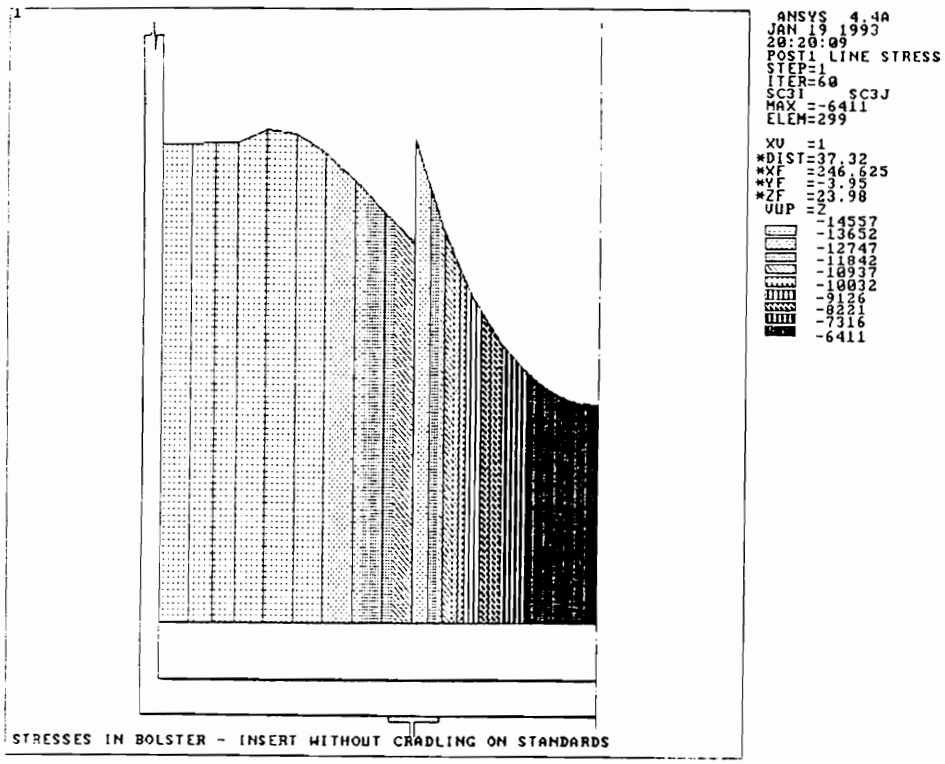

b)

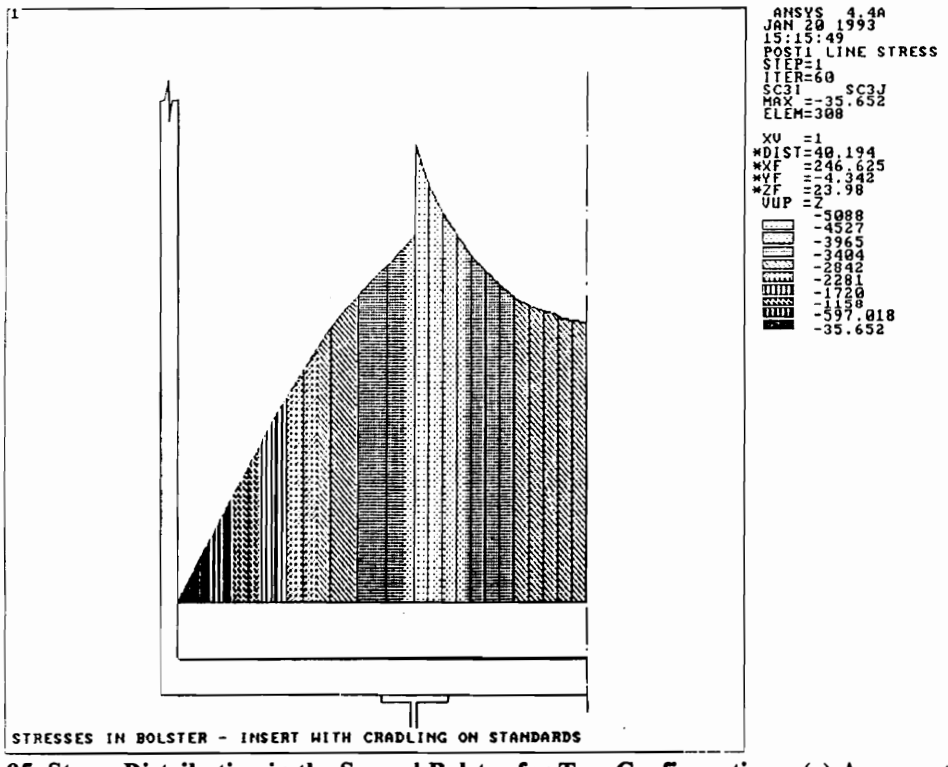

Figure 95. Stress Distribution in the Second Bolster for Two Configurations: (a) A conventional insert is used, and (b) insert with cradling on standards is used.

a)

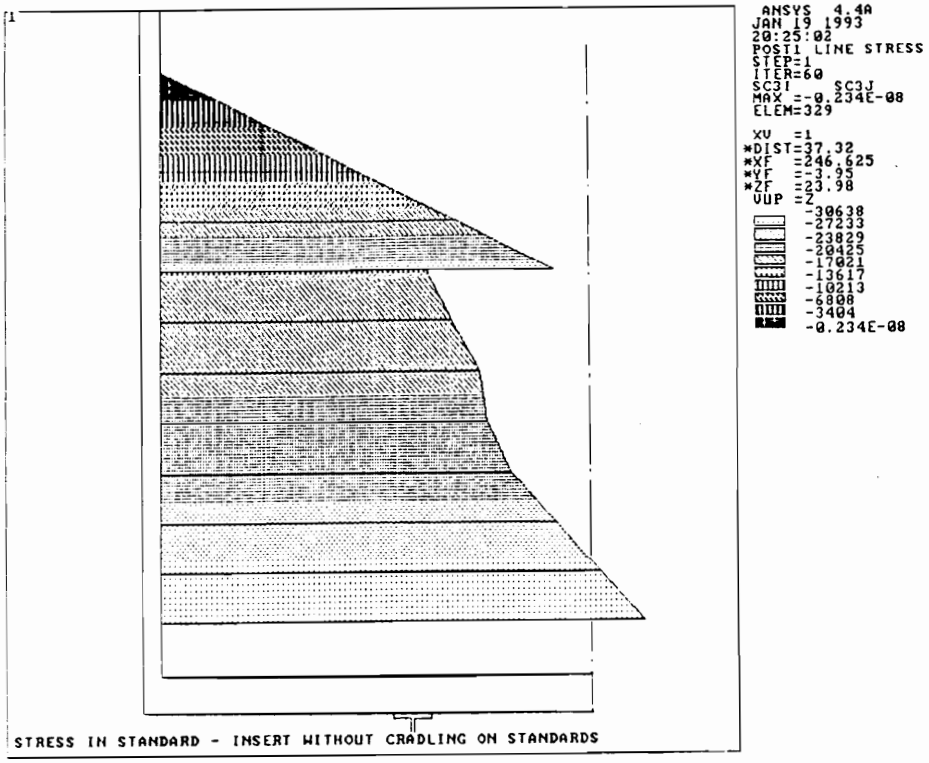

b)

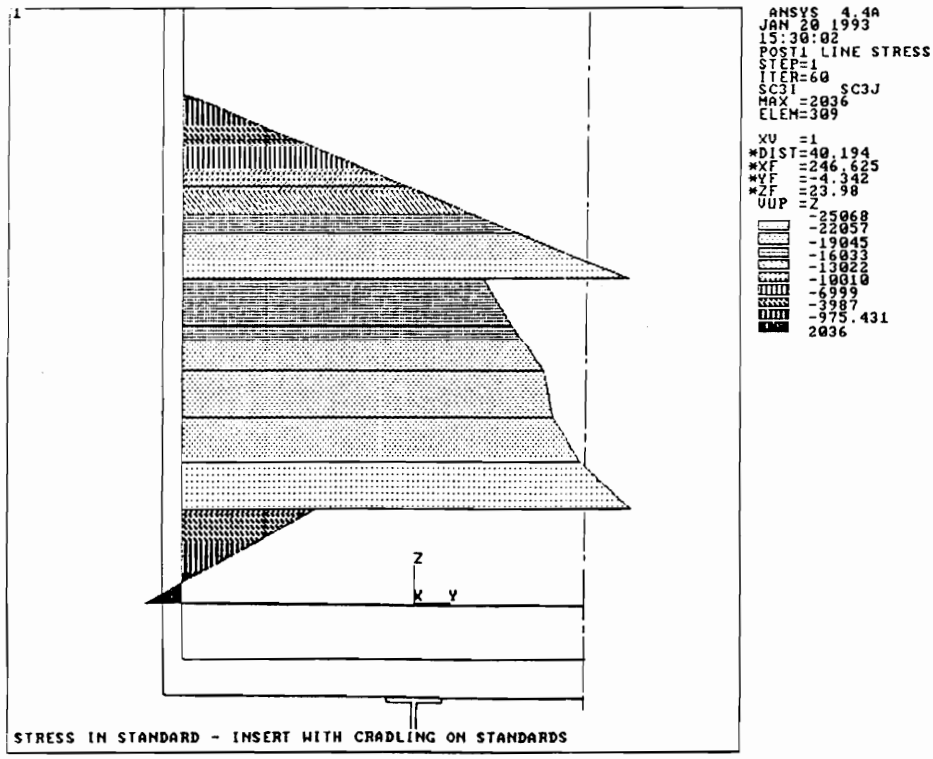

Figure 96. Stress Distribution in the Second Standard for Two Configurations: (a) A conventional insert is used, and (b) insert with cradling on standards is used.

a)

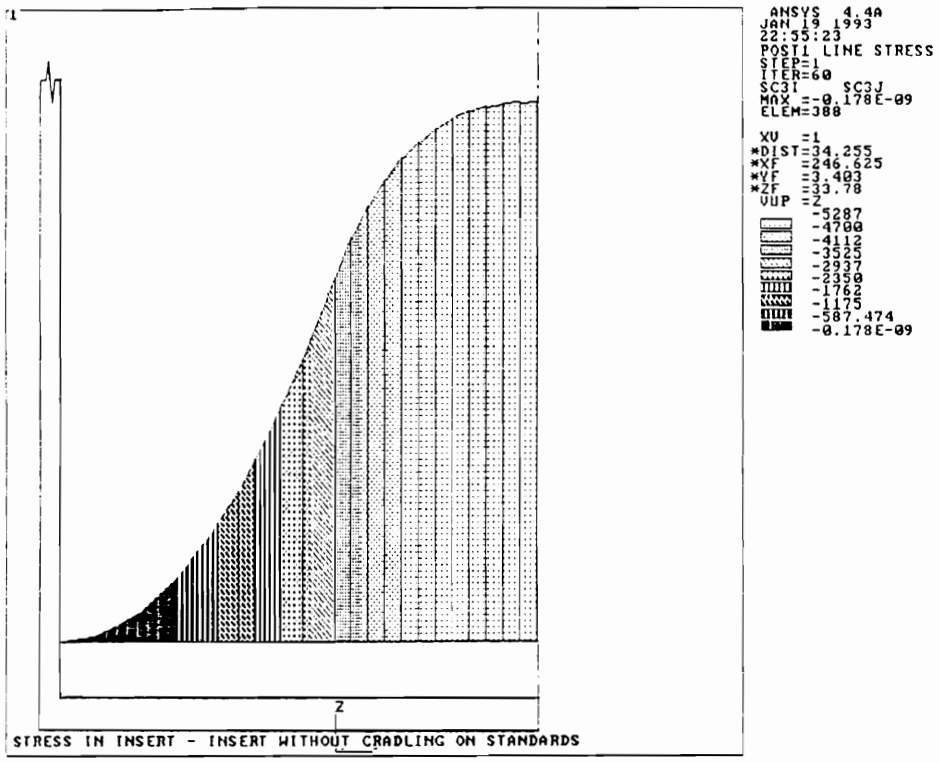

b)

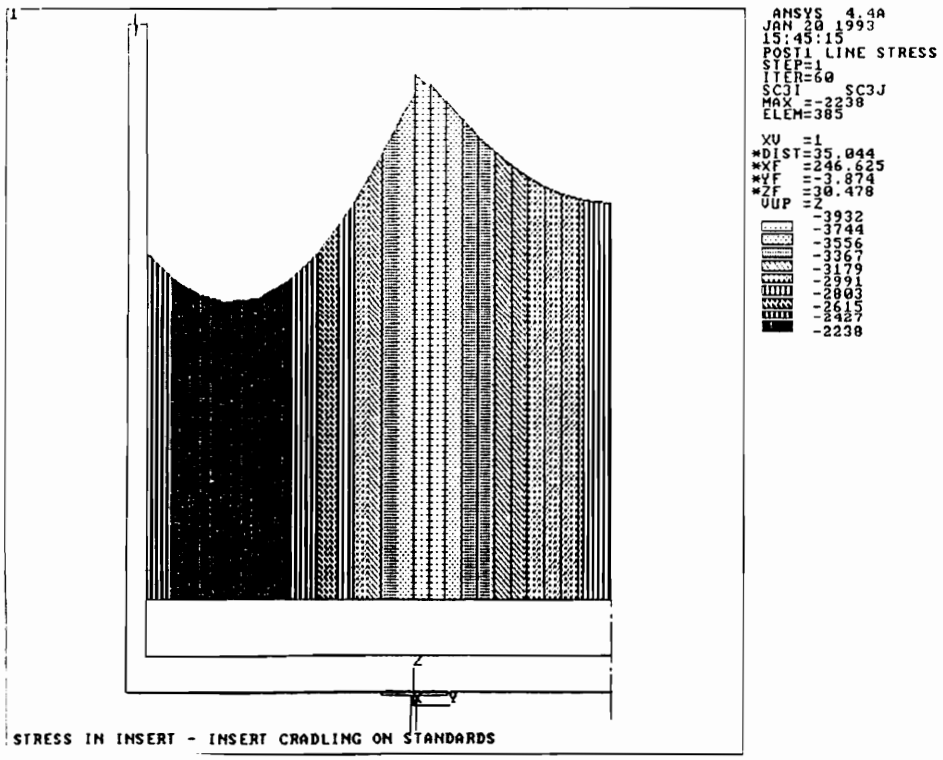

Figure 97. Stress Distribution in the Insert for Two Configurations: (a) A conventional insert is used, and (b) insert with cradling on standards is used.

a)

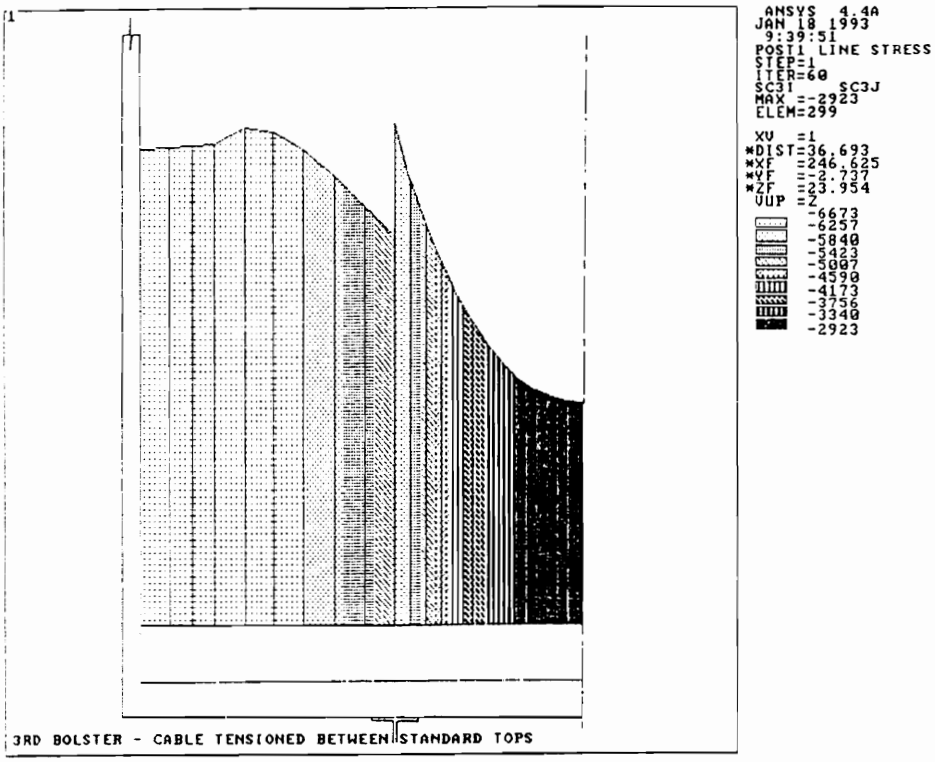

b)

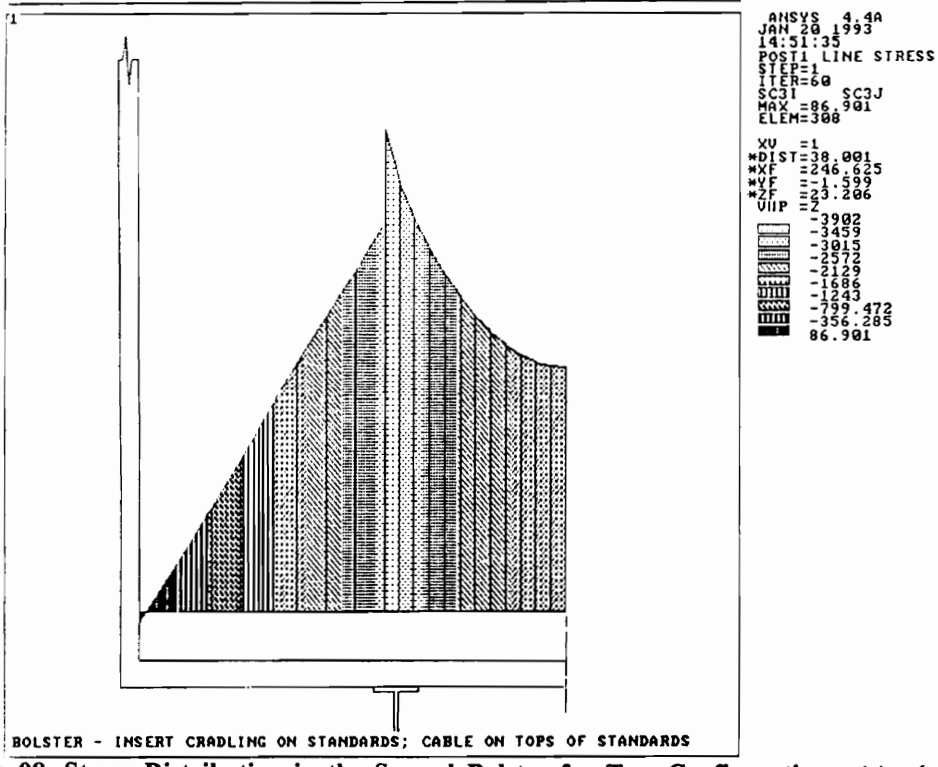

Figure 98. Stress Distribution in the Second Bolster for Two Configurations: (a) when a cable is placed between standard tops after the trailer is loaded, and pretensioned, and (b) pretensioned cable combined with an insert cradling on standards.

a)

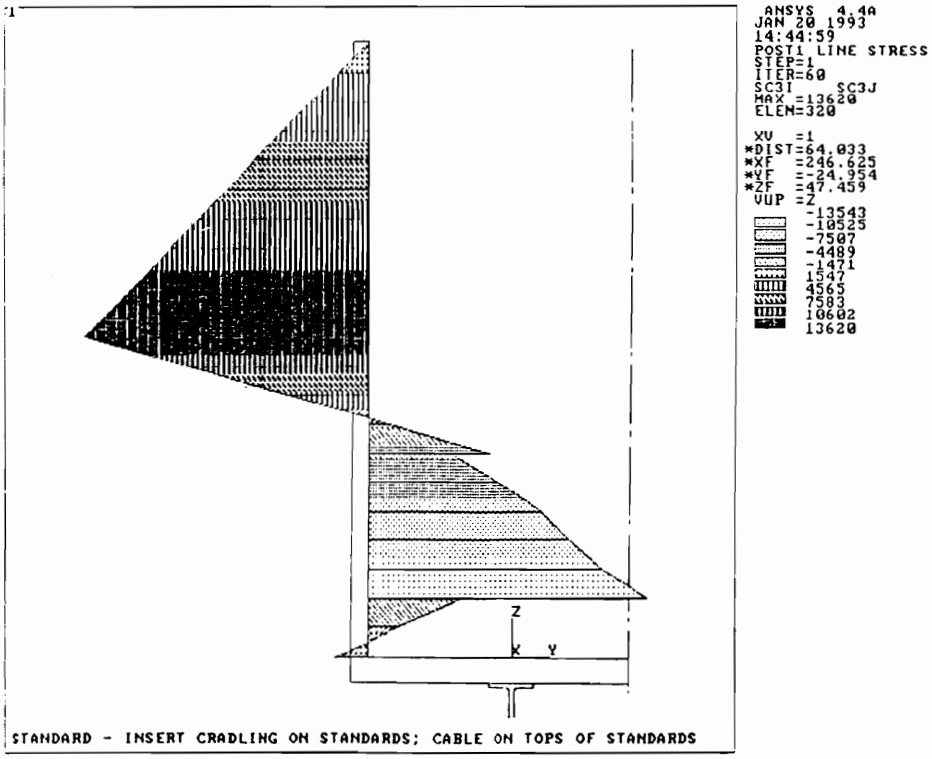

b)

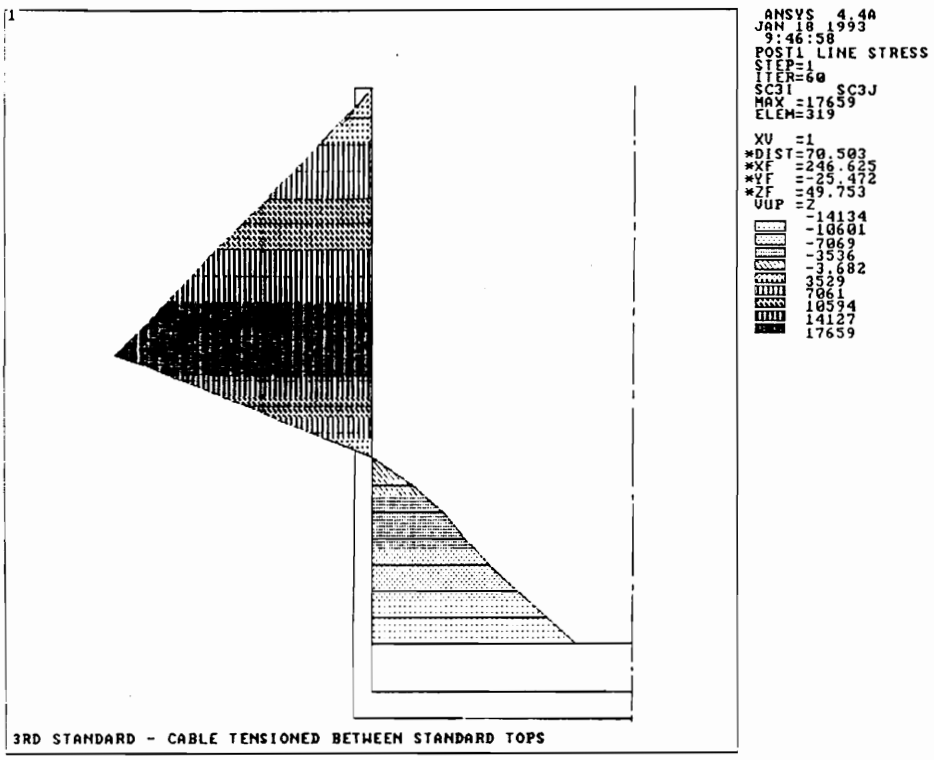

Figure 99. Stress Distribution in the Second Standard for Two Configurations: (a) when a cable is placed between standard tops after the trailer is loaded, and pretensioned, and (b) pretensioned cable combined with an insert cradling on standards.

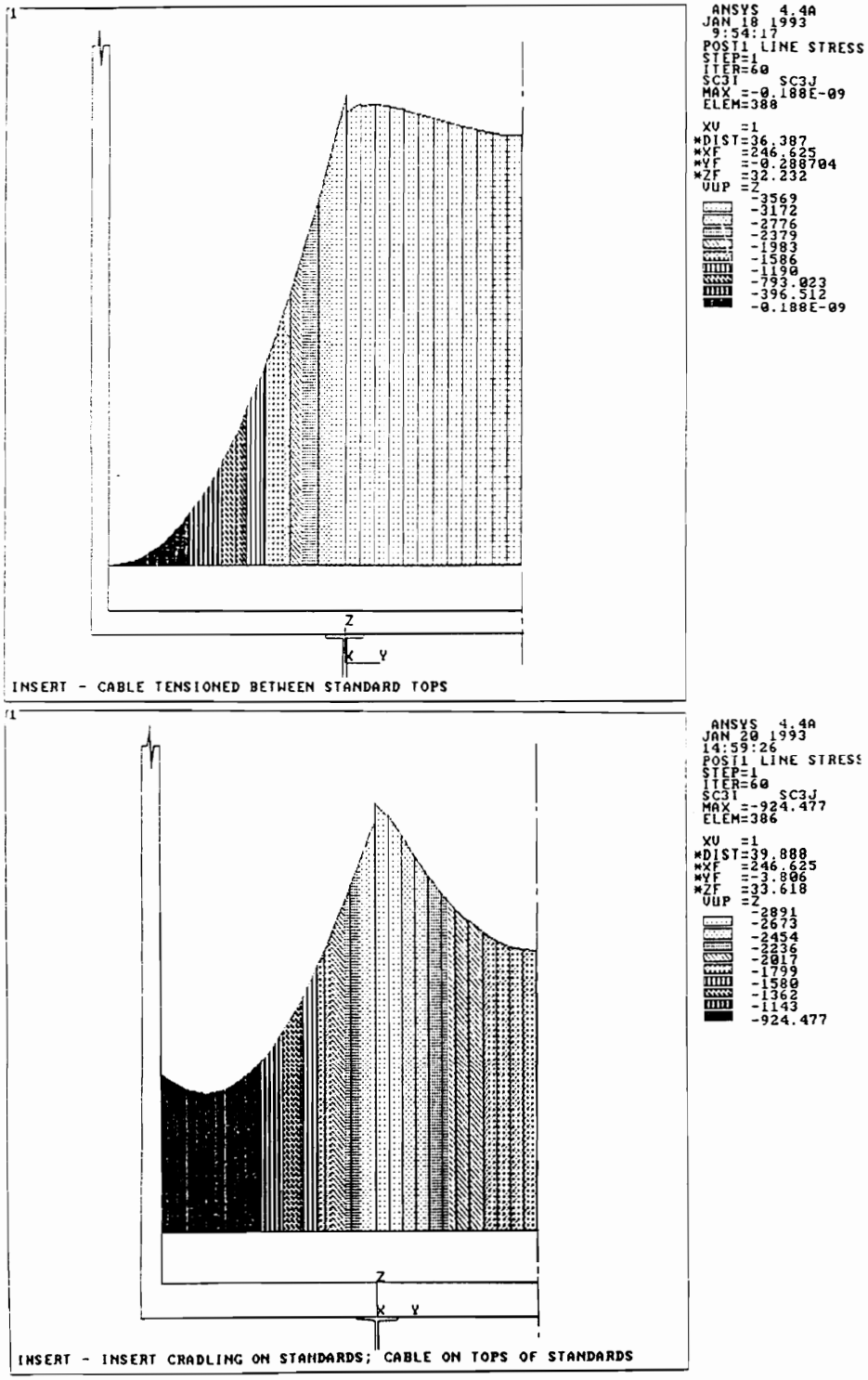

Figure 100. Stress Distribution in the Insert for Two Configurations: (a) when a cable is placed between standard tops after the trailer is loaded, and pretensioned, and (b) pretensioned cable combined with an insert cradling on standards.

The results are very interesting. They indicate that putting a cable between the tops of standards after the loading operation and pretensioning it diminishes stresses in both the bolster and the standard by a factor over 2. Stresses in the insert are also lower by about 32%.

Combining the pretensioned cable over the tops of standards and the cradling mechanisms on inserts diminishes maximum combined stresses by a factor 3.73 in the bolster, by a factor 2.25 in the standard, and by a factor 1.83 in the insert!

It follows that using some kind of a simple cradling of the inserts around the standards (e.g. by bolting ends of the inserts to the standards) and a slightly pretensioned cable between the tops of standards will increase the trailer safety, or allow for a significantly reduced tare weight, or a combination of both.

Full-Tree Trailer 3-D Model

The full-tree trailer included in the study is one of the lightest trailers in this category. It is 45 feet long, has three bolsters, is equipped with a cage incorporating two additional bolsters, and still weighs only 9,600 pounds. Its maximum legal payload is over 27 tons (i.e. assuming tractor weight equal to 16,000 pounds). The light weight was achieved by modifications of the main beam design, and by using slightly lighter members for bolsters and standards. Increased number of bolsters allowed diminishing loadings on each of the bolsters, and proportionally on the standards, as was discussed in the previous section.

The construction of the main beam was based on the W16x26 wide flange section. It has been tapered to the depth of 9 and 7/8 inches at a central section to introduce the 12-inch clearance between logs and the frame to facilitate unloading with a single-grip portal crane. A 6-inch wide, 5/8-inch thick bar was used as a top flange of the beam at the cut out section. A bow-string truss with a 4-inch wide, 1/2-inch thick strap 3 inches below the bottom flange of the beam was also added. Both the stronger beam flange and the truss had the objective of increasing the main beam stiffness against bending moments. Webs of the main beams were also reinforced by adding oval plate sections (3/8-inch thick) on both sides, under the second bolster, and on the outer sides only under the third bolster. Usual stiffeners were introduced at hangers and equalizer locations in the rear of the beams. These had the objective of increasing stiffness against shear due to vertical forces from the load. All the modifications resulted in a rather complicated geometry of the main beams (Figure 101).

There are two other very important features of the design. First, all the bolsters (except for the bolsters in the cage) were supported by struts running from the bottom of the beam web to the end of the bolster. Gussets were not used to feed stresses evenly from a bolster to the main beam through the rigid joint. The second feature is that the trailer was built employing stick-electrode welding technique without any pre- and/or post heating, or any other post-fabrication stress-relief operation.

Figure 102 shows the final, 3-D tapered unsymmetrical elastic beam model of the full-tree trailer. Altogether 378 elements (including 4 spring-damper elements: 3 simulating trailer's running gear and 1 modeling the kingpin and fifth/wheel connection) and 400 nodes were used in the model. Figure 102 shows the geometry only, while symbols of all boundary conditions are included in Figure 103. A 58,320-pound full-tree payload (i.e. 7.2% overload) was assumed for the analysis. Figure 104 hows the deformed geometry of the trailer under the load.

Figure 101. The Full-Tree Trailer: Main Beam Design.

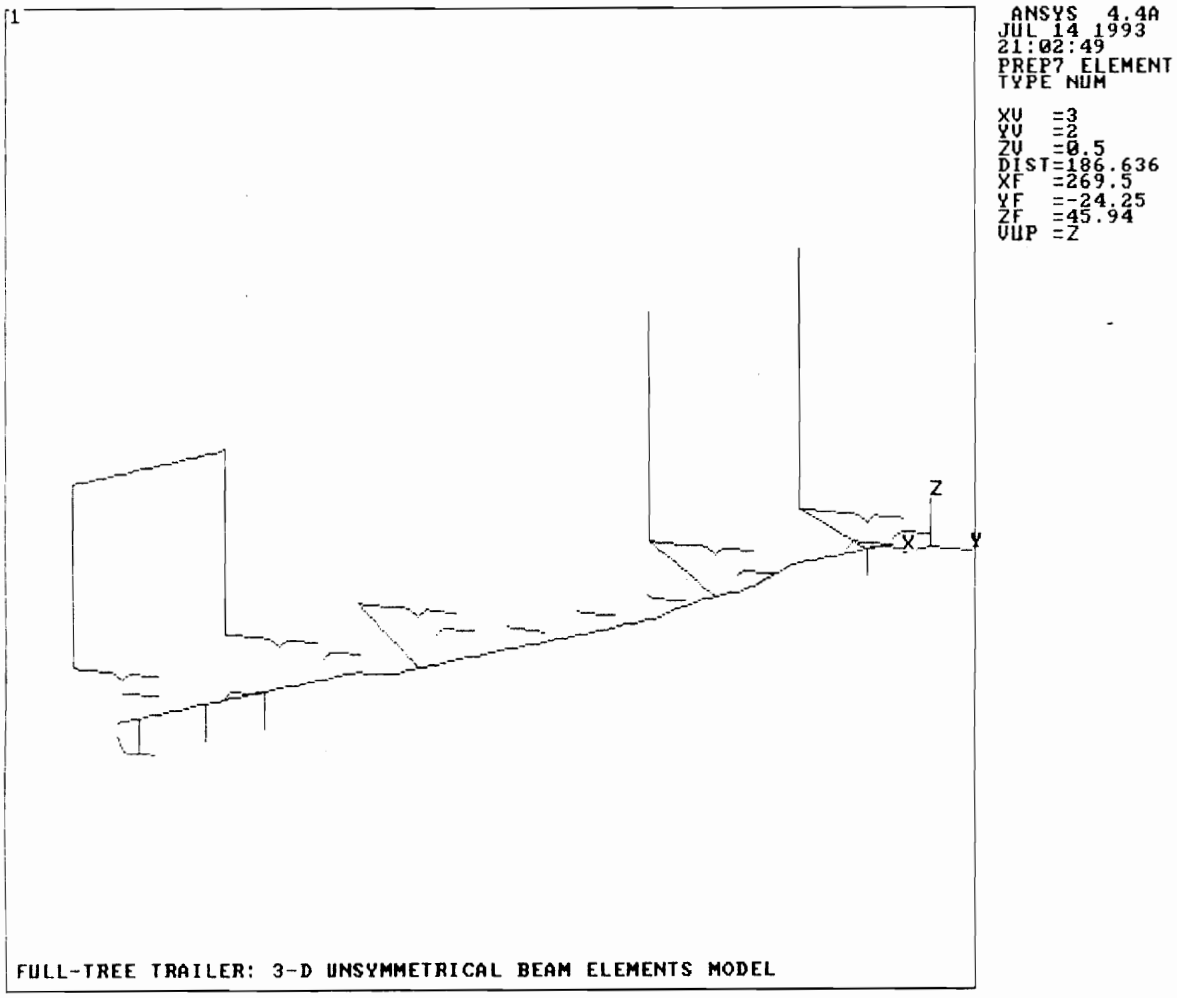

Figure 102. The 3-D Tapered Unsymmetrical Beam Elements Model of the Full-Tree Trailer.

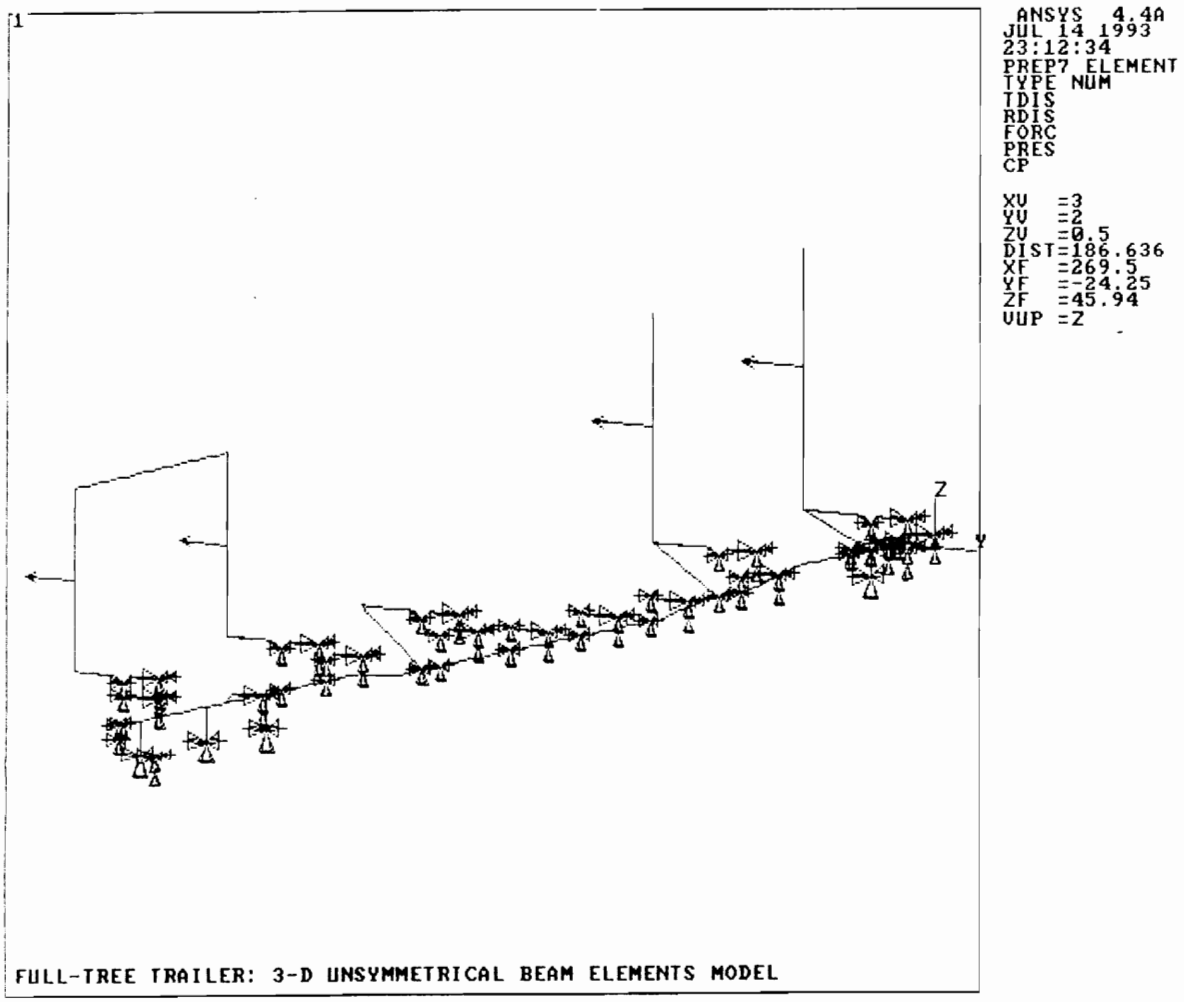

Figure 103. The 3-D Tapered Unsymmetrical Beam Elements Model of the Trailer: All boundary conditions are represented in the plot.

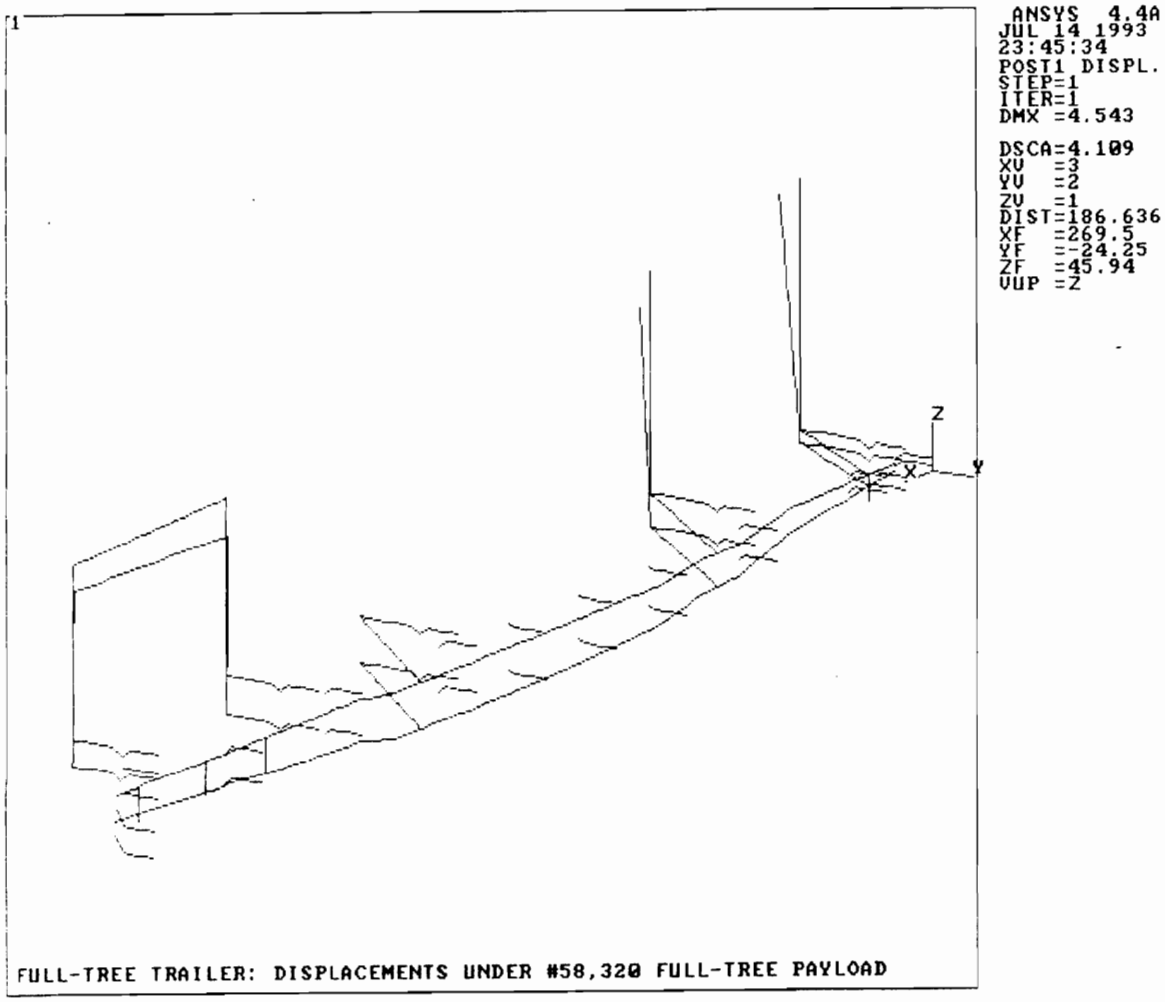

Figure 104. Deformed Geometry of the Full-Tree Trailer under 55,320-Pound Static Load Imposed on the Undeformed Geometry of the Trailer.

A plot of the maximum combined normal stresses in the structure is shown in Figure 105. The cut-out section of the main beam and struts supporting bolsters were identified as the most stressed locations on the trailer, in addition to the previously indicated critical spots: bottom sections of standards, bolsters, and places on the main beam under the second and the third bolsters. In general, the distribution of the stresses in the trailer appears very irregular and reveals many stress concentrations in the structure.

Figure 106 compares distributions of the maximum normal stresses in bottom flanges of the front and the rear bolster. The plots reveal completely different stress distributions. In the front bolster, maximum stress (8,759 psi in compression) occurs at the end of the member where bending moments are transmitted from the standard and the strut (Figure 106a). Much lower stresses, in the range of 550 psi to 476 psi, are present at the bolster and the main beam joint. It indicates that the dynamic stress fluctuates from tensile into compression and vice-versa at this location. Repeated loading causing fully reversed stresses is known to accelerate fatigue damage of steel structures. Therefore, the outside locations of the bolster and the main beam weldments are identified as the possible places where fatigue cracks could originate. This is due to the altered stress distribution in the bolster caused by adding the supporting strut.

Comparative FEM Static Stress Analysis

The trailers considered in this analysis represent three different main frame designs. The designs were categorized as follows: the gooseneck trailer as a single-drop frame, the full-tree trailer as a cut-out design, and the Clark trailer as a center-drop frame trailer. The main emphasis in the analysis was placed on the behavior of the three different main beam designs.

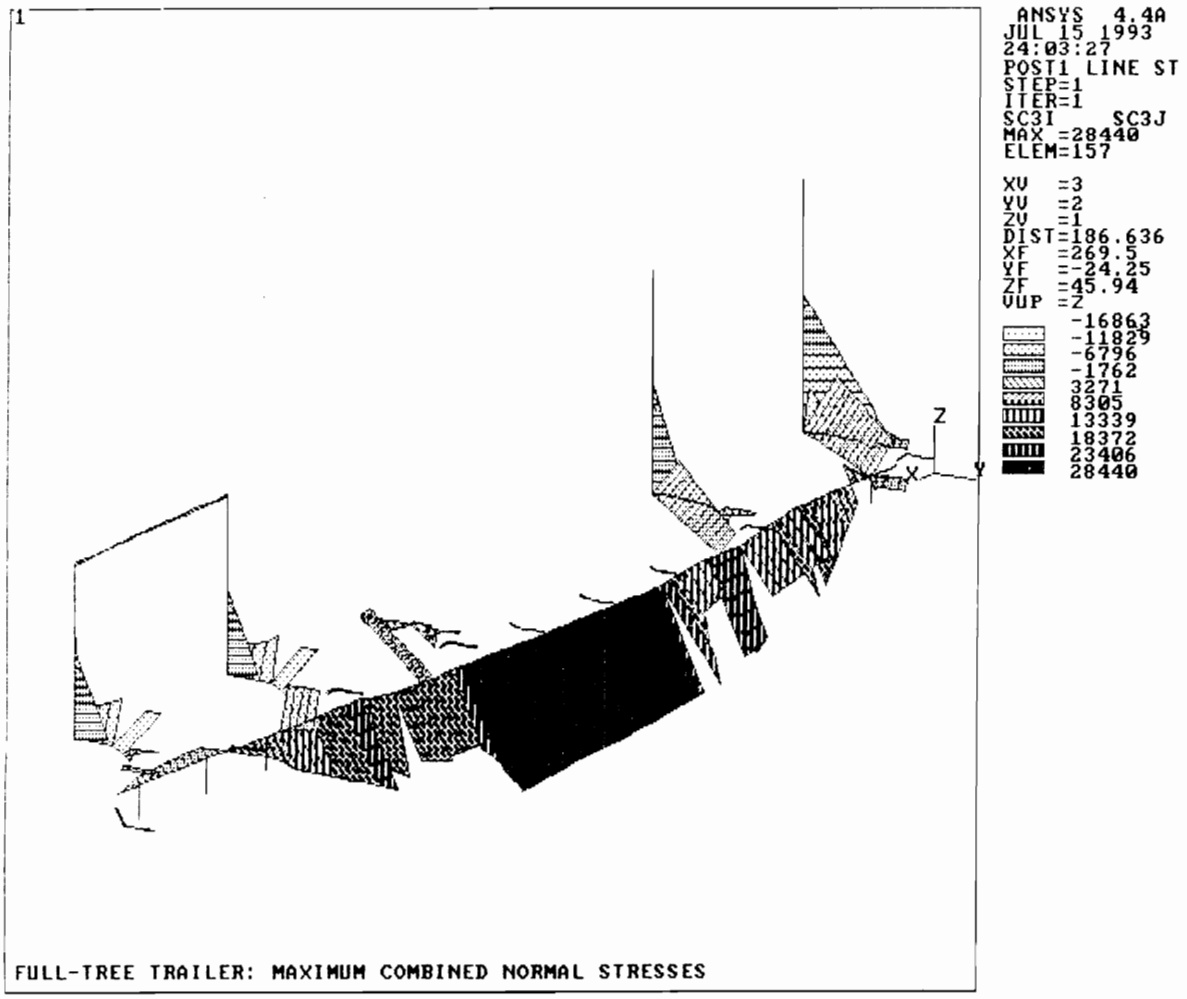

Figure 105. Maximum Combined Normal Stresses in the Full-Tree Trailer under the Static Load.

a)

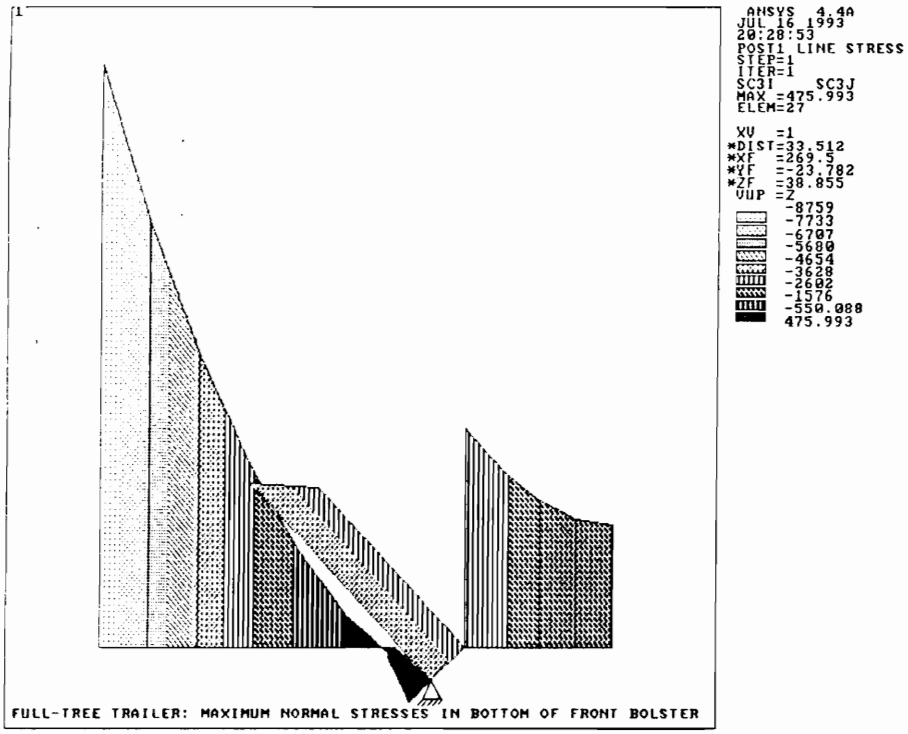

b)

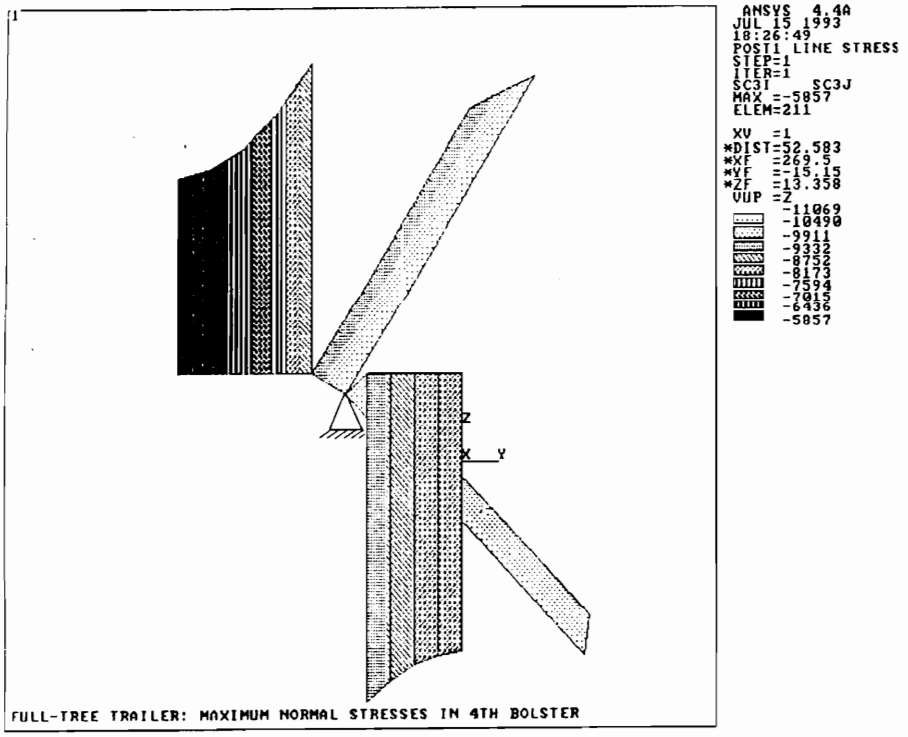

Figure 106. Comparison of Stress Distributions between the First and 4th Bolster: (a) front bolster, and (b) 4th bolster.

Static stress analysis was performed for each of the trailers, assuming the same payload and the same distance between log butts and load CG location. The loading scheme was assumed to correspond to the tree-length material placed on the second and the third bolsters. Figure 107 shows maximum normal stresses in the main beams of the trailers. A close examination of the plots reveals the following:

1. The drop-center trailer exhibits the desired, very smooth stress distribution in the main frame (Figure 107a). This design is considered superior to the other two.

2. The frame of the gooseneck trailer has a fairly uniform stress distribution, but variations in the neighboring cross-sections are present, which may lead to fatigue problem (Figure 107b). The "seesaw" stress pattern along the truss under the main beam is especially undesired.

3. The stress distribution in the cut-out frame design appears deficient compared with the other two. Uneven stress pattern with multiple abrupt changes reveals possible serious fatigue problems of the design (Figure 107c). The location under the second bolster is the most dangerous.

Frequency and Modal Analysis

Models representing the entire geometry of the structure were required for the frequency and modal analysis of the trailers. Figures 108 and 109 show models of the gooseneck trailer and the full-tree trailer, respectively. They were created by mirror reflections with regard to the longitudinal symmetry plane of each of the trailers, using models from the previous analyses. A hundred degrees of freedom (DOF) with the highest mass-to-stiffness ratios were requested to be selected automatically by the ANSYS program as the master DOF for the modal analysis.

a)

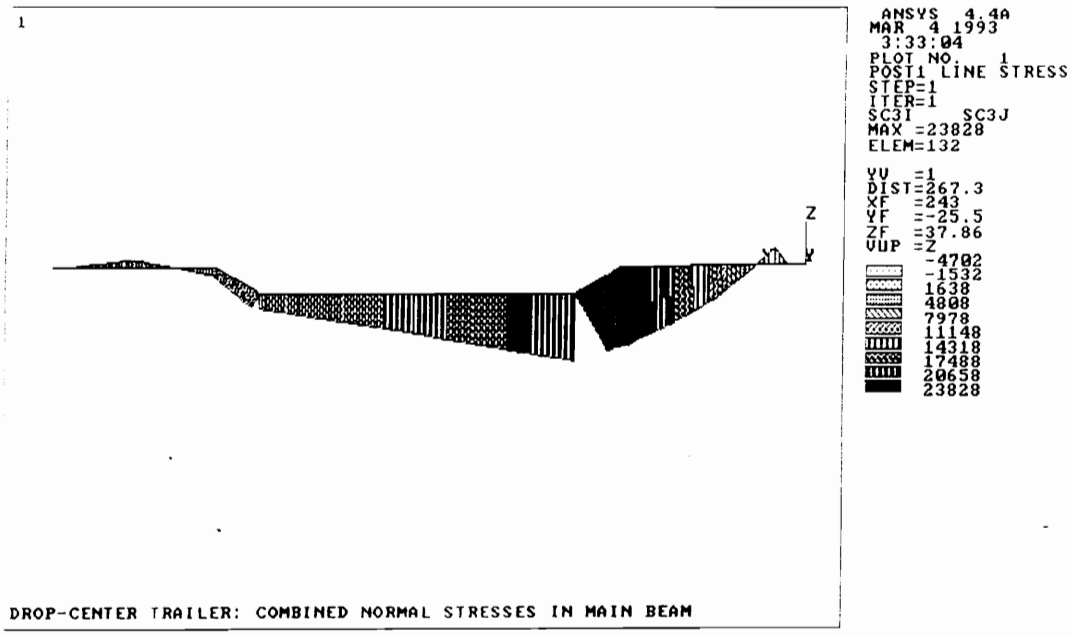

b)

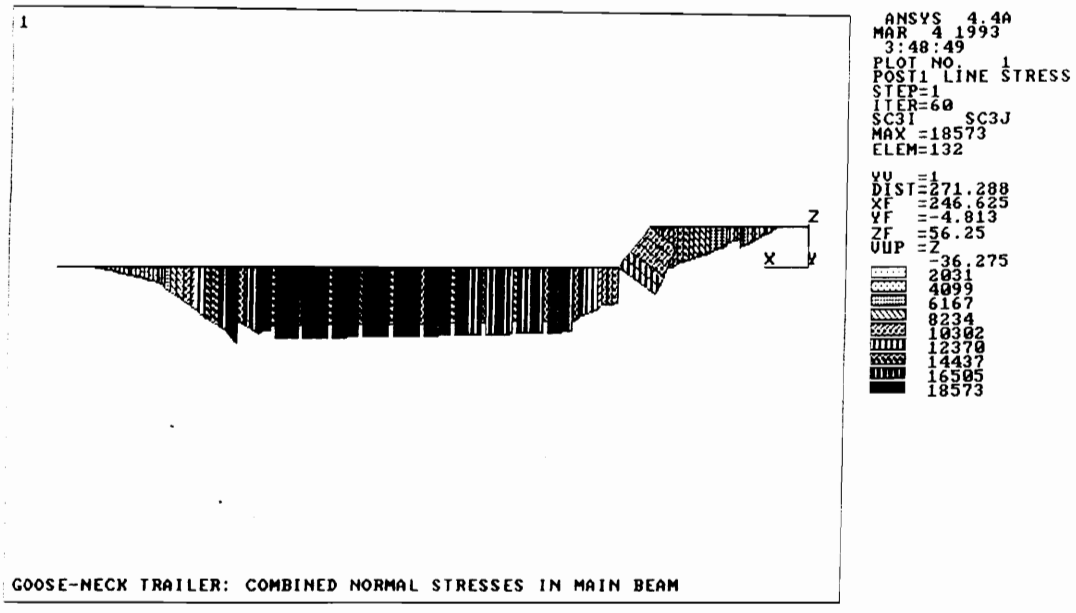

Figure 107. Maximum Normal Stresses in Main Beams of the Three Trailers: (a) Double-Drop Trailer, (b) Gooseneck Trailer, and (c) Full-Tree trailer.

c)

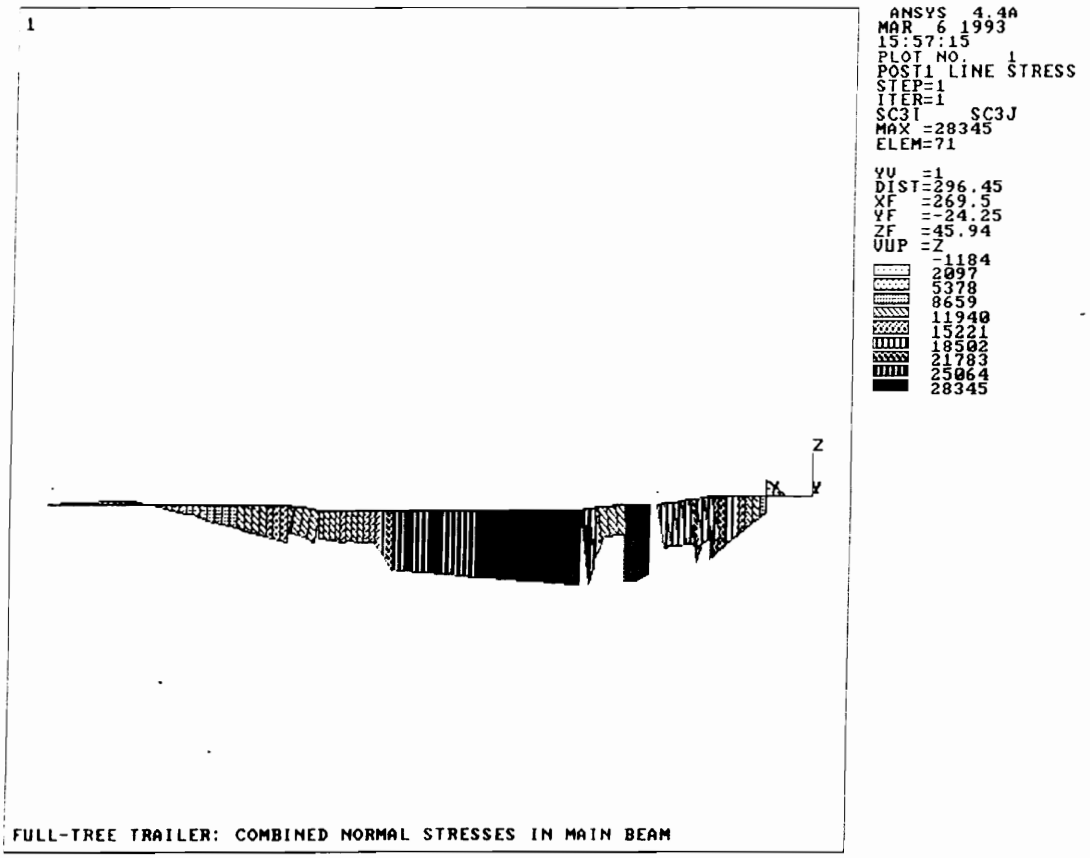

Figure 107 Continuation. Maximum Normal Stresses in Main Beams of the Three Trailers: (a) Double-Drop Trailer, (b) Gooseneck Trailer, and (c) Full-Tree trailer.

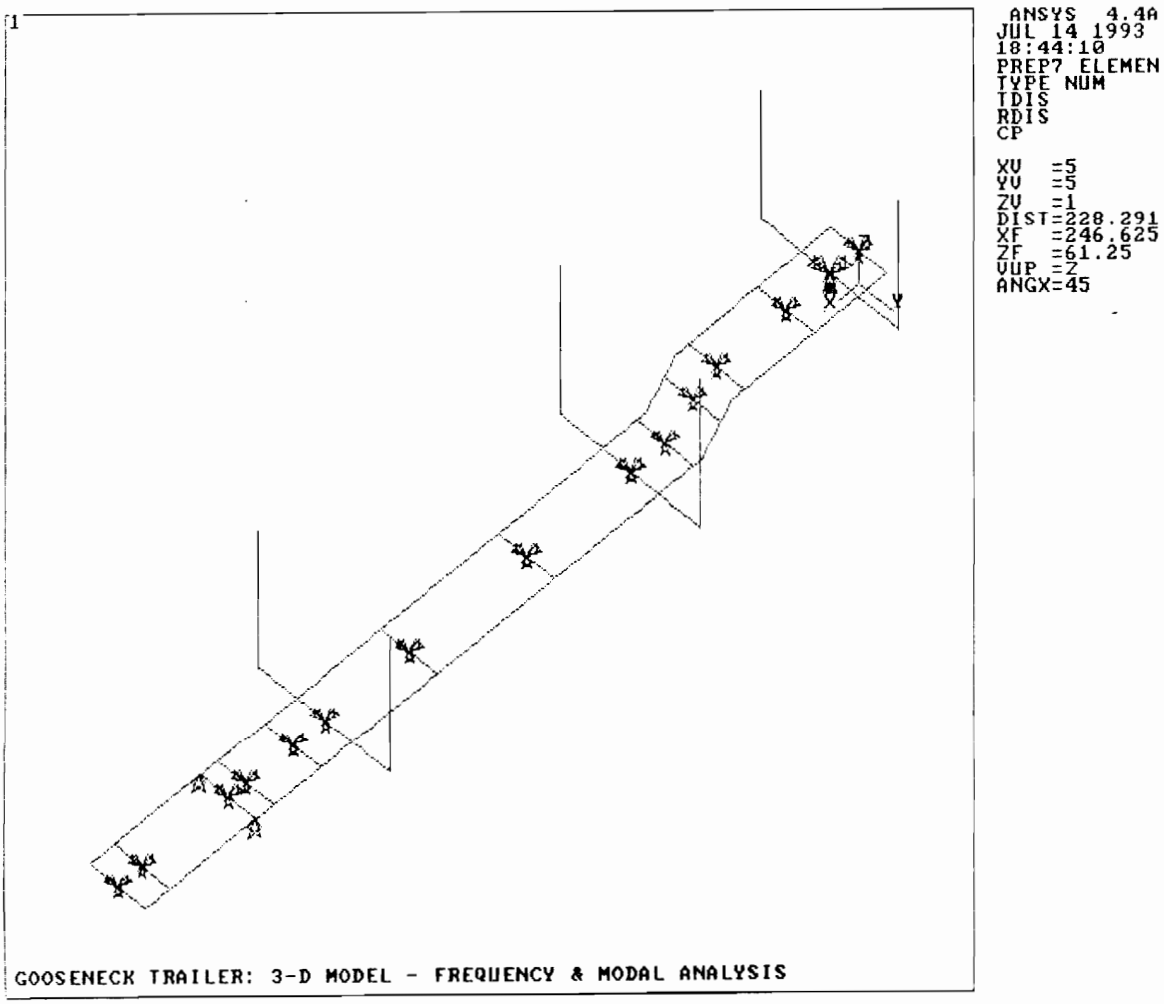

Figure 108. Frequency and Modal Analysis Input Model for the Gooseneck Trailer.

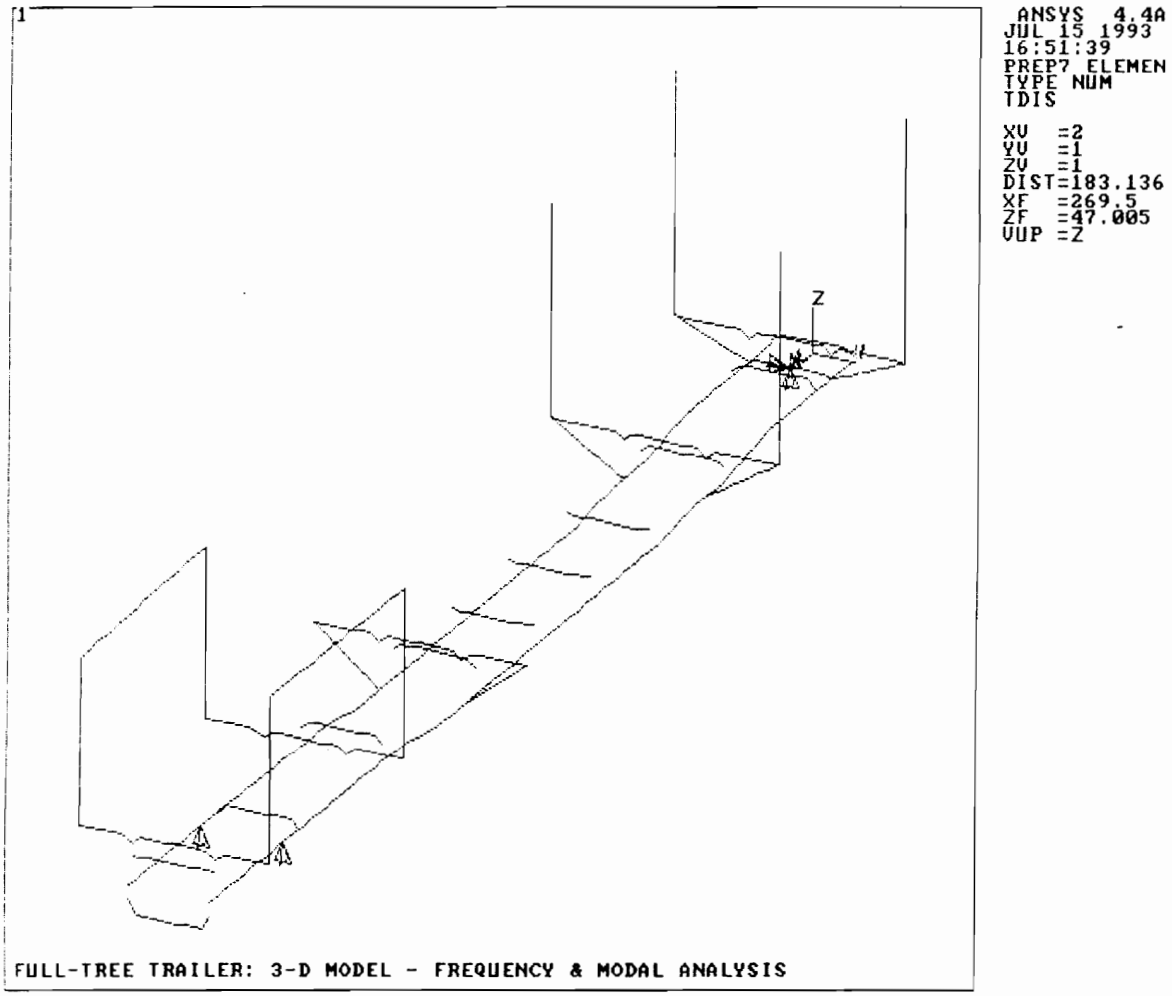

Figure 109. Frequency and Modal Analysis Input Model for the Full-Tree Trailer.

The first three lowest natural frequencies computed for the two trailers are given in Table 16. A careful inspections were performed of the structure displacements associated with vibration modes corresponding to the given natural frequencies. It indicated that the displacements for the third lowest frequencies coincide with "up-and-down swaying" frame vibrations of both trailers,which were very commonly observed to be excited by signals from the road. This mode of vibrations for the gooseneck trailer and the full-tree trailer has been shown in Figures 110 and 111, respectively.

The computed frequencies agree with the frequencies of "resonance" responses of the trailers measured during the experimental stress analyses (see Figures 78 thorough 81).

It is concluded that a suspension system which has harmonics removed from the range of 7 to 8 Hz should be selected for the trailers to prevent a mechanical resonance of the structures as a result of the excitation from the road when the trailers are driven empty.

Table 16. The First Three Lowest Natural Frequencies of the Gooseneck and the Full-Tree Trailer.

First Lowest Frequencies	Gooseneck Trailer	Full-Tree Trailer
1st Lowest	1.175 Hz	0.621 Hz
2nd Lowest	3.846 Hz	6.509 Hz
3rd Lowest	7.162 Hz	7.749 Hz

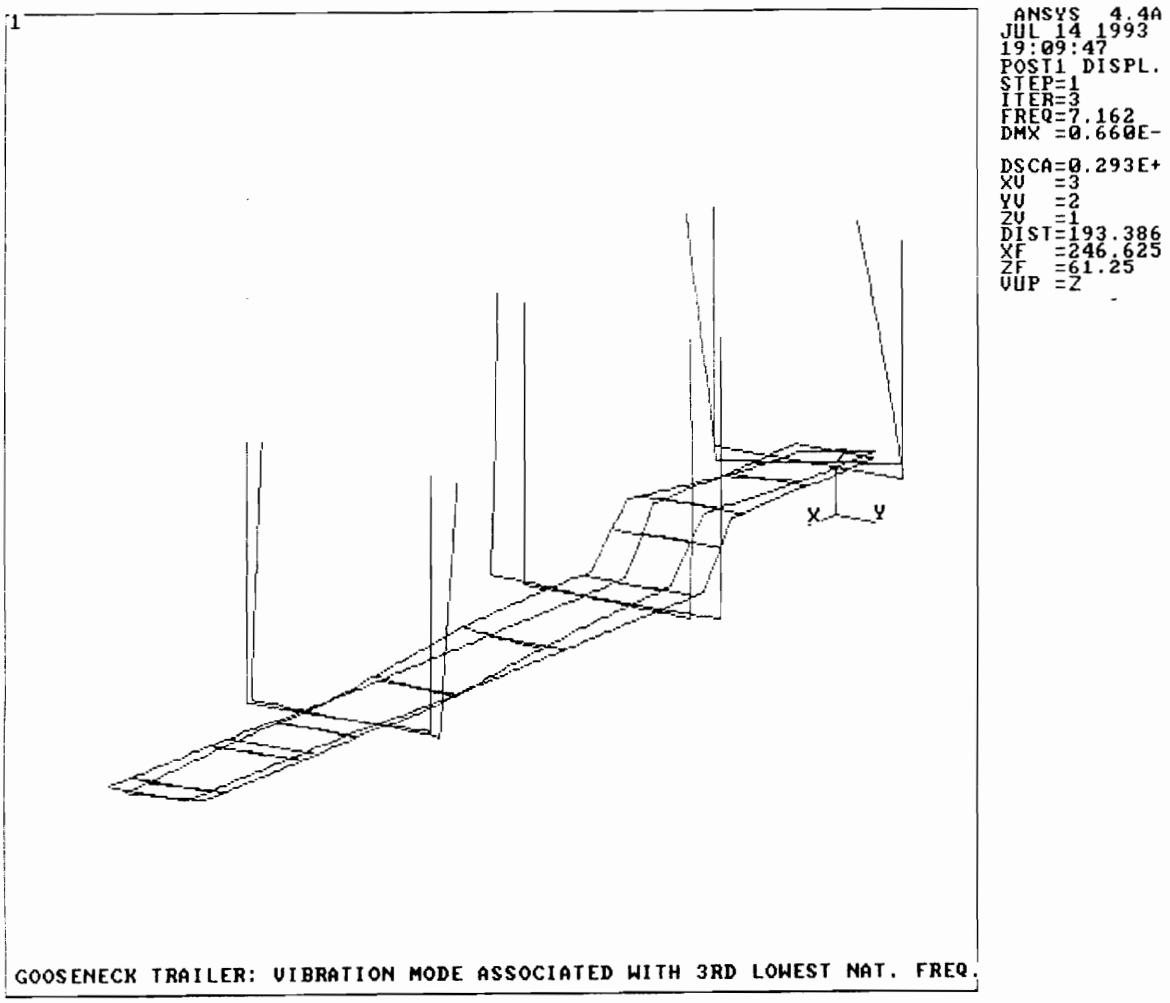

Figure 110. Vibration Mode of the Gooseneck Trailer Associated with the 3rd Lowest Natural Frequency.

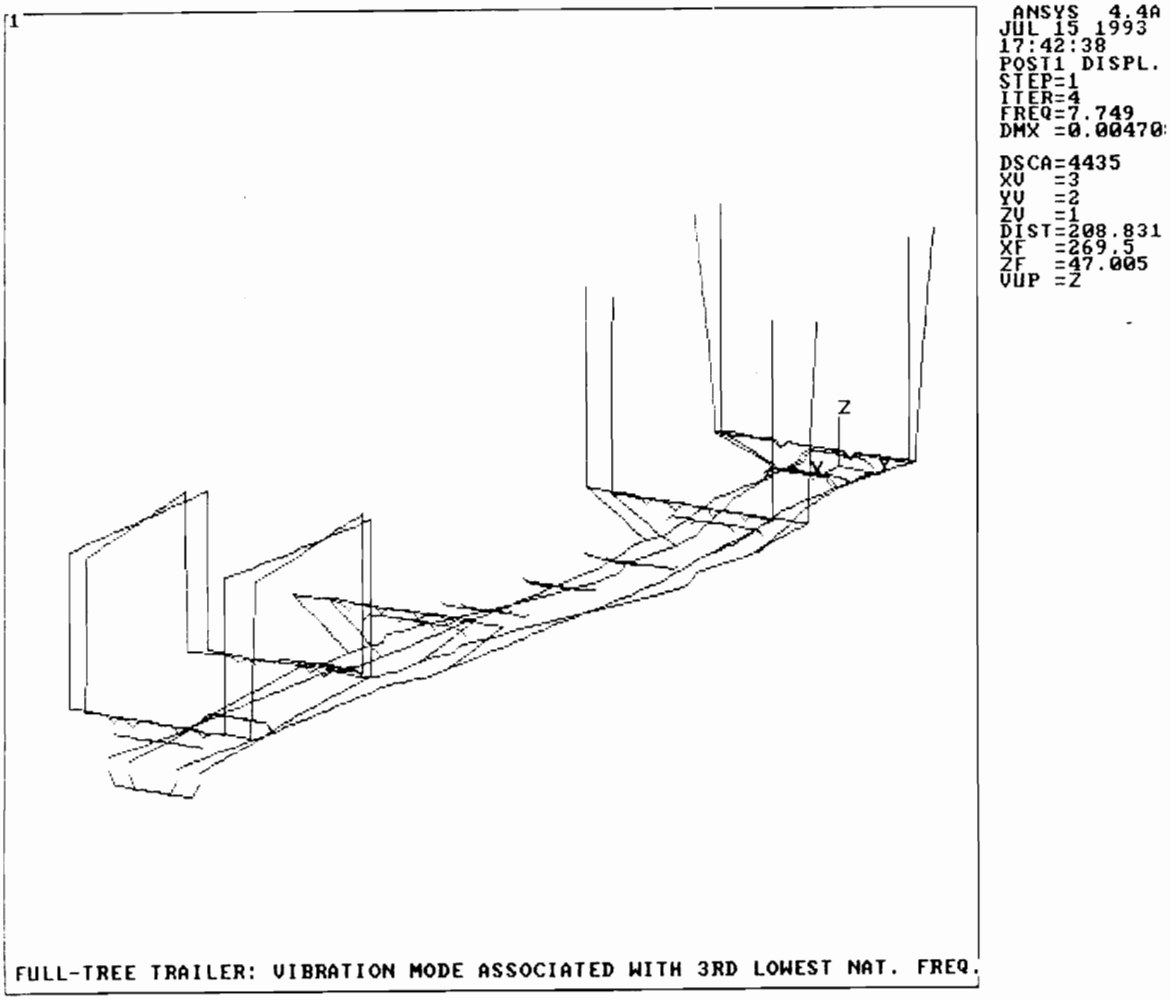

Figure 111. Vibration Mode of the Full-Tree Trailer Associated with the 3rd Lowest Natural Frequency.

CHAPTER 7. FATIGUE OF LOG TRAILERS

Introduction

Maximum nominal dynamic stresses were measured at critical locations on selected trailers while simulating extreme situations and during typical work cycles. The stresses were found to be below yield points of the material. The lowest safety factor (computed against a yield point) SF = 1.31 was detected in a main beam when the gooseneck trailer was tested under extreme cornering conditions. The trailer was carrying a heavy payload corresponding to a 12.7% overload placed between the second and the third bolster, which induced unfavorable load distribution in the beam. At this most dangerous situation, a safety buffer of 30% of the material strength was still left.

The experimental data indicate therefore, that it is unlikely that trailers will fail by extensive yielding (i.e. plastic deformation) due to excessive nominal stresses induced into the structure under "normal conditions". Normal conditions are understood as those excluding situations when a trailer is: tipped over, crushed by a crane grapple, loaded with loads other then logs, crushed in a traffic accident, or any other condition resulting from an obvious misuse of the trailer.

A careful examination of the second tested full-tree trailer revealed many fatigue cracks in the structure. There was a number of factors contributing to this phenomenon. These included: inherent features of the design (i.e. struts used instead of gussets, and the modified frame design), fabricating technique (i.e. stick-

electrode welding), and materials used for building the trailer (i.e. low tensile steel). Observations during experimental stress analysis indicated that the structure was subject to larger twisting torques than the other trailer, because center of gravity of the full-tree-load was shifted to the back of the vehicle. These torques caused frequent "racking" of the trailer's frame ("racking" is understood here as a situation when the frame was undergoing severe displacements as a result of the combined effect of large bending moments and twisting torques). Data recorded, when the trailer was traveling over Florida State Highway 19, revealed that a frequency of the repeated dynamic load from the concrete highway at about 55 mph, when the trailer was driven empty, and at 45 mph, when the trailer was driven loaded, coincided with the natural frequencies of the structure. The trailer was at the end of its third year of service at the time of the experiment. It was carrying heavy payloads (approximately 27 tons) four times a day and five days a week. All the above factors contributed to the fatigue damage of the trailer.

These observations with the full-tree trailer lead to a survey of other trailers for fatigue cracks. Examination of a number of log trailers across the Southeast revealed common places where fatigue cracks originated:

1) inside standard and bolster junction (Figure 112);

2) where bolsters are mounted rigidly on flanges of the main beams (Figures 113 through 116);

3) where cross member flanges are welded to flanges of main beams (Figure 117);

4) where cross member flanges are welded to webs of main beams;

5) at transitions between flexible and stiff components (e.g. main beam/fifthwheel plate junctions); and

6) along the bow-string truss added under the main beam to increase its section modulus (Figure 118).

These findings indicated that a log trailer, unless over designed, fails (or may eventually fail) by fatigue, i.e. progressive brittle fracture. This mode of failure results from repeated loadings and occurs by fracture without visual evidence of yielding at nominal stress levels well below the strength of the material.

Usually, fatigue cracks initiate and propagate at points of high localized stresses. The following conditions cause stress at a point in a simple member to attain significantly higher values than the nominal (i.e. computed from ordinary formulas):

1) abrupt changes in cross-section properties;

2) residual stress resulting from fabrication (e.g. machining, welding, drilling);

3) high pressure at points of load application;

4) cracks and scratches on a surface of the member resulting from material impurity, manufacturing process, etc.; and

5) corrosion pits on a surface of the component created by environmental conditions.

These places of higher than nominal stresses (i.e. stress raisers) are always accompanied by high stress gradients as the phenomenon is of a very localized character.

Figure 112. Fatigue Crack Inside of Standard and Bolster Junction.

Figure 113. Fatigue Crack at Bolster and Main Beam Weldment.

Figure 114. Fatigue Crack at the Tip of the Bolster Reinforcing Gusset.

Figure 115. Fatigue Crack in the Outside Section of the 3rd Bolster of the Full-Tree Trailer.

Figure 116. Fatigue Crack in the Inside Section of the 3rd Bolster of the Full-Tree Trailer.

Figure 117. Fatigue Crack at the Corner Where the Flange of the Cross Member is Welded to the Flange of the Main Beam.

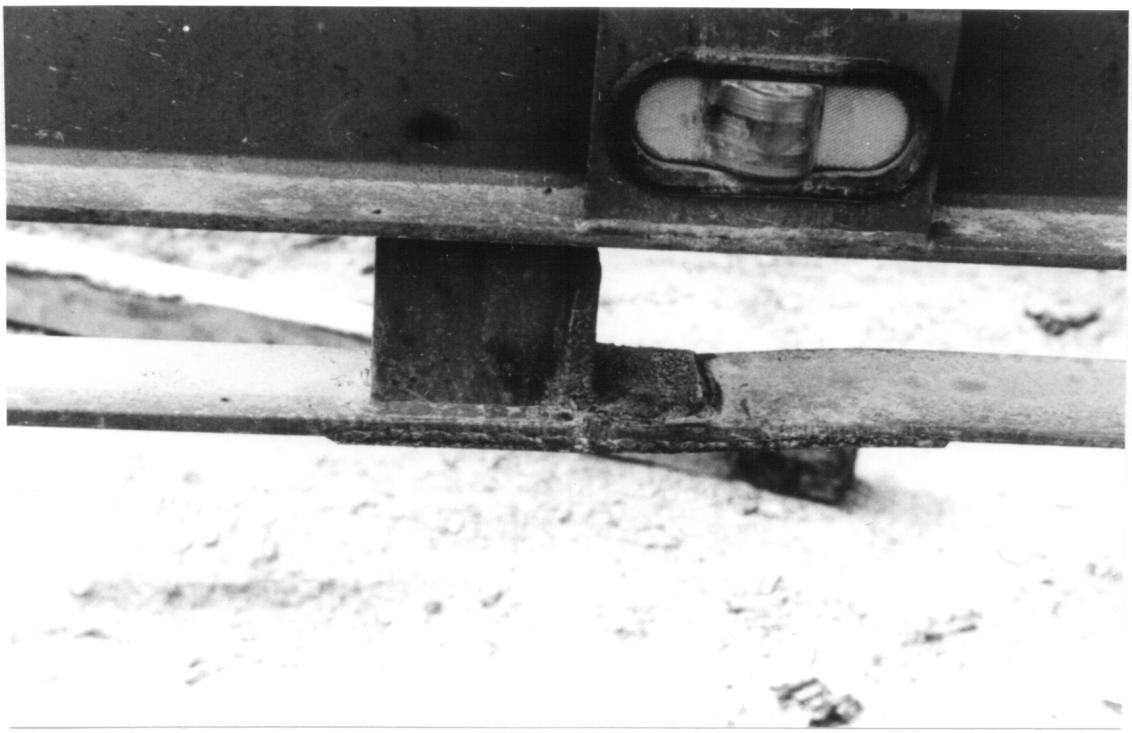

Figure 118. Fatigue Crack in the Bow-String Truss under Main Beam.

A combination of the three phenomena: a notch effect, residual stress from welding and large highly localized stresses due to restrained warping of I-sections contribute to fatigue cracking of log trailers.

The notch effect due to a sudden change of stiffness was present at every location identified as a common place for crack origination on a log trailer. The bow-string truss under the main beam of many log trailers is an excellent example of this common design mistake. Figure 118 shows the truss on a shortwood trailer. The very spot where a short rectangular tube spacer is welded to the strapping becomes a stress concentration point due to the sudden change in stiffness of the beam. This location experiences the largest nominal stresses (with the exception of the outside fibers in the strap). This is a spot where the residual stresses are introduced by welding (which can be as high as yield point of the material). As the photo shows fatigue crack originated at and propagated at this location. The problem of cracking bow-string trusses is more pronounced on double-bunk trailers since their frames experience higher bending moments from the load. The W 18x35 wide flange I-beam with the reinforcing truss underneath is used so widely in building trailers because it is easily available (e.g. used in construction) and fairly inexpensive. A fabricated I-beam of an increased depth or with a thicker or wider flanges would be much lighter and stronger than the "hybrid structure", provided that the fabrication does not induce excessive residual stresses.

Welding operations induce residual stresses locally around the "heat affected zone" in the members joined. Weldments also introduce stress concentrations due to the bead geometry. Fatigue strength of a welded joint depends on many factors: weld type, joint geometry, welding technology, heat operation prior to and after welding, and the characteristic of the applied loads. Design fatigue strength of steel weldments for alternating stresses at 2 million cycles ranges usually from one third to one ninth of the yield strength of the material (Fuchs and Stephens, 1980). Figure 119 shows distribution of residual stresses in welded beam (after Rice edit., 1988).

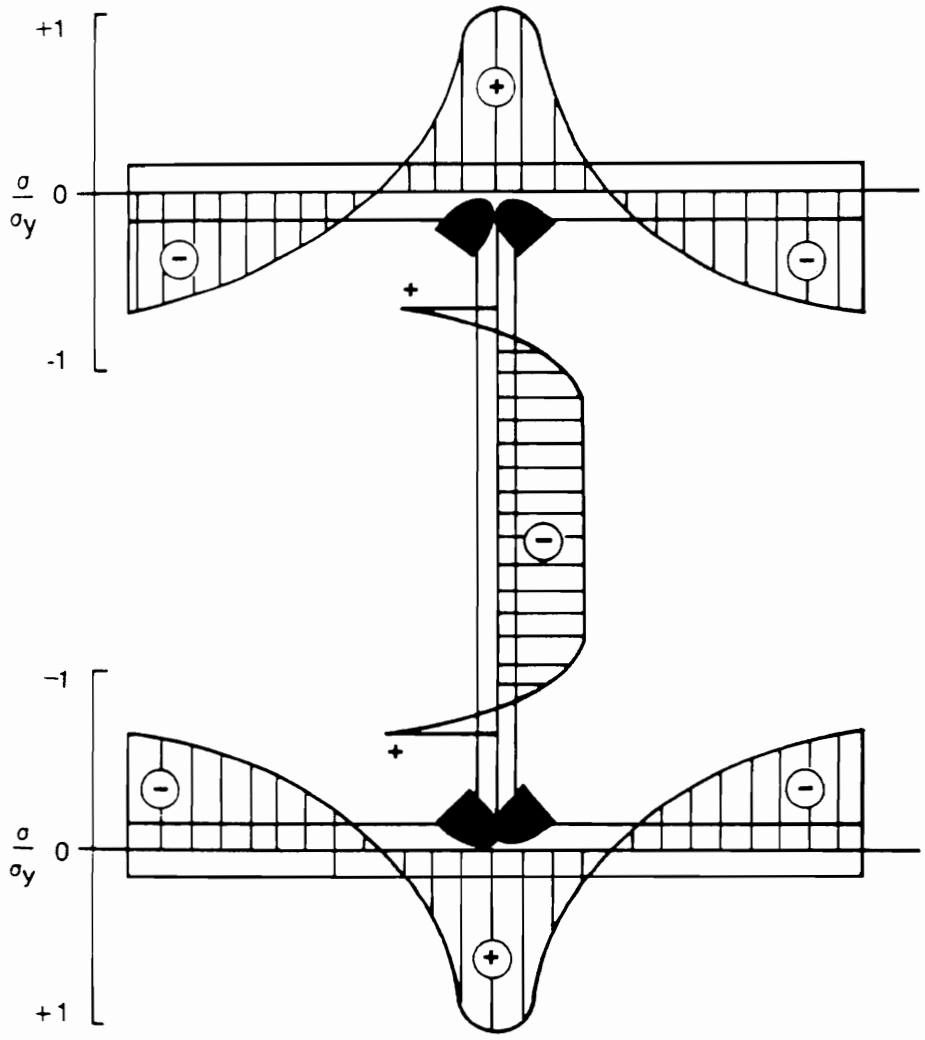

Figure 119. Residual Stresses in Welded Beam.

Figure 119 shows clearly that the maximum residual tresses in the welds of welded I-beam can easily approach the yield strength of the material.

Heat treatments are employed to remove the residual stresses induced by high temperature gradients created during welding operation. The thermal stress-relief can increase fatigue strength of weldments at lives greater than one million cycles provided that the stress ratio is less than or equal zero and notches are present in the weldment (Rice edit., 1988).

A stick-electrode welding can have a disastrous affect on some assemblies. Figure 120 shows the front bolster of the full-tree trailer. The bolster was mounted rigidly directly on the top flange of the main frame. A fatigue crack originated at the front tip of the weldment due to the notch affect, residual stress from welding, and a fluctuating, fully reversed dynamic loading. When the crack reached a length of about 2.5 inches, it was repaired by stick-electrode welding without pre- or post-heating. The welding operation worsened instead of repairing the situation in the crack. The brittle weld fell off creating a large opening. The weakened cross-section of the bolster was now so reduced that the crack propagated even faster. It went all around the bolster (Figure 121). The bolster was, finally, plastically deformed while the trailer was being loaded, a week after this photograph was taken.

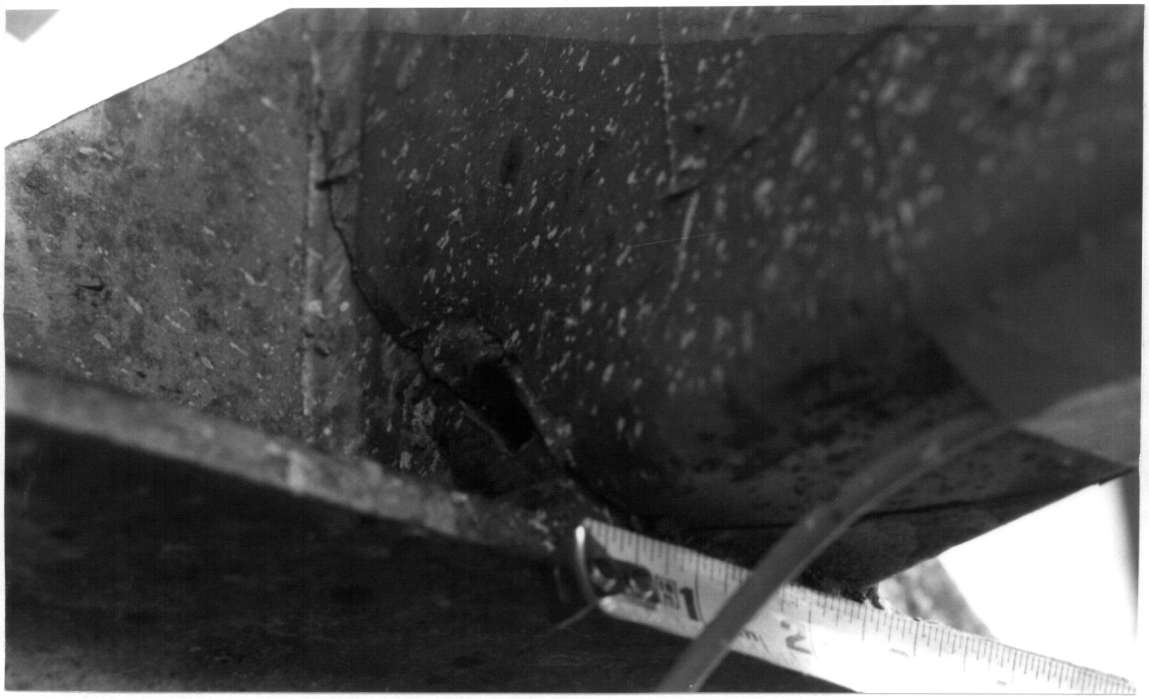

Figure 120. Fatigue Crack in the Front Bolster of the Full-Tree Trailer; It's propagation was accelerated by stick-electrode welding.

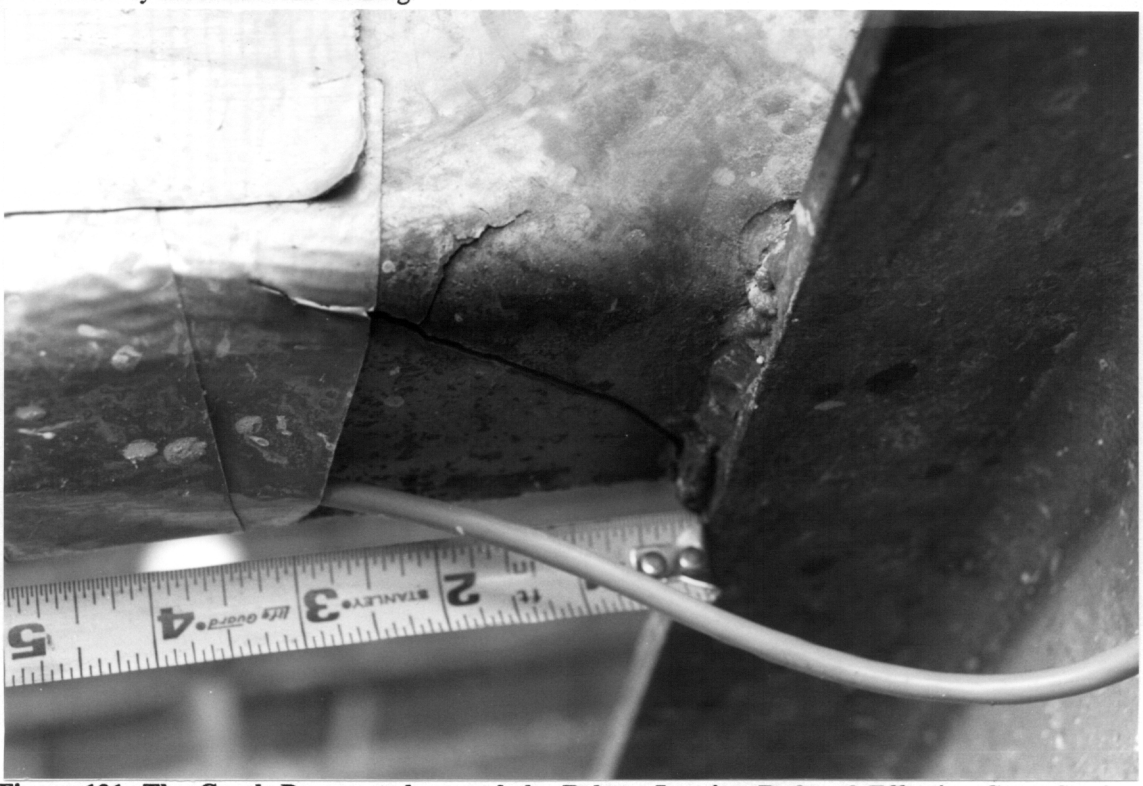

Figure 121. The Crack Propagated around the Bolster Leaving Reduced Effective Cross-Section; The bolster failed by plastic deformation a week after this photo had been taken.

Torsion of I-Beam with Restrained End

Data from the dynamic stress measurements show that a log trailer is subjected to a combination of bending moments, twisting torques and axial forces. The "racking" situation of a trailer was identified as the most severe loading on the trailer. This situation was frequently observed when the vehicle was negotiating tight curves, passing over deep ditches on low-quality roads, or transferring from dirt to paved road. Wide flange I-beams are, almost exclusively, used as main beams in log trailers. A rolled section is a poor member to support such a combination of loadings (Boresi and Sidebottom, 1985). They undergo excessively large rotations in torsions, because rolled sections are not particularly suited to resist large torsional moments.

A single I-beam, when subjected to a twisting torque, warps at every cross-section like any other torsional member with a noncircular cross section. If the beam is rigidly fixed to supports, warping at the restrained cross-sections is prevented. Therefore, in addition to the shearing stresses that counterbalance the torsional load, normal stresses develop at the restrained sections. These highly localized normal stresses are significant compared with the nominal stresses in the cross-section.

Figure 122 shows an I-beam fixed rigidly to a wall and subjected to a twisting torque T. At a section close to the wall the torsional load is transmitted mainly by lateral shearing forces V in each flange (Boresi, and Sidebottom, 1985). As the result, a linear normal stress distribution in each flange is produced at the wall. At small distances away from the wall partial warping occurs, and the torsional load is transmitted partly by the shear forces $V' < V$ in the flanges and partly by a shear stress distribution in torsion. At greater distances from the wall, the effect of the restrained warping diminishes rapidly and the torque is transmitted mainly by torsional shearing stress distribution.

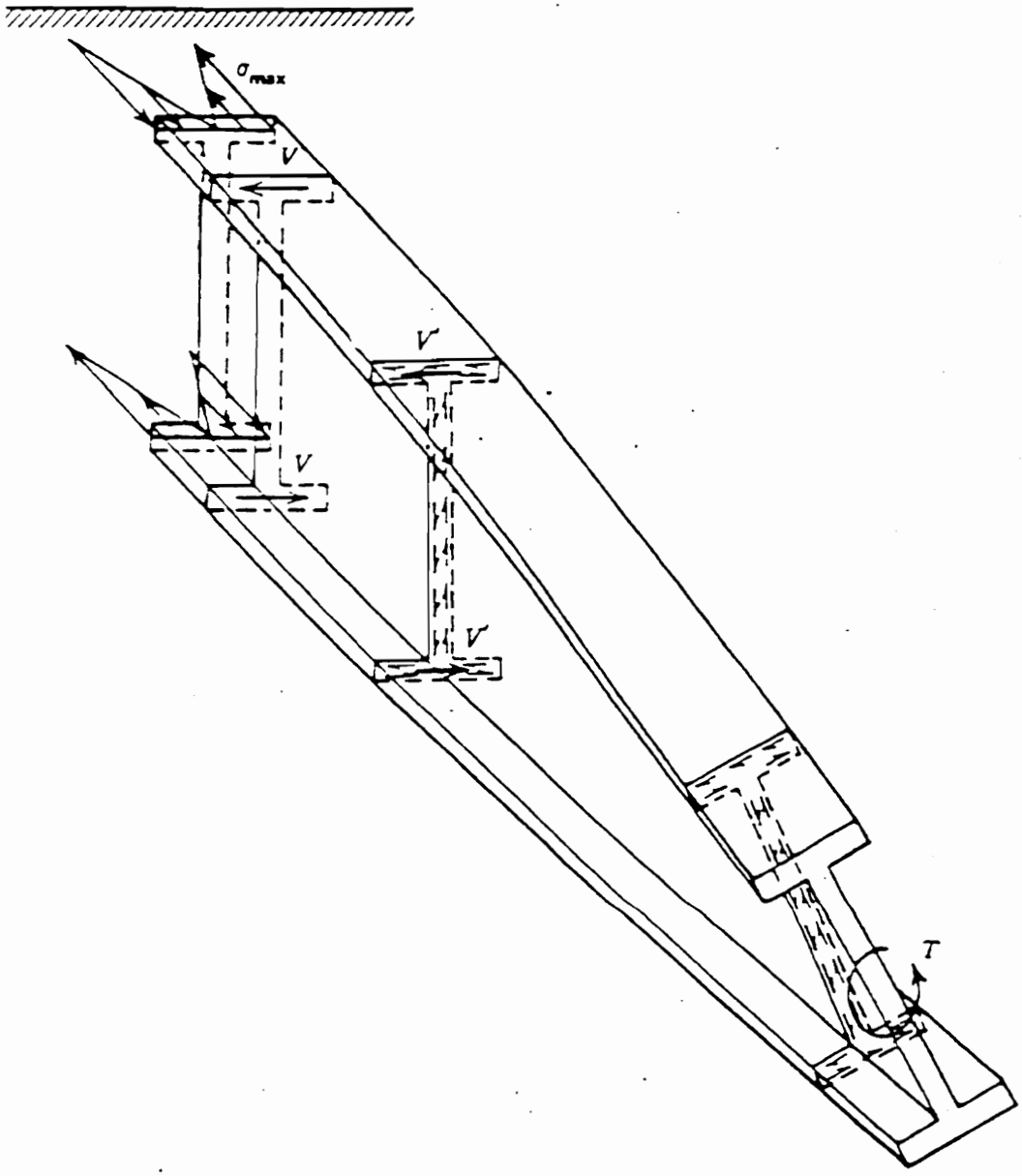

Figure 122. I-Beam Fixed Rigidly at One End and Subjected to Twisting Torque at the Other End.

The localized normal stresses in I-beams subjected to twisting torques with cross sections restrained from warping are one of the main causes of stress concentrations in log trailers.

Rectangular Box Sections Free from Warping

Box beams are generally used in earth-moving, construction and mining equipment not only because the box section saves weight, but because it also offers an excellent combination of torsional and bending resistance. The walls of the box are made thick enough to carry the normal stresses due to bending. The ends of the box beams are usually welded to other members so that at the fixed ends warping is prevented. This adds additional torsional stiffness and transverse shearing stiffness to the structure.

Unlike wide flange rolled sections, some noncircular thin-wall hollow members, under certain conditions, twist without warping.

A solution for the problem of a thin-walled cylinder under an nonuniform twist was presented by von Karman and Chien in 1946. The authors showed that constant thickness hollow torsion members having a cross-section of an equilateral polygon do not warp. Therefore, a square box beam does not warp and does not develop normal stresses at the restrained cross sections. However, a square box beam of the same section modulus as the corresponding wide flange rolled section would be heavier by about 30%. Thus, a solution for a strong and light cross-section should be sought in a rectangular box beam.

Thin-walled members of rectangular box section and uniform thickness were shown to warp when subjected to twisting torques. The distribution of normal stresses at restrained cross-sections was found

nonlinear with vanishing stresses at midpoints of the sides and maximum values occurring at the corners (Figure 123).

Smith et al. (1970) investigated the influence of cross-section dimensions of the beam on the stresses at the restrained sections. They found that the maximum normal stresses at the restrained end section of a 20-inch long, 8-inch high, 3-inch wide, and of 1/4-inch wall thickness, box beam was 0.18486 psi per inch-pound of twisting torque. While in a box of the same outside dimensions but with the thickness of a shorter side increased to 3/4 inch the maximum normal stress was computed to be 0.19680 psi/(in.*lb.). This indicated that putting more material in the shorter side slightly increases the stresses. Conversely, if the short side were reduced in thickness from 1/4 inch to 3/32 inch the stresses would vanish completely. In general, the authors discovered that if the cross product of the length and thickness of the sides of the rectangular box beam is a constant (e.g. for the 8 in. X 3 in. X 1/4 in. X 3/32 in. beam the cross product is 8*(3/32) = 3*(1/4) = 3/4) then no warping occurs, and hence the localized normal stress do not develop at the restrained sections.

It follows that rectangular box sections free from warping used for main beams in log trailers would decrease the localized stresses at all the places where the members are welded together. This in turn would directly increase the fatigue life of the structure. And finally, more importantly, delayed initiation and propagation of unavoidable cracks would significantly increase safety of log trailers.

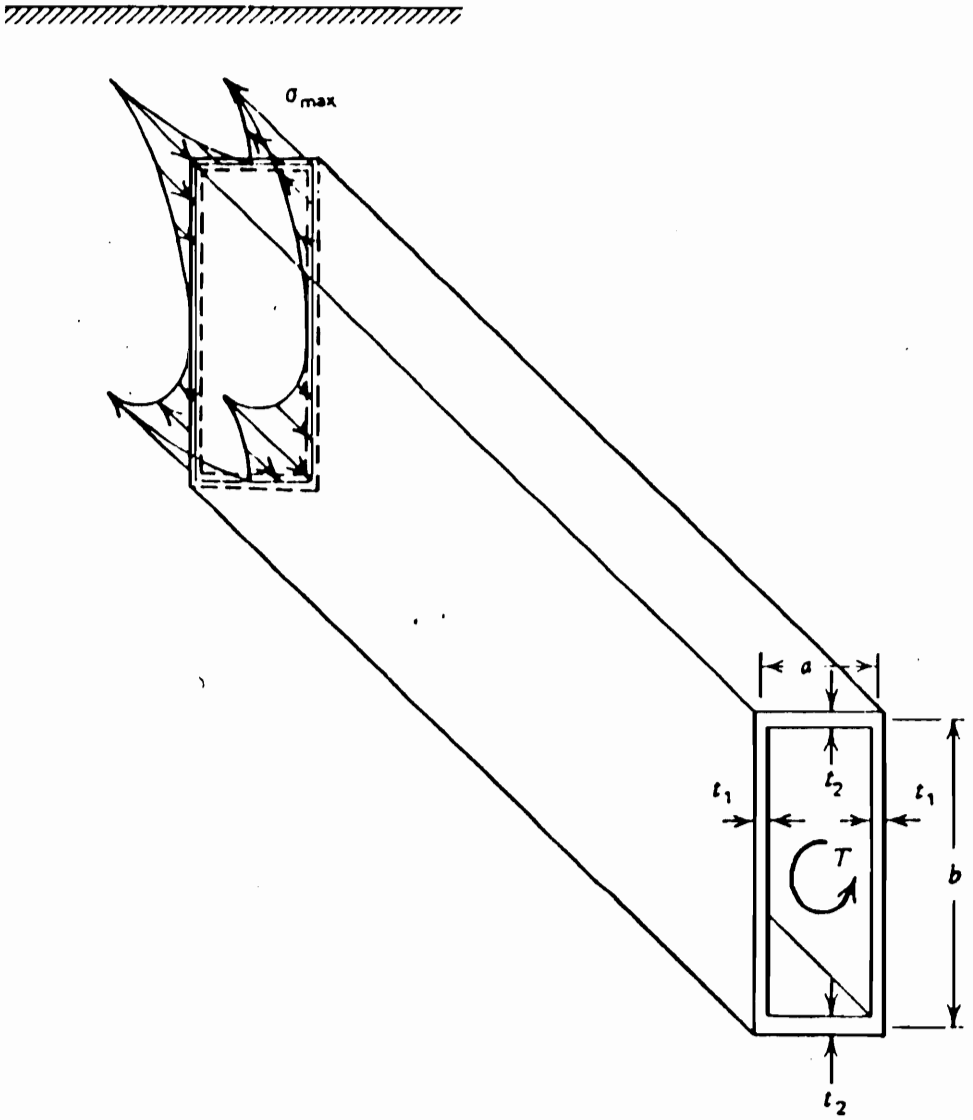

Figure 123. Some Thin-Wall Hollow Members Twist Without Warping and Do Not Develop the Large Stresses in the Corners.

An existing log trailer built of rectangular box tubing was spotted when delivering wood to the Union Camp Company woodyard in Lattimore, North Carolina (Stephenson, 1993). Its main frame was built of 12-inch high, 8-inch wide rectangular tubing. High tensile steel, ASTM A500 of 50 ksi minimum yield strength, was used as a primary material. The main beams had a telescopic design so that the rear section of the trailer and the tandem assembly could slide about 4 to 5 feet to lengthen or shorten the trailer. The frame had a low gooseneck in the front. A third rectangular tubing was used as a center beam in the neck, because the main beams had a lower depth there. It terminated at a large tubular cross-section in the transition area between the gooseneck and mainframe. Some of the cross members were severely cracked because the box sections did not satisfy the geometrical condition required for the non-warping behavior.

Comparison of I-Beam with Box Section

It will be instructive to illustrate the problem by computing the maximum stresses at a restrained cross section for both a wide flange I-section and the equivalent box section. Computations of the stresses by an approximate analytical method follow in this section, these will be later compared with the FEM solution.

W 16 x 36 I-beams are frequently used in manufacturing light log trailers. Let us consider a single 15-foot long cantilever beam of this section with one end rigidly built into a wall (Figure 124). The beam is subjected to a combination of a bending moment and a twisting torque by the means of the concentrated 1000 pound force applied at the distance of 2 feet from the plane of symmetry of the beam. As it has been pointed out, the maximum normal stresses due to restrained warping at the fixed end occur at the edges of the flanges. Using the approximate solution given by Boresi and Sidebottom (1985) we find the stresses equal to 37.1 ksi. The nominal maximum bending stress at this location is only 3.19 ksi. Therefore, the

stress concentration factor at the cross-section built into the wall due to the restrained warping is Sc = 11.6! (computed as a ratio of the maximum normal stress to the nominal stress in the cross-section). At the very corner of the flange torsional shearing stresses vanish. Shearing stresses due to the lateral force P are insignificant in the flange and can be neglected. For ductile materials the maximum shearing stress criterion of failure is the most often used. Thus, the state of stress at the point on the edge of the flange is represented by the maximum shearing stress, which equals to 20.15 ksi.

Let us now, consider the 16 x 8 x 5/16 box beam which has the same stiffness against bending in the vertical plain as the W 18 x 36 I-beam (Figure 125). In order to obtain a box section free from warping at the restrained end we add 16" x 12" x 5/16" plates on each longer side. At the distances greater than 12 inches from the wall the box has a uniform thickness but warping at these sections is permitted. The loading and other boundary conditions are identical as before.

The modified box section satisfies the condition that the cross product of the length and thickness of the sides is a constant at the restrained cross-section. Therefore, the only normal stresses in the cross section at the fixed end are due to bending. The maximum values of stresses occur at the corner junction of the sides. The nominal normal stresses are about 3 ksi. Using an approximate solution for thin-walled multiply-connected cross sections the torsional shear stress at the corner is computed equal to 0.32 ksi. The rectangular tube has a reentrant corner, thus a considerable shearing stress concentration may take place at this location. According to the elasticity solution, if the ratio of the radius of the filet to the greater thickness of a wall is 0.5, the stress concentration factor should not exceed 1.8 (Timoshenko and Goodier, 1985). Thus, accounting for the effect of the reentrant corner, the torsional shearing stress is about 0.6 ksi. Since the length-to-depth ratio for the beam is greater then 10 the shear stresses due to the lateral shearing force can be neglected. Finally, the maximum shearing stress at the point is computed for the box section equal to 1.62 ksi.

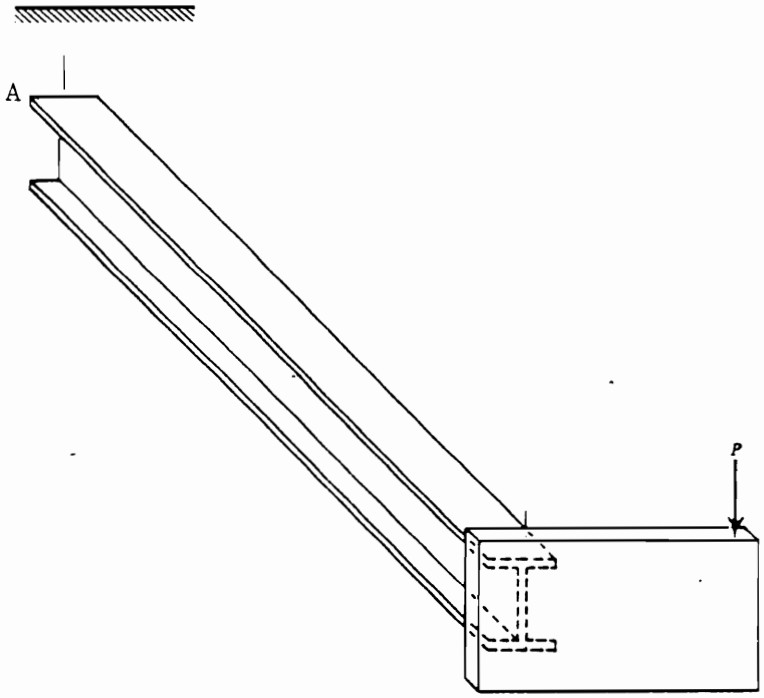

Figure 124. W 16x36 I-Beam Subjected to Combination of Bending and Twisting Torque.

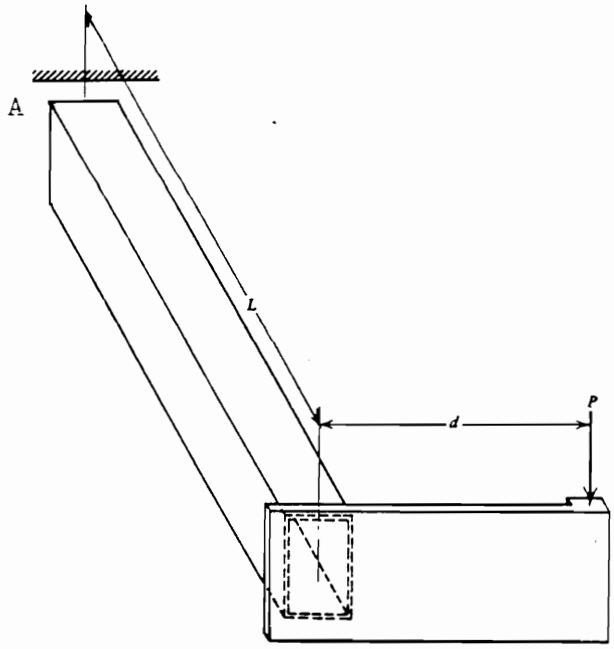

Figure 125. The 16x8x5/16 Box Beam Subjected to the Same Loading.

It has been shown therefore, that the maximum stresses at the fixed end are over 12 times lower for the modified box beam than for the I-beam, using approximate solution. The 16 x 8 x 5/16 box beam is heavier than W 18 x 36 but this can be easily offset by making cut-outs in webs of the box beam, or preferably by decreasing the number of cross members.

Elastic Shell Element Models

Utility of rectangular box sections in log trailer construction has been verified by finite element stress analysis using elastic shell elements.

Models of two simple frames, equivalent in terms of weight and stiffness in longitudinal vertical plane, were built. The first frame consists of two 8-foot-long W 10x12 I-beams and two 34.5-inch-long cross members of the same section geometry. The second frame has the same main I-beams but uses 6 x 4 x 3/16 box beams as cross members. They represent a neck section of a log trailer's frame. The two frames are subjected to the same loading with a twisting couple of 1,000-pound forces applied at corners on one end. This loading corresponds to the racking situation of the trailer. The midpoint of the cross member bottom flange on the opposite end of the frame is restrained from movement, simulating a kingpin connection. Figure 126 shows models of the two frames.

The static analysis was performed, and displacements and stresses were computed for each of the frames.

a)

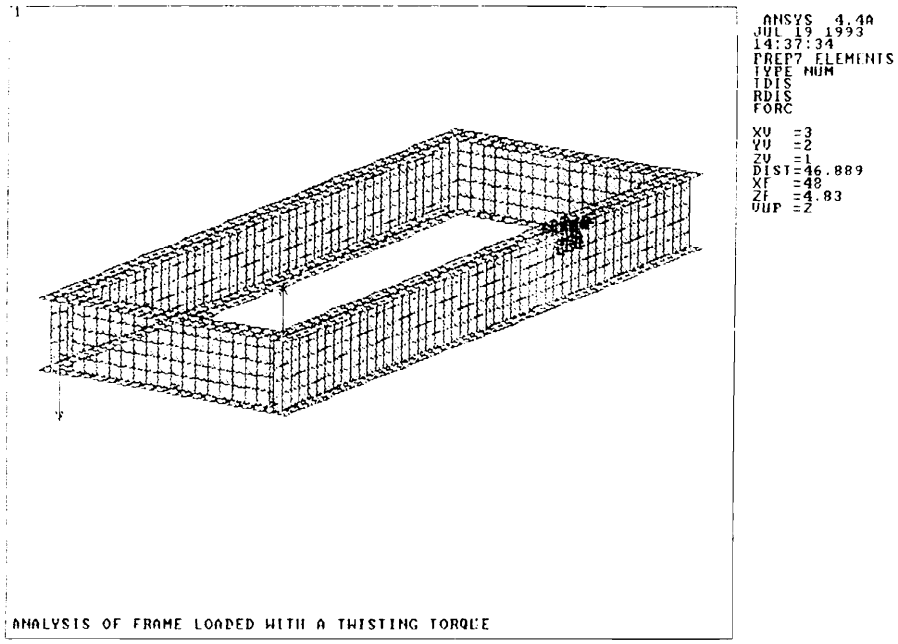

b)

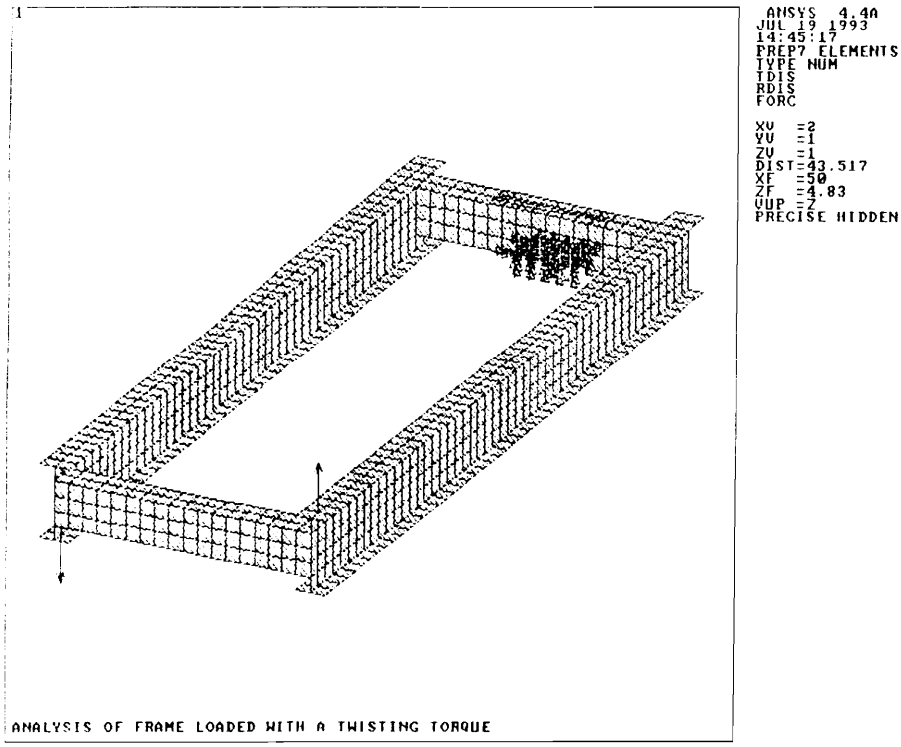

Figure 126. Elastic Shell Element Models of Two Simple Frames; (a) first uses I-beam section of the same geometry as the main beam for cross members, (b) the second utilizes box beams for cross members.

The maximum displacements for the first frame (i.e. the one using I-beam cross members) amounted to 4.49 inches, while these displacements for the second frame (i.e. the one using box tubes for cross members) were computed to be equal to 0.46 inches. It was found, therefore, that the first structure displaces almost 10 times more than the second one under the same loading.

The overall distribution of von Mises equivalent stresses for each of the frames are shown in Figure 127. The plots clearly indicate that the first frame tends to highly concentrate stresses in flanges of the main beams and the I-beam cross members, while the second frame distributes stresses evenly throughout the structure. The behavior of the two structures can be evaluated easily by examining stress distributions at the beam-cross-member junction. Figures 128 and 129 show the von Mises equivalent stresses at the junction for the first and the second frame, respectively. These plots clearly indicate the frame made of I-sections concentrates stresses at places where flanges are welded to each other, while the frame with box cross members tends to distribute them along the perimeter of the tubular cross member. The effect is that the maximum stresses are several (i.e. 5.76) times higher for the all-I-beam structure than the stresses at the same location for the frame with the tubular cross members.

The corner of the main beam and the cross member junction is a geometrical stress concentration point. In the model, the very tip of the corner must be specified as a concentration keypoint for the area meshing to be able to compute the stress value at this location with higher precision. Figure 130 shows the modified model for the all-I-beam frame. Computed stress distribution for this formulation clearly indicate behavior of the frame at this location. The stress at the tip of the corner where flanges are welded to each other is computed to equal 102.12 ksi. This stress would cause local yielding for a 80 ksi yield strength material of the flanges.

a)

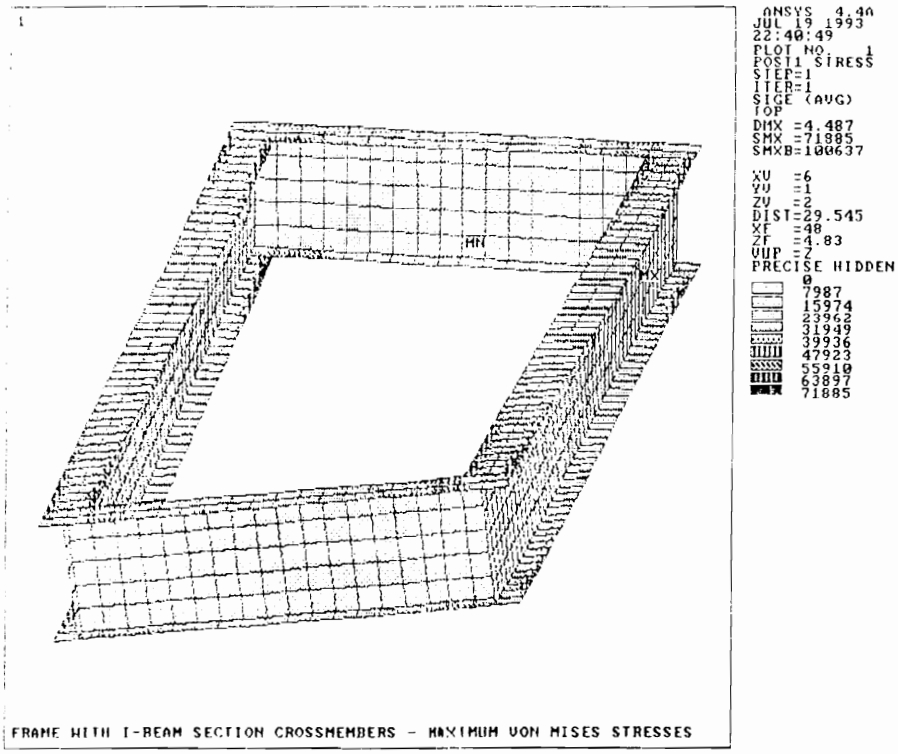

b)

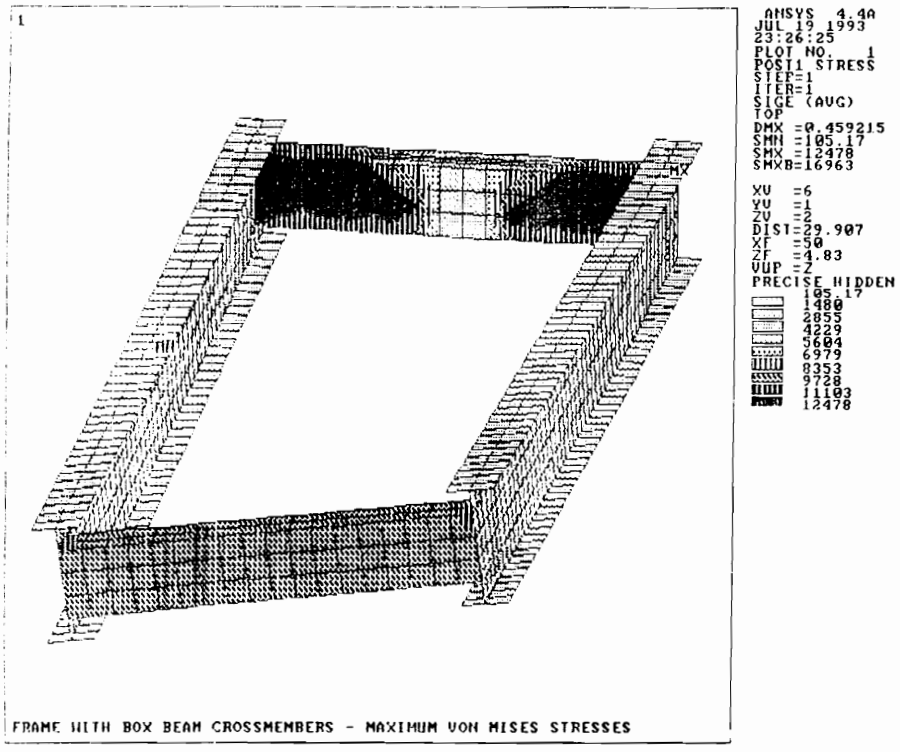

Figure 127. Overall Stress Distribution in the Two Frames; (a) for the all-I-beam frame, and (b) for the frame with box cross members.

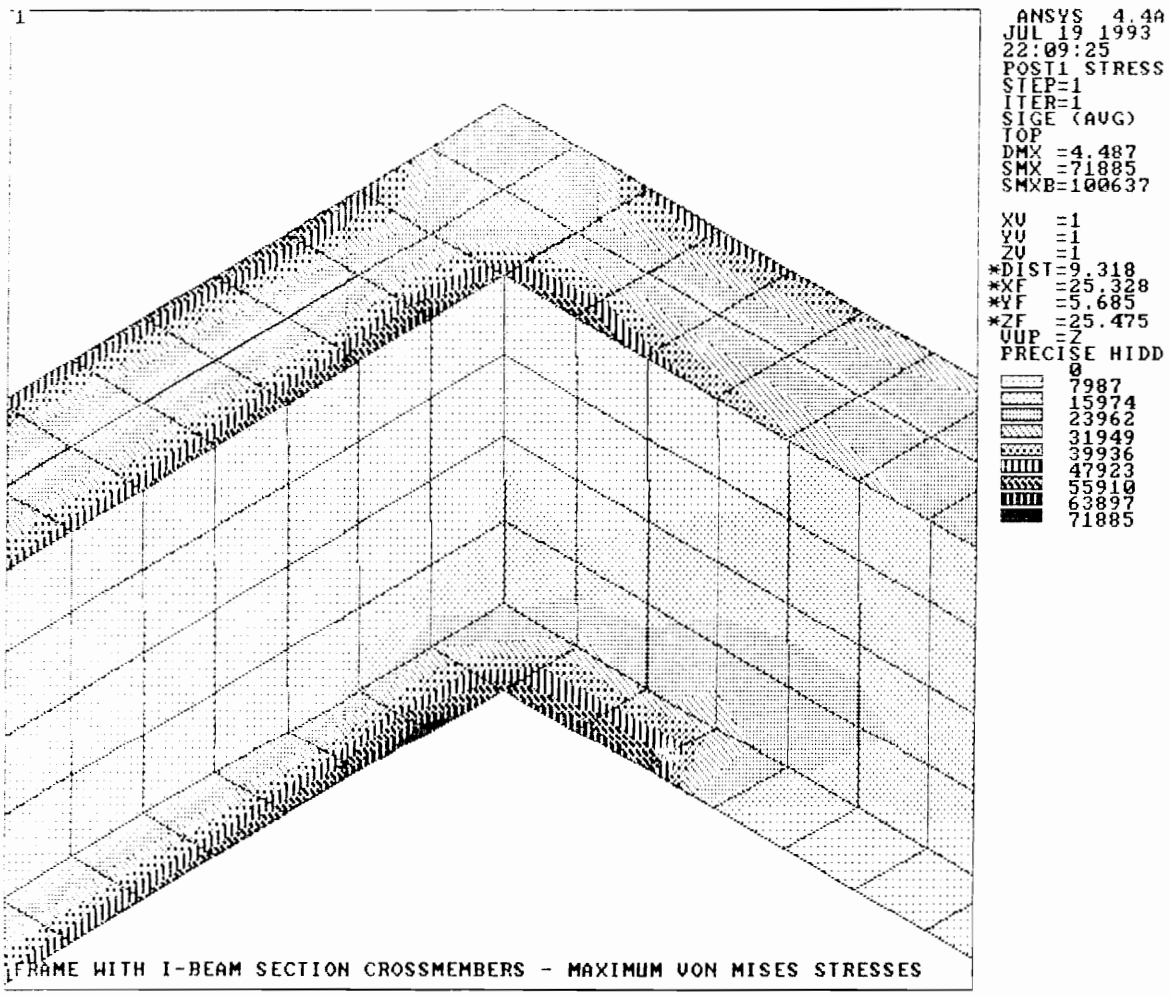

Figure 128. Stress Distribution at the Cross Member/Main Beam Junction for the First Frame.

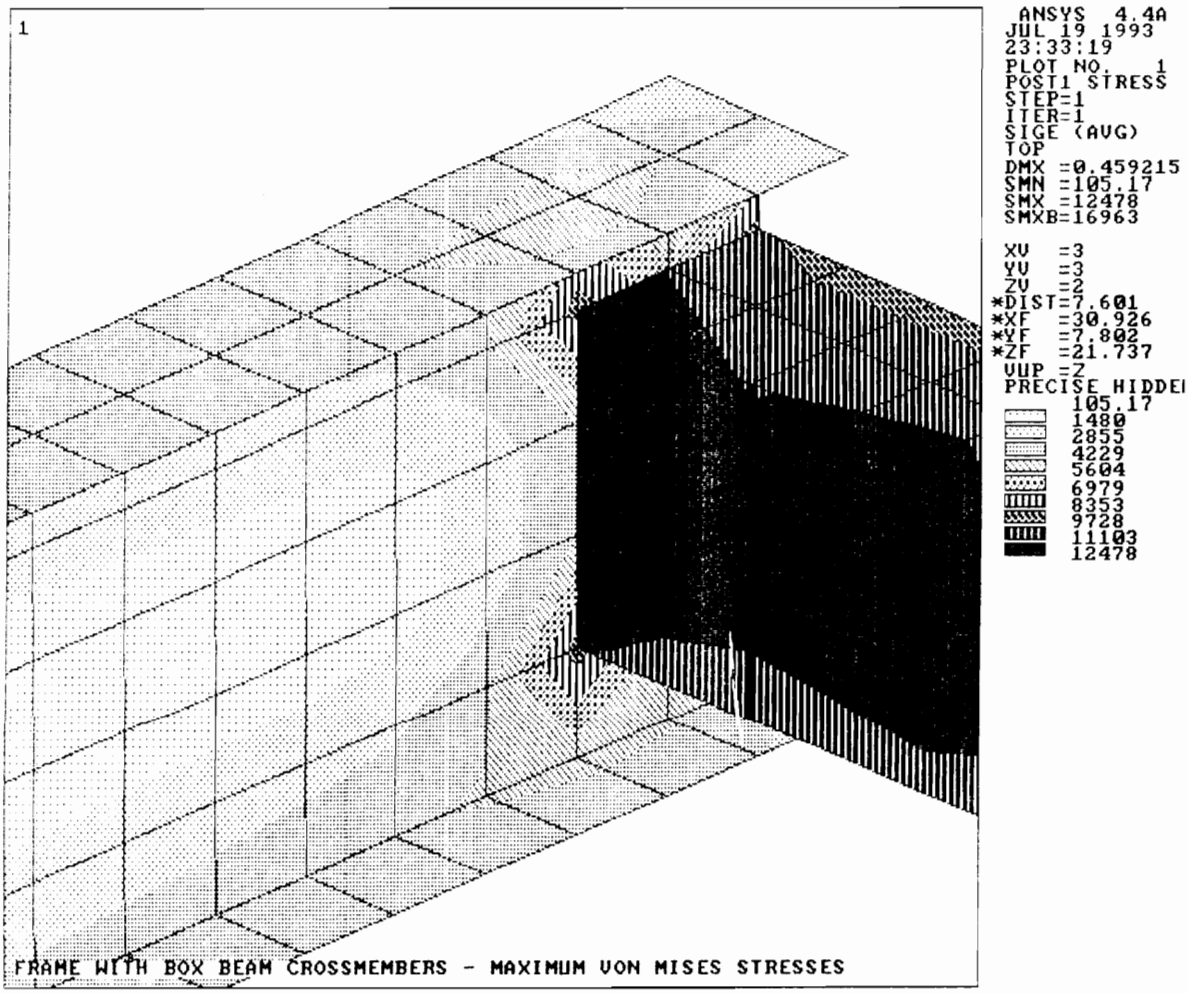

Figure 129. Stress Distribution at the Cross Member/Main Beam Junction for the Second Frame.

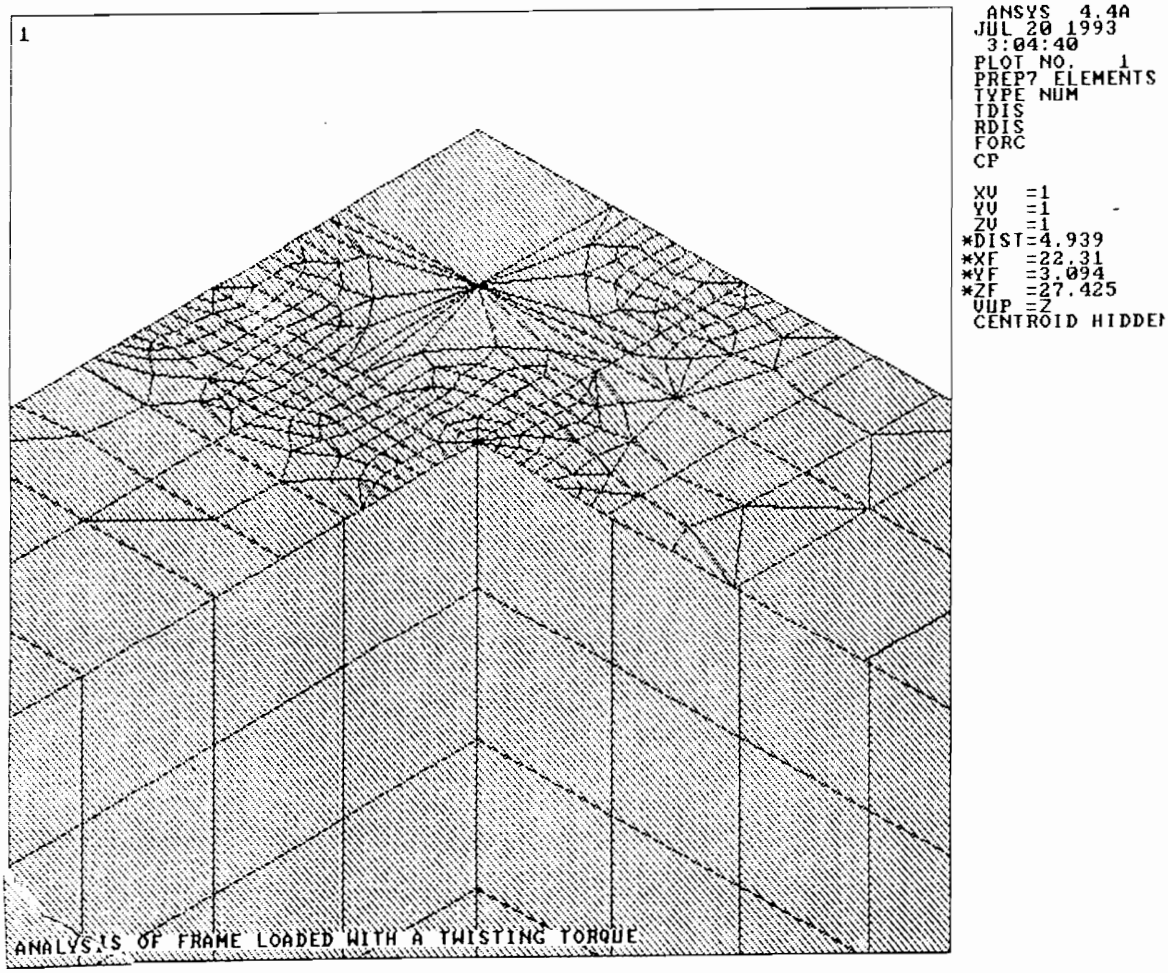

Figure 130. a) Modified Meshing of the All-I-Beam Frame with the Stress Concentration Keypoint at the Tip of the Corner.

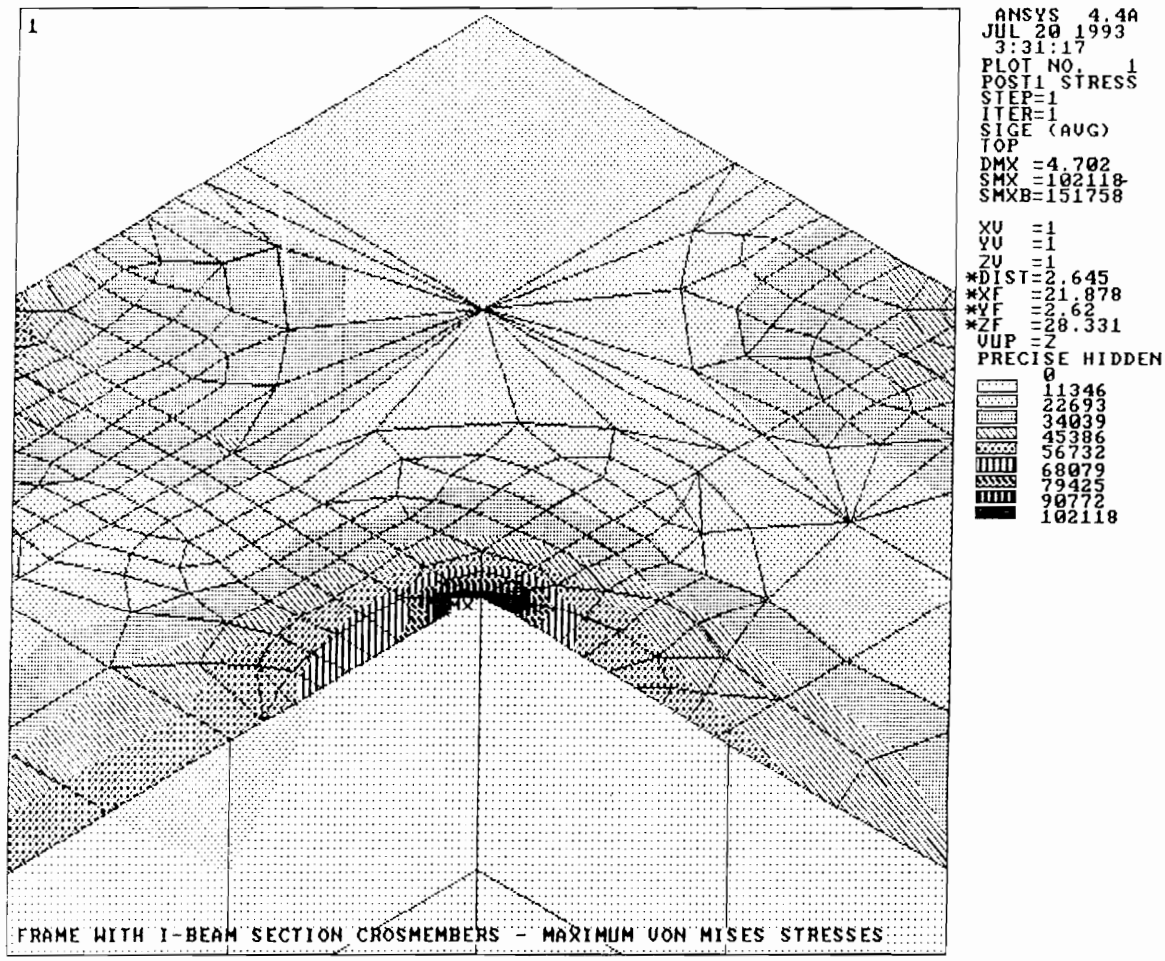

Figure 130. b) Stress Distribution at the Tip of the Corner.

Fatigue Life Predictions

Fatigue life estimates for the two tested trailers were computed using the *nominal-stress method* which is based on the linear-elastic stress analysis.

Gooseneck Trailer

The front standard was selected as the member controlling a fatigue behavior of the trailer. An estimated *S-N* curve for the member was constructed taking into account the effects of: stress concentration, loading type, member size, and surface quality. The dominant loading exerted on the standard is bending, however, due to the presence of shear lateral forces the loading type coefficient, C_l , was assumed 0.8. The factor accounting for the member size, C_d , and that accounting for the surface quality, C_s , were assumed 0.8 and 0.55, respectively (after Reifsnider, 1991). The *S-N* curve was constructed for the member using procedures presented in Appendix C.

Service stress-time histories recorded for the front standard of the gooseneck trailer were analyzed to identify the greatest stress range, which is the most responsible for the fatigue damage of the member. The actual stress range in the standard-bolster junction was extrapolated using the value recorded at the point of measurement, and assuming that the dynamic stress distribution pattern in the member was the same as that computed under static conditions.

The elastic stress concentration factor, K_t , and the notch sensitivity, q, had to be assessed for the standard/bolster weldment bead in the calculations. K_t was assumed to be equal to 2.1 using Peterson's stress concentrations diagrams for three-dimensional shoulder fillets in bending (Peterson, 1974). The

notch sensitivity, q, was taken as equal to 0.8 (Reifsnider, 1991). Finally, the adjusted stress range in the weldment was computed equal to 26.64 ksi (see Appendix C), and the number of the cycles required to fracture was obtained from the *S-N* curve to be equal $N = 530{,}942$ cycles (Figure 131).

Full-Tree Trailer

The front bolster was selected as the member controlling fatigue life of the full-tree trailer. The same computational procedures as that used for the gooseneck trailer were applied. Figure 132 shows the constructed *S-N* curve for the full-tree trailer. The adjusted stress amplitude at the bolster/main-frame weldment was computed as equal to 15.49 ksi. Finally, the number of cycles required to fracture was determined as equal to 418,931 (Figure 132).

The number of cycles to fracture obtained for both trailers may be treated as an approximate fatigue life of the structures. These were computed to be comparatively low--about half of a million of cycles.

In case of the gooseneck trailer, low fatigue life was a result of the high mean stress (28.5 ksi), and the stress range (21.0 ksi). Tapering the standard so that its very bottom section has an increased cross-section area would elevate the problem. The other solution is to use a cable or strap to tie the tops of standards together after loading, and to constantly tension the cable/strap during the trip.

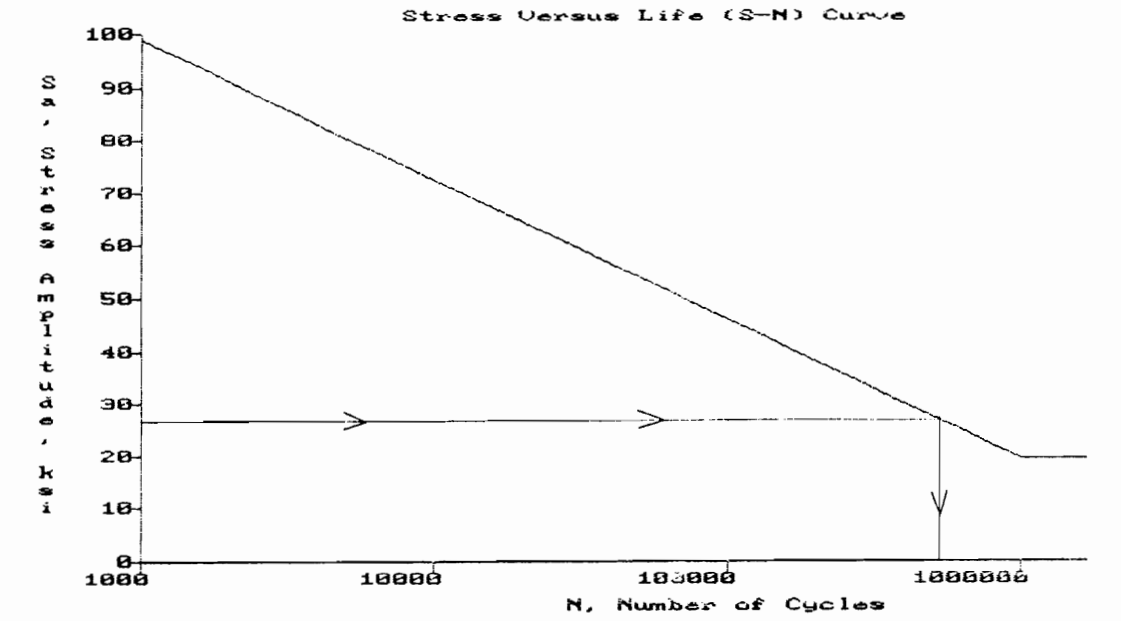

Figure 131. *S-N* Curve Constructed for the Gooseneck Trailer.

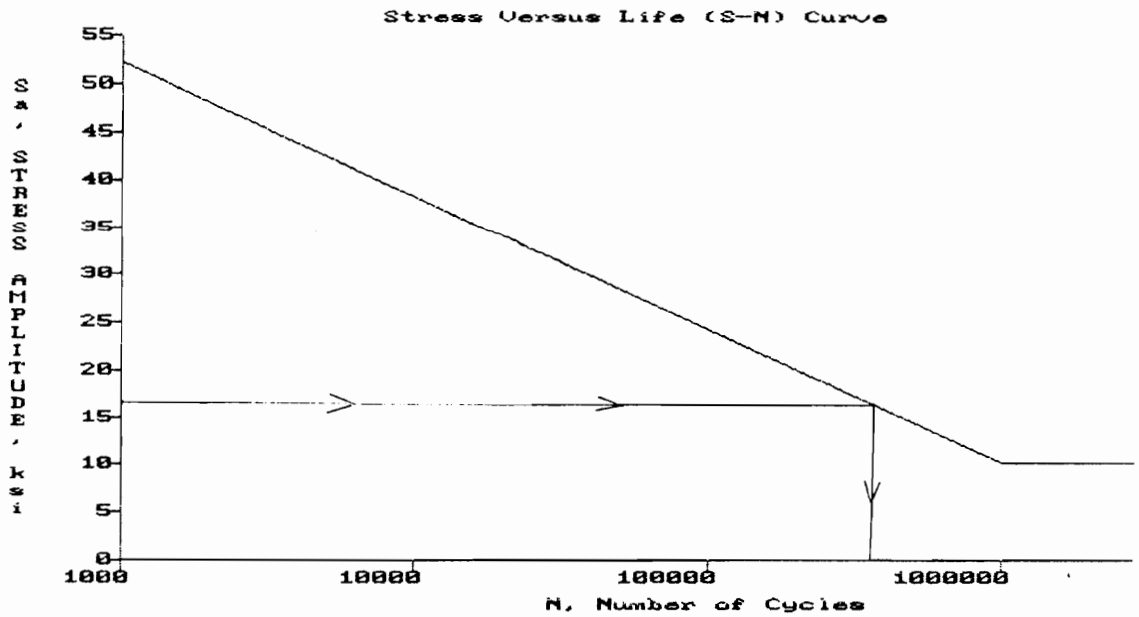

Figure 132. *S-N* Curve Constructed for the Full-Tree Trailer.

Using supporting struts instead of gussets, which altered the stress distribution in the bolster, and frequent overloading of the member contributed to short fatigue life for the full-tree trailer.

Fatigue life estimation results for both trailers indicate the need to apply a detailed design to avoid stress concentrations in the structure, and to carefully inspect the manufacturing process if the design specifications are not changed in the final product.

Corrosion Fatigue of Log Trailers

Environmental effects on fatigue of metals may sometimes be more severe than sharp stress concentrations (Fuchs and Stephens, 1980). Quantitative fatigue life predictions are often not possible because of the many interacting factors that influence environmental fatigue behavior. This places great emphasis on real-life product testing, inspection, and service history analysis.

Log trailers working in the Southeast are subjected to an air environment, which is usually corrosive due to a high relative humidity and moderately elevated temperature. Moisture and oxygen are two the most important that factors accelerate the process of corrosion. Water, dirt, and salt are also common elements of this environment. Also log trailers are usually subjected to varying temperature conditions during a day-night cycle.

Fuchs and Stephens (1980) compared typical constant amplitude *S-N* diagrams obtained from laboratory fatigue tests at room temperature under four key conditions: vacuum, air, presoak, and submerged in corrosive solution (Figure 133).

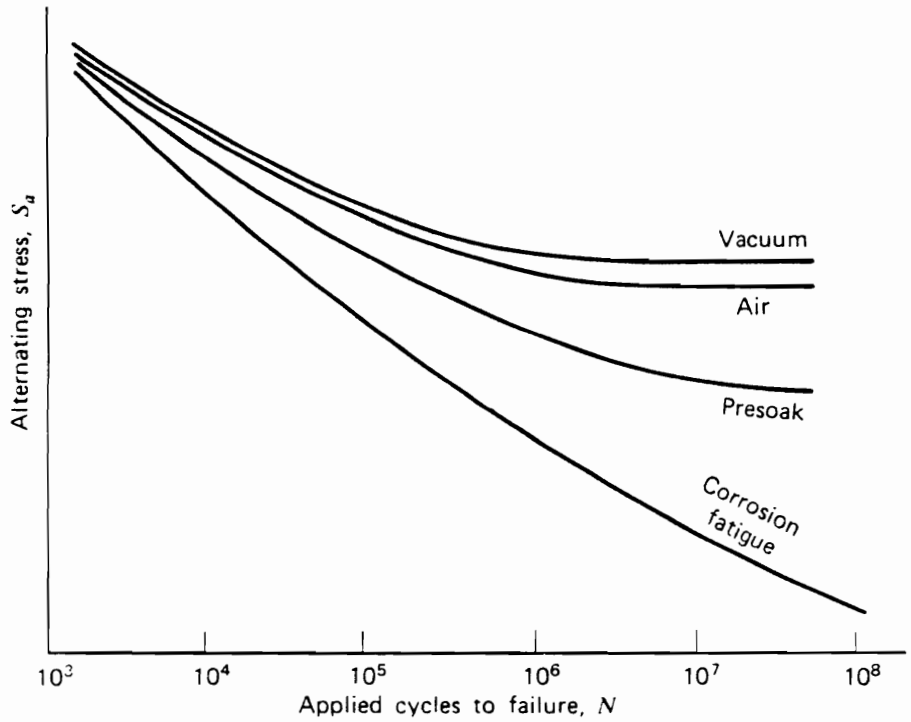

Figure 133. Relative Fatigue Behavior under Various Environmental Conditions (after Fuchs and Stephens, 1980).

It is obvious that presoaking fatigue specimens in corrosive liquid followed by cyclical stressing significantly decreased their fatigue lives. Therefore, we may suspect that high humidity air can be quite detrimental to fatigue behavior of a log trailer. The *S-N* curve for corrosion fatigue (i.e. for the specimens submerged in corrosive liquid) do not reveal a fatigue limit at all (i.e. the *S-N* curve do not become flat after 10^6 - 10^7 cycles). Such a situation may be present when a log trailer is covered locally with a thick layer of dirt that absorbs and holds moisture and has acid reaction from air pollutants. When the expected life of the component decreases, all four conditions tend to converge primarily due to insufficient time for corrosion to be effective (Figure 133).

In summary, it is has been experimentally determined that both crack initiation life and crack growth life are significantly reduced under corrosion fatigue conditions. The number of cracks on the component's surface increases at the same time.

The principal way to reduce corrosion fatigue is to choose materials of improved corrosion resistance in the service environment. This solution is rather impractical when applied to log trailer design--using stainless steel, for instance, would be cost prohibitive. Increased corrosion fatigue resistance can also be accomplished through various surface treatments, such as shot-peening, cold working, which induce desirable surface compressive self-stresses. Surface coatings such as paint, oil, and polymers can protect against corrosive air and liquid environments if they remain continuous. However, under service conditions it is impossible for paint coatings to retain complete continuity. Broken or disrupted coatings can eliminate the beneficial effects. Corrosion inhibitors that form an adherent corrosion resistant chemical film on the metal surface have been somewhat successful (Fuchs and Stephens, 1980). Chromates and dichromates have been widely used for this purpose.

CONCLUSIONS

It would be advantageous to use rectangular box sections free from warping for cross members and main beams of a log trailer. This solution would decrease the localized stresses at all places where the members are welded together, and, in turn, would directly increase the fatigue life of the structure. More importantly, delayed initiation and propagation of cracks would significantly increase the safety of log trailers. Frames built of box beams possess also a potential of having fewer cross members, because box sections offer excellent combination of stiffness against bending and torsion. Box beams are about 30% heavier than strength equivalent I-beams, which can be offset by making large oval cutouts in webs (at cross-section neutral axis) of the box main beam. A tare weight of the trailer can be further decreased by limiting the number of cross members.

C-Channels in Building Log Trailers

C-channels have been considered in the process of selecting a suitable section geometry for main beams and cross members of a log trailer. These cross-sections have many advantages. Two matched C-channels fitting one inside the other, can make a box beam; this would be an excellent member cross-section for bolsters and standards. Channels are manufactured out of high tensile low-alloy steel. They are cold formed and heat treated. Therefore, the material has at least 110 ksi yield strength. Channels can be formed by stamping so a variable web depth and flange width can be introduced. C-channel sections have a potential to be very efficient members for main beams and cross members of log trailers.

CHAPTER 8. EXTRA-LIGHT LOG TRAILER DESIGN

Introduction

One of the objectives of this research was to develop an efficient and economically feasible extra-light log trailer design that would utilize most, if not all, formulated recommendations. The design, if successful, would be used for manufacturing a prototype trailer, which would then be followed by comprehensive testing and final product development. All parties involved in this research effort have been hoping that the design will help to improve log trucking safety and profitability.

Main Features of the Design

The extra-light log trailer design was completed and documented through detailed engineering drawings. It does not utilize the recommendation for the folding frame, because implementation of this concept would significantly complicate the design and require additional time. It was more important to develop a design in a short time, which would implement all the other findings. At the same time three major trailer manufacturers were challenged with the folding frame concept by presenting them the outcome of this research.

A concise description of the extra-light log trailer design follows in this chapter.

The most important features of the design are (Figure 134):

1. Reduced tare weight of 7,770 pounds.

2. Sound structural integrity; e.g. the design factor is greater than 6 when the trailer is loaded with tree-length material spanning all four bolsters.

3. Material of high strength and toughness used throughout.

4. Welds replaced with elastic friction joints for fatigue resistance.

5. Moveable bunks.

6. Replaceable bolsters and standards.

7. Constant tensioning device for load binders.

Tare Weight

The proposed extra-light log trailer weighs about 3,000 pounds less than an average log trailer in the Southeast. Previous IFO research revealed that each pound of an increased payload generates about $5 of additional profit over the life of the rig (Beardsell, 1986). The three thousand pounds of increased payload would yield additional income of approximately $15,000, which would constitute the entire initial trailer investment cost (e.g., trailers currently available on the market cost between $9,000 and $11,000). The above cost/return calculation should be an excellent argument for marketing a commercial version of the trailer.

ITEM	QTY	PART NO	DESCRIPTION	REF DRWG	ITEM	QTY	PART NO	DESCRIPTION	REF DRWG
5	1	1.006.000	BUMPER ASSEMBLY	1.006.000	1	1	1.001.000	FRAME ASSEMBLY	1.001.000
6	1		5TH WHEEL PLATE		2	2	1.003.000	FRONT BOLSTER ASSEMBLY	1.003.000
7	1		BINKLEY LANDING GEAR		3	1	1.003.000	MIDDLE BOLSTER ASSEMBLY	1.003.000
8	4		U-BOLT 1-8 X 25 GR8; 5 7/8 BETWEEN LEGS		4	1	1.003.100	BOLSTER	1.003.100

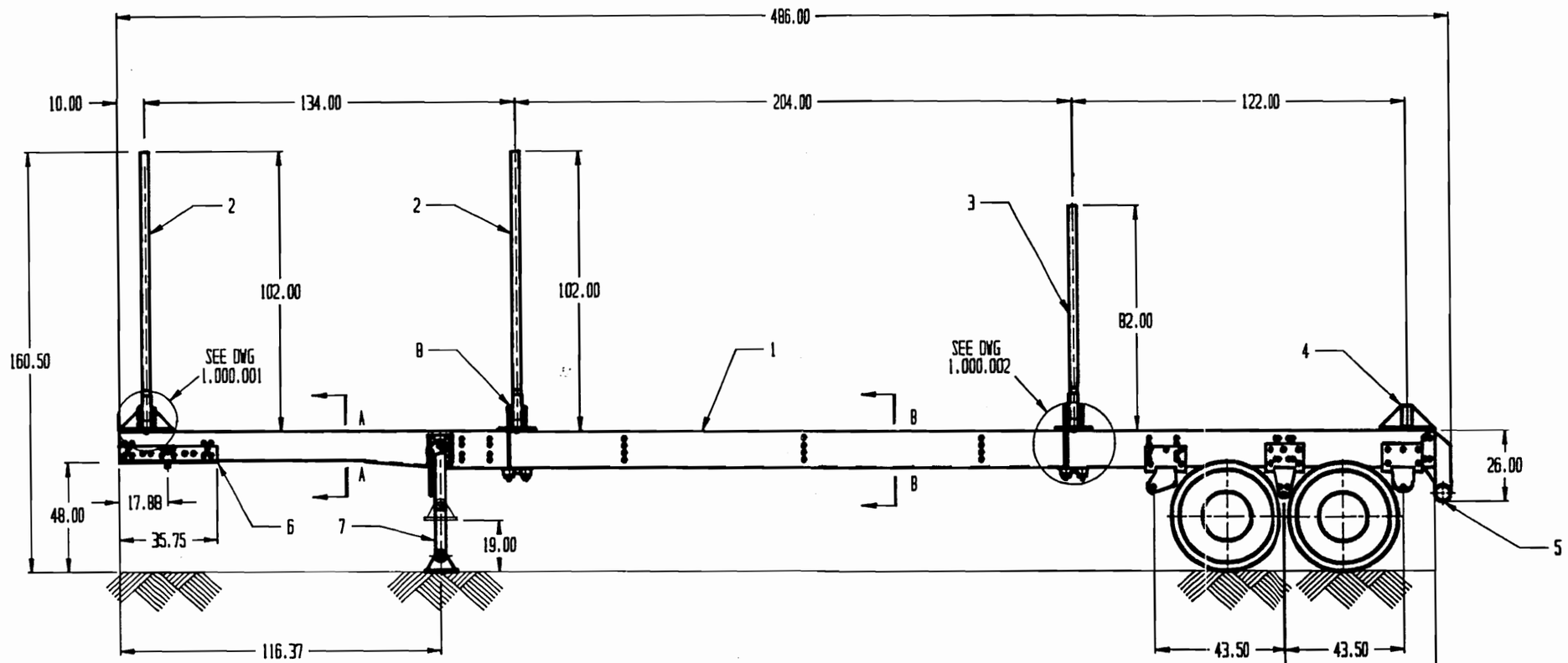

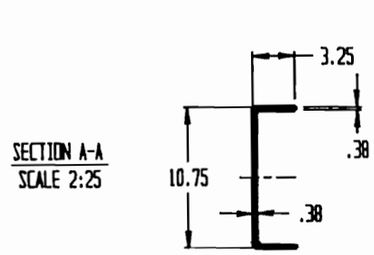

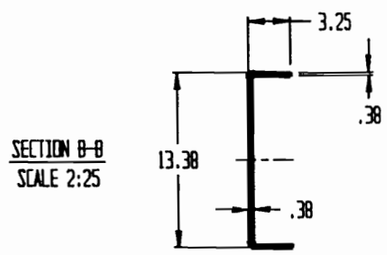

TITLE: IFO LOG TRAILER	INDUSTRIAL FORESTRY OPERATIONS COOPERATIVE-VIRGINIA TECH	
DWN. A.WYLEZINSKI DGND. A.WYLEZINSKI APVD. W.STUART	WEIGHT: 7,769 lbs TOLERANCES: ±0.06	SCALE: 1 : 50 DWG NO. 1.000.000

Figure 134. Extra-Light Log Trailer Design.

Table 17 shows the weight breakdown for the extra-light design. Comparing it with the tare weight break down for a typical double-bunk log trailer (see Table 6), it follows that the greatest weight savings were obtained for the main beams (about 30%), standards and bolsters (about 26%), and the running gear (about 22%). These weight savings were achieved by utilizing high-strength, heat treated steel for the trailer's members, and by using super-wide-singles and aluminum wheels.

Two groups of components were designed heavier than those for a conventional double-bunk trailer: cross member assemblies (by about 25%), and a bumper (by about 30%). The trailer's cross members are designed for fatigue strength; they have large, stiff flanges, by which they connect to main beam webs through specially designed friction joints. These flanges are the source of the increased tare weight.

The need for a stronger and heavier bumper was frequently identified by interviewed loggers; trailers, and sometimes entire vehicles, are frequently pushed by a bumper when they get stuck in difficult terrain.

Strength

The extra-light trailer is, at the same time, stronger than the two tested designs as well as any surveyed in the course of the project. The extra-light design is based on high-strength, heat treated, cold formed channels. The yield strength of the material is 110 ksi minimum. The channels are also characterized by an increased toughness.

Table 17. Tare Weight Breakdown for the Extra-Light Log Trailer Design.

EXTRA-LIGHT LOG TRAILER WEIGHT BREAKDOWN

Item	Material	Qty	Weight
Main Beams	C 13.38x3.25x.38	2 @ 990 lbs	1,980 lbs
X-members	C 8.00x3.50x.25	3 @ 78 lbs	234 lbs
	C 10.62x3.5x.31	2 @ 109 lbs	218 lbs
	C 10.62x3.5x.31	1 @ 85 lbs	85 lbs
	Double above	1 @ 170 lbs	170 lbs
	Composite Xmember	3 @ 35 lbs	105 lbs
Standards & Bolsters	Front	1	581 lbs
	2nd	1	581 lbs
	3rd	1	527 lbs
	Rear	1	203 lbs
Landing Gear	Binkly LG 4002-9	1	54 lbs
5th Wheel Plate	36x40x.38	1	152 lbs
Bumper	8.5 ft	1	203 lbs
Running Gear	Axles	2 @ 319 lbs	638 lbs
	Suspensions	2 @ 271 lbs	542 lbs
	Springs	4 @ 87 lbs	348 lbs
	Wheels, Drums, Breaks & Cups	2 @ 466 lbs	932 lbs
5/8 Dia. Huck-Fit-Fasteners		110	66 lbs
Miscellaneous			150 lbs
		TOTAL =	7,769 lbs

This material is available in the form of C-channels of any required web-depth, flange-width, and gage (i.e. wall thickness). Rails having a drop of up to 20 inches between the neck and the middle section are also available. These rails are used in the heavy truck industry, thus there are good chances of utilizing standard components and controlling the material cost.

A 13.38-inch-high, 3.25-inch-wide-flange, and 0.375-inch-gage side-rail, used in heavy truck manufacturing was selected for the main beam of the extra-light log trailer (Figure 135). These rails are tapered to 10.75-inch depth in the front end, which ideally suits the strength and size requirements of the trailer's neck. The rails have 110 ksi minimum yield strength, 3 times the strength of commonly used ASTM A36 steel. This resulted in a resisting bending moment (RBM), greater by 8.13% than that of the gooseneck trailer main beam. At the same time, the rail weighs 42% less than the gooseneck trailer beam. Table 18 shows a comparison of the proposed trailer specifications with those of the tested trailers.

Two heat treated C-channels fitting one inside the other and arranged to make a box beam are used for assembling bolsters. They are 72% stronger than bolsters on the other trailers (Table 18). Only the standards are designed to be welded using 100 ksi minimum yield strength low-alloy steel (e.g. T-1). These standards can be stress-relieved by heat treating since they are members of much smaller sizes.

Friction Joints

The second principal feature of the extra-light design is that the members are assembled by bolting with Huck-Fit Fasteners. These threaded fasteners have some exceptional features. They use cold-swaged collars instead of conventional nuts. These fasteners do not loosen due to vibrations. They are superior to other threaded fasteners also because they ensure sustained clamping force within +/- 5% accuracy, by virtue of the installation process (Huck Manufacturing Company, 1988).

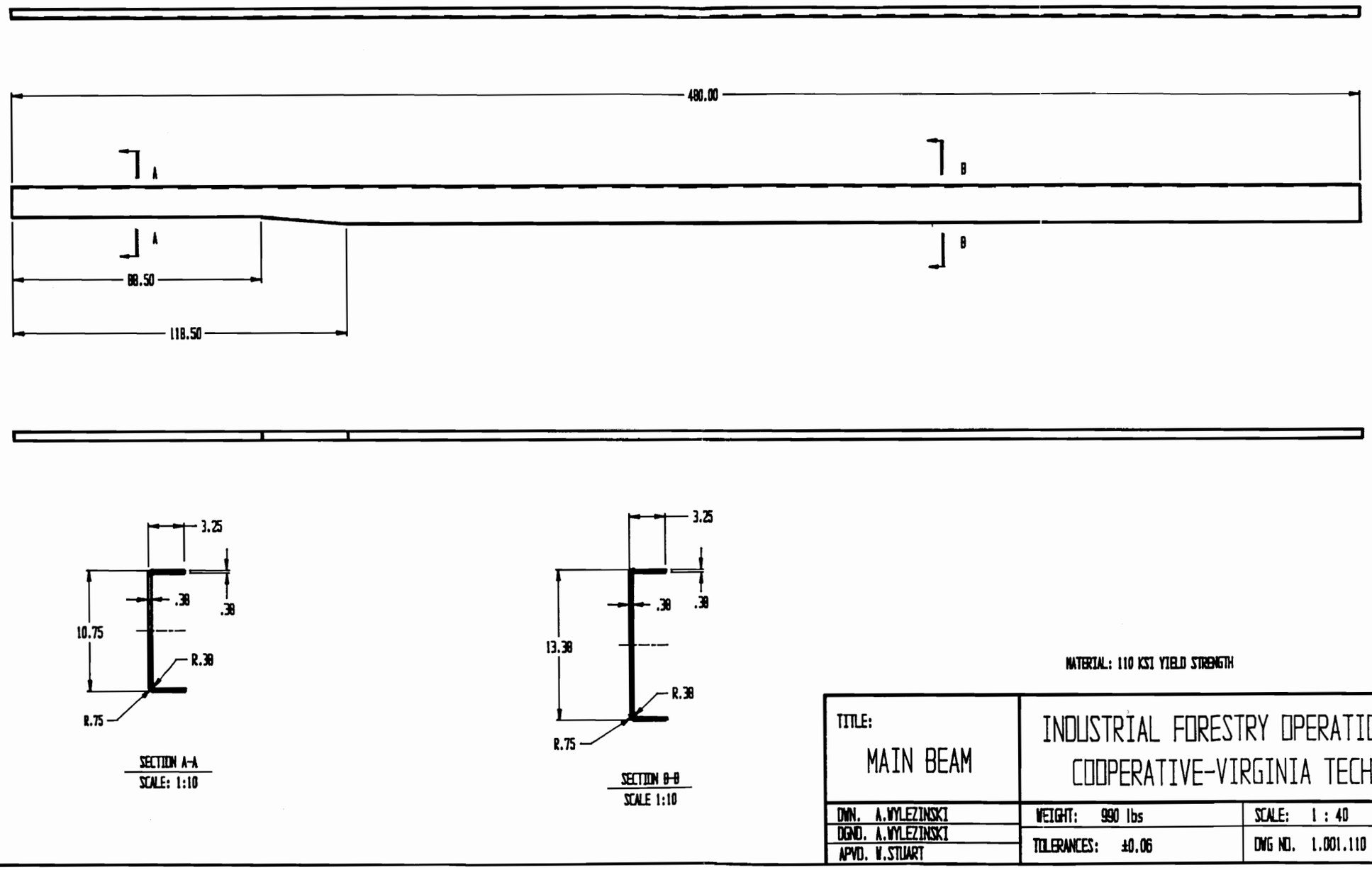

Figure 135. Side Rails (C-Channels) Used as Main Beams.

Table 18. Log Trailer Specification Comparison.

Main Frames/Side Rails

Equipment	Section Modulus [cu. in.]	Material Yield Strength [ksi]	RBM Thousand [in.-lb.]	Weight [lb/ft]
Gooseneck Trailer				
Neck: W 12x35	45.60	36	1,642	35.0
Drop: W 18x3 w/ truss	70.10	36	2,520	41.8
Double-drop Trailer				
Neck: W10x22 Fabricated	1.21	80	1,698	22.3
Drop: W 12x25 Fabricated	30.29	80	2,423	24.9
Extra-Light Log Trailer				
Neck:				
[- 10.75x3.25x0.38	18.00	110	1,980	21.0
Drop:				
[- 13.38x3.25x0.38	24.78	110	2,725	24.4

Bolster Specs

Equipment	Section Modulus [cu. in.]	Material Yield Strength [ksi]	RBM Thousand [in.-lb.]	Weight [lb/ft]
Gooseneck Trailer				
1st & 2nd Bolsters:				
9 x 5 x 5/16 Box w/ Bar	22.60	46	1,040	35.2
3rd: 9 x 5 x 5/16 Box	19.90	46	915	28.4
Double-drop Trailer				
All: 8 x 6 x 1/4 Box	15.00	46	960	22.4
Full-tree Trailer				
1st & 2nd Bolsters:				
6 x 4 x 3/8 Box	9.90	46	455	22.4
3rd & Cage Bolsters	7.03	46	323	17.0
Extra-Light Log Trailer				
All Bolsters:				
Combined C 8.0x3.5x0.25				
and C 7.5x3.5x0.25	16.29	110	1,789	24.2

Table 18 Continuation. Log Trailer Specification Comparison.

Standard Specs				
Equipment	**Section Modulus [cu. in.]**	**Material Yield Strength [ksi]**	**RBM Thousand [in.-lb.]**	**Weight [lb/ft]**
Gooseneck Trailer				
1st Standard: 4 x 3 x 1/4 Box	4.27	100	427	12.3
2nd and 3rd: 7.5 x 3.0 x 1/4 Box	9.37	100	937	20.0
Double-Drop Trailer				
All: 5" N.D. Schedule 80	7.43	46	342	20.8
Full-Tree Trailer				
1st & 2nd Standards: 6 x 4 x 3/8 Box	9.90	46	455	22.4
Cage Standards:	3.23	46	149	10.5
Extra-Light Log Trailer				
All Standards: 5 1/2 x 4 x 3/8 Box	8.80	100	880	18.3

The pin has a pintail with a breakneck groove. It allows the installation tooling to grasp the pin during the collar swaged cycle. After the collar is swaged onto the pin's locking grooves, the nose assembly continues pulling on the pintail until, at a pre-defined stress point, the pintail separates form the installed collar and pin. The sustained clamping force is extremely important for the sustained integrity of friction joints, and thus the entire structure. The fasteners do not require retorquing, thus the maintenance is very simplified. The other very important characteristic of the fasteners is their special fatigue design. Improved fatigue strength was achieved by introducing a stress relieving groove in the head/bolt fillet and a wide streamlined locking groove in the pin.

The extra-light log trailer design uses friction joints between the members (incorporating a design factor at least 4), which are based on stiff flanges and a greater number of less stiff fasteners for increased fatigue strength.

The design features also include replaceable standards and bolsters, and moveable bunks. This solution makes the design very flexible; it can be configured to haul shortwood, tree-lengths, and shorter thinning material. Standards of different height can be installed on the trailer depending on the material being hauled. Repair should also be much easier. The location of bolsters can be quickly changed to improve weight distribution over the axles. Using wooden standards (made of engineered wood) has been also considered. Oak 10-inch-by-5-inch standards would be equally strong (RBM = 1,041,667 inch-pound) but still lighter than the T-1 welded design (by about 15%). Bolsters are anchored to main beams by U-bolting. Hard rubber pads, 1.25-inch thick, are placed between the members to dampen vibrations and limit dynamic loads exerted on the members. Similar elastic joints have been employed in the standard-bolster connection (Figure 136).

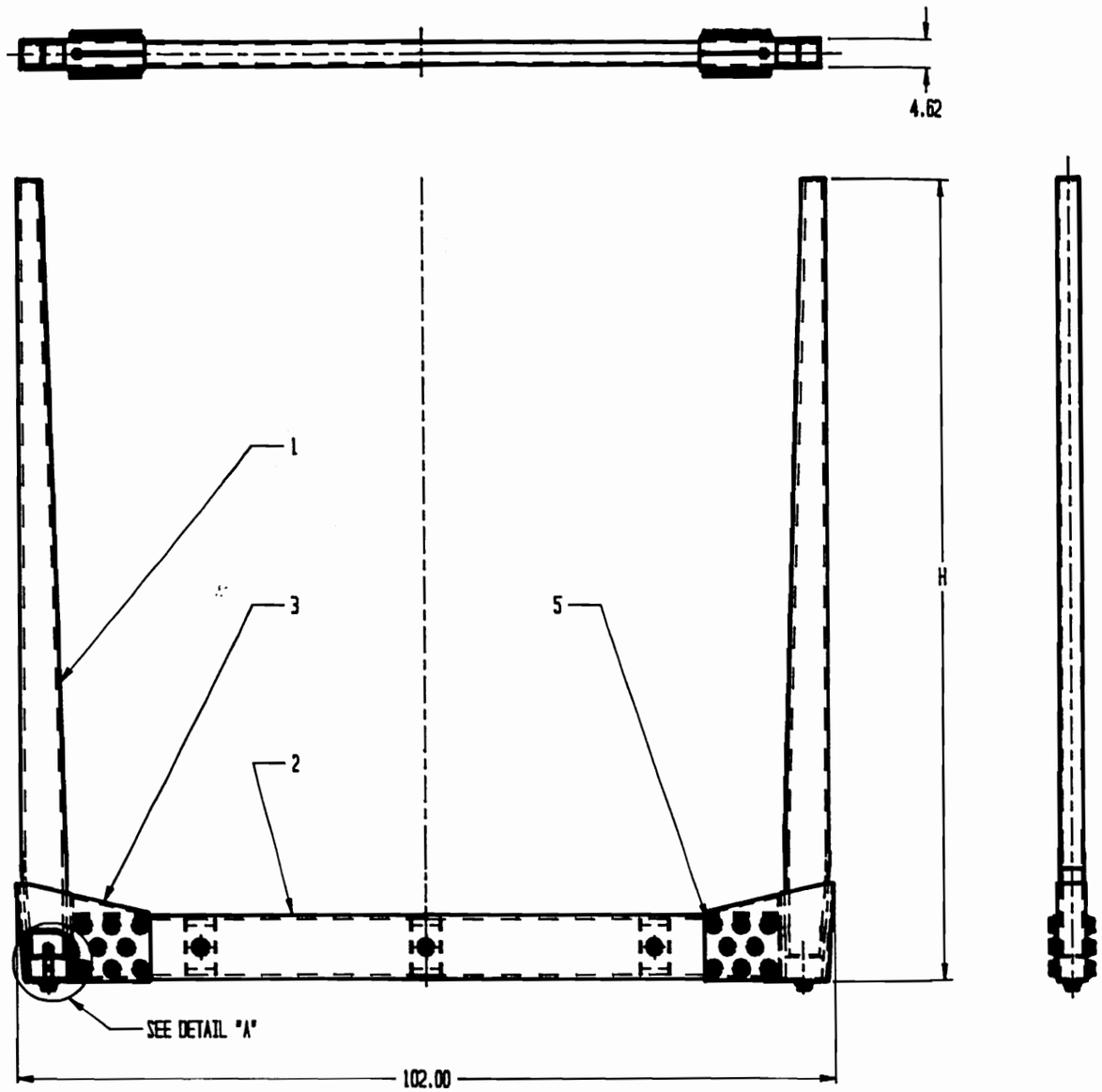

ITEM	QTY	PART NO	DESCRIPTION	REF DRWG
1	2	1.004.000	STANDARD	1.004.000
2	1	1.003.100	BOLSTER	1.003.100
3	2	1.003.300	BRACKET	1.003.300
4	4		HARD RUBBER	
5	16		7/8 DIA HUCK-FIT FASTENERS	
6	2		7/8 - 9 UNC BOLT	

BOLSTER	H	WEIGHT
FRONT	101	# 581
MIDDLE	81	# 527
REAR	51	# 439

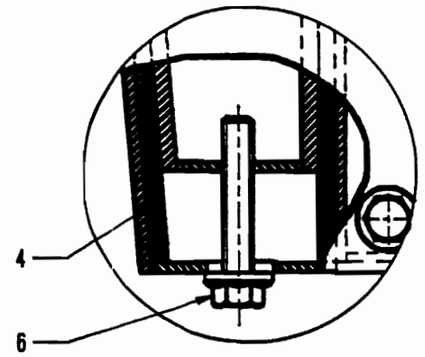

DETAIL "A"

MATERIAL: 110 KSI YIELD

TITLE: BOLSTER ASSEMBLY	INDUSTRIAL FORESTRY OPERATIONS COOPERATIVE-VIRGINIA TECH	
DWN. A.WYLEZINSKI	WEIGHT:	SCALE: 1 : 20
DGND. A.WYLEZINSKI	TOLERANCES: ±0.06	DWG NO. 1.003.000
APVD. W.STUART		

Figure 136. Bolster Assembly.

Load Binder Constant Tensioning Device

Load binders are usually tightened only once after loading the trailer on the in-woods landing. Experimental measurement of the dynamic loads acting on a log trailer revealed that loosely bound logs relocate on the trailer--load shifts occur when the trailer negotiates curves, brakes, accelerates or drives on rough or inclined surface. These shifts result in surges of dynamic load on one side of the trailer. Wood is a structural material which performs very well under various loading configurations. Unfortunately, log trailers do not utilize the stiffness of the logs. Taking advantage of the structural strength of the material being carried would require strapping the wood to the trailer's frame and maintaining a tension in the binder for the entire haul.

It has been proposed that the extra-light log trailer be equipped with a constant tensioning device for load binders. The objective of the latter is to constantly tie the load to the trailer, thus limiting dynamic loading on standards and bolsters, and adding extra stiffness to the trailer's frame. The other task of the device is to allow the driver to remove binders remotely from the truck's cab after arriving at a mill. This possibility would significantly enhance safety of the unloading operation. At least one driver is killed by a falling logs during unbinding operation at a mill woodyard in the Southeast every year.

Figure 137 shows a schematic of the proposed hydrostatic drive circuit for one version of the constant tensioning device. It is planned to use three synthetic web straps of 12,000-pound breaking strength. A high-torque and low-speed hydrostatic motor is used to tension each strap. It is believed that a force in the range of 2,000 to 3,000 pounds would be sufficient. Further research (including building a prototype rig and field testing) is required for a full development of the device.

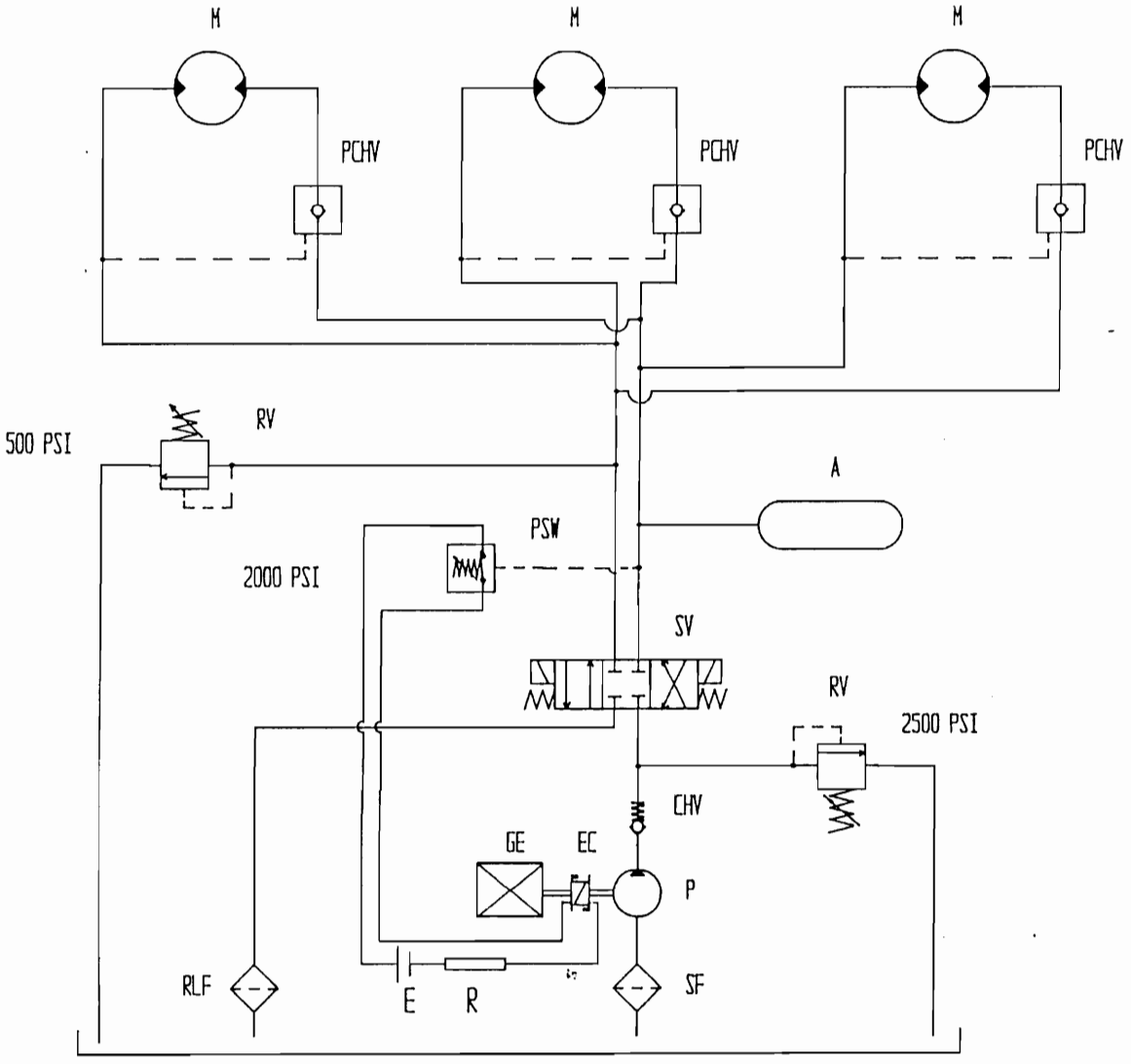

Figure 137. Hydrostatic Drive Circuit for the Proposed Load Binder Constant Tensioning Device.

Table 19. Component List for the Hydrostatic Drive System of the Proposed Load Binder Constant Tensioning Device.

LIST OF COMPONENTS	
ABBREVIATION	**DESCRIPTION**
M	Hydraulic Motor
PCHV	Pressure Controlled Check Valve
A	Hydraulic Accumulator
RV	Relieve Valve
PSW	Pressure Switch
SV	Spool Valve
CHV	Check Valve
P	Hydraulic Pump
GE	Gasoline Engine
EC	Electric Clutch
SF	Suction Filter
RLF	Return Line Filter
E	12 V Truck Battery
R	Resistor in Pressure Switch Circuit

CHAPTER 9. LOG TRAILER DESIGN RECOMMENDATIONS

Introduction

In the synthesis phase of this design process, information on the existing extra-light log trailers was gathered and selected designs were thoroughly analyzed. The research involved dynamic loading measurement, experimental stress analysis and finite element modeling of the designs, surveying trailers for fatigue cracks and estimating their fatigue life.

General Design Recommendations

1. Maximum working dynamic stresses in a log trailer should be assumed between 2.1 and 2.4 times larger than the static ones. In other words, all trailer structural members should incorporate a safety factor **greater than 2.4** (computed as a ratio of the yield strength of the material to the maximum predicted static stresses).

2. If the above condition is satisfied, it seems unlikely that the trailer will fail by plastic deformation due to excessive stresses induced in the structure during "normal operation" (excluding an obvious trailer misuse, such as tipping it over, crushing it with a crane grapple, loading with loads other than logs, etc.).

The **trailer will fail by fatigue**. This mode of failure results from repeated loadings and occurs without visual evidence of yielding at nominal stress levels far below the strength of the material. The process usually develops over an extended period of time. It operates at local areas rather than throughout the entire component. Typically, fatigue cracks initiate at points of highly localized stresses. After a crack has initiated at a stress raiser, the fluctuating stress activates its propagation. A fatigue failure is often sudden, with no external warning. The ultimate cause of all fatigue failures is that the crack has grown to a point at which the remaining material can no longer withstand the stresses, and sudden fracture occurs.

In conclusion, from the standpoint of trailer design, fatigue resistance is as critical as structural strength.

Improving fatigue resistance can be achieved in the following ways:

a) using **materials**:

- of higher strength (e.g. 50 ksi, or preferably 80, ksi yield strength);
- of higher fracture toughness;
- of improved purity;
- of improved grain structure from heat treatment;

b) **improving surface quality** (as the most fatigue cracks originate on the structure surface):

- desirable compressive stresses in the surface of a member can be induced by local heating, shot- or hammer-peening, surface rolling and tensile overloading;
- thermal stress relief is often used to reduce undesirable tensile residual stresses;
- grinding butt welds flush and smooth to reduce geometrical stress concentrations;

- protecting from corrosion greatly improves fatigue life of members; surface coatings such as paint, oil, or corrosion resistant chemical film should be always used; also capping tops of standards or opening their bottoms is desirable;

c) **designing the trailer for fatigue strength**:

- a smooth flow of stresses through the structure must be provided for;
- any cross-section property of a member should change very gradually;
- sudden passages from stiff to flexible regions must not be allowed;
- all joints should be located in regions of low stresses (e.g. at neutral axis of a member in bending);
- joints with large variations in stiffness must be removed from the structure;
- undercuts, notches, grooves, small holes, scratches, and any other stress risers in the structure are not allowed;
- loadings should be spread out on the structure as much as possible;

d) **improving welding operations** (e.g.: lack of penetration in a weldment provides a precrack; tungsten-arc inert-gas technique and dressing welds improves weld profile and removes entrapped inclusions at the weld toe);

- manual stick-electrode welding should be replaced by semi-automatic and automatic process whenever possible;
- welding operation should eliminate gas pockets and slag inclusions;
- weldments should be dress welded at critical locations to obtain surface smoothness and increase the thickness of material;
- over welding must be avoided;

e) **using butt welds instead of lap joints;**

f) **avoiding intermittent welds** (i.e., start and stop positions; weld ends are common locations for fatigue cracks);

3. Monitoring the dynamic loads acting on a log trailer traveling empty revealed high frequency and large amplitude stress variations. They were fully reversed, and a resonance response was frequently observed. Traveling empty is suspected of significantly contributing to fatigue damage of the trailer and affecting its fatigue life.

A folding frame trailer is a possible solution to this problem. It offers an increased productivity due to shorter turn-around time, less tire, brakes and suspension wear, and lower fuel consumption when in the return haul.

4. Data from the experimental stress analysis of log trailers indicate that the cyclic force which tends to cause the main frame to vibrate has a frequency between 7 and 8 Hz. A frequency and modal analyses of the selected trailers revealed that natural frequencies associated with the commonly observed "up-and-down swaying" vibrations of the frames are actually: 7.162 Hz for the gooseneck trailer, and 7.749 for the full-tree trailer. Therefore, to prevent a mechanical resonance of the structures, a suspension system having harmonics removed from the range of 7 to 8 Hz should be selected.

Recommendations for Trailer Member Design

Main Beams

1. Wide flange I-beams are used almost exclusively as main beams in log trailers. Data from dynamic loading measurements show that a log trailer is subjected to a combination of bending moments, axial forces, and twisting torques. These twisting torques become quite large while "racking" the trailer. Rolled sections are extremely poor members to support such loadings. They undergo excessively large rotations, and more importantly, develop highly concentrated stresses at places where they are welded to the other members (due to a restrained warping). Rectangular thin-wall hollow members twist without warping under certain conditions. Using rectangular tubing sections free from warping for main beams would dramatically increase the stiffness of the frame. The greater weight (by about 30%) than that of a wide flange cross-section of the same section modulus can be offset by introducing cutouts in the webs, and by using fewer number of cross members (e.g., 9 or 10). The beams should also be tapered for a better weight control (constant stress members).

If I-beams or other rolled sections (e.g., C-channel) are used as main beams, a totally different approach in the frame design should be assumed. Flexible main beams require more elastic connections with cross members than weldments. Bolted joints, if properly designed, will provide the required elastic connections.

2. **Cross members, landing gear fixtures,** as well as **any other attachments to the main beam should be joined to the web of the beam close to its neutral axis.** In special cases, the attachment may be made by means of a gusset running along the flange center line.

3. **The increased spacing between the main beams reduces loading surges** on bolsters on one side when the trailer leans on sharp corners. External frame design seems very promising.

4. **Logs on the trailer should be supported by three or four bolsters rather than two or three only.** The additional weight of an extra bolster (in this case a bolster without standards could be used) may be offset by the decreased weight of the frame (the primary contributor to the trailer tare weight). This weight reduction would be possible because of distributing the load along the trailer diminishes the bending moments exerted on the beams. With four bolsters, a trailer can still haul shortwood as well as longwood. Maximum normal stresses in the main beam of the gooseneck trailer were compared for two loading schemes: when the load was placed between the second and third bolsters versus the situation when it spanned all three bolsters. The stresses are 25% lower when the same load is supported by three bolsters.

It is important that the second and third bolsters be located as close as possible to the kingpin and the trailer bogie, respectively. This design feature again helps to limit the bending moments exerted on the main beams.

5. **A cross-section of the main beam should be kept very simple** and should have smooth passages at drops and tapers. I-beams must not be stiffened by adding bow-string trusses under the bottom flange, or by adding extra plates to the webs. All these "improvements" inevitably create geometric stress raisers, where fatigue cracks will originate (not to mention residual stresses from welding).

The comparative FEM stress analysis of the three selected trailer designs revealed that a combination of simple I-beam design and high tensile material (i.e. 80 ksi yield strength for flanges, and 50 ksi yield strength for the web) resulted in a design factor above 3 (computed as a ratio of the yield point of the material to the maximum static stress), whereas the main beams of a combined design (i.e. I-beam stiffened with the bow-string truss) had lower design factors (as low as 1.29 in one case).

Bolsters and Standards

6. **Bolsters should be recessed in webs of main beams, or raised on pedestals**, instead of mounted rigidly on top flanges. Top mounting induces highly concentrated stresses due to a restrained warping of I-sections and eventually leads to fatigue failure. A recessed bolster also increases the loading space of the bunk.

7. The alternative is to **mount bolsters on main beam top flanges using flexible (elastic) joints** (e.g.: clamping with rubber pads in between the members).

8. **Gussets rather than struts should be used to reinforce bolsters**; they help to distribute stresses more evenly.

The gussets should come out from almost the entire depth of the main beam web and avoid the corner of the web and flange weldment. The bolster and its gusseting must not be welded to the flanges of the main beam in order to remove stress concentrations due to the restrained warping of the I-section.

9. **Gussets stiffening bolsters should be used also in between the main beams.** This will diminish maximum stresses in bolsters at places where they meet with main beams by at least 15%.

10. If an **insert** is used to raise logs to facilitate unloading operations and/or to clear the taillights, it **should be equipped with some cradling mechanism** to restrain the outward deflections of the standards. This solution would **reduce the maximum stresses in the bolster almost by a factor of 3!** Also, the maximum stresses in standards would be lowered by about 20%.

11. **Putting a cable between tops of standards and tensioning it after loading is completed will diminish stresses in both standards and bolsters by a factor of 2!**

12. **Combining insert with a cradling mechanism on standards and placing a cable between the tops would result in maximum stresses lower in the bolsters, standards, and inserts by a factor of 3.7, 2.2 and 1.8, respectively!**

Cross members

13. **Rectangular tubing is the most efficient section for cross members**. Stresses are fed more smoothly into the main beam web.

14. Some cold-formed sections (e.g. channels), and fabricated sections (i.e. fabricated I-beams) have a potential to be efficient sections for main beams and other trailer's members. If these sections are used for cross members they **must not be welded to the flanges** of the main beam, since this will concentrate stresses. FEM stress analysis of two simple frames was performed, subjecting them to identical loading combination. The first frame used cross members of the same section geometry as the main I-beam, while the second one utilized tubular cross members. Maximum stresses at the joint of a box cross member with the main beam web were computed to be equal to only 17.4% of the magnitude of the corresponding stresses for the I-section cross member!

Summary

The following are the most important recommendations for extra-light log trailer:

1. Log trailer should be designed for fatigue resistance.

2. It should fold for return travel.

3. It should be equipped with a load binder constant tensioning device.

4. The cross-section of the main beam should be kept very simple.

5. Rectangular tubing, or cold formed shapes, should be used for cross members.

6. Bolsters should be mounted on top of main beams using flexible joints, or they should be recessed in the webs.

7. Cross members, landing gear fixtures, and other attachments to the main beam should be joined to the web at the neutral axis.

CHAPTER 10. SUMMARY AND FUTURE RESEARCH

The extra-light log trailer design was undertaken in a response to a need for safe and light log trailers for economical road transportation of timber.

The design process necessitated the experimental measurement of dynamic loads exerted on a log trailer and a comprehensive stress analysis of the structure. After an exhaustive survey of the existing designs, two light-weight, prototype, log trailers were selected for the study. Finite element models (FEM) were developed for each of the trailers using three-dimensional tapered unsymmetrical beam elements. Static stress analysis was performed to identify critical spots in the structures and to estimate stresses encountered at these locations. These spots were then selected as strain gage placements for the experimental dynamic stress analysis.

A special data acquisition system based on an STD bus computer was designed, assembled, programmed, and tested for the experimental force and strain measurements. External sensors included: strain gages, accelerometers detecting dynamic accelerations in three directions of space, a vehicle speed transducer, a brake monitor, and an event switch box to mark predefined events in the computer file. The data logger consisted of the STD Bus computer and system monitor and control console (a laptop computer was used for this purpose).

Experimental stress analysis of each of the selected trailers was performed. Dynamic loads and the resultant strains at critical locations were measured, both while simulating extreme situations, and during typical work cycles. The recorded service stress-time histories were then used to identify peak values of the maximum dynamic loading and the structure response. Stress distributions throughout the structures were obtained using the FEM models.

The two most important results of the experimental study of the selected trailers are:

1. The maximum dynamic loading exerted on a log trailer (given as the load CG acceleration expressed in terms of gravity acceleration "g") was detected to be:

- Vertical = 2.10 g;
- Lateral = 1.12 g;
- Longitudinal = 0.25 g;
- Resultant (Vector Sum) = 2.39 g.

2. It is unlikely that the two tested trailers will fail in excessive plastic deformation due to a dynamic overloading under normal conditions (i.e., excluding situations of the obvious trailer misuse). It was identified, however, that the most likely failure mode for a log trailer is a fatigue fracture.

Comparative FEM static stress analysis of selected designs revealed a potential for decreasing loadings exerted on standards and bolsters by using: inserts with cradling mechanisms on standards, and pretensioned ties between tops of standards (on loaded trailer).

The recorded service load spectra were utilized to assess a fatigue life of each of the designs. The estimated number of stress cycles to fracture computed for both trailers was found to be comparatively low, about a half of a million of cycles, as a result of a high mean stress, geometrical stress raisers present in the structures, and residual stress from fabrication.

A survey of log trailers for fatigue cracks revealed many locations were these cracks originate and propagate. The causes for fatigue cracking of log trailers were investigated through elastic shell element FEM modeling. It has been identified that a combination of four phenomena: notch effect due to sudden change in stiffeners, self stresses from welding, highly localized stresses due to restrained warping of I-sections, and environmental effects on fatigue of metals contribute to fatigue cracking of log trailers.

An efficient and economically feasible extra-light design was developed utilizing advanced materials and manufacturing technology.

The most important features of the proposed design are:

1. Light tare weight of 7,770 pounds.
2. Sound structural integrity.
3. Material of high strength and toughness used throughout.
4. Improved fatigue resistance (e.g. welds were replaced by elastic friction joints).
5. Movable bunks.
6. Replaceable bolsters and standards.
7. Constant tensioning device for load binders.

Finally, recommendations for an ultimate extra-light log trailer were formulated based on the results of the experimental stress analyses, finite element modeling, fatigue analyses, and engineering parameters and insights gained during the evaluation process.

Suggestions for Further Research

The extra-light design was documented through detailed engineering drawings, coupled with technical data from the manufacturers of components. Design concepts and specifications were presented to trailer manufacturers for evaluation and development of a final product. At this time two major trailer manufacturers are completing their preliminary designs of the extra-light folding log trailer for production.

A third trailer manufacturer is finalizing preparations for production of the prototype extra-light log trailer according to the design suggested in this dissertation (i.e. the straight-frame extra-light trailer).

It is planned that the design process of these trailers will be completed by a comprehensive product testing. The following further research is suggested:

1. Building a prototype is the best practical verification of a new design. Assembly stresses resulting from geometric imperfections, fabrication tolerances, and poor fits in the actual structure should be measured at this time using the "PhotoStress" method. These stresses may be detrimental for satisfactory fatigue life of the trailer. All alternations for practical reasons during assembly should be thoroughly analyzed and possibly included in the verified version of the design. If possible, more than two prototype trailers of each

type should be built. The first experiences with acquiring the components, fabricating the members, and assembly of the trailer will be invaluable in refining the design.

2. The trailer prototypes of the two trailer designs, when put into service, should be monitored for: the payloads carried and distances traveled (broken down into road categories, and their condition), loading and unloading equipment, etc. The trailers ought to be closely monitored for loosened fasteners (if any) and condition of the friction joints. The latter should be very carefully protected from grease and any other possible lubricants. If conventional bolts (of at least the same strength) are used instead of the Huck-Fit Fasteners the trailer should be monitored for possible optimal retorquing schedule.

3. At least one trailer of the two designs should be instrumented with strain gages and static stress analysis performed for various loading schemes (e.g. tree-lengths, shortwood, full-trees, etc.). The "PhotoStress" method (full stress field measurement technique) can be used at this stage to detect stress distributions in joints between members when simulating severe overloading.

4. A prototype constant tensioning mechanism for load binders should be built for tests. A dynamic stress analysis of the trailer should be performed for two situations: when the device is constantly tensioning load binders, and when the conventional binders are used. The experimental measurements should allow for detecting the effect of the device on the dynamic stresses induced in the trailer structural members. Tests with different tension in the binders should be also carried out to determine the optimal tension force in the binders.

5. The prototype tensioning device should be designed for remote binder removal. All necessary alternations for the present conceptual design should be thoroughly evaluated.

6. Economic performance of the trailers in terms of productivity and cost should be investigated and compared with that of a conventional double-bunk trailer. Fuel consumption for the folding frame trailer during a return trip empty should be experimentally measured (possibly using the data logger) for two situations: when the trailer is folded and when it is towed as a straight-frame trailer. Such an experiment could verify how much of the air drag and rolling resistance is reduced when the trailer is folded for the empty travel.

7. The present research was limited to trailers equipped with mechanical suspensions (i.e. 3-point 4-spring suspensions). It is recommended that one of the prototype vehicles of each group have air-ride suspension. Experimental dynamic stress measurements at critical locations could be then performed to identify the apparent advantages of using this type of suspension.

BIBLIOGRAPHY

Alt, C.B. 1990. Pulpwood truck unbinding rack. APA Technical Release 90-R-15. APA, Washington, DC.

American Pulpwood Association. 1981. Southern guide to Federal and State trucking regulations. APA Report 81-A-5, Washington, D.C., 101 p.

Anonymous. 1992. Super single tires. International Paper Comp. Applied Technology & Research. Logging Bulletin No. 43. Hattiesburg, MS.

Anonymous. 1993a. Trailer distributor assembles almost half of what it sells. Trailer/Body Builders. p 44-46.

Anonymous. 1993b. New equipment for construction industries introduced at ConExpo. Trailer/Body Builders. p 84-96.

Baas, P.H. and J.A. Stulen. Safety in log transport: an investigation into load securing devices and methods. New Zealand Logging Industry Research Assoc. Project Report No. 23.

Baumgrass, J.E. 1975. How to avoid axle-weight overloads on tandem-axle log trucks. Modern Logger and Timber Processor. p 14-15.

Beardsell, M. G. 1986. Decreasing the Cost of Hauling Timber through Increased Payload. Ph. D. Dissertation. Virginia Polytechnic Inst. & State Univ. Blacksburg, VA. 133 p.

Beer, F.P. and E.R. Johnston. 1981. Mechanics of Materials. McGraw-Hill Book Company. New York.

Boresi, A.P. and O.M. Sidebottom. 1985. Advanced Mechanics of Materials. Fourth edition. John Wiley & Sons. New York.

Burkhart, H., R.C. Parker, M.R. Strub and R.G. Oderwald. 1972. Yields for old-field loblolly pine plantations. Publication FWS-3-72, Div. of For. & Wildlife Res. Virginia Polytechnic Inst. & State Univ. Blacksburg, VA.

Buxbaum, O. 1979. Random load analysis as a link between operational stress measurement and fatigue life assessment. Service fatigue loads monitoring, simulation, and analysis. ASTM STP 671. Abelkis, P.R. and J.M. Potter, Eds., American Society for Testing and Materials. 1979. p 5-20.

Cao, Q.V. and H.E. Burkhart. 1980. Cubic-foot volume of loblolly pine to any height limit. Southern Journal of Applied Forestry. Vol. 4, No. 4. p 166-168.

Carruth, S. 1991. Personal communication. Westvaco Corp. Summerville, SC.

Clark, M. and D.R. Giles. 1988. Orientation of log butts on highway trucks: an economic analysis. Forest Engineering Research Inst. of Canada, Technical Report No. TR-85.

Cook, R.D., D.S. Malkus and M.E. Plesha. 1989. Concepts and Applications of Finite Eement Analysis. 3rd edition. John Wiley & Sons. New York.

Dieter, G.E. 1983. Engineering Design. A Materials and Processing Approach. McGraw-Hill Book Company. New York. p 27-67.

Dohrenwend, C.O. and W.R. Mehaffey. 1950. Electrical-resistance gages and circuit theory. *In* Handbook of Experimental Stress Analysis, Hetenyi, M., editor. John Wiley & Sons, Inc. New York.

Dowling, N.E. 1987. A review of fatigue life prediction methods. SAE Technical Paper 871966. Society of Automotive Engineers, Inc. Warrendale, PA.

Dowling, N.E. 1993. Mechanical Behavior of Materials: Engineering Methods for Deformation, Fracture, and Fatigue. Prentice Hall, Englewoods Cliffs, NJ.

Dykstra, D.P. and J.J. Garland. 1978. Log trucking in Oregon- a survey. Transactions of the ASAE, Vol. 21, No. 4. p 628-632.

Elphinstone, G.J. 1992. Personal communication. Elphinstone Engineering,Tribunana, Australia.

EXTE Fabrics AB, no date. Gebannte Landung. EXTE Fabrics AB, Farila,Sweden. 6 p. (In German).

Ford, E.C. III. 1976. Predictions of Tree Weights and Center of Gravity for Various Species of Appalachian Hardwoods. M. S. Thesis. Virginia Polytechnic Inst. & State Univ. Blacksburg, VA.

Ford, E.C. III. 1993. Personal communication. International Company, Hattiesburg, MS.

Fuchs, H.O. and R.I. Stephens. 1980. Metal Fatigue in Engineering. John Wiley & Sons. New York.

Gordon, R.D. 1980. Log truck axle layouts: an economic comparison of 5-axle and 6-axle layouts. New Zealand Logging Industry Research Assoc. Project Report No. 10. 23 p.

Green, D. and B. Jackson. 1992. Georgia logging vehicle monitoring system. APA Technical Release 92-R-68. APA, Washington, DC.

Hannah, R.L. and S.E. Reed, editors. 1992. Strain Gage User's Handbook. Elsvier Applied Science. London and New York. Society for Experimental Mechanics, Inc.

Hatenyi, H. editor. 1950. Handbook of Experimental Stress Analysis. John Wiley & Sons. New York.

Hendry. A.W. 1964. Elements of Experimental Stress Analysis. Pergamon Press. Oxford.

Ilzar, B. 1980. Federal and state trucking regulations confuse wood transportation outlook. Pulp and Paper, June. p 79-81.

Ilzar, B. 1983. Review of market and transportation requirements and future trends. *In* Harvesting the South's Small Trees. FPRS Conference, April 1983. Proceeding 7340. FPRS, Wisconsin. p 89-96.

Keesee, M. J. 1990. Reducing Log Truck Transfer of Mud to Public Roads. M.S. Thesis. Virginia Polytechnic Institute & State University. Blacksburg, VA. 78 p.

Knight, C.E. 1989. FEPC - Finite Element Personal Computer Program. Dept of Mechanical Engineering, Virginia Polytechnic Inst. & State Univ. Blacksburg, VA.

Knight, C.E. 1990. The Finite Element Method in Mechanical Design. Dept of Mechanical Engineering, Virginia Polytechnic Inst. & State Univ. Blacksburg, VA.

Lavoie, J.-M. 1980. The transport of full trees from the stump are to the mill woodyard. Forest Engineering Research Inst. of Canada, Technical Report No. TR-44, 36 p.

Lavoie, J.-M. 1981. Securing Systems for truck loads of tree-lengths. Forest Engineering Research Inst. of Canada, Technical Note No. TN-41. Feb.

LAXO Mekan AB, no date. LAXO .....for sequring the timber load. LAXO Mekan AB, Laxa, Sweden.

Lineback, D. 1987. Strain gage measurement systems. *In* Experimental Stress Analysis Notebook. Issue 6. May. Measurements Group, Inc. Raleigh, NC.

Marsh, K.J. and N.E. Frost. 1968. Problems in Service--Engineering Considerations. *In* Avoidance of failures. Proceedings from the 22nd Autumn Course. Institution of Mechanical Engineers, Eastbourne, UK, England.

McCormack, R.J. 1990. Measuring and Evaluating Log Truck Performance in a Variety of Operating Conditions. Ph.D. Dissertation. Virginia Polytechnic Institute & State University. Blacksburg, VA. 138 p.

Measurement Group, Inc. 1992. Seminar on Experimental Stress Analysis Techniques for the Teaching Labolatory. July 13-17. Raleigh, NC.

Nole, B. 1992. Double-bunk loading method for pulpwood from thinnings. APA Technical Release 92-R-47. APA, Washington, DC.

Overboe, P.D. 1987. Optimizing Log Truck Payload through Improved Weight Control. M.S. Thesis. Virginia Polytechnic Institute & State University. Blacksburg, VA.

Peerless Co. 1986. Short logger. Bulletin 123. Tualatin, OR.

Perry, C.C. 1982. The professional stress analyst. Epsilonics, Vol. II, Issue 3, Dec.

Peters, L.C. and R.B. Hopkins. 1986. The designer and the designer's problems. *In* Standard Handbook of Machine Design, Shigley J.E. and C.R. Mischke editors. McGraw-Hill Book Company. New York. p 2-45.

Peterson, R.E. 1974. Stress Concentration Factors. John Wiley & Sons, New York.

Rice, C.R. 1988. Fatigue Design Handbook. Society of Automotive Engineers, Inc. Warrendale, PA.

Rinn, R.J. 1992. Personal communication. Measurement Group, Inc. Raleigh, NC.

Shaffer, R.M. and W.B. Stuart. A checklist for efficient log trucking. Virginia Cooperative Extension Service. Virginia Tech and Virginia State. Publication 420-094. Dec. 7 p.

Shigley, J.E. 1977. Mechanical Engineering Design. 3rd edition. McGraw-Hill, Inc. New York.

Smith, D.G. 1981. Computer aided comparison of 5-, 6-, and 7-axle log trucks for long distance highway hauling. Forest Research Inst. of Canada, Pointe Clare, Quebec, Technical Report No. TR-49. 56 p.

Stadden, K. 1990. Shake it, don't break it. Heavy Duty Trucking, March 1990. p 56-63.

Stainhilb, H.M. and J.R. Erickson. 1970. Weights and centers of gravity for quaking aspen trees and boles. USDA For. Service. Research Paper NC-91, 4 p.

Stainhilb, H.M. and J.R. Erickson. 1972. Weights and centers of gravity for red pine, white spruce and balsam fir. USDA For. Service. Research Paper NC-75, 7 p.

Stephenson, E.H. 1988. On-board air scales for timber transport. APA Technical Release. APA, Washington, DC.

Stephenson, E.H. 1991. Constant-tension web strap winch for long-log railcars. APA Technical Release 91-R-77, Nov. APA, Washington, DC.

Stephenson, E.H. 1993. Personal communication. Union Camp Corp. Savannah, GA.

Stuart, W.B. 1992. Improving trucking economics. Timber Harvesting, May, 1992. p 29-35.

Stulen, J.A. 1984. Securing loads on logging trucks. New Zealand Logging Industry Research Assoc. Report. Vol. 9, No. 2. 4 p.

Stulen, J.A. 1985. Log truck axle layouts: an economic comparison of log transport layouts. New Zealand Logging Industry Research Assoc., Project Report 24. 17 p.

Swanson Analysis Systems, Inc. 1989. ANSYS Engineering Analysis System User's Manual. Revision 4.4. Swanson Analysis Systems, Inc. Houston, PA.

Taylor, P. 1989. Folding Bailey Bridge Trailers in New Zealand. New Zealand Logging Industry Research Assoc. Report. Vol. 14, No. 11. 7 p.

Titus, A.C., J.A. Titus and D.G. Larsen. STD Bus Interfacing. Blacksburg Continuing Education Series. Haward W. Sams & Co., Inc. Indianapolis, IN.

Trevitt, D. 1991. Truck/trailer weight-reduction program. APA Technical Release 91-R-23. March 1991. APA, Washington, DC.

US. DOT. 1982. Bridge Gross Weight Formula. Federal Highway Administration. Washington, DC. 11 p.

Watson, W.F. and T.G. Matney. 1984. Predicting axle loads on trucks hauling tree-length logs. Southern Journal of Applied Forestry, Vol. 9, No. 3. p 157-161.

Wilson, F. G. 1980. Truck transport of longwood calls for new equipment and regulations. Pulp and Paper, June. p 99-103.

Appendix A. Derivation of Weight Distribution and Member Loadings on the Gooseneck Trailer

Definitions:

L1 = 209" - distance measured from the tractor steering axle to the kingpin;

L2 = 215" - distance measured from the tractor steering axle to the tractor tandem midpoint;

L3 = 609" - distance measured from the tractor steering axle to the trailer tandem midpoint;

L4 [in.] - distance from the steering axle to the location of the tractor center of gravity;

L5 [in.] - distance measured from the kingpin to the trailer center of gravity;

L6 [in.] - distance measured from the kingpin to the location of the payload center of gravity;

F1 [lbs] - measured weight of the steering axle of the tractor;

F2 [lbs] - measured weight of the driving tandem axles of the tractor;

F3 [lbs] - measured weight of the trailer tandem axles;

F4 [lbs] - derived reaction force at kingpin;

W1 [lbs] - derived mean empty weight of the tractor;

W2 [lbs]- derived empty trailer weight;

W3 [lbs]- measured payload;

H1, B1 [in.] - measured inside height of the second standard and inside width of the second bolster;

H2, B2 [in.] - measured inside height of the third standard and width of the third bolster;

Fs [lbs] - total horizontal force acting on a standard from the load;

Hs [in.] - distance measured from the direction of the force Fs to the top surface of the bolster;

Ms [in.-lbs] - bending moment due to the force Fs.

Figures 138 and 139 show force distribution exerted on the empty and loaded trailer, respectively. The weight and axle spacing data were obtained by actual measurement for two payloads of tree-length thinning material: 54,100 and 58,320 pounds. The payload was placed between the second and third bolster each time.

Forces acting on the tractor and trailer and the locations of the centers of gravity for the tractor, trailer and payloads were determined from the equilibrium condition.

Finally, the static loading exerted on each member of the trailer was derived using both methods of computing loadings on standards (i.e. the hydrostatic pressure, and the group of logs partially supported by a standard concept), and assuming a symmetrical weight distribution on the trailer.

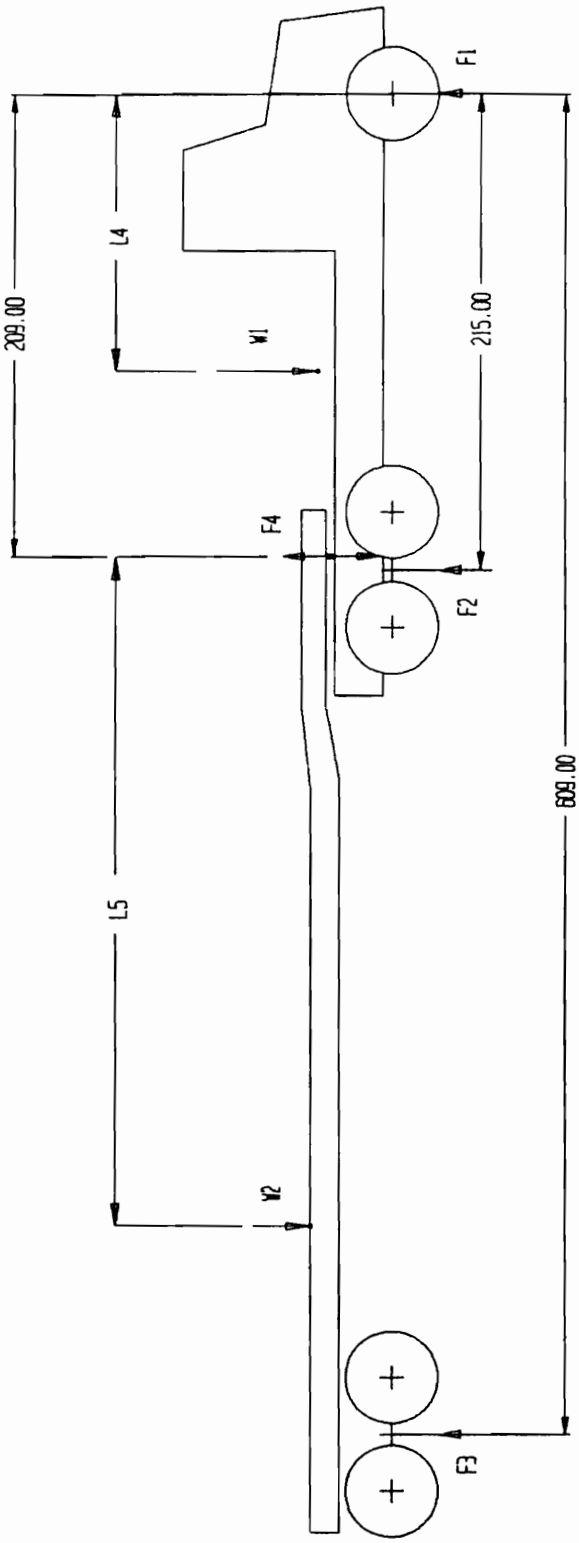

Figure A1. Distribution of Forces Exerted on the Empty Gooseneck Trailer.

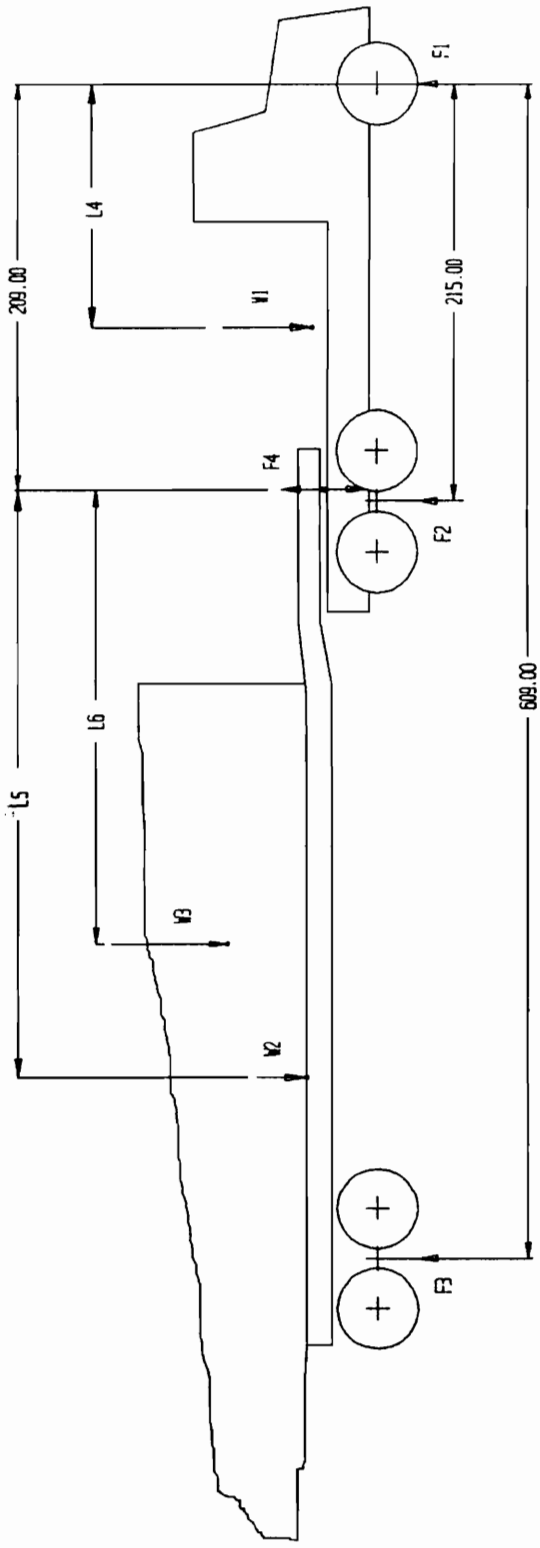

Figure B2. Distribution of Forces Exerted on the Loaded Gooseneck Trailer.

GOOSENECK TRAILER

I. AXLE SPACING DATA [IN.]

from \ to	Front Drive	Rear Drive	Front Trailer	Rear Trailer
Steering Axle	189	241	583	635

Front Drive = Rear Drive - (4*12 +4)

from \ to	King Pin	Drive Axles Midpoint	Trailer Bogie Midpoint
Steering Axle	209	215	609

Drive Axle Midpoint = Tractor - Steering Axle
Trailer Bogie Midpoint = GVW - Tractor

II. AXLE WEIGHTS [LBS]

	Steering Axle	Tractor	GVW	Drive Midpt.	Bogie Midpt
1. Empty	8,320	22,800	31,120	14,480	8,320
1. Loaded	9,920	45,180	85,220	35,260	40,040
2. Empty	8,380	22,700	31,020	14,320	8,320
2. Loaded	9,860	47,340	89,340	37,480	42,000

III. EMPTY WEIGHTS (in lbs)

Mean Steering Axle Weight =	8,350
Mean Driving Axles Weight =	14,400
Mean Tractor Weight =	22,750
Mean Tractor Tare Weight =	20,170

Trailer Tare Weight =	10,900

IV. STEERING AXLE TO BUTTS DISTANCE [IN.]

Case 1.	309
Case 2.	308

V. LOCATION OF THE TRAILER AND TRACTOR CENTER OF GRAVITY - L4 & L5 [IN.]

Trailer: L5=F3*(L3-L1)/W2 =	305.32	(from Kingpin)
Tractor:L4=(F2*L2-F4*L1)/W1 =	126.76	(from Kingpin)

VI. LOCATION OF THE PAYLOAD CENTER OF GRAVITY - L6 [IN.]

Case	Payload (lbs)	Location of the Payload CG from:		
		Kingpin	Butts	2nd Bolster
1.	54100	234.53	134.53	100.53
2.	58320	231.00	132.00	97.00

Location of the Payload CG (from Kingpin)= (F3*(L3-L1)-W2*L5)/LOAD L6

VII-A. BOLSTER LOADS - COMPUTING METHOD "ONE"

Loading Case		Concentrated [lb]	Distributed [lb/in.]	Bending Moment [in.*lb]
1.	2nd Bolster:	27,407	292.35	636,003
1.	3rd Bolster:	26,693	302.46	561,085
2.	2nd Bolster:	30,555	325.92	709,042
2.	3rd Bolster:	27,765	314.62	583,629

CROSS-SECTIONAL AREA OF LOADING SPACE AT BOLSTERS [SQ.IN.]

2nd Bolster:	H1*B1 =	114.25*93.75=	10,710.9
3rd Bolster:	H2*B2 =	105.50*88.25=	9,310.4

Bending Moment = 1/3(F5*(H ^ 2)/(2*B)

STANDARD AND BOLSTER WEIGHTS [LBS]

	Single Standard	Bolster
2nd Bolster:	134.2	166.8
3rd Bolster:	124.8	121.0

VIII-A/1. LOADS EXERTED ON STANDARDS - METHOD "ONE"/LOADING 1

STANDARDS ON 2ND BOLSTER

Element	Distance from top of standard	Total shear force at this level (lbs)	Shear force acting on the element (lbs)	Bending Moment acting on the elem. (in.*lbs)
	0	0	0	0
1	5.5	39	38.70	71
2	10.5	141	102.35	256
3	15.5	307	166.32	416
4	20.5	538	230.29	576
5	25.5	832	294.27	736
6	30.5	1,190	358.24	896
7	35.5	1,612	422.21	1,056
8	40.5	2,099	486.18	1,215
9	45.5	2,649	550.15	1,375
10	50.5	3,263	614.12	1,535
11	55.5	3,941	678.09	1,695
12	60.5	4,683	742.06	1,855
13	65.5	5,489	806.03	2,015
14	70.5	6,359	870.00	2,175
15	75.5	7,293	933.97	2,335
16	80.5	8,291	997.94	2,495
17	85.5	9,353	1061.92	2,655
18	90.5	10,479	1125.89	2,815
19	95.5	11,669	1189.86	2,975
20	100.5	12,922	1253.83	3,135
21	105.5	14,240	1317.80	3,294
22	110	15,481	1240.71	2,792
23	111.5	15,906	425.09	319
24	113	16,337	430.84	323
25	114.25	16,700	363.43	227
				39,235

STANDARDS ON 3ND BOLSTER

Element	Distance from top of standard	Total shear force at this level (lbs)	Shear force acting on the element (lbs)	Bending Moment acting on the elem. (in.*lbs)
	0	0	0	0
1	5.5	43	43.36	79
2	10.5	158	114.68	287
3	15.5	344	186.35	466
4	20.5	602	258.03	645
5	25.5	932	329.70	824
6	30.5	1,333	401.38	1,003
7	35.5	1,807	473.05	1,183
8	40.5	2,351	544.72	1,362
9	45.5	2,968	616.40	1,541
10	50.5	3,656	688.07	1,720
11	55.5	4,415	759.75	1,899
12	60.5	5,247	831.42	2,079
13	65.5	6,150	903.09	2,258
14	70.5	7,125	974.77	2,437
15	75.5	8,171	1,046.44	2,616
16	80.5	9,289	1,118.12	2,795
17	85.5	10,479	1,189.79	2,974
18	90.5	11,741	1,261.46	3,154
19	95.5	13,074	1,333.14	3,333
20	100.5	14,479	1,404.81	3,512
21	105.5	15,955	1,476.49	3,691
				39,859

VIII-A/2. LOADS EXERTED ON STANDARDS - METHOD "ONE"/LOADING 2

STANDARDS ON 2ND BOLSTER

Element	Distance from top of standard	Total shear force at this level (lbs)	Shear force acting on the element (lbs)	Bending Moment acting on the elem. (in.*lbs)
	0	0	0	0
1	5.5	43	43.15	79
2	10.5	157	114.11	285
3	15.5	343	185.42	464
4	20.5	599	256.74	642
5	25.5	927	328.06	820
6	30.5	1,327	399.38	998
7	35.5	1,798	470.69	1,177
8	40.5	2,340	542.01	1,355
9	45.5	2,953	613.33	1,533
10	50.5	3,638	684.65	1,712
11	55.5	4,394	755.96	1,890
12	60.5	5,221	827.28	2,068
13	65.5	6,119	898.60	2,246
14	70.5	7,089	969.91	2,425
15	75.5	8,131	1041.23	2,603
16	80.5	9,243	1112.55	2,781
17	85.5	10,427	1183.87	2,960
18	90.5	11,682	1255.18	3,138
19	95.5	13,009	1326.50	3,316
20	100.5	14,406	1397.82	3,495
21	105.5	15,876	1469.14	3,673
22	110	17,259	1383.20	3,112
23	111.5	17,733	473.90	355
24	113	18,213	480.32	360
25	114.25	18,618	405.17	253
				43,741

STANDARDS ON 3ND BOLSTER

Element	Distance from top of standard	Total shear force at this level (lbs)	Shear force acting on the element (lbs)	Bending Moment acting on the elem. (in.*lbs)
	0	0	0	0
1	5.5	45	45.11	83
2	10.5	164	119.29	298
3	15.5	358	193.84	485
4	20.5	627	268.39	671
5	25.5	970	342.95	857
6	30.5	1,387	417.50	1,044
7	35.5	1,879	492.06	1,230
8	40.5	2,446	566.61	1,417
9	45.5	3,087	641.16	1,603
10	50.5	3,803	715.72	1,789
11	55.5	4,593	790.27	1,976
12	60.5	5,458	864.83	2,162
13	65.5	6,397	939.38	2,348
14	70.5	7,411	1,013.93	2,535
15	75.5	8,500	1,088.49	2,721
16	80.5	9,663	1,163.04	2,908
17	85.5	10,900	1,237.60	3,094
18	90.5	12,212	1,312.15	3,280
19	95.5	13,599	1,386.70	3,467
20	100.5	15,060	1,461.26	3,653
21	105.5	16,596	1,535.81	3,840
				41,460

VII-B. LOADS EXERTED ON BOLSTERS - COMPUTING METHOD "TWO"

Loading Case		Concentrated lb	Distributed lb/in.	Bending Moment in.*lb
1.	2nd Bolster	27,407	292.35	375,885
1.	3rd Bolster	26,693	302.46	335,448
2.	2nd Bolster	30,555	325.92	419,053
2.	3rd Bolster	27,765	314.62	348,926

CROSS-SECTIONAL AREA OF BOLSTER LOADING SPACE [SQ.IN.]

2nd Bolster:	H1*B1 =	114.25*93.75=	10,711
3rd Bolster:	H2*B2 =	105.50*88.25=	9,310

WEIGHTS SUPPORTED BY STANDARDS [LBS]

CROSS-SECTIONAL AREA OF THE LOAD SUPPORTED BY STANDARDS [SQ.IN.]

2nd Bolster: (@TAN(1.047)*(93.75/2))*(93.75/2)/2+(114.25-(@TAN(1.047)*93.75/2))*93.75/2=
= 3,453

3rd Bolster: @TAN(1.047)*(88.25/2)*(88.25/2)/2+(105.5-(@TAN(1.047)*88.25/2))*88.25/2 =
= 2,970

FRACTION OF THE LOAD RESTING ON SINGLE STANDARD

2nd Bolster:	0.3224
3rd Bolster:	0.3190

VIII-B. LOADS EXERTED ON STANDARDS - METHOD "TWO"

STANDARDS ON 2ND BOLSTER

Horizontal force exerted on standard due to the load resting on it - Fs [LBS]

	Loading	
	Case 1.	Case 2
Fs = 27407.48*0.32242*TAN(30 deg) =	5,102	5,688

Point of Application of the Force Fs - Hs [IN.]

Hs = CENTROID of the load resting on the bolster =	73.68

Bending Moment due to force Fs - Ms [IN.*LBS]

	Loading	
	Case 1.	Case 2.
Ms = Fs * Hs	375,885	419,053

STANDARDS ON 3RD BOLSTER

Horizontal Force acting on standard due to the load resting on it - Fs [LBS]

	Loading	
	Case 1.	Case 2.
Fs = 26692.5153*0.318977*TAN(30 deg) =	4,916	5,113

Point of Application of the Force Fs - Hs [IN.]

Hs = CENTROID of the load resting on the bolster =	68.24

Bending Moment due to Force Fs - Ms [IN.*LBS]

	Loading	
	Case 1.	Case 2.
Ms = Fs * Hs	335,448	348,926

IX-1. LOADS EXERTED ON THE MAIN BEAM [LBS] - METHOD "TWO"/LOADING CASE 1

At Kingpin = 0.5(PAYLOAD + TRAILER WEIGHT - REACTION ON BOGIE MIDPOINT) =
= .5(PAYL-W2+ = 0.5 * 24960= 12,480

At 2nd bolster = 0.5 * F5 = 13,704

Distributed load due to trailer weight = 11900/477 = 24.95 [LBS/IN.]

At 3rd bolster = 0.5 * F6 = 13,346

At trailer bogie midpoint = 0.5 * F3 = 20,020

IX-2. LOADS EXERTED ON THE MAIN BEAM [LBS] - METHOD "TWO"/LOADING CASE 2

At KingPin = 0.5(PAYLOAD + TRAILER WEIGHT - REACTION ON BOGIE MIDPOINT) =
= .5(PAYL-W2+ = 0.5 * 27220= 13,610

At 2nd bolster = 0.5 * F5 = 15,278

Distributed load due to trailer weight = 11900/477 = 24.95 [LBS/IN.]

At 3rd bolster = 0.5 * F6 = 13,883

At trailer bogie midpoint = 0.5 * F3 = 21,000

Appendix B. Sample of Conventional Stress Analysis Method Calculations

Definitions:

$w = 292.35$ [lbs/in.]	- uniformly distributed load on the bolster;
$F_a = 5201.9$ [lbs]	- total horizontal force acting on a standard (and conveyed to the bolster);
$M_S = 375{,}885$ [in.-lbs]	- total bending moment applied to a standard (and conveyed to the bolster);
$W_S = 134$ [lbs]	- weight of the standard;
$W_b = 166$ [lbs]	- weight of the bolster;
R_b, R_d [lbs]	- reaction forces at fixed supports B and D, respectively;
M_b, M_d [in.-lbs]	- reaction moments at fixed supports B and D, respectively;
V_x [lbs]	- shearing force acting at the cross-section located x inches from the origin of the coordinate system;
M_x [in.-lbs]	- bending moment acting at the cross-section located x inches from the origin of the coordinate system;
$l = 28.25$ [in.]	- length of the outside (cantilevered) section of the bolster;
$L = 37.25$ [in.]	- length of the center section of the bolster (between the webs of the I beams);

Application of conventional methods in stress analysis of a log trailer is illustrated taking the second bolster of the gooseneck trailer as an example. Loading Cases 1 and 2, and Methods 1 and 2 of computing loadings on standards are considered as discussed in Chapter 4.

B1. Double Integration of the Elastic Curve Differential Equation

It is assumed that the bolster is rigidly supported at the weldments attaching it to the two main beams of the trailer. Figure B1 shows loading exerted on the bolster. It is also assumed that the bolster is a prismatic beam (i.e. has a constant cross-section). Later on, we will consider the actual properties of each cross-section, when computing stress magnitudes.

From the free-body diagram of Figure B2 it is seen that there are 4 unknowns (R_b , M_b , R_d , M_d), and only two independent equilibrium equations are available. Thus, the structure is indeterminate to the second degree. The geometry of the loaded beam is utilized to obtain the additional relations needed for evaluation of the unknown reactions. Two boundary or matching conditions are required in addition to those necessary for the determination of the constants of integration. These extra boundary conditions, when substituted in the appropriate elastic curve equations (slope and deflection), will yield the necessary additional equation.

The equations of equilibrium are:

$- F_a + F_b = 0$ (only for $0<x<28.25$);

$F_e - F_d = 0$ (only for $65.5<x$);

$R_b + R_d - 2W_s - W_b - w(2l + L) = 0$;Eq. 1

$M_s + R_b l + R_d(l + L) - 0.5w(2l + L)^2 - 0.5W_b(2l + L) + M_b + M_d - W_s(2l + L) - M_s = 0$;Eq. 2

At points B ($x=X_1$) and D ($x=X_3$) the deflections and slopes of the bolster are zero (fixed supports):

$\theta_1 (x=X_1) = 0$; Eq. 3

$y_1 (x=X_1) = 0$; Eq. 4

$\theta_2 (x=X_3) = 0$; Eq. 5

$y_2 (x=X_3) = 0$; Eq. 6

Point C ($x=X_2$) is used as a matching point: deflections and slopes of the beam sections in front and past the point C must be equal:

$\theta_1 (x=X_2) = \theta_2 (x=X_2)$;Eq. 7

$y_1 (x=X_2) = y_2 (x=X_2)$;Eq. 8

Thus, the six additional equations (Eq. 3 to Eq. 8) have been obtained. They can be used now for finding the unknown reactions at supports (utilizing also the equilibrium conditions Eq. 1 and Eq. 2).

The method using differential equation of an elastic curve requires the following simplifying assumptions:

1. The bolster is an elastic curve.
2. The square of the slope of the bolster at any cross-section is negligible compared to unity.
3. The bolster deflections due to shearing stresses are negligible.
4. The values of Young's modulus (E) and moment of inertia (I) of a cross-section are constant for any interval along the beam.

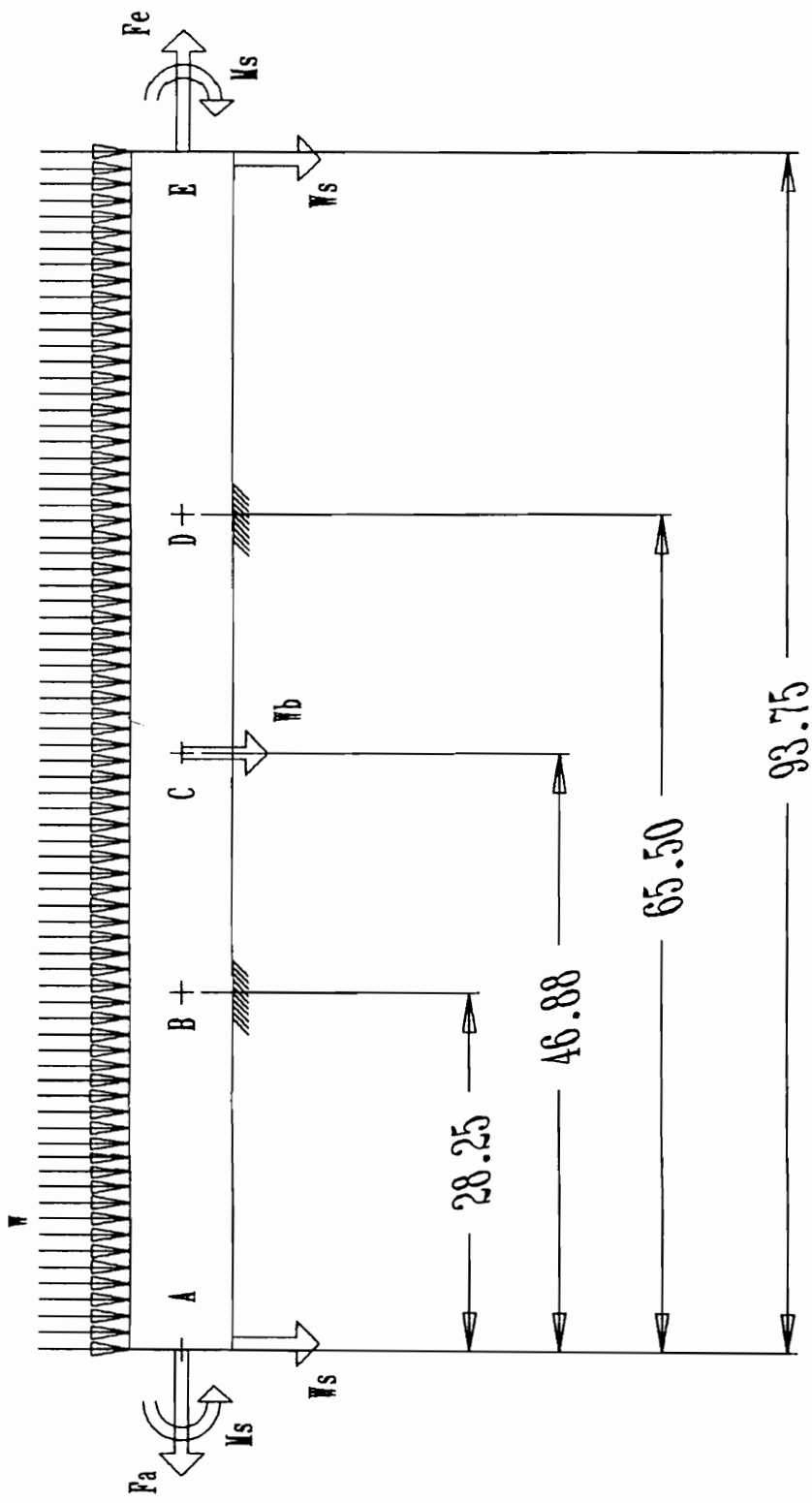

Figure B1. Schematic of the Second Bolster of the Gooseneck Trailer.

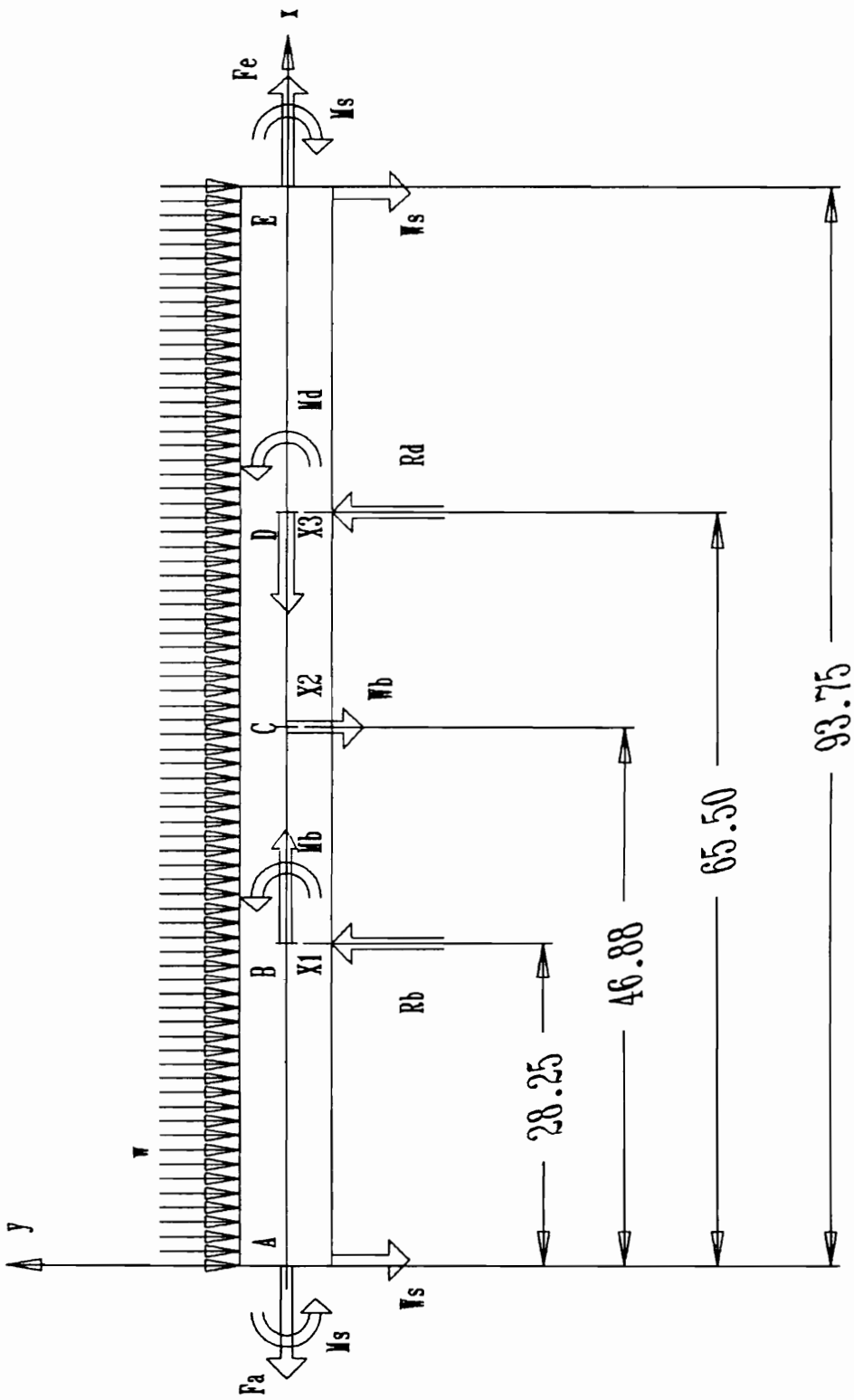

Figure B2. Free-Body-Diagram of the Bolster.

The elastic curve equations for the unique intervals of the bolster are given as:

for $0 < x < 28.25$ interval (Figure B3):

$$EI\,(d^2y/dx^2) = M_1(x) = -0.5wx^2 - W_s x - M_s$$

integrating once in we get:

$$EI\,(dy/dx) = EI\,\theta_0(x) = -(1/6)wx^3 - 0.5x^2 W_s - M_s x + C1$$

integrating again gives:

$$EI\,y_0(x) = -(1/24)wx^4 - (1/6)W_s x^3 - 0.5M_s x^2 + xC1 + C2$$

Similarly, the relationships for the slope and deflection in the other intervals of the bolster are obtained:

for $28.25 < x < 46.875$ (Figure B4):

$$EI\,(d^2y/dx^2) = M_2(x) = R_b(x-l) - 0.5wx^2 - W_s x - M_s - M_b$$

$$EI\,(dy/dx) = EI\,\theta_1(x) = R_b(0.5x^2-lx) - (1/6)wx^3 - 0.5x^2W_s - M_s x - M_b x + C3 \qquad ;Eq.\ 9$$

$$EI\,y_1(x) = R_b\{(1/6)x^3 - 0.5lx^2\} - (1/24)wx^4 - (1/6)W_s x^3 - 0.5M_s x^2 - 0.5M_b x^2 + xC3 + C4 \qquad ;Eq.10$$

for $46.875 < x < 65.5$ (Figure B5):

$$EI\,(d^2 y/dx^2) = M_3(x) = R_b(x-l) - 0.5wx^2 - W_s x - M_s - M_b - W_b(x - l - 0.5L)$$

$$EI\,(dy/dx) = EI\,\theta_2(x) = R_b(0.5x^2 - lx) - (1/6)wx^3 - 0.5W_s x^2 - M_s x - M_b x - W_b\{0.5x^2 - x(l + 0.5L)\} + C5 \quad ;\text{Eq. 11}$$

$$EI\,y_2(x) = R_b\{(1/6)x^3 - 0.5lx^2\} - (1/24)wx^4 - (1/6)W_s x^3 - 0.5M_s x^2 - 0.5M_b x^2 - W_b\{(1/6)x^3 - 0.5x^2(l + 0.5L)\} + xC5 + C6 \quad ;\text{Eq. 12}$$

TK Solver version 2.0 was used to solve the set of equations Eq. 1 to Eq. 12. Table B1 contains the solutions for the unknown reactions at the supports.

Exploring a symmetry of the structure we could have arrived at the same solution much quicker. However, setting that:

$$R_b = R_d \quad ;\text{Eq. 13}$$

and

$$M_b - M_d = 0 \quad ;\text{Eq. 14}$$

The two equilibrium equations (Eq. 1 and Eq. 2) are now dependent on each other and cannot yield a solution. The problem is now indeterminate to the first degree. Only one elastic curve equation has to be written and only one boundary (or matching) condition is needed in addition to the two for determination of the integration constants.

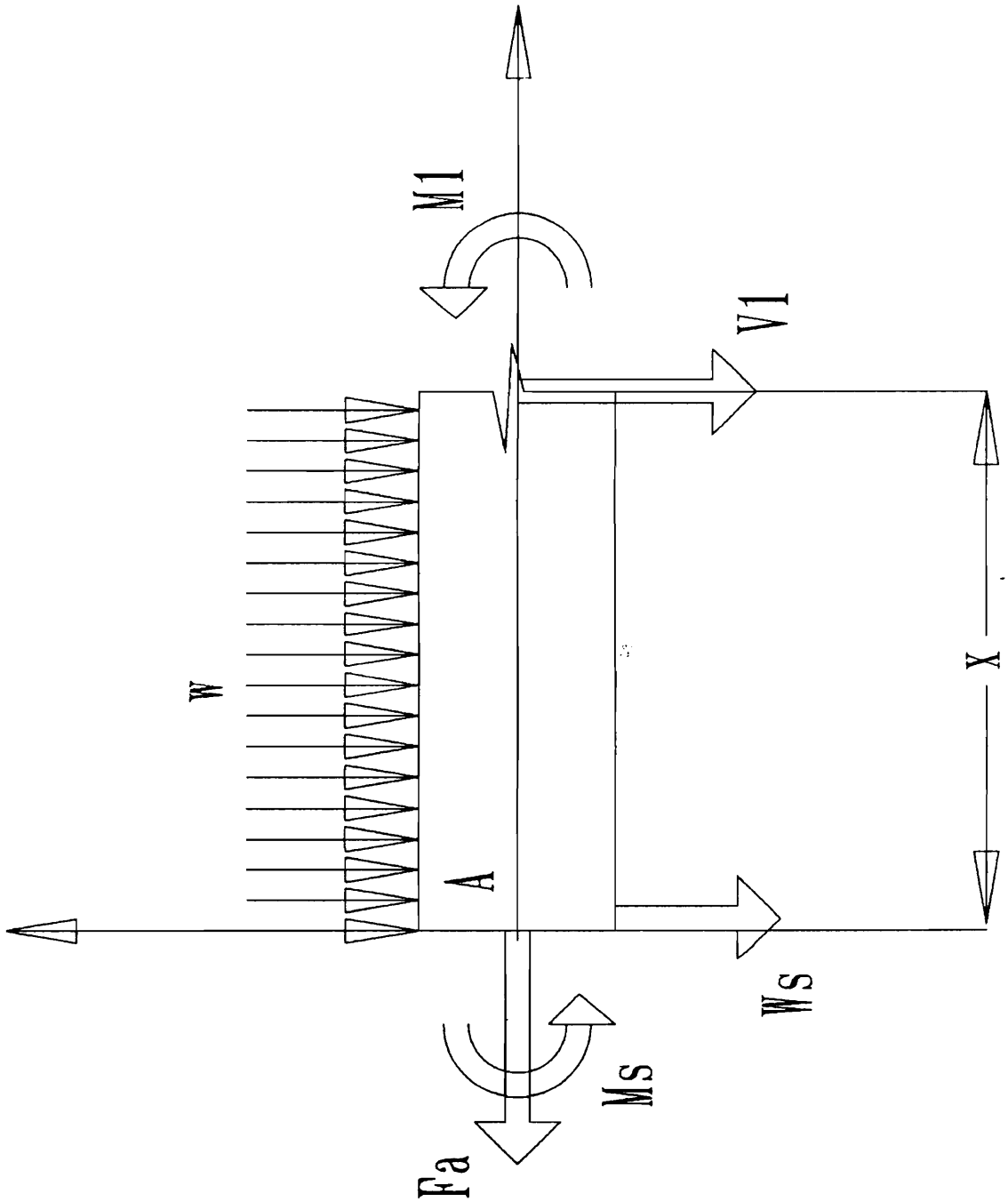

Figure B3. Free-Body Diagram of the First Interval: $0 < x < 28.25$.

The slope of the standard at point C ($x=X_2$) is zero due to the symmetry:

$\theta_1 (x=X_2) = 0$;Eq. 15

Using equations Eq. 13 to 15 along with the second equilibrium condition (Eq. 2) we arrive at the identical solution having utilizing only one equation of elastic curve; i.e. Eq. 9. Only one beam interval was used i.e.:

$46.875 < x < 65.5$

Table B2 shows the equations used and solution obtained by TK Solver program.

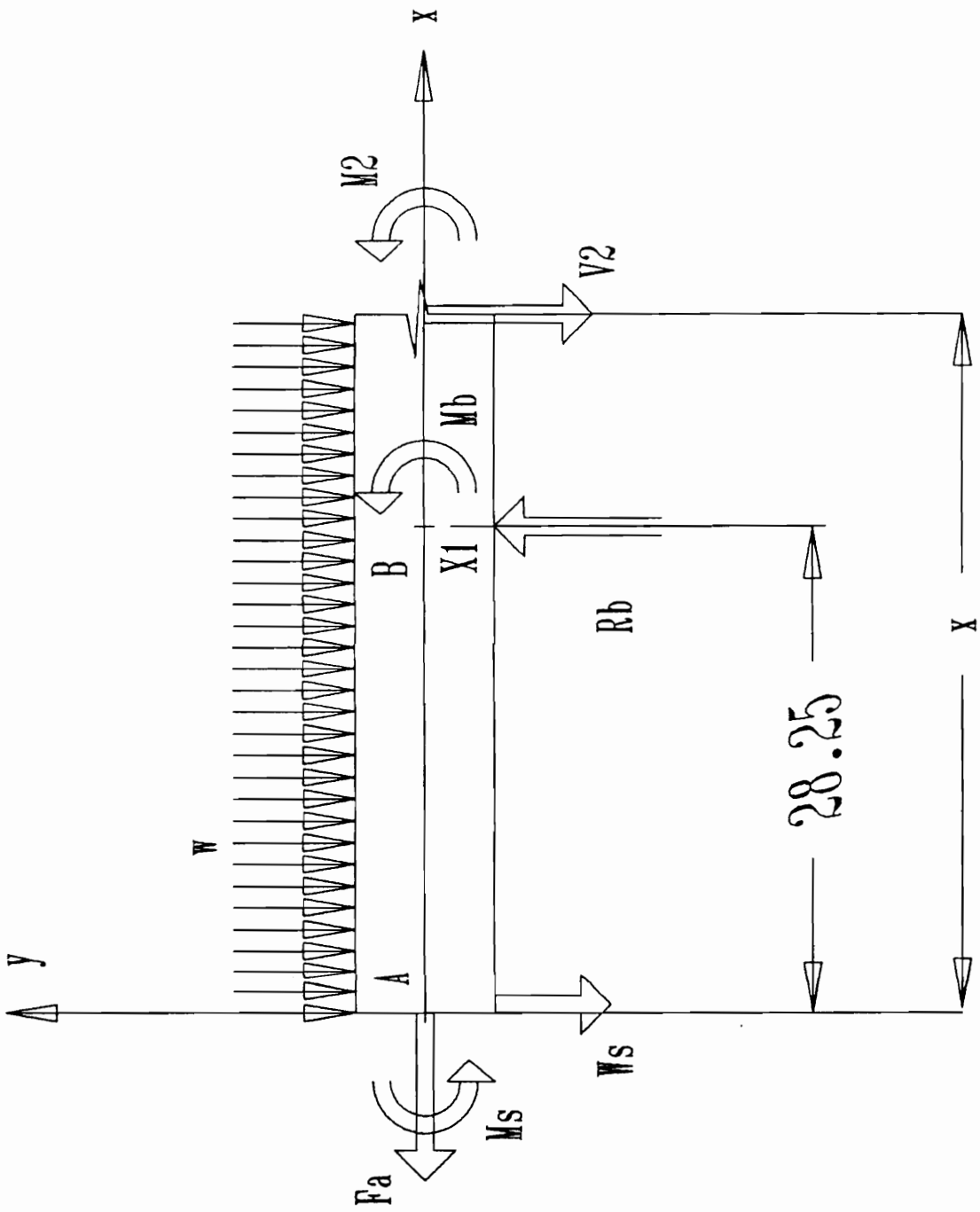

Figure B4. Free-Body Diagram of the Second Interval: 28.25 < x < 46.875.

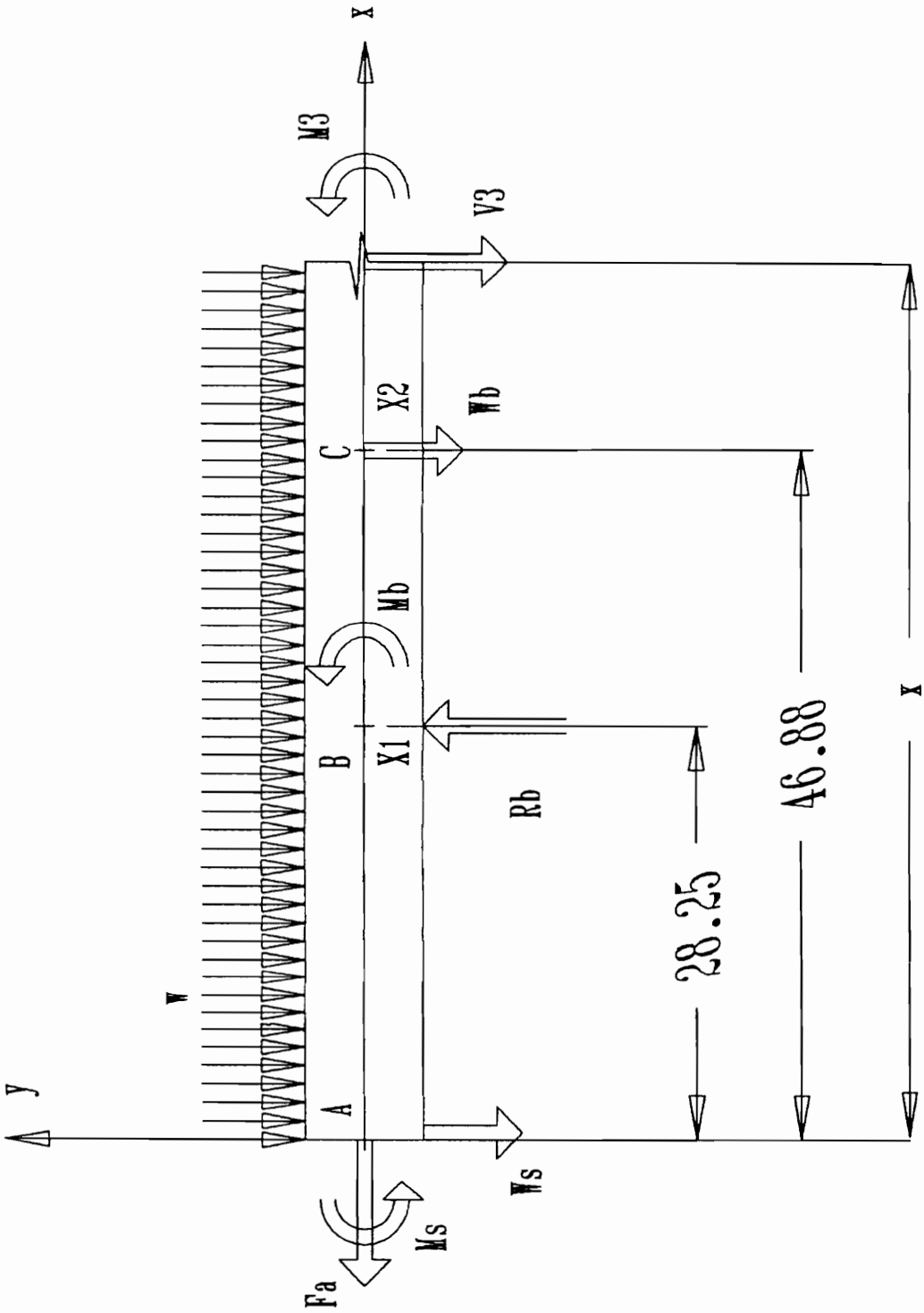

Figure B5. Free-Body Diagram of the Third Interval: 46.875 < x < 65.5.

Table B1. Solution for Unknown Reactions M_b and M_d (by TK Solver Ver. 2.00).

VARIABLE SHEET — For Academic Use Only

St	Input	Name	Outpu	Unit	Comment
	13921.451	Rb			Reaction force at point B
	13921.451	Rd			Reaction force at point D
	134.17	Ws			Weight of standard on 3rd bolster
	292.35	w			Linearly distributed load on bolster
	28.25	l			Outside length of 3rd bolster
	37.25	L			Inside span length of bolster
	166.75	Wb			Weight of 3rd bolster
	375885	Ms			Bending moment acting on standard
		Mb	-461751.2		Reaction moment at point B
		C3	4281431		Constant of integration
	28.25	X1			X1 = l
		Md	461751.17		Reaction moment at point D
		C4	-42330336		Constant of integration
	46.875	X2			X2 = l + 0.5 * L
	65.5	X3			X3 = l + L
		C5	4098233.9		Constant of integration
		C6	199509666		Constant of integration
		EIxETA2	1.8626E-9		EI x Slope at point C from right side
		EIxETA1	1.8626E-9		EI x Slope at point C from left side
		EIxY1	237466852		EI x Deflection at point B
		EIxY2	237466852		EI x Deflection at point D

Table B2. The Solution by Exploring Symmetry of the Structure (TK Solver Ver. 2.00).

VARIABLE SHEET

St	Input	Name	Output	Unit	
	13921.451	Rb			Reaction force at point B
	13921.451	Rd			Reaction force at point D
	134.17	Ws			Weight of standard on 3rd bolster
	292.35	w			Linearly distributed load on bolster
	28.25	l			Outside length of 3rd bolster
	37.25	L			Inside span of bolster
	166.75	Wb			Weight of 3rd bolster
	375885	Ms			Bending moment acting on standard
		Mb	-461751.2		Reaction moment at point B
		C3	4281431		Constant of integration
	46.875	X2			X2 = l + 0.5 * L
		Md	461751.17		Reaction moment at point D

RULE SHEET

S	Rule	
	Rb+Rd-2*Ws-Wb-w*(2*l+L)=0	; EQ1
	Rb=Rd	; EQ2
	Mb+Md=0	; EQ3
	C3=0.5*Rb*l^2+Ms*l+0.5*Ws*l^2+(1/6)*w*l^3+Mb*l	; EQ4
	Rb*(0.5*X2^2-l*X2)-Ms*X2-0.5*Ws*X2^2-(1/6)*w*X2^3-Mb*X2+C3=0	; EQ5

B2. Superposition Method

The superposition method utilizes a principle that a slope or deflection due to several loads is the algebraic sum of the slopes or deflections at the same location on the beam due to each of the loads acting individually. The method is frequently used in practice to provide the deformation equations needed to supplement the equilibrium equations in the solution of statically indeterminate beam problems. Most structural and mechanical engineering handbooks include tables giving the deflection and slopes of beams for various loadings and types of support to facilitate the task of practicing engineers. However, the maximum deflection cannot be obtained by simply adding the maximum deflections of the individual load components if these deflections occur at different points on the beam. Some of the tables would include expressions of the deflection in relation to the location on the beam. Differentiating these relations once would yield expressions for the slope, differentiating twice would give expressions for the bending moment, and so on.

The approach is outlined as follows. Two intervals on the beam may be identified: the cantilevered outside section of the bolster and the inner portion between the main beams (Figure B6).

The first interval of the structure is represented as a superposition of loading cases as in Figure B7. A solution for displacements, slopes, bending moments and lateral forces is obtained by algebraic addition of the appropriate parameters at the given location in the interval.

The second interval represents a beam indeterminate to the second degree (Figure B8). We designate the reactions at the second support (point D) as redundant. They are treated now as an unknown loads which, together with the other loads, must produce deformations compatible with the original supports. The

displacement boundary conditions at points B and D (where deflections and slopes are zero) are used to determine the redundant reactions R_d and M_d .

$\theta(x=X_3) = 0;$

and

$y(x=X_3) = 0;$

The sum of the deformations (expressions of which were taken from Beer and Johnston, 1981) caused by the individual loads and the redundant reactions at point D must satisfy the above equations, therefore we have:

$$- wl^3/6EI - W_b l^2/8EI + R_c L^2/2EI + M_c L/EI = 0 \quad \text{;Eq. 16}$$

$$- wl^4/8EI - 5W_b L^3/48EI + R_c L^3/3EI + M_c L^2/2EI = 0 \quad \text{;Eq. 17}$$

These equations are now supplemented with the equilibrium equations for the interval:

$$- wl - W_b + R_b + R_d = 0 \quad \text{;Eq. 18}$$

$$M_b - 0.5wL^2 - 0.5W_b L + M_c + R_c L = 0 \quad \text{;Eq. 19}$$

A solution for the unknown reactions in the supports are obtained by simultaneously solving equations Eq. 16 through Eq. 19.

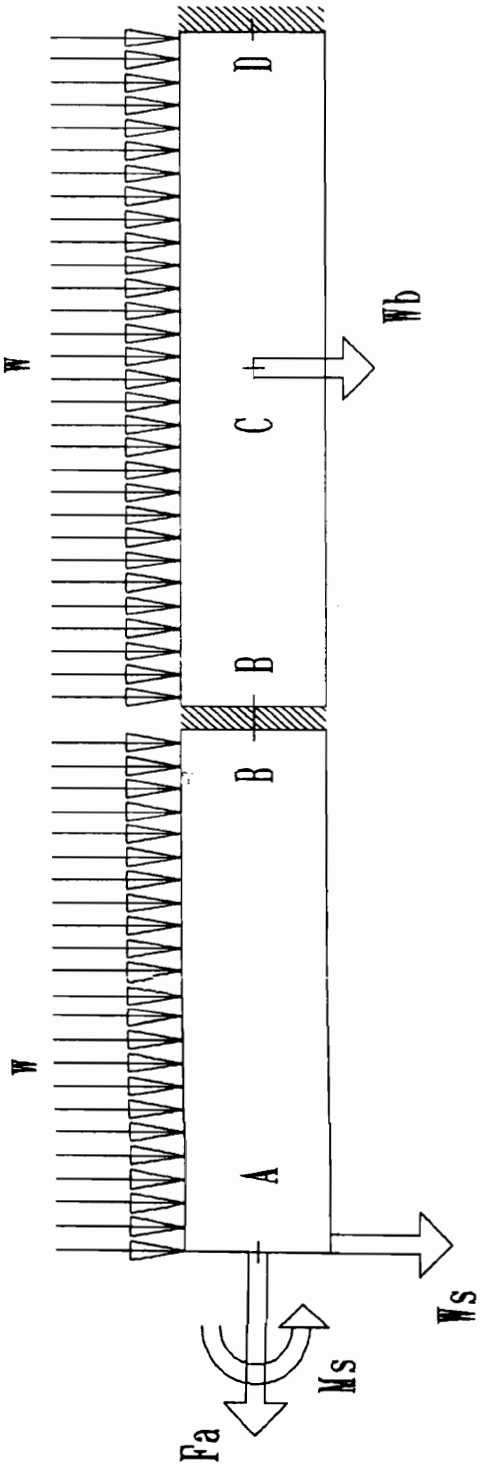

Figure B6. Schematic of the Simplified Bolster. The bolster is represented by two distinct intervals.

Figure B7. Bolster Solution by Superposition Method. First interval: $0 < x < 28.25$.

Figure B8. Bolster Solution by Superposition Method. Second interval: $28.25 < x < 65.50$.

B3. Stress Analysis

Having determined the reactions in the supports we can proceed to usual stress analysis of the bolster. We consider the intervals separately and determine the formulas for the shear force and bending moment in each cross-section of the bolster. The shear and bending moment diagrams are shown in Figures B9 and B10, respectively. Now, we use the actual cross-section properties of the bolster. Stresses are computed using usual formulas of the straight beam theory.

The stress distribution is obtained in agreement with the results of the FEM analysis. The computed maximum combined normal stresses differ from the FEPC solution only by 1%.

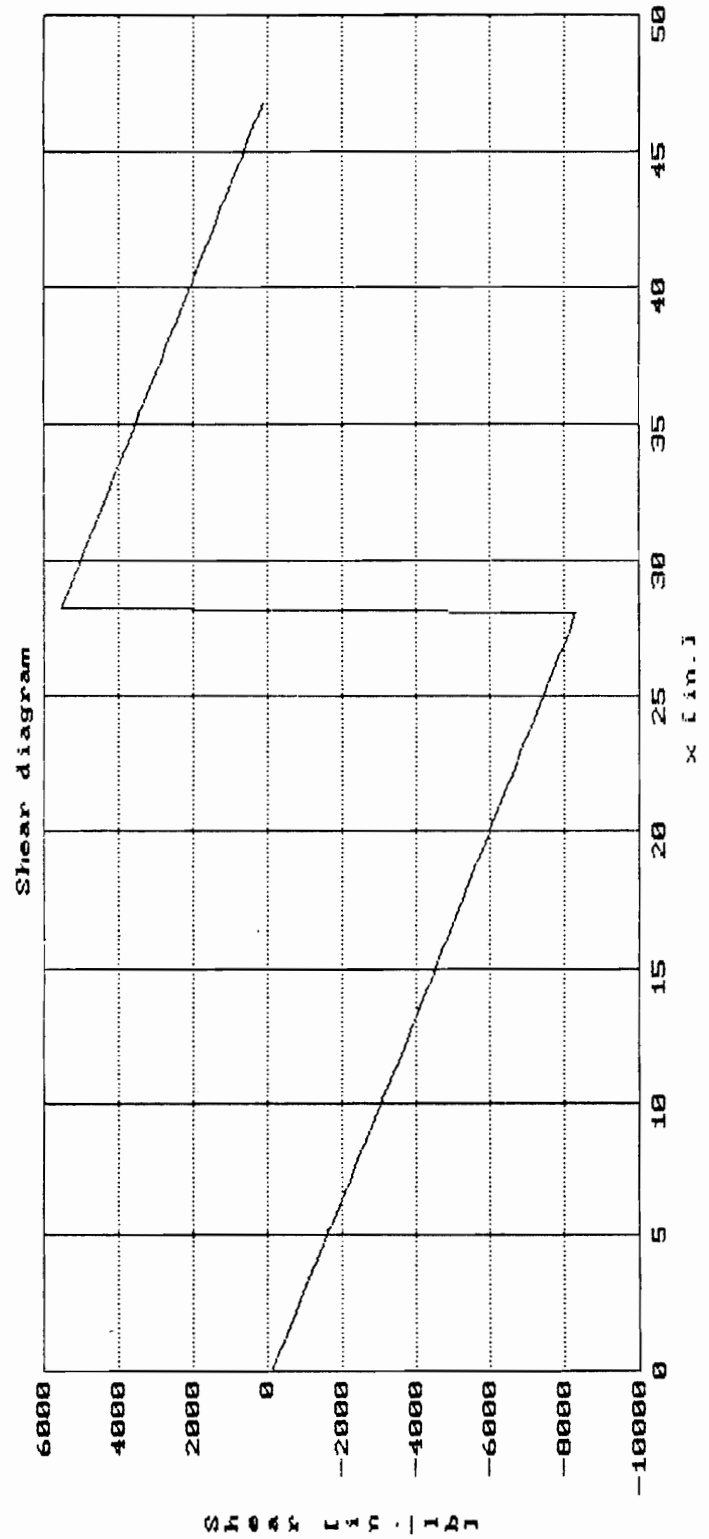

Figure B9. a) Shear Force Diagram for the Bolster: Interval $0 < x < 46.875$.

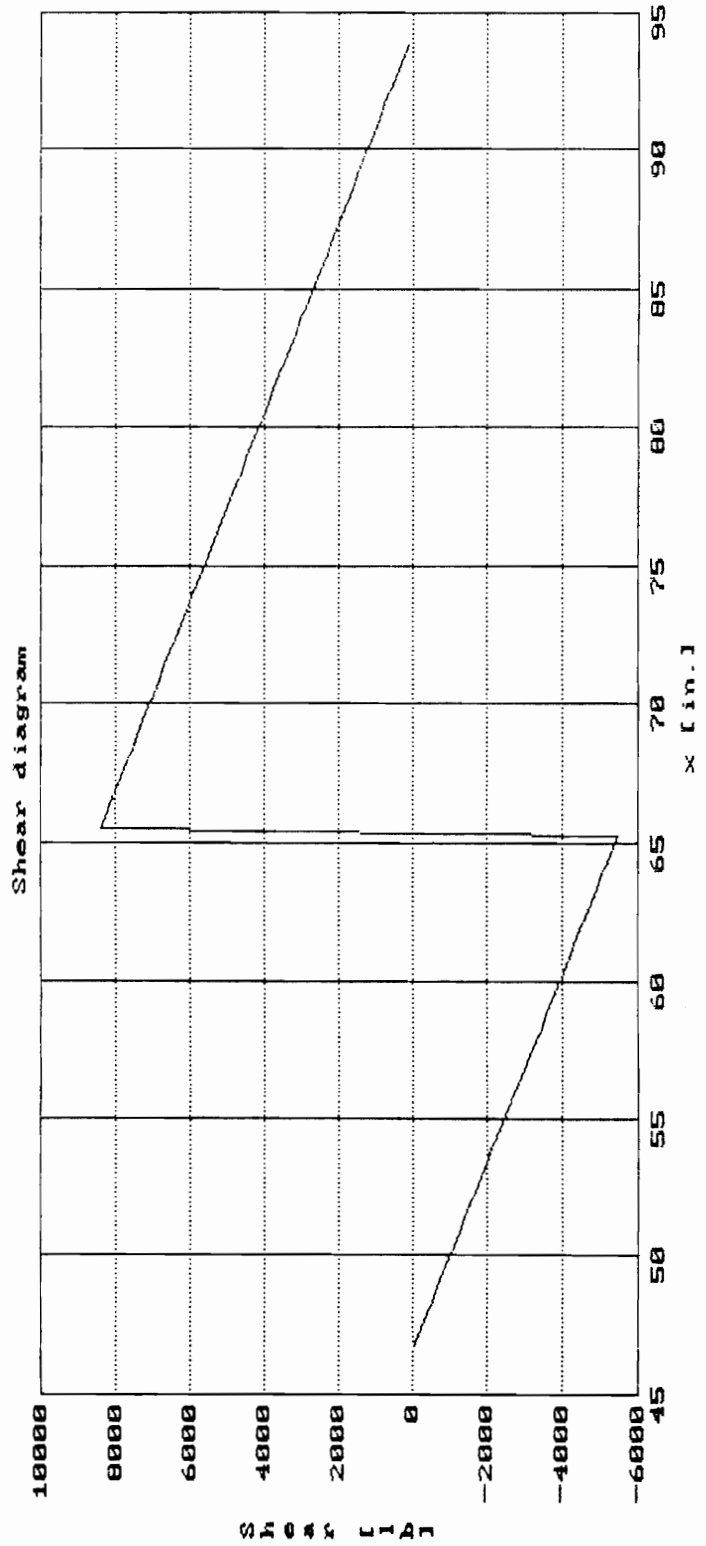

Figure B9. b) Shear Force Diagram for the Bolster: Interval $46.875 < x < 93.75$.

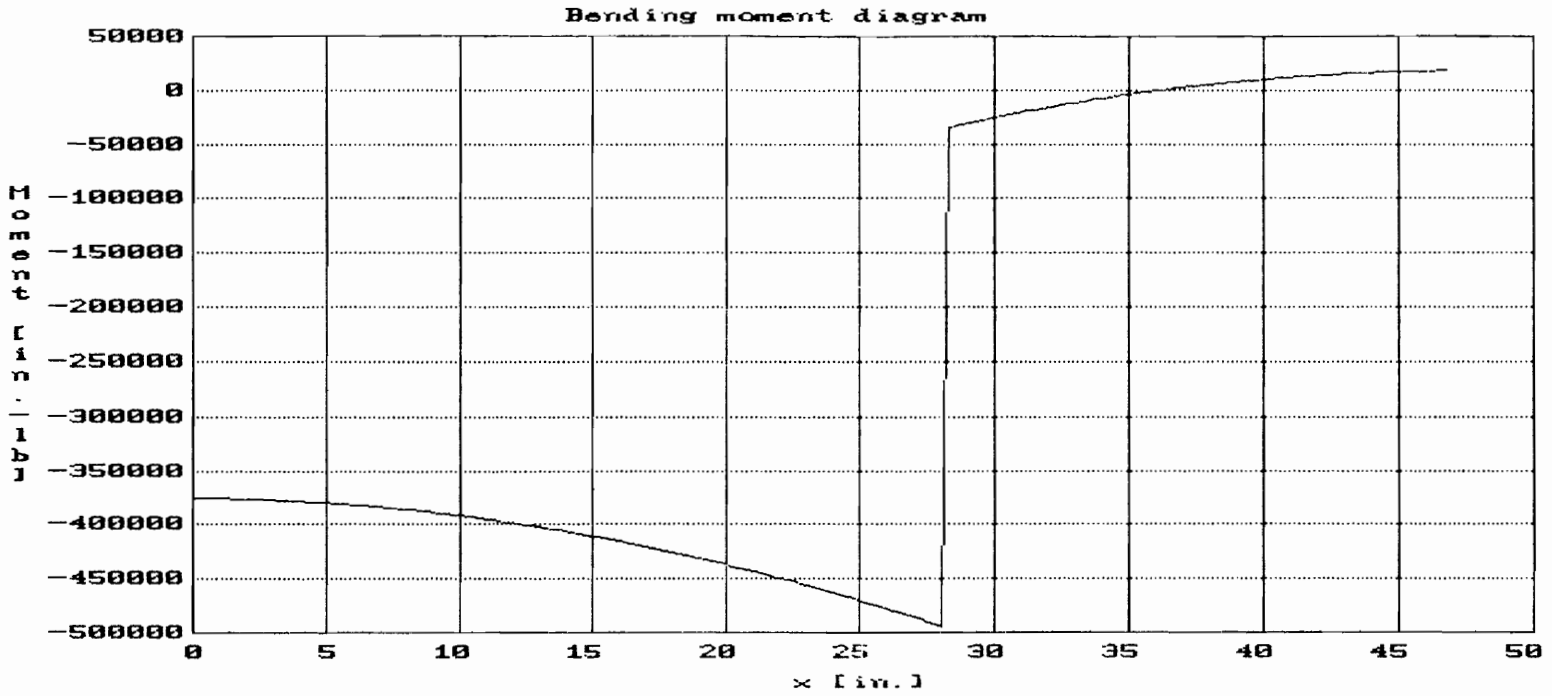

Figure B10. a) Bending Moment Diagram for the Bolster: Interval $0 < x < 46.875$.

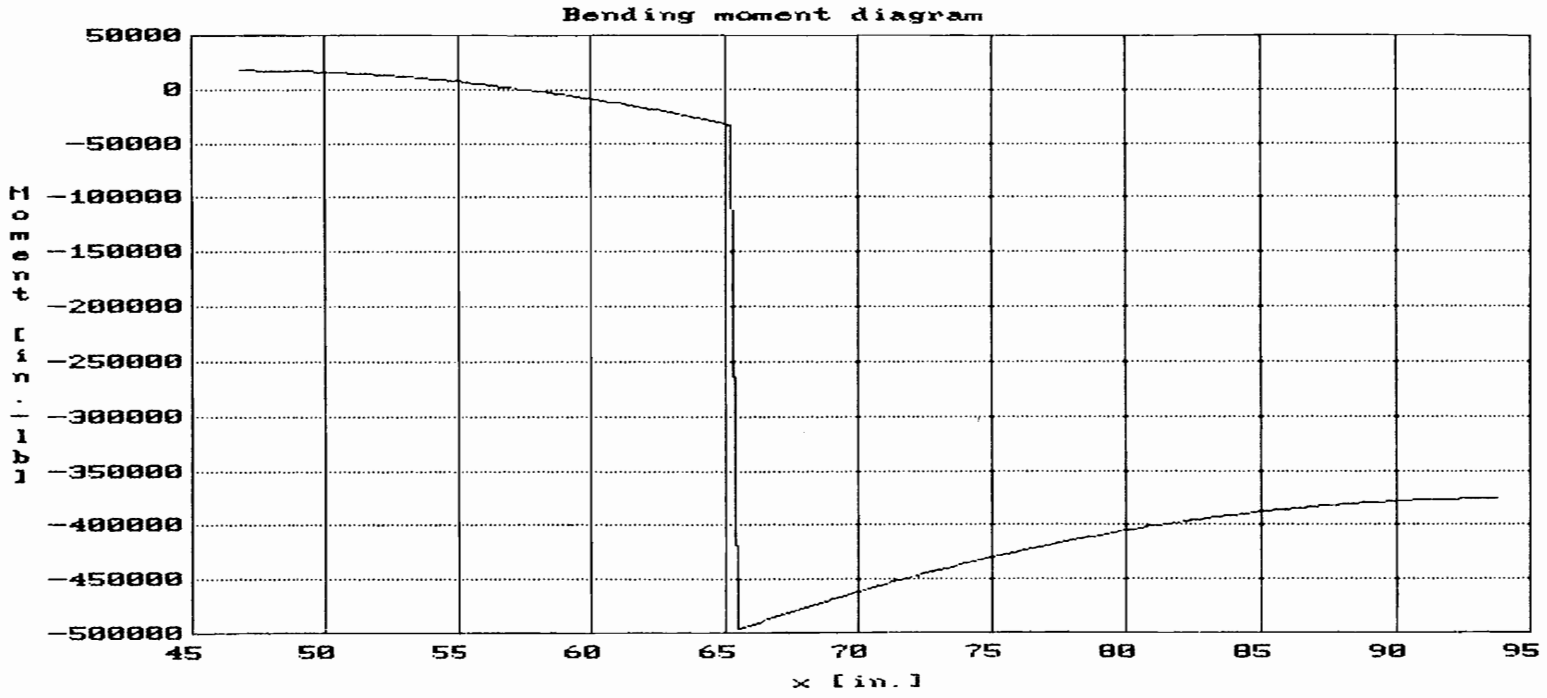

Figure B10. b) Bending Moment Diagram for the Bolster: Interval $46.875 < x < 93.75$.

Appendix C. Fatigue Life Prediction Using Nominal-Stress Approach

Definitions:

N - number of cycles;

S_a - stress amplitude for a notched member;

S_u - ultimate tensile strength of the material;

S_n - fatigue limit - endurance limit;

S_m - mean stress;

S_r - stress range;

S_{max} - maximum stress;

S_{min} - minimum stress;

C_l - coefficient accounting for loading type;

C_d - coefficient accounting for member size;

C_s - coefficient accounting for surface quality;

K_f - fatigue notch factor;

K_t - elastic-stress concentration factor;

q - notch sensitivity;

S' - stress amplitude adjusted for notch effect and mean stress;

R - stress ratio;

A - amplitude ratio;

N_f - fatigue life for the given stress amplitude S' and other factors;

C1. Constructing *S-N* Curve

A curve representing the stress amplitude, *S*, as a function of the number of cycles required to fatigue fracture, *N*, for the given material, component, and testing conditions is called the *S-N curve*. The number of cycles to failure changes very rapidly with stress level and may range over several orders of magnitude. *S-N curve* is, thus, plotted on logarithmic scale. The curve is approximated as a straight line on a log-linear plot separately for two life ranges: $10^3 < N_f < 10^6$, and $N_f > 10^6$. In the first interval the *S-N* relationship is following:

$$S = C + D \log N;$$

where C and D are fitting constants for experimental data.

S-N curve for the first interval is approximated as a straight line by joining together two characteristic points. These points are:

$S(10^3)$ - estimated stress amplitude for the fatigue life of 10^3 cycles; and

$S(10^6)$ - estimated stress amplitude for the fatigue life of 10^6.

These two characteristic values of stress amplitude are computed as (for bending as the dominating loading mode):

$$S(10^3) = 0.9\ S_u;$$

$$S(10^6) = 0.5\ C_l\ C_d\ C_s\ S_u;$$

For some materials, notably plain-carbon and low-alloy steels, there is a distinct stress level below which fatigue failure does not occur under ordinary conditions. *S-N* curve appears to become flat and to asymptotically approach the stress level S_n (Figure C1). Such lower limiting stress amplitude is called the *fatigue limit* or *endurance limit*. It is usually, assumed that the fatigue limit is attained by the material after 10^6 cycles, i.e.:

$$S_n = S(10^3);$$

Finally, the *S-N* curve is obtained for a given component and test conditions (Figure C1).

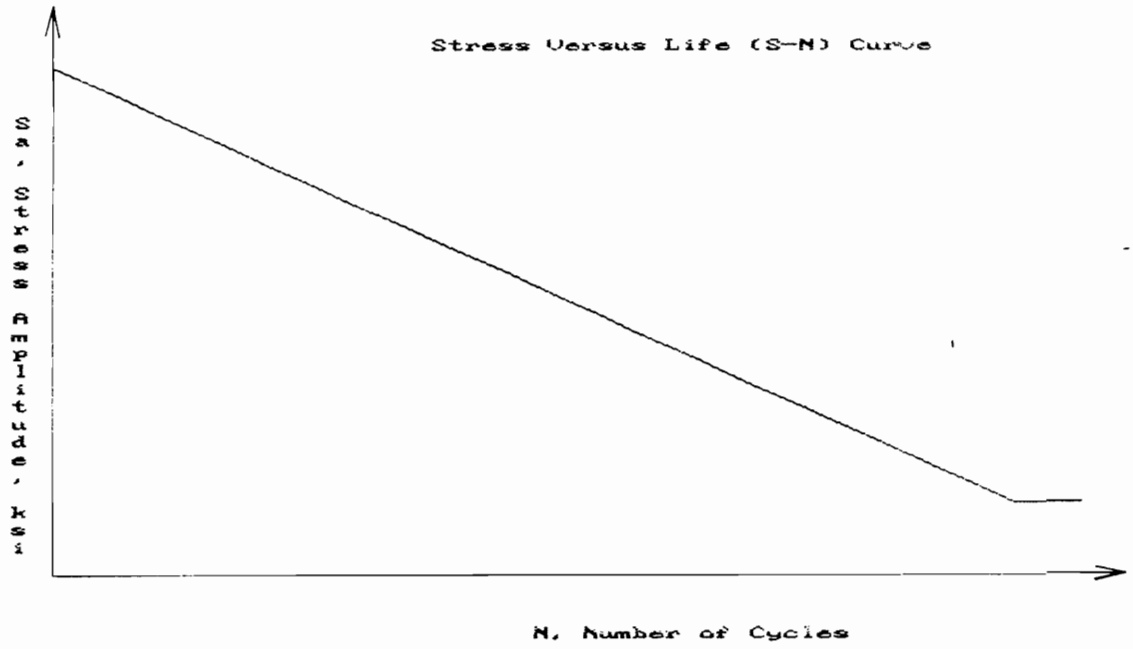

Figure C1. *S-N* **Curve.**

C2. Estimating Fatigue Life for Given Stress Amplitude - S_a

Parameters of the cycling stress: S_{min}, and S_{max} are obtained from the loading conditions or, preferably, from the experimental stress measurement. The other parameters are computed as:

$$S_a = 1/2 \, (S_{max} - S_{min});$$

$$S_m = 1/2 \, (S_{max} + S_{min});$$

The adjusted stress amplitude, S', is computed to account for the notch effect, and the mean stress:

$$S' = S_a \, K_f / \{1 - (S_m / S_u) \};$$

where, K_f is evaluated as:

$$K_f = 1 + (K_t - 1)q.$$

VITA

The author was born on the 17th of February, 1959 in Warsaw, Poland. After graduating from Klement Gottwald Gymnasium in Warsaw, he began his college education at Agricultural Academy, Warsaw, Poland. He subsequently completed the Bachelor of Science and Masters of Science (1983) degrees in Agricultural and Forest Engineering. He entered the Industrial Forestry Operations program at Virginia Polytechnic Institute and State University as a graduate research assistant in August, 1986. He received his Doctor of Philosophy degree in Forestry, Forestry Industrial Operations in August, 1993.

Since 1981 he worked in the area of forest engineering for the Department of Agricultural and Forest Engineering at the Agricultural Academy in Warsaw. Areas of his expertise include design of new forestry equipment, timber harvesting systems development, and industrial forestry operations. In 1986 he participated in Young Scientists' Summer Program at the International Institute for Applied System Analysis (IIASA) in Laxenburg, Austria. During 1987 and 1988 the author was a member of the Research Team investigating Implications of Forest Decline in Poland. This research endeavor was a part of the Biosphere Project at IIASA studying forest decline in Europe.

Andrzej T. Wylezinski